Regulation of *HPGD* and *SLCO2A1* in Colorectal Cancer Development

Spyridon Papagrigoriou

Submitted in accordance with the requirements for the degree of

Doctor of Philosophy

The University of Leeds

Faculty of Medicine and Health

September 2018

The candidate confirms that the work submitted is his own and that appropriate credit has been given where reference has been made to the work of others.

Acknowledgments

I would like to thank Dr Christine Diggle, Dr Ian Carr, Professor David Bonthron, and Sir Alex Markham for giving me the opportunity to undertake this PhD, and for their invaluable advice, help and support throughout this work

I would also like to thank Dr Laura Wastall, Dr Caroline Young, Mr Mike Shires, and Ms Lisa Allinson for their help and advice in interpreting the cellular localisation of the labelling in immunohistochemistry.

Abstract

A wide range of lipid mediators are synthesised from Polyunsaturated Fatty Acids. These mediators regulate inflammation and many other processes in the human body, and perturbation of their signalling can contribute to the survival and proliferation of cancer cells. Prostaglandin E2 has the most diverse range of functions amongst the prostaglandins and other lipid mediators, and increased PGE2 signalling has been associated with promoting tumour growth and survival by a number of mechanisms. NSAIDs target the synthesis side of the prostaglandin pathway through PTGS2, but only recently has the importance of the degradation component, involving the enzyme HPGD and prostaglandin transporter SLCO2A1 been discovered.

Although a number of publications have shown that *HPGD* is downregulated in colorectal cancer, in addition to other malignancies, the mechanisms by which this takes place remain unclear. Only a few studies have indicated a comparable role for SLCO2A1, and the potential for these two genes to be co-regulated. Therefore, understanding how these two genes are regulated could reveal the mechanisms by which their expression is lost, and potentially how they could be upregulated to complement the action of NSAIDs when used prophylactically, or as an adjunct to chemotherapy.

HPGD and *SLCO2A1* expression was characterised, and the genes' transcriptional start sites identified using two colorectal cancer cell lines. This information was used to design and carry out a promoter deletion series, which revealed the importance of the proximal 364 bp *SLCO2A1* promoter region in driving transcription. Further analysis of this region revealed a possible role for the intestinal and colonic epithelium-specific transcription factor CDX2 for driving SLCO2A1 expression. Further experiments provided evidence to

suggest that the TGF-β pathway, which is known to drive *HPGD* expression, may also co-regulate *SLCO2A1.*

Table of Contents:

List of Figures

List of Tables

List of Abbreviations

°C	degrees Celsius
15-PGDH	15-Hydroxyprostaglandin dehydrogenase
5’-UTR	5’-Untanslated region
AA	Arachidonic acid
ABCC4	ATP-binding cassette subfamily C member 4
ALOX12	Arachidonate 12-lipoxygenase
ALOX15	Arachidonate 15-lipoxygenase
ALOX5	Arachidonate 5-lipoxygenase
APC	Adenomatous polyposis coli
BAC	Bacterial artificial chromosome
BLAST	Basis local alignment sequence tool
bp	Base pair
BSA	Bovine serum albumin
CCND	Cyclin D
CDX2	Caudal-type homeobox protein 2
cGMP	cyclic Guanosine monophosphate
CK1α	Casein kinase 1α
CIP	Calf intestinal phosphatase
COX2	Cyclo-oxygenase 2
DAB	3,3′-diaminobenzidine
DEPC	Diethyl pyrocarbonate
DHA	Docosahexenenoic acid
DNA	Deoxyribonucleic acid
dNTP	Deoxynucleoside triphosphate

Dlv	Dishevelled
EDTA	Ethelenediaminetetraacetic acid
EGR	Early growth response
EMT	Epithelial to mesenchymal transition
EPA	Eicosapentaenoic acid
EST	Expressed sequence tag
g	Gram
g	Force of gravity = 9.81 m/s^2
GAPDH	Glyceraldehyde-3-phosphate dehydrogenase
GSK3β	Glycogen synthase kinase 3β
h	Hour
HDAC	Histone Deacetylase
HPGD	Hydroxyprostaglandin dehydrogenase
HRP	Horseradish peroxidase
IgG	Immunoglobulin G
IHC	Immunohistochemistry
KRAS	Kristen rat sarcoma viral oncogene homologue
LB	Lysogeny broth
LRP5/6	Low density lipoprotein receptor family member 5/6
M	Molar (1 mole/decilitre^3)
ml	millilitre
mM	miniMolar
MOPS	3-Morpholinopropane-1-sulphonic acid
MRP4	Multidrug resistance protein 4
MYC	c-Myc (c-Myelocytomatosis)
ng	nanogram

nM	nanoMolar
NSAID	Non-steroidal anti-inflammatory drug
PBS	Phosphate buffered saline
PCR	Polymerase chain reaction
PGD_2	Prostaglandin D_2
PGE_2	Prostaglandin E_2
PGF_2	Prostaglandin F_2
PGH_2	Prostaglandin H_2
PGI_2	Prostaglandin I_2
PTGER1	Prostaglandin E receptor 1
PTGER2	Prostaglandin E receptor 2
PTGER3	Prostaglandin E receptor 3
PTGER4	Prostaglandin E receptor 4
PTGES	Prostaglandin E synthase
PTGES2	prostaglandin E synthase 2
PTGES3	prostaglandin E synthase 3
PTGS1	Prostaglandin-endoperoxidase synthase 1
PTGS2	Prostaglandin-endoperoxidase synthase 2
PUFA	Polyunsaturated fatty acids
PVDF	Polyvinylidene fluoride
RB1	Retinoblastoma-associated protein 1
RIPA	Radioimmonoprecipitation assay
RLM-RACE	RNA ligase-mediated rapid amplification of 5’-cDNA ends
RNA	Ribonucleic acid
RPM	Revolutions per minute
RT-PCR	Reverse-transcriptase polymerase chain reaction

SAG	Smoothened agonist
SAP	Shrimp alkaline phosphatase
SDS	Sodium dodecyl sulphate
S.O.C.	Super optimal broth with catabolite suppression
SLCO2A1	Solute organic anion transporter family member 2A1
SMAD2	Small / mothers against decapentaplegic homologue 2
SMAD3	Small / mothers against decapentaplegic homologue 3
SMAD4	Small / mothers against decapentaplegic homologue 4
SP	Specificity protein
TAE	Tris acetate ethylenediaminetetraacetic acid
TAP	Tobacco acid pyrophosphatase
TBS	Tris buffered saline
TGFBR1	Transforming growth factor β receptor 1
TGFBR2	Transforming growth factor β receptor 2
TGFBR3	Transforming growth factor β receptor 3
TGF-β	Transforming growth factor β
TP53	Tumour protein p53
TSS	Transcriptional start site
TXA_2	Thromboxane A_2
VEGF	Vascular endothelial growth factor
V	Volt
w/w	Mass concentration as weight per weight
w/v	Mass concentration as weight per volume
Wnt	Wingless-type mouse mammary tumour virus integration site
β-TrCP	β-transducin repeat containing E3 ubiquitin protein ligase
µg	microgram

µl	microlitre

Chapter 1 Introduction

1.1 Lipid Mediators

1.1.1 Polyunsaturated fatty acid-derived signalling factors

Lipid mediators, eicosanoids, have been implicated in numerous biological processes including those in reproduction, cardiovascular physiology, and the immune system. The mediators include prostaglandins, leukotrienes, thromboxanes, prostacyclins, lipoxins, resolvins and protectins, all of which can be synthesised from polyunsaturated fatty acids (PUFAs) (Figure 1.1) (Umar et al., 2016). Dietary PUFAs are typically classified by the position of the first carbon double bond from the end of the fatty acid hydrocarbon chain, the third or sixth, as ω-3 or ω-6, respectively (Innes and Calder, 2018). This distinction is important because the enzymes of the different mediator pathways are able to process more than one fatty acid substrate (Bannenberg and Serhan, 2010) The resulting mediators can have different or even opposing effects, depending on whether the original substrate was an ω-3 or ω-6 fatty acid (Liu et al., 2006; Thuresson et al., 2002; Laneuville et al., 1995).

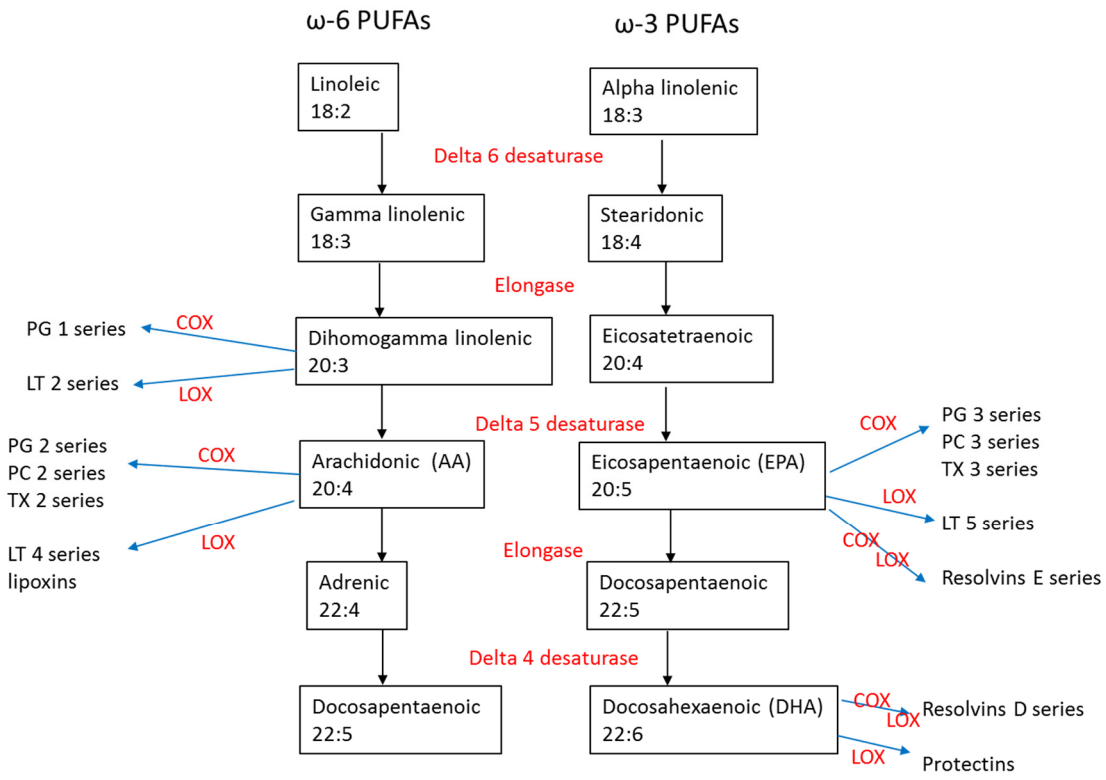

Figure 1.1: Polyunsaturated fatty acid (PUFA) and eicosanoid synthesis Outline of ω-6 and ω-3 PUFA metabolism, demonstrating that the different classes of lipid mediator are synthesised from the different intermediate products. Desaturase enzymes introduce C=C carbon bonds into the fatty acid chain, while the elongases extend it by two carbon atoms. The ratios indicate the total number of carbon atoms in the fatty acid chain to C=C double bonds. Prostaglandin (PG), prostacyclin (PC), leukotriene (LK), thromboxane (TX), cyclooxygenase (COX)

In the immune system, the ω-6-derived mediators typically act to both drive and to resolve inflammation, and the recruitment of immune cells such as leucocytes (Kaley and Weiner, 1971). Arachidonic acid (AA) (or eicosatetraenoic acid) are the substrates from which a number of pro-inflammatory prostaglandins, such as PGE_2, and leukotrienes are synthesised (Bannenberg and Serhan, 2010). Likewise, the lipoxins and resolvins, which exert an anti-inflammatory action and initiate resolution of inflammation, are also produced from AA (Serhan et al., 1984a; Serhan et al., 2000; Serhan, 2007). On the other hand, ω-3 fatty acids, such as eicosapentaenoic acid (EPA) and docosahexenenoic acid (DHA), result in the generation of lipid mediators, such as the resolvins and protectins that drive resolution of inflammation (Serhan et al., 2000; Ariel et al., 2005).

The enzymes that catalyse the first reactions in the lipid mediator synthesis pathways are the cyclooxygenases (PTGS1 and PTGS2) (Chulada et al., 2000) and the lipoxygenases (ALOX5, ALOX12 and ALOX15) (Gronert et al., 2005; Vainio et al., 2011) (Figure 1.1). The cycloxygenase pathway generates the prostaglandins, prostacyclins, and thromboxane (Hamberg et al., 1975), while the lipoxygenases produce the leukotrienes, lipoxins, resolvins and protectins (Shimizu et al., 1984; Serhan et al., 1984b). The relative abundance of the ω-6 and ω-3 substrates can bias the generation of one type of mediator over another (Magrum and Johnston, 1983; Wada et al., 2007). Furthermore the potential for cell specific expression of the enzymes and their relative activity when competing for substrates, can allow substantial control of the mediators generated, impacting on cellular processes (Abeywardena et al., 1987).

Many of the individual eicosanoids are as yet not well understood in regards to their functional significance in health and disease, however that eicosanoids have an important role modulating the immune system is well established. The prostaglandins are of particular interest due to their role in regulating the initiation of acute inflammation, and the pathology resulting from sustained activity that results in chronic inflammation (Serhan et al., 2015).

1.1.2 Overview of the Prostaglandin Pathway

Prostaglandins are a subclass of lipid mediators derived from PUFAs via the enzymatic pathways downstream of the cyclooxygenases (Hamberg and Samuelsson, 1971; B Samuelsson et al., 1975; Tootle, 2013). PUFAs, for example AA, when released from the membrane phospholipids through the action of phospholipase A2, can be converted to prostaglandin H_2 (PGH_2) by cyclooxygenases (Figure 1.2). PGH_2 becomes the substrate for specific prostaglandin synthases (Ruan et al., 2011). The prostaglandins generated can then be exported from the cell, and exert their effects in an autocrine or paracrine manner through G-protein coupled cell surface receptors. Prostaglandins are short-lived molecules, as they can be subsequently rapidly removed from the extracellular space by transport into the cell by the prostaglandin transporter (PGT/SLCO2A1) (Hamberg and Samuelsson, 1971). They can then be deactivated, which is performed enzymatically by 15-hydroxy prostaglandin dehydrogenase (15-PGDH/HPGD). That prostaglandins can be rapidly metabolised, ensures that once they have performed their physiological function, homeostasis can be readily restored.

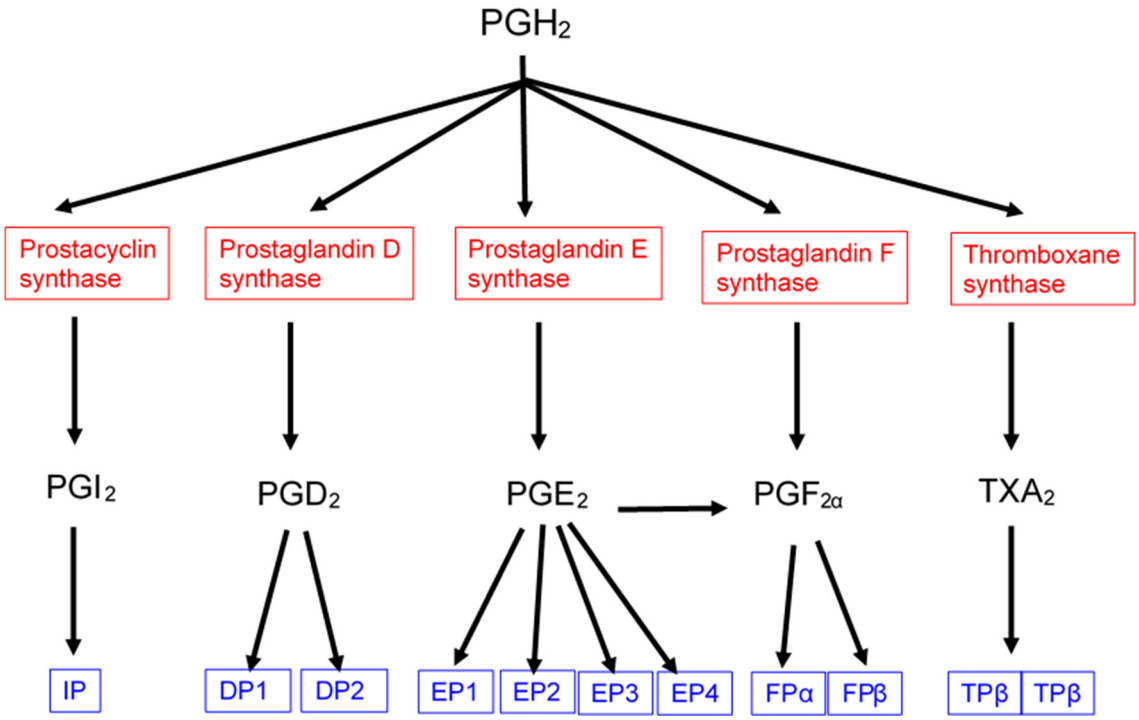

Figure 1.2: The 2-series prostaglandins and their receptors

1.1.3 Prostaglandin synthesis

Series 2 prostanoids (prostaglandins, prostacyclins and thromboxanes) are generated from arachidonic acid which is normally stored as part of the endoplasmic reticulum membrane and becomes available through membrane phospholipid hydrolysis by phospholipase A2 (Figure 1.4) (Gustafson-Svard et al., 1996). The cyclooxygenases PTGS1 and PTGS2 constitute the next step by production of PGH_2 (Laneuville et al., 1995). This is the rate-limiting reaction in PGE_2 synthesis (Yan et al., 2004). PTGS1 is generally considered to be a constitutively expressed enzyme, while PTGS2 is inducible following exposure for example to injury and inflammation (Umar et al., 2016). The 3-series prostanoids (PGD_3, PGE_3, PGF_3, PGI_3, and TXA_3) are generated through the ability of PTGS2, but not PTGS1, to use EPA as a substrate (Yang *et al.*, 2014c). The enzymatic reactions with EPA and the PGH_3 are approximately 30% as efficient compared to AA and PGH_2, meaning that the 3-series intermediates act as competitive inhibitors and reduce 2-series prostaglandin generation.

Specific prostaglandin synthases metabolise the PGH_2 precursor to generate Prostaglandin D2 (PGD_2), prostaglandin E_2 (PGE_2), and prostaglandin F2 (PGF_2) through isomerisation reactions (Wada et al., 2007). Prostaglandin I_2 (PGI_2)/prostacyclin and thromboxane A_2 (TXA_2) can also be synthesised from PGH_2 (Figure 1.4). The microsomal prostaglandin E synthase (PTGES) is the main enzyme that converts PGH_2 to PGE_2 (Jegerschöld et al., 2008). Two more prostaglandin E synthases exist (PTGES2 and PTGES3), however, PTGES is considered to be the predominant enzyme, considering that knockout of *Ptges2* in mice does affect overall PGE_2 synthesis (Langenbach et al., 1995; Morham et al., 1995). PTGES is an inducible enzyme, and its upregulation coincides with

that of COX-2, therefore, suggesting a preferential increase in PGE_2 synthesis over other prostaglandins (Hara et al., 2010).

The control of prostaglandin production has been a means by which drugs act to reduce inflammation. The non-steroidal anti-inflammatory drugs (NSAIDs) exert their action through inhibition of PTGS1 (COX-1) and PTGS2 (COX-2) (Ku et al., 1975; Serhan, 2002) (Bygdeman, 2003). While this effectively blocks the synthesis of 2-series prostaglandins and thromboxanes, it causes AA to be shunted across to the unaffected lipoxygenase pathways, so increasing the generation of alternative bioactive lipids (Bannenberg and Serhan, 2010). The archetypical NSAID, aspirin, is a non-selective inhibitor that irreversibly inactivates PTGS1 and PTGS2 by acetylating their active sites, and altering the latter's substrate specificity, in addition to preventing the oxidation of AA, it increases the enzyme's specificity for DHA and EPA (Rome et al., 1976; Serhan et al., 2000). The intermediate products formed then are further metabolised by the lipo-oxygenases to generate the D-series and E-Series of resolvins (from DHA and EPA, respectively). The prostaglandin synthases can also metabolise these intermediates to generate the 3-series prostaglandins (such as PGE_3), which as described above further inhibit the action of the 2-series prostaglandins (Bannenberg and Serhan, 2010). Aspirin also promotes the synthesis of the anti-inflammatory lipoxin 15-epi-LXA_4 (from AA), which is more resistant to degradation (Takano et al., 1997).

Although NSAIDs such as aspirin have been highly successful in treating a range of conditions, they have potentially serious side effects (Fanaroff and Roe, 2016). These include bleeding, ulceration, and renal, cardiovascular and gastrointestinal toxicity (Robert et al., 1976; Fung et al., 1974). Furthermore, these drugs are not suitable for certain patient groups, e.g. it may causes

aspirin-exacerbated respiratory disease in 7% of all asthma patients (Fanaroff and Roe, 2016). One key prostanoid that contributes to aspirin's side effects is thromboxane A2 (TXA_2). The anticoagulant side effects of aspirin is due to the preferentially inhibition by aspirin of COX-1, compared to COX-2, which is required for the production of the blood clotting lipid TXA_2 in the platelets (Patrignani et al., 2003). Consequently, high doses of aspirin reduce the ability of blood clots to form where they would have life threatening consequences.

COX-2 has been the subject of intense research as a drug target, not only as this would avoid COX-1 inhibition adverse effects, but also due to its upregulation, particularly during inflammation and in cancer, and as the rate-limiting step in prostaglandin production, and its ability to alter the enzyme's substrate specificity to generate anti-inflammatory mediators (Gustafson-Svard et al., 1996; Asting et al., 2011; Fink et al., 2014; Maeng et al., 2014; Pereira et al., 2014; Zelenay et al., 2015). A number of COX-2-selective inhibitors have been developed, and COX-2 remains the most studied member of the PGE_2 metabolic pathway, and the key drug target for suppressing PGE_2 synthesis (Wang et al., 2018). COX-2 specific inhibitors do not detrimentally effect thromboxane A_2 levels, but do however substantially impact on the balance with prostacyclin levels. Prostacyclin is a potent vasodilator that also inhibits platelet aggregation (Coceani et al., 1978; Johnson et al., 1977). These inhibitors have therefore been associated with higher levels of cardiovascular events, such as myocardial infarction, stroke, hypertension and congestive heart failure, with the altered prostacyclin levels relative to TXA_2 thought to be the major contributory factor.

As PTGES acts downstream of PTGS1 and 2, and as the specific synthase that generates PGE_2, it has also been of interest as an alternative

drug target to decrease PGE_2 synthesis. Although a number of inhibitors have been identified and entered clinical trials, as yet none have approved clinically (Koeberle and Werz, 2015). Certainly, it would be expected that there would be fewer side effects, by acting downstream of the COX enzymes, however, there could still be some shunting of the PGH_2 precursor towards other synthase pathways. Consequently, there is interest in additional parts of the prostaglandin pathway that act further downstream that may affect fewer prostanoids thereby reducing harmful side effects.

1.1.4 Prostaglandin export

PGE_2 is secreted from the cells through multidrug resistance protein 4 (MRP4) (Figure 1.4), which is encoded by the ATP-binding cassette subfamily C member 4 (ABCC4) gene (Chen and Tiwari, 2011). In addition to PGE_2 and PGE_1, MRP4 is also capable of exporting other substrates, including cyclic nucleotides (such as cGMP) and steroid derivatives, as well as glutathione (Chen and Tiwari, 2011; Reid et al., 2003). In the context of PGE_2 synthesis pathway, MRP4 has an important role in accelerating PGE_2 release, which would otherwise be much slower by simple diffusion or passage through other less efficient transporter proteins (Maeng et al., 2014).

NSAIDs have also been found to inhibit MRP4's export of PGE_2, in addition to their effects on PTGS1 and PTGS2 (Reid et al., 2003; Kochel and Fulton, 2015). However, as the mechanism of PGE_2 secretion is not fully understood, and given MRP4's ability to transport anions other than PGE_2, this membrane transporter may not be an ideal drug target (Shirasaka et al., 2013; Shimada et al., 2015).

1.1.5 Prostaglandin receptor activation

The prostanoids can activate downstream signalling pathways through a variety of cell surface receptors (Figure 1.4). Unlike the other prostanoids, which have one or two receptors that are expressed only in certain organs or tissues, there are four PGE_2 receptors (EP1, EP2, EP3 and EP4) (Tootle, 2013). PGE_2 mediates its effects by binding to receptors, EP1-EP4 (Figure 1.2 and Figure 1.4), encoded by the genes *PTGER1*, *PTGER2*, *PTGER3* and *PTGER4*, respectively) (Edwards et al., 2012). These receptors are expressed by a range of cell types, and afford PGE_2 signalling greater complexity, and the ability to control a range of functions, in addition to the local triggering of acute inflammation and initiation of resolution (Innes and Calder 2018). EP1 to EP4 are all G-protein coupled receptors, which trigger an increase (EP2, EP4) or decrease (EP3) in intracellular cAMP, or trigger the release of intracellular Ca^{2+} (EP1) (Tootle, 2013). The EP2 and EP4 receptors are important because of their ability directly or indirectly trigger a positive feedback loop to increase PGE_2 synthesis by upregulating PTGS2 and PTGES (Fujino, 2016).

In addition, further cellular non-enzymatic dehydration and isomerisation reactions can generate additional products, e.g. PGE_2, PGE_1 and PGD_2 can produce PGA_2, PGA_1, and PGJ_2 respectively, that are all bioactive (Coceani et al., 1978; Eklund and Carlson, 1980; Straus and Glass, 2001). Some prostanoid products do not require G-protein involvement in their mechanism of action, as they are ligands for nuclear hormone receptors thereby altering transcription, e.g. 15-Deoxy-$\Delta^{12,14}$-Prostaglandin J_2 and PGI_2 can bind PPAR's (Forman et al., 1995; Kliewer et al., 1995). The potential downstream pathways activated from a single precursor molecule is therefore theoretically large.

1.1.6 Termination of prostaglandin signalling through the actions of HPGD and SLCO2A1

Extracellular prostaglandins can be actively removed and internalised in order to terminate signalling. The prostaglandin transporter, encoded by the *SLCO2A1* gene, fulfils this role (Kanai et al., 1995). This gene belongs to the solute organic anion transporter superfamily, which consists of eleven genes in the human, divided into six families (SLCO1, SLCO2, SLCO3, SLCO4, SLCO5 and SLCO6) (Tamai et al., 2000; Hagenbuch and Stieger, 2013). SLCO2A1 is believed to function by importing prostaglandins such as PGE_2 into the cell through the exchange of lactate ions that pass in the opposite direction (Chan et al., 2002b; Bao et al., 2002).

SLCO2A1 (Figure 1.3) was first cloned and characterised in the rat and human more than two decades ago (Kanai et al., 1995; Lu and Schuster, 1998). In spite of subsequent research on prostaglandin transporter function, largely by the same research team, and the identification of potent inhibitor compounds with potential utility for example in hypertension, very little work has been carried out to elucidate the actual regulation of the *SLCO2A1* gene (Bao et al., 2002; Chan et al., 1999; Chang et al., 2010; Chi et al., 2006; Chi et al., 2008; Schuster et al., 2015). Few publications from other groups suggest possible regulators of the prostaglandin transporter, as little research on the actual control at the transcriptional level has been carried out (Topper et al., 1998; Chi et al., 2006; Gao et al., 2007).

This is despite SLCO2A1's importance in being the rate-limiting step for PGE_2 degradation (Nomura *et al.*, 2004; Schuster *et al.*, 2015). While drugs can act as agonists or antagonists on receptors and components of signalling cascades, or inhibit the function of transporter proteins and enzymes, adequate

expression of the target gene that encodes the protein drug target is a prerequisite for their action. Therefore, in situations where the objective is to upregulate a particular gene, knowledge of its transcriptional regulation is essential so that any drugs can be targeted to the upstream pathway elements to stimulate expression or inhibit repression.

15-Hydroxyprostaglandin Dehydrogenase (15-PGDH, encoded by the *HPGD* gene) (Figure 1.3) is the enzyme that oxidizes PGE_2 that is taken up into the cell by SLCO2A1. In this way, PGE_2 signalling is terminated, as the intracellular PGE_2 concentration is lowered, reducing the amount that could be potentially secreted through MRP4. Therefore, SLCO2A1 and HPGD constitute the degradation arm of the PGE_2 metabolic pathway (Ensor et al., 1990; Chang et al., 2010).

Unlike SLCO2A1, the 15-PGDH enzyme was discovered much earlier. 15-PGDH was first isolated from pig lung in 1966, and from human placenta in 1974 (Änggård and Samuelsson, 1969; Braithwaite and Jarabak, 1975; Nakano et al., 1969; Thaler-Dao et al., 1974). While most studies to characterise HPGD's expression were historically conducted largely in the reproductive biology field (Braithwaite and Jarabak, 1975; Greenland *et al.*, 2000; Nandy *et al.*, 2003), *HPGD* gained attention as a tumour suppressor-like gene through the research by Dr. Sanford D. Markowitz' group (Myung *et al.*, 2006; Yan *et al.*, 2004), which has since led to renewed interest in this gene's contribution to cancer development and progression. Both SLCO2A1 and HPGD represent potential new targets for the control of prostaglandin production. As they act further downstream than the prostaglandin synthesis enzymes, this may suggest that fewer adverse side effects would be expected, as there would be less perturbation of other parts of the lipid mediator pathways.

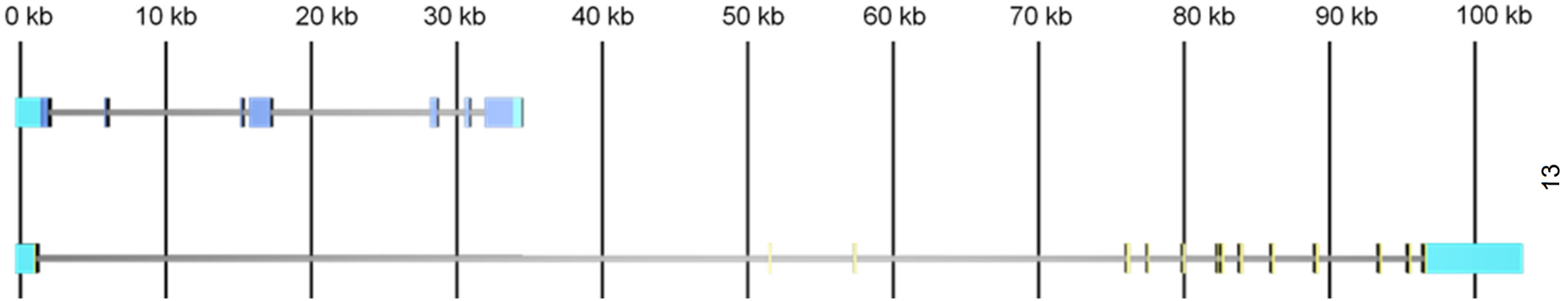

Figure 1.3: Schematic representation of the *HPGD* and *SLCO2A1* genes
HPGD is a 32.7 kb gene located on chromosome 4q34.1, with eight coding exons. *SLCO2A*1 is 101.9 kb in size, located on chromosome 3q22.1 to 3q22.2, with fourteen coding exons. The genes are represented to scale. *HPGD* exons (blue), *SLCO2A1* exons (yellow), untranslated region (cyan), introns (grey)

1.1.7 Prostaglandin E2

Although prostaglandins have a number of additional functions, such as the initiation of labour and parturition (PGE_2, $PGF2_\alpha$) (Davis et al., 1999; Lim et al., 1997), or platelet aggregation during clot formation (TXA_2), (Hamberg et al., 1975), PGE_2 remains one of the most intensely studied prostaglandins (Pelus and Hoggatt, 2011) because of the diverse range of biological processes it is involved in, and, unlike the other prostaglandins the complexity in its signalling through four G-protein-coupled receptors (Chi et al., 2014; Castellone et al., 2005). Prostaglandin E_2 belongs to a class of lipid cytokines that are synthesized from the fatty acid precursor arachidonic acid (all-*cis*-5,8,11,14-Eicosatetraenoic acid), and generally acts locally in an autocrine or paracrine manner (Reid *et al.*, 2003), given that its half-life in the bloodstream is less than one minute (Hamberg and Samuelsson, 1971). The main site of PGE_2 clearance in the blood are the lungs, which means that any PGE_2 that enters venous blood is prevented from returning to systemic circulation (Piper et al., 1970; Nakanishi et al., 2015). PGE_2 has a wide range of functions that vary depending the organs and tissue types, and initiating stimulus.

Although generally considered to be an inflammatory mediator, as described above, PGE_2 displays an array of functions which depend on the context of its release and the organ where this takes place. In its role as an inflammatory mediator, release of PGE_2 by damaged tissues leads to increased capillary endothelium permeability, the recruitment of immune cells to the site of injury, and sensitisation of sensory neurones that leads to hyperalgesia (Grösch et al., 2017). Yet, PGE_2 also has a role in resolving inflammation, as its action on the neutrophils and macrophages is generally inhibitory (Dakin et al., 2017; Martínez-Colón and Moore, 2018). However, some authors have argued that

PGE_2 also contributes to the resolution phase of acute inflammation, as evidenced by the effect of *Ptges1* knockout in mouse models (Langenbach et al., 1999; Frolov et al., 2013). In this context, PGE_2 also stimulates cell proliferation and angiogenesis, which promotes restoration of normal tissue function and wound healing (Liu *et al.*, 2015; Shao *et al.*, 2015). PGE_2 also contributes to the regulation of body temperature, and it is largely responsible for triggering pyrexia during infection (Grösch *et al.*, 2017). Impairment of PGE_2 synthesis and transport was shown to disrupt the increase in temperature in mice challenged with injected lipopolysaccharide (Nakamura et al., 2018; Poon et al., 2015).

Stimulation of cell proliferation can be seen in primary hypertrophic osteoarthropathy (PHO) patients who have germline mutations in *HPGD* and *SLCO2A1*, where this causes the characteristic dermal hyperplasia, due to the reduced ability to degrade PGE_2 or prevent it from entering the circulation (Seifert *et al.*, 2012; Uppal *et al.*, 2008). Interestingly, the dermal and bone features differ between patients with *HPGD* or *SLCO2A1* mutations, emphasising the importance of prostaglandin compartmentalisation in the microenvironment for downstream effects. Furthermore, there are sex differences in PHO patients. Both men and women have similar features when *HPGD* is mutated, but women who have *SLCO2A1* mutations are less likely to be identified as displaying PHO features, and are more susceptible to a form of chronic enteropathy with ulcer formation in the small intestine, which suggests that PGE_2 signalling may be differentially regulated in men and women to result in these phenotypes (Uchida *et al.*,2017; Umeno *et al.*, 2018). As PGE_2 is not the only substrate for these to proteins, the effects in PHO patients may be due to other prostaglandin molecules.

PGE_2 also affects haematopoiesis, where it reduces haematopoietic stem cell apoptosis by downregulating pro-apoptotic enzymes such as caspase-3, and stimulates cell cycle progression (Pelus and Hoggatt, 2011). From the range of PGE_2 actions however, it is clear how the effects on cell proliferation, angiogenesis, and suppression of granulocytes could promote tumour survival.

PGE_2 also regulates blood pressure, in part by inhibiting the reuptake of sodium ions and water in the kidneys' collecting duct, promoting salt and water excretion (Qi et al., 2002); (Chi et al., 2008). This results in a reduction of blood plasma volume, and therefore blood pressure. PTGS, HPGD and SLCO2A1 are known to be expressed in renal collecting ducts, which demonstrate the autocrine and paracrine nature of PGE_2 signalling (Nomura *et al.*, 2004). Similarly, inhibition of SLCO2A1 in hypertensive rats has been also demonstrated to reduce blood pressure (Chi *et al.*, 2015). This effect is largely mediated by the EP2 receptor (Kennedy et al., 1999).

In the colon, PGE_2 also controls motility, predominantly through the EP3 receptor (Iizuka et al., 2014). In addition, PGE_2 has been implicated in the regulation of water and electrolyte absorption. Although it has been demonstrated to promote secretion of fluids in rodent models, the same observations were not seen in human subjects (Rampton and Sladen, 1984; Rivière et al., 1991). Prostaglandins, including PGE_2 also induce cervical maturation and contractions of the uterine smooth muscle. PGE_2, and synthetic prostaglandin analogue such as carboprost, gemeprost or misoprostol, can thus be used for the induction of labour in a gynaecology setting (Bygdeman, 2003). Clearly, PGE_2 has a range of tissue and cell specific effects, and attempts to control its level to resolve one aspect of its function, could potentially impact on other physiological processes.

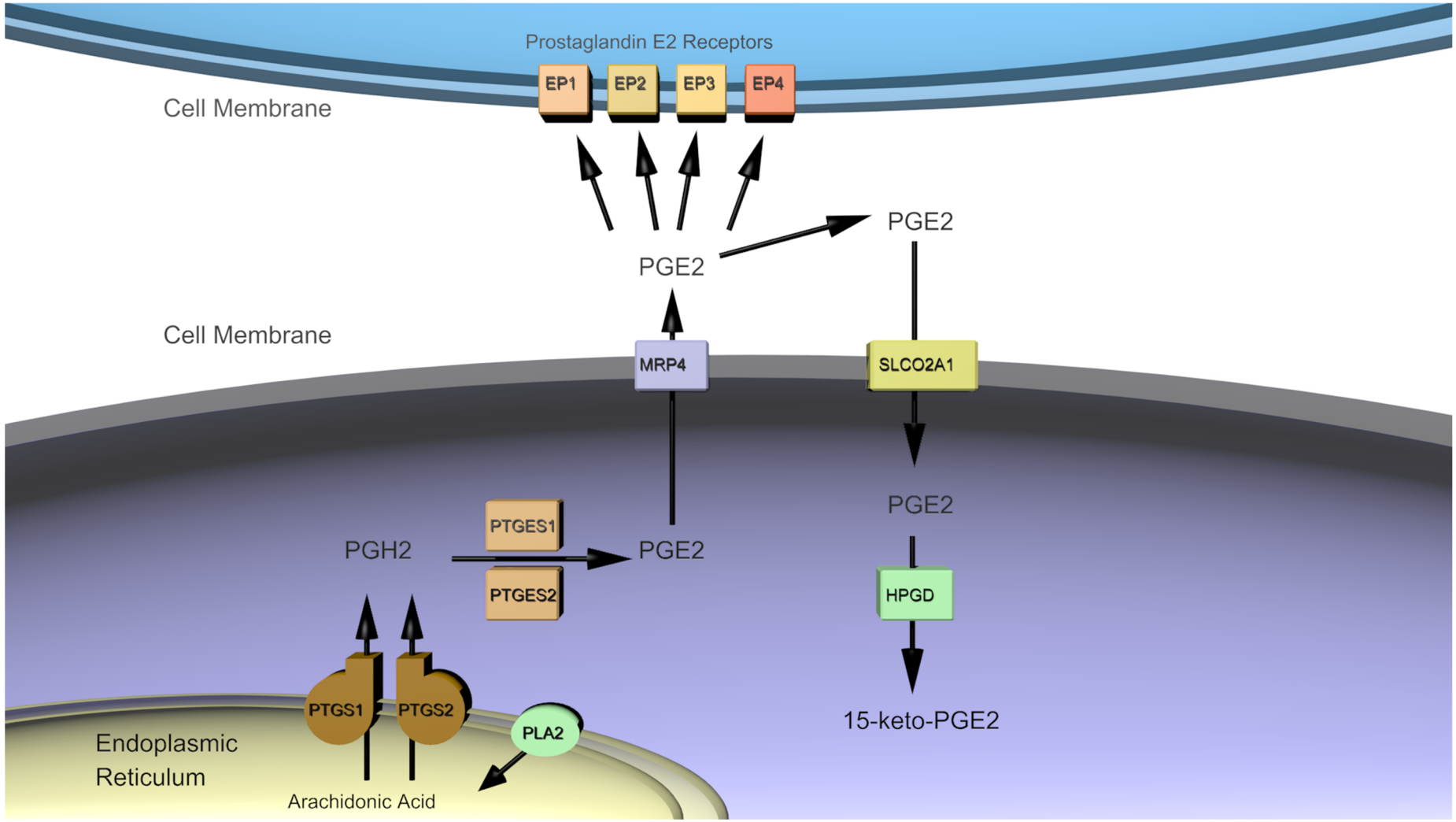

Figure 1.4: Outline of the Prostaglandin E2 metabolic pathway

1.2 Colorectal cancer

1.2.1 Overview of Colorectal cancer

Colorectal cancer incidence ranks third in men and second in women worldwide (Fitzmaurice et al., 2017). The highest incidence rates occur in Australia, Europe and North America, which accounts for considerable morbidity, particularly amongst the ageing population (Torre et al., 2015). In Europe, colorectal cancer is the second-most common malignancy in both men and women (Ferlay et al., 2018). Known risks included lifestyle factors such as smoking, amount of dietary fibre and processed meat consumed, but also environmental factors (e.g. radiation), and genetic predisposition. The incidence in the UK is not increasing and the overall survival rates are estimated to be approximately 60%. A high proportion of diagnoses are however made at a late stage, where survival rates are lower. Developing therapies for prevention and also detection and treatment of early stage disease is therefore of interest. The most common type of colorectal cancer is the colorectal adenocarcinoma, which develops from the colonic mucosal epithelium (Hugen et al., 2014; Bagante et al., 2018).

The sequences of events that progressively lead to colorectal tumorigenesis were established first by the observation of chromosomal deletions, and later, the aberrant activation of oncogenes (such as *KRAS*), and the loss of tumour suppressor genes (such as *APC* and *TP53*) (Powell et al., 1992). The process, briefly, involves the stages where normal epithelium begins to proliferate excessively, which leads to the formation of benign adenomas that can then progress to adenocarcinoma once there is invasion of the mucosa (Fearon and Vogelstein, 1990).

Rare forms of hereditary colorectal cancer syndromes have been crucial in establishing the key genes (such as *APC* in familial adenomatous polyposis (FAP) and pathways that become deregulated in sporadic cases of colorectal cancer (Knudson, 1985; Nishisho et al., 1991). Inactivating *APC* mutations are known to be one of the earliest events (Powell et al., 1992), and the mechanism by which this leads to uncontrolled epithelial cell proliferation has been characterised more recently (Barker et al., 2008; Bellis et al., 2012; Boman and Fields, 2013). The stem cells at the base of the crypts of Lieberkühn have been identified as the starting point for colorectal carcinogenesis, where *APC* mutations and consequent increase of β-catenin expression (which is normally targeted for degradation by APC) disrupt the normal asymmetric cell division that maintains the stem cell population and produces cells that differentiate into columnar epithelium as they migrate towards the colon lumen (Potten et al., 1992; Bellis et al., 2012).

While colorectal tumorigenesis has been traced to a specific cell type of origin (Barker et al., 2008), the sequence of key mutagenesis events leads to the aberrant activation or suppression of other genes' expression that enable a tumour to grow in a self-sustaining manner. These common characteristics, or "hallmarks", that are consistent across all cancers are increased proliferative signalling, insensitivity to growth suppressors, resistance to apoptosis, induction of angiogenesis, immortalisation and the ability to invade tissues and metastasize to distant sites (Hanahan and Weinberg, 2011). More recently, four more hallmarks have been added to the original six, and include genomic instability, inflammation (Van Den Brenk et al., 1974), immunosuppression in the tumour environment and dysregulation cellular respiratory pathways (Hanahan and Weinberg, 2011).

This classification has aided the development of therapies that target each of the hallmarks, although alone, such treatments prove inadequate due to the tumours' capacity to evolve and adapt to the environmental stress (Hanahan, 2014). Signalling pathways typically influence many downstream genes, and ultimately, mechanisms that promote tumour survival (Fearon, 2011). The importance of the tumour stroma and the cell types that are recruited by the cancerous cells, is also recognised, and more effective treatment regimens are envisioned to target multiple components to reduce the chance of the tumour being able to adapt (Hanahan, 2014). Therefore, understanding these pathways and manipulating them pharmacologically is a key strategy in the development of new anticancer drugs that can be used in addition to conventional chemotherapy and radiotherapy that target a tumours' rapidly-dividing cells.

1.2.2 Dysregulation of the Wnt/β-catenin in colorectal cancer

The Wnt/β-catenin signalling pathway is evolutionarily conserved, and has a diverse range of functions, including regulating cell proliferation, cell polarity, asymmetric cell division, cell migration, calcium deposition in bones, embryonic development or insulin sensitivity (Kahn, 2014; Mohammed et al., 2016; Bellis et al., 2012). There are nineteen Wnt ligand genes encoded in the human genome (MacDonald et al., 2009; Kahn, 2014). The prototypical Wnt1 was first characterised in the mouse (Nusse et al., 1984), and later in Drosophila melanogaster (Baker, 1988), where evolutionary sequence conservation led to researchers adopting of the current "Wnt" name for this gene family to replace the preceding names for homologs between species (van Ooyen et al., 1985; Nusse et al., 1991).

β-catenin is a protein that functions both as a cell adhesion adaptor in complex with E-cadherin at the cytoplasmic side of the cell membrane (Gumbiner and McCrea, 1993), and as a transcriptional activator (Korinek et al., 1997). When the pathway is not activated, (Figure 1.5) free β-catenin in the cytoplasm is unstable and is targeted for proteosomal degradation (Aberle et al., 1997). Activation of the signalling pathway by Wnt ligands prevents β-catenin phosphorylation (Figure 1.4 and Figure 1.5), leading to its accumulation and translocation to the nucleus where it binds to activating TCF factors or displaces repressive members, driving expression of target genes (Mohammed et al., 2016). The signalling cascade can activate other downstream effectors in addition to β-catenin, such as small GTPases, or by inducing intracellular calcium cation release (Kikuchi et al., 2012; Mehdawi et al., 2016; Mohammed et al., 2016)

However, dysregulation of the Wnt/β-catenin signalling pathway is a recurring event in range of malignancies, including breast, melanoma, hepatocellular and gastrointestinal cancers (Takayama et al., 1996; Ilyas et al., 1997; Korinek et al., 1997; Morin et al., 1997; Chiurillo, 2015). Amongst the earliest direct downstream targets of the signalling cascade to be discovered were the proto-oncogenes c-Myc (MYC) and Cyclin D (CCND), which stimulate cell cycle progression and cell proliferation (MacDonald et al., 2009; Fearon, 2011). Therefore, this unregulated proliferation would promote the accumulation of further mutations as the cells become resistant to cell cycle checkpoint signals and apoptosis.

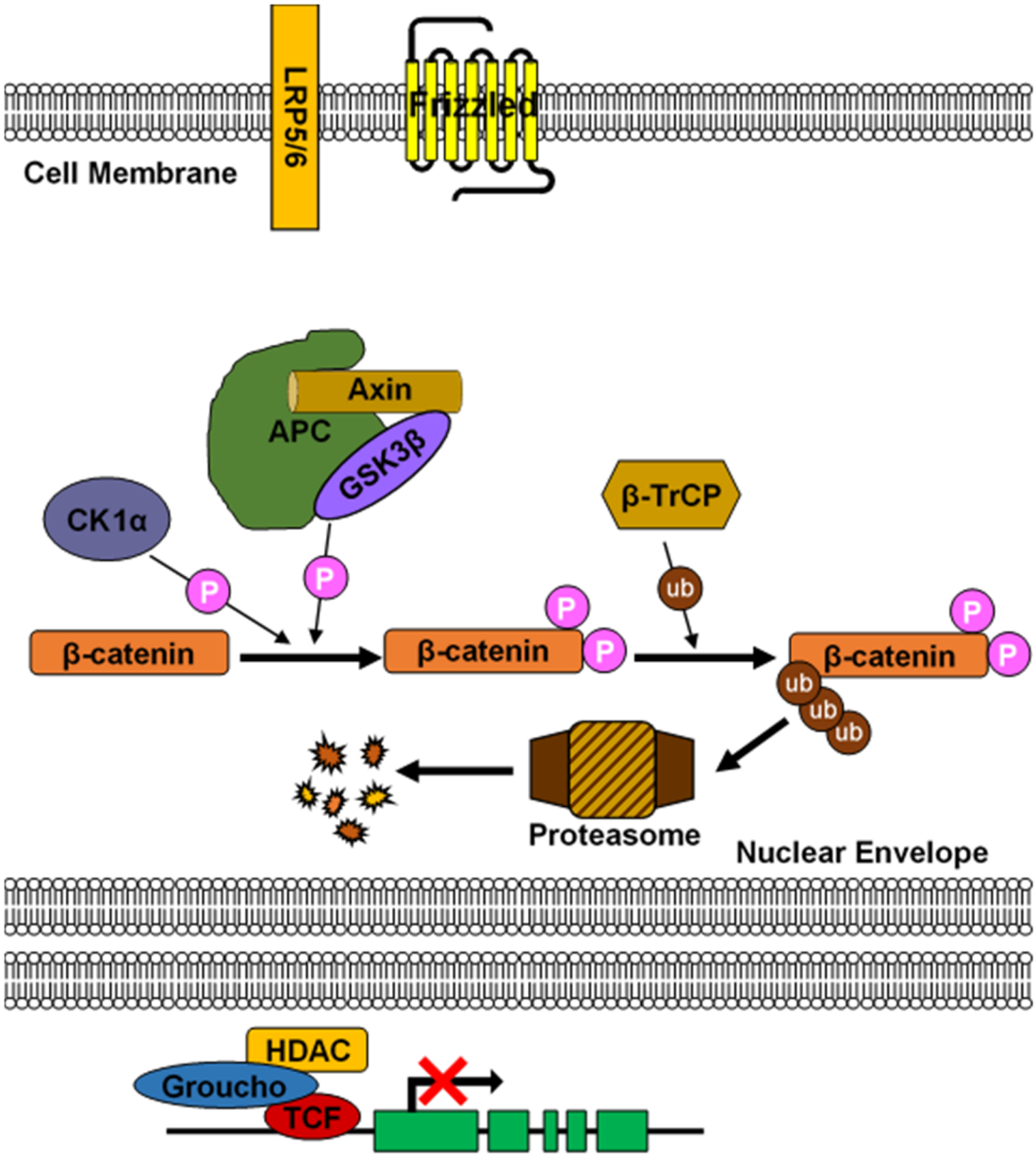

Figure 1.5: Outline of the Wnt/β-catenin signalling pathway (inactive state)

In the absence of Wingless-type (Wnt) ligand the Frizzled receptor and Low-density lipoprotein receptor family 5/6 (LRP5/6) co-receptor do not associate, and intracellular β-catenin targeted for degradation. Ademomatous polyposis coli (APC), Axin and GSK3β form a “destruction complex” that phosphorylates β-catenin. Casein Kinase 1α (CK1α) also participates in β-catenin phosphorylation. Phosphorylated β-catenin is subsequently recognised by the E3 ubiquitin ligase β-TrCP, and ubuquitination targets β-catenin for proteosomal degradation. This prevents β-catenin accumulation in the cytoplasm and subsequent translocation to the nucleus. Therefore, T-cell specific factor (TCF) proteins that bind to the promoters of target genes associate with transcriptional repressors such as Groucho and Histone deacetylates (HDAC) are not displaced, leading to the repression of the target genes.

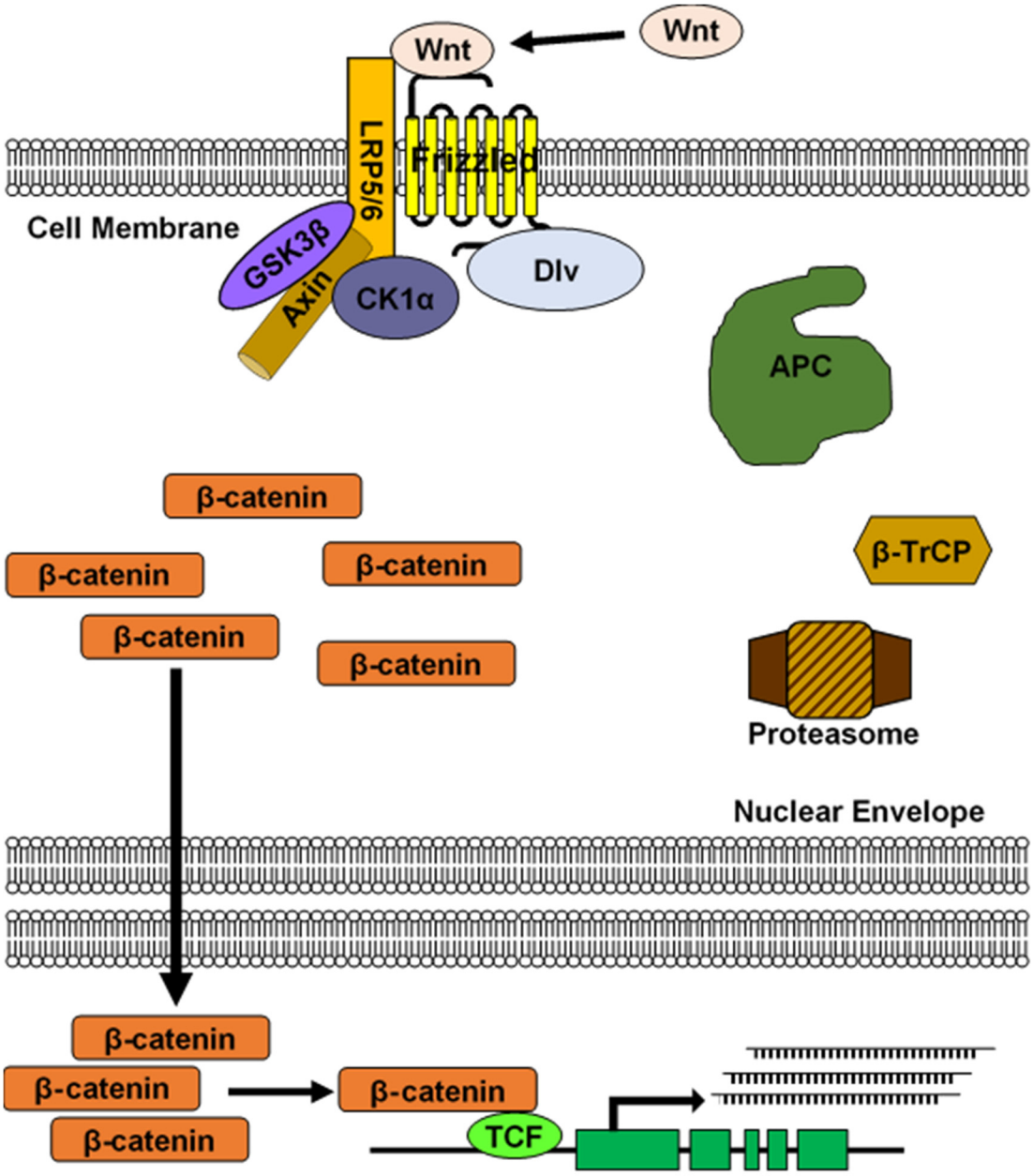

Figure 1.6: Outline of the Wnt/β-catenin signalling pathway (activated) Wnt binding to the Frizzled and LRP5/6 receptor complex. This recruits Dishevelled (Dlv) to the Frizzled intracellular domain. This induces translocation of Axin, GSK3β and CK1α to the LRP co-receptor cytoplasmic domain, which results in the dissociation of the APC/Axin/GSK3β complex. This prevents phosphorylation and ubiquitination of cytoplasmic β-catenin. β-catenin thus accumulates in the cytoplasm and is able to translocate to the nucleus where it displaces transcriptional repressors associated with repressor TCF factors (such as TCF3), and recruits TCF family members that drive transcription, (such as TCF4). In this way, β-catenin functions as a transcriptional activator in, driving expression of target genes.

In sporadic colorectal cancer, aberrant Wnt/β-catenin pathway activation is one of the earliest initiating events (Rubinfeld et al., 1993; Munemitsu et al., 1995; Takayama et al., 1996; Boman and Fields, 2013). Germline mutations in APC were first discovered in the hereditary Familial Adenomatous Polyposis syndrome, and later in sporadic colorectal cancer cases (Fearon and Vogelstein, 1990; Nishisho et al., 1991; Powell et al., 1992). APC mutations often disrupt APC protein's ability to bind β-catenin, and therefore enable phosphorylation by GSK3β (Rubinfeld et al., 1993; Fearon, 2011). Although mutations in other components of the pathway do occur (such as mutations or N-terminal deletion of β-catenin leading to the loss of its phosphorylation site), they are comparatively rare (Fearon, 2011).

APC also has a role in controlling cell polarity and mitosis. Its function is essential for regulating asymmetric cell division, as would be the case of a stem cell, where one daughter cell maintains its stem cell phenotype, while the other differentiates. This process is critical for renewing epithelia such as that of the intestinal and colonic on the luminal surface of the mucosa (Boman and Fields, 2013). Therefore, in addition to their effects on proliferation, APC mutations also disrupt the stem cells' polarity and capacity to divide asymmetrically, as discussed in section 1.2.1 above (Quyn et al., 2010; Bellis et al., 2012).

1.2.3 TGF-β signalling in colorectal cancer

Transforming Growth Factor β (TGF-β) is a member of a superfamily of related cytokines (bone morphogenetic peptides, activins, inhibins and growth and differentiation factors), which share as common characteristics a disulphide bond-linked dipeptide homodimer as the active agent, similar receptor subunit structure, and post-translational modification to generate the active dipeptide

(Hinck and O'Connor-McCourt, 2011; Poniatowski et al., 2015). TGF-β exists in three isoforms, TGF-β1, TGF-β2 and TGF-β3, of which TGF-β1 and TGF-β2 have greater affinity for the TGF-β receptor complex. The receptor (Figure 1.6) exists as a heterotetramer of two Type I receptors and two Type II receptors, with the type III receptors functioning as adaptors to assist binding between the active TGF-β and the receptor complex. This triggers a phosphorylation cascade, which in the case of TGF-β consists of the SMAD2 and SMAD4 transcription factors that bind to the promoters of target genes to activate transcription.

The TGF-β pathway is amongst one of the key signalling pathways that are dysregulated in colorectal cancer (Markowitz et al., 1995), where mutations lead to constitutive activation. The TGFβ type II receptor *(TGFBR2*) is mutated in approximately 25% of colorectal cancer cases, while mutations to the downstream SMAD2, SMAD3 or SMAD4 are less frequent (Fearon, 2011; de Miranda et al., 2015). The constitutive activity of the TGF-β pathway is a facilitating, rather than initiating, event in colorectal carcinogenesis. It is known to inhibit early tumour growth (Engle et al., 1999), a likely contributing factor being its suppression of Prostaglandin E_2 signalling (discussed in sections 1.2.4 and 1.2.5 below) (Yan et al., 2004). However, TGF-β signalling accelerates the growth of more advanced or metastatic tumours, and therefore the pathway components' genes are generally viewed as tumour suppressors (Zhao et al., 2018). *Smad4*$^{+/-}$ heterozygous mice do not develop intestinal polyps, but compound *Apc*$^{+/\Delta 716}$ *Smad4*$^{+/-}$ heterozygotes developed fewer, but larger number of polyps than the *Apc*$^{+/\Delta 716}$, mouse model, and several developed into carcinomas. This can also be seen in the cooperative role of SMAD proteins and mutant, but not wild-type, p53 in inducing target gene transcription to

promote metastasis (Dupont et al., 2004; Adorno et al., 2009). Therefore, this suggests that the TGF-β pathway becomes oncogenic in the presence of dysregulation in other suppressor pathways.

TGF-β drives colorectal carcinogenesis is by increasing tumour cell metastatic potential through triggering epithelial to mesenchymal transition, and sustaining an immunosuppressive tumour microenvironment (Kasai et al., 2005; Takahashi et al., 2010; Tirino et al., 2013; Tauriello et al., 2018). Its ability to induce epithelial to mesenchymal transition has been observed in a number of cancer cell lines, (Kasai et al., 2005; Tirino et al., 2013; Yeung et al., 2013; Wu et al., 2014). This causes the downregulation of cell adhesion proteins, such as E-cadherin, and promotes cell motility, which facilitates tissue invasion (Tauriello et al., 2018; Lampropoulos et al., 2012). This has led to TGF-β pathway activation being one of the key markers used to classify colorectal cancer according to gene expression patterns (Guinney et al., 2015; Dienstmann et al., 2017).

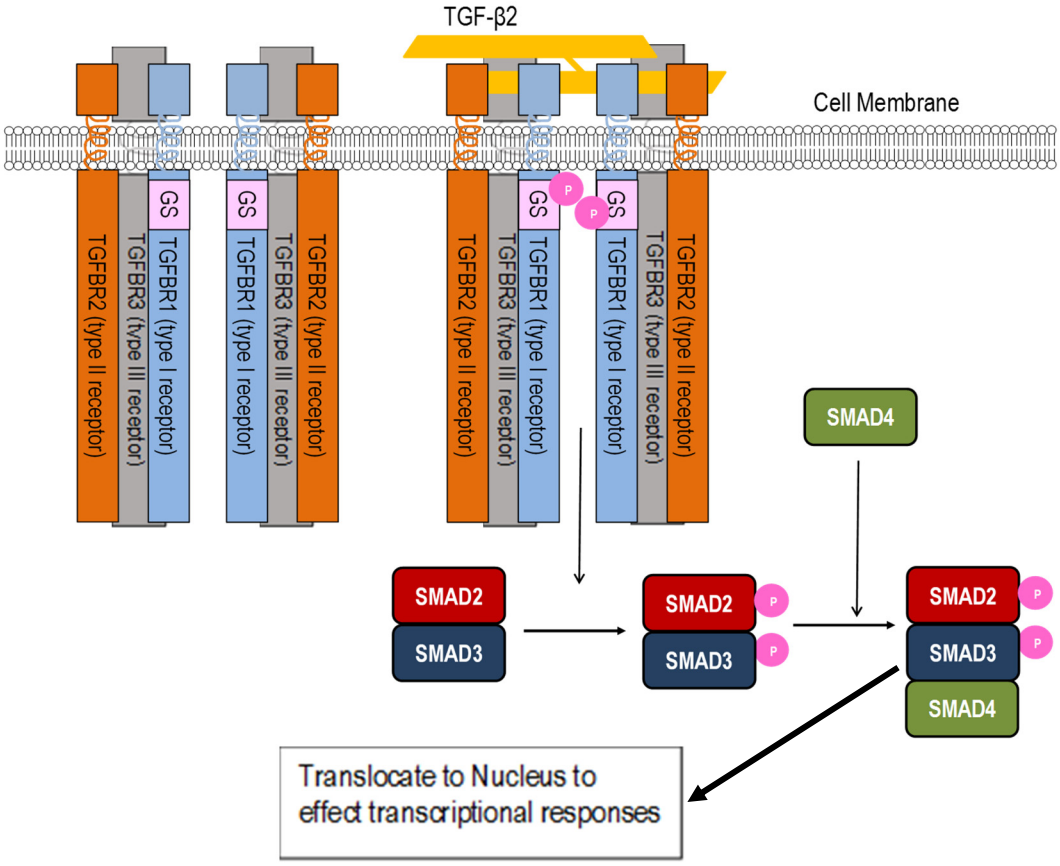

Figure 1.7: Overview of the TGF-β signalling pathway
The TGF-β receptor is a tetramer consisting of two TGFBR1 Type I receptors and two TGFBR2 Type II receptors. The TGFBR3 is a Type III receptor that facilitates the ligand's binding to the receptor. The TGF-β disulphide-linked dimer binds to the extracellular domains of the TGFBR1 and TGFBR2. TGFBR2 then phosphorylates the TGFBR1 in the glycine-serine repeat box (GS box) to expose the active site. The TGFBR1 in turn phosphorylates SMAD2 and SMAD3 (Hinck and O'Connor-McCourt, 2011). The co-activator SMAD4 forms a complex with the phosphorylated SMAD2 and SMAD3, which translocates to the nucleus to mediate transcriptional activation

1.2.4 PGE2's role in Colorectal Cancer

PGE_2's normal actions can be subverted by tumours to promote their survival and sustain their continued growth. Due to its influence on inflammation, it has the ability to drive many of the hallmarks of cancer (Hanahan and Weinberg, 2011; Van Den Brenk et al., 1974). This includes cell proliferation (Castellone et al., 2005), angiogenesis (Kochel and Fulton, 2015), inhibition of apoptosis (Tai, 2011), inflammation (Choi and Zelig, 1994); (Gustafsson et al., 2010; Zhao et al., 2017), metastasis (Guillem-Llobat et al., 2016; Wang et al., 2015), and immunosuppression in the tumour microenvironment (Hauptmann et al., 1993).

In a study in 1987, it was found that colorectal tumours had increased levels of AA and PGE_2, but not other prostaglandins, relative to normal colon, which in the context of more recent work, highlighted the importance of PGE_2 in particular for promoting tumour survival (Bennett et al., 1987). PTGS2 (COX-2) was later discovered to be consistently upregulated not only in colorectal cancer (Eberhart et al., 1994; Sano et al., 1995; Gustafson-Svard et al., 1996; Soumaoro et al., 2004) but in other malignancies including breast (Wolf et al., 2006), lung, (Maeng et al., 2014), prostate (Lodygin et al., 2005) and head and neck squamous cell carcinoma (St John et al., 2012), though the role of prostaglandins in colon cancer has been most widely studied. That $APC^{+/Min}$ mice with deleted COX-2 had reduced intestinal tumours highlighted the mechanistic importance of COX-2 (Oshima et al., 1996). Moreover PTGS2 expression is not only upregulated within the tumour cells, but also in the surrounding stromal cells (Hara et al., 2010). As a result, the high local PGE_2 concentrations would promote tumour survival. In addition, PGE_2 also drives a positive feedback loop, where, mainly through action on the EP2 and EP4

receptors (Fujino et al., 2003), induces the upregulation of PTGS2, as well as PGES (Seo et al., 2009; Sjögren et al., 2013) and MRP4 (Hara et al., 2010), thereby increasing both PGE_2 synthesis and the capacity to export it into the extracellular environment.

The utility of NSAIDs to inhibit PTGS2 (and drive the synthesis of anti-inflammatory resolvins, as described in section 1.1.3 above) as a prophylactic treatment have been already established, where low-dose aspirin was found to reduce the risk of developing colorectal cancer (Hial et al., 1976; Pollard and Luckert, 1981; Kune et al., 1988; Thun et al., 1991) and Ptgs2 inhibition in *Apc*$^{+/min}$ mice (Jacoby et al., 2000). These drugs, such aspirin or celecoxib, can be used as adjuvant therapy following adenoma resection to reduce the chance of recurrence (Hua et al., 2018). However, their effectiveness is limited by the adverse effects that can result by PGE_2, as well as other prostaglandins.

PGE_2 is required for gastric epithelium mucus secretion, and NSAIDs, particularly when used long-term, in high doses, can lead to the development of gastric ulcers (Grösch et al., 2017). Likewise, the global inhibition of prostaglandins and thromboxanes also has an anticoagulant effect by reducing platelets' ability to aggregate (Weiss et al., 1968; Zucker and Peterson, 1968). Given that PGE_2 is the prostaglandin responsible for tumour growth, these adverse effects could be addressed by targeting PGE_2 more specifically. However, COX-2-selective inhibitors have been associated with cardiovascular adverse effects, in spite of their reduced gastrointestinal side effects (Patrignani et al., 2003; Qi et al., 2002).

Furthermore, not all patients who undergo aspirin treatment experience a reduction in colorectal cancer risk (Fink et al., 2014). This is because, although NSAIDs act on one of the earliest steps in the PGE_2 synthesis pathway,

compensatory mechanisms may evolve, or already exist to counteract the action of the NSAIDs. Low expression of HPGD was found to correlate with the loss of aspirin's prophylactic effect, since this would result in longer PGE_2 persistence in the extracellular space (Fink et al., 2014). This reflects one of the major challenges in cancer treatment, where a tumour's heterogeneous nature and its capacity to evolve to compensate against the inhibition of one pathway component, often result the development of resistance, and a more aggressive relapse. Therefore, targeting multiple components of the PGE_2 metabolic pathway could offer a means to reduce the chance of compensatory mechanisms counteracting the action of NSAIDs (Hanahan, 2014).

1.2.5 Loss of HPGD and SLCO2A1 expression

Within the past decade, there has been a shift in literature to also study the degradation component of the PGE_2 pathway. Pioneering work by Dr. Sanford D. Markowitz (Yan et al., 2004; Myung et al., 2006) and other researchers established the loss of *HPGD* expression in colorectal, breast, and other cancers, demonstrating that both the synthesis and degradation arms of the pathway are dysregulated (Backlund et al., 2005; Castellone et al., 2005; Wolf et al., 2006).

The ability of HPGD to antagonise the action of PTGS2, was first demonstrated in mRNA and protein expression levels between normal colon epithelium, and adenocarcinoma or colorectal cancer cell lines and the effects on cell and xenograft tumour growth (Yan et al., 2004; Backlund et al., 2005). Germline knockout of the mouse *Hpgd* gene, on its own, was shown to be insufficient to induce tumorigenesis, but when combined with a pre-existing genetic predisposition ($Apc^{+/Min}$) or a carcinogen exposure (Azoxymethane), the

tumour burden in the mouse small intestine and colon was increased (Myung et al., 2006). As such it became clear that the control of PGE_2 degradation was as important as the regulation of its synthesis. Furthermore, the above study also demonstrated that *HPGD* loss can stimulate colorectal cancer growth through prolonging PGE_2 action, *HPGD* itself is not a tumour suppressor gene (in contrast to *RB1* (Knudson, 1971) or *APC* (Powell et al., 1992).

In colorectal adenocarcinoma samples, as well as other cancers, it was found that *HPGD* was downregulated, but not mutated, meaning that loss of *HPGD* expression was caused by perturbations in the gene's transcriptional regulation (Yan et al., 2004). Therefore, stimulation *of HPGD* expression has been considered to be a mechanism to reduce PGE_2 signalling within the tumour, a treatment that could be used in conjunction with, or as an alternative to, NSAIDs (Kaliberova et al., 2009; Na et al., 2011). Already, this has been attempted by one group, who trialled a drug on colorectal cancer cell lines that can induce HPGD expression (Seira et al., 2017).

However, although the loss of HPGD in cancer has been demonstrated, as has its value as a prognostic marker, its transcriptional regulation remains to be fully determined (Thompson et al., 2013; Kang et al., 2014; Yang et al., 2014; Hu et al., 2015).

Two studies characterised the proximal *HPGD* promoter, and were able to demonstrate with considerable evidence, that *HPGD* could be positively regulated by three transcription factor families (AP-1, Ets, and CREB), which bind directly to the promoter to exert their effect (Greenland et al., 2000; Nandy et al., 2003). AP-1 transcription factors, which consist of the Jun and Fos proteins, are expressed in colonic epithelial cells, and in adenocarcinomas (Zhang et al., 2005). Although they do not appear to influence tumour growth,

evidence suggests that their activity contributes to the tumour cells' ability to metastasize (Bae et al., 2014; Iskit et al., 2015). Similarly, the Ets family of transcription factors has been implicated in driving carcinogenesis and tumour survival through a number of mechanisms (Sizemore et al., 2017). In colorectal cancer, Ets1 and Ets2 (Leprince et al., 1983) are expressed in adenocarcinomas, but not normal colon epithelium or in adenomas with low to medium dysplasia (Nakayama et al., 2001; Ito et al., 2002), with Ets1 expression negatively correlated with patient survival in colorectal cancer patients (Peng et al., 2014). Although both AP-1 and Ets can upregulate *HPGD* expression, their established role in favouring the development of colon cancer indicates they would not be an ideal mechanism through which to increase *HPGD* levels. CREB is considered to be a ubiquitous transcription factor that regulates many aspects of cell proliferation and survival (Sakamoto and Frank, 2009). As CREB can be activated by upstream phosphorylation cascades that result from increased intracellular cAMP, this may suggest a potential negative feedback mechanism for PGE_2 to upregulate *HPGD* through the EP2 and EP4 receptors (Nishihara et al., 2004). However, its role in colon cancer aetiology is not well established, suggesting that manipulating its expression to increase *HPGD* transcription must be viewed with caution at present. The other study to follow up the work on the *HPGD* promoter found an inverse correlation of β-catenin and HPGD expression in both human and mouse intestine and colon, and proposed that β-catenin and TCF transcription factors act to suppress HPGD expression (Smartt et al., 2012b). Although their evidence and arguments to support this mechanism were not as robust, they established that loss of HPGD, as well as SLCO2A1, is an event that coincides with *APC* mutations and aberrant β-catenin activity, which is considered to be the initiating

event in colorectal cancer development (Smartt et al., 2012b; Barker et al., 2008; Quyn et al., 2010; Boman and Fields, 2013). Therefore, their results suggested that *HPGD* and *SLCO2A1* may be co-regulated by β-catenin (Smartt et al., 2012a; Smartt et al., 2012b).

In contrast to *HPGD*, even less is known about *SLCO2A1*, and how it is regulated. The literature has generally appeared to be more biased towards HPGD, despite SLCO2A1's important role to transport PGE_2 into the cell and make it accessible to HPGD (Schuster et al., 2015). It has been observed that SLCO2A1 expression is also lost in colorectal cancer, and like *HPGD,* loss of *SLCO2A1* can be associated with a poorer prognosis (Holla et al., 2008; Takeda et al., 2015). Moreover, while their analysis of SLCO2A1 was more superficial compared to that of HPGD, Smartt et al, (2012) demonstrated a potential for *SLCO2A1* and *HPGD* to be co-regulated by β-catenin (Smartt et al., 2012a; Smartt et al., 2012b).

SLCO2A1's function has generally been accepted as an importer of PGE_2 into the cell, based on evidence on a number of studies on cell line systems and immunohistochemistry (Bao *et al.*, 2002; Nomura *et al.*, 2005), rodent models (Chang *et al.*, 2010; Chi *et al.*, 2015; Liu *et al.*, 2015), and PHO patients (Li et al., 2017b). However, a series of more recent studies have proposed that it may also function to transport PGE_2 bidirectionally in certain cases, and possibly contribute to PGE_2 secretion (Kasai *et al.*, 2016; Shimada *et al.*, 2015; Shirasaka *et al.*, 2013). This was based on the theory that SLCO2A1 localised on cytoplasmic exosomes membranes may concentrate PGE_2 prior to exocytosis (Kasai *et al.*, 2016).

The potential for *HPGD* and *SLCO2A1* co-regulation is a possibility, considering how PGE_2 is able to drive expression of its major synthesis

enzymes and exporter protein (Hara et al., 2010). An inverse relationship has been observed between *PTGES2* and *HPGD* in one study on lung cancer cells, where upregulation of one gene led to the downregulation of the other (Tong et al., 2006a). Whether this relationship is important in colon cancer cells has yet to be determined. However with the observation that generally COX-2 is upregulated whilst HPGD expression is reduced or lost, indicates that both the synthesis and degradation components of the pathway are important in increasing PGE_2 release and prolonging its action by a much reduced degradation rate.

However*, SLCO2A1* has not received comparable attention in the literature, in the context of colorectal cancer, with little information on transcriptional regulation beyond the in silico prediction of its transcriptional start site and predicted transcription factor binding sites (Lu and Schuster, 1998). A clearer understanding of transcriptional regulation of *HPGD* and *SLCO2A1* could lead to understanding the mechanisms by which their function is lost during carcinogenesis (Smartt et al., 2012a; Smartt et al., 2012b). This in turn could be used to develop strategies to reactivate and increase their expression to supplement or replace NSAIDs to which some patients do not respond (and which also have the adverse effects of reducing stomach mucus secretion, and COX-2 selective inhibitors' association with cardiovascular problems).

1.3 Aims

Characterise the regulation of the *HPGD* and *SLCO2A1* promoters using colorectal cancer cell lines as a model system

Determine whether HPGD and SLCO2A1 have associated downregulated expression patterns in sporadic colorectal adenocarcinomas relative to normal colon mucosa.

Chapter 2 Methods

2.1 Protein procedures

2.1.1 Paraformaldehyde fixation and paraffin embedding of mouse organs

The use of mouse tissues was covered under the project licence PPL 70/7965. Lungs, kidneys, small intestine and colon from euthanized *Apc*$^{+/Min}$ and wild-type (WT) male mice were isolated and fixed overnight in 4% w/v paraformaldehyde solution at room temperature. The organs were subsequently washed in 1 × PBS and stored at room temperature in 70% w/w ethanol. The tissue samples were paraffin-infiltrated using a Leica ASP200 automated vacuum processor, and subsequently embedded into sectioning blocks. Formaldehyde-fixed paraffin-embedded (FFPE) blocks were stored at room temperature.

2.1.2 Preparing sections and slides from formaldehyde-fixed paraffin-embedded section mouse tissue

Paraffin blocks were sectioned on a Leica RM2255 microtome, at 5-µm thickness, and dried at 37°C overnight on Superfrost Plus slides (Thermofisher Scientific, Massachusetts, USA). A second plain paraffin section was applied over the tissue to protect it from oxidation. Slides were then stored at 4°C and used for immunohistochemistry within two weeks of sectioning.

2.1.3 Immunohistochemistry on formaldehyde-fixed paraffin-embedded tissue sections

Immunohistochemistry was carried out on 5-µm FFPE tissue sections to assess the efficacy of available commercial anti-HPGD and anti-SLCO2A1 antibodies (Table 9) in staining human and mouse tissue. Ethical approval for the use of normal human kidney, colon and lung tissue sections for immunohistochemistry was covered by the GIFT ethics, reference number 05/H00903/62.

Sections were dewaxed and rehydrated by incubating for 5 minutes in 3 serial xylene baths followed by 1 minute in 3 absolute (100% w/w) ethanol baths and then tap water for 5 minutes. Heat-induced epitope retrieval was carried out by microwaving the sections at full power for 10 minutes in pre-warmed sodium citrate buffer (pH 6.0), followed by cooling at room temperature for 20 minutes. Endogenous peroxidase blocking was carried out in 0.3% w/w hydrogen peroxide in methanol for 10 minutes at room temperature. Sections were blocked in 1 × Casein in Antibody Diluent solution (Vector Laboratories, UK) incubated at room temperature for 30 minutes before the addition of antibodies. The sections were incubated overnight at 4°C. Antibody specificity was evaluated using non-specific host antibodies (rabbit IgG), and a negative control with no primary antibody.

The sections were washed in 1 × TBS + 0.01% w/w Tween-20 twice and once in 1 × TBS for 5 minutes. Horseradish peroxidase-conjugated anti-rabbit secondary antibody (EnVision, Dako. Agilent Technologies, California USA) was applied, and the slides incubated for 30 minutes at room temperature. Sections were washed in 1 × TBS + 0.01% w/w Tween-20 twice and once in 1 × TBS for 5 minutes. 100 µl of 3,3′-diaminobenzidine (Invitrogen, Massachusetts,

USA) was applied to each section for 10 minutes. After washing for 2 minutes under running water, the slides were counterstained with Mayer's haematoxylin for 30 s, followed by 1 minute under running tap water, 1 minute in Scott's tap water, and 1 minute under running tap water.

Sections were dehydrated through the same 3 absolute ethanol and 3 xylene baths in the reverse order and mounted using dibutyl phthalate in xylene (DePeX). They were visualised under a light microscope to assess antibody staining, and sections of interest were then imaged under a Nikon Eclipse 1000 microscope fitted with a digital camera. Images were taken under the × 4, × 10 and × 40 objective lenses.

2.1.4 Protein extraction from cultured cells

A modified preparation of radioimmonoprecipitation assay (RIPA) buffer was used for cell lysis (50 mM Tris-HCl (pH8.0), 150 mM NaCl, 1% w/w Triton X-100, 2% w/w SDS and 0.5% w/w sodium deoxycholate). Working aliquots of buffer were supplemented with 1 × PhosSTOP phosphatase inhibitor cocktail (product code 04906845001, Roche, UK) 1 mM dithiothreitol, in the final volume. The cells were washed in ice-cold 1 × PBS, lysed with the buffer and then placed on ice for 10 minutes. Cell lysates were scraped, transferred to centrifuge tubes and incubated on ice for a further 10 minutes. They were then centrifuged for 20 minutes at 4°C at 12,000 × *g*, and supernatants stored at −80°C.

2.1.5 Protein concentration measurement using bicinchoninic acid

Protein concentration was determined against a BSA standard curve, using the bicinchoninic acid protein assay (product code 71285-3, Novagen, Wisconsin, USA). BSA standards and sample lysates were aliquoted in duplicate on a clear 96-well plate. Working solution was added, the reaction mixed for 30 s on a shaker, and then incubated for 30 minutes at 37°C. After cooling to room temperature for 10 minutes, the absorbance was measured on a Mithras LB 940 multimode microplate reader (Berthold Technologies, Bad Wildbad, Germany) with a 2 second exposure through a 570 nm filter. The results were transferred to a spreadsheet to plot a standard curve using the BSA standards.

2.1.6 Polyacrylamide gel electrophoresis of cell lysate proteins

1 µl NuPAGE Sample Reducing Agent (NP0004) and 4 µl of NuPAGE lithium dodecyl sulphate loading buffer (NP0007) were added to 16 µl of cell lysates containing 21–30 µg total protein. The mixture was boiled at 100°C for 5 minutes and immediately transferred to ice to prevent protein refolding. Polyacrylamide gel electrophoresis was carried out using precast 4–12% w/v gradient 10-well gels (NuPAGE), in 1 × MOPS SDS running buffer (product number NP0001, Invitrogen, Massachusetts, USA) at 180 V for 60 minutes.

2.1.7 Transfer of proteins to PVDF membrane

1 × NuPAGE transfer buffer, (product number NP0006-1, Invitrogen, Massachusetts, USA) containing 10% w/w methanol was used to carry out the

transfer of proteins to a polyvinylidene fluoride (PVDF) membrane (Amersham Hybond P, General Electric Healthcare Bio-Sciences, Massachusetts, USA). The membrane was pre-treated with 100% w/w methanol for 30 s, followed by two 5-minute washes in dH_2O, and 20 minutes in 1 × transfer buffer + 10% w/w methanol. Proteins were transferred onto the membrane at 12 V for 16 hours.

2.1.8 Probing blotted proteins with SLCO2A1 and ACTB antibodies

The membrane was blocked in 1 × PBS + 0.1% w/w Tween-20 + 5% w/v dried non-fat milk for 1 hour at room temperature. Primary antibodies were diluted in 1 × PBS + 0.1% w/w Tween-20 + 1% w/v dried non-fat milk. The primary antibody was applied to the membrane at 4°C for 16 hours.

After this, the membrane was washed 3 times in 1 × PBS + 0.1% w/w Tween-20 for 5 minutes. The pig anti-rabbit HRP-conjugated secondary antibody (product number P0217, Dako, UK) was diluted in 1 × PBS + 0.1% Tween-20 + 1% w/v dried non-fat milk at (1:130,000 initially) 1:3000. The membrane was incubated with the primary antibody for 1 hour at room temperature.

The membrane was then washed 3 times in 1 × PBS + 0.1% w/wTween-20 for 5 minutes, and visualised using a Luminol-based chemiluminescence kit (Super Signal West Femto Maximum Sensitivity Substrate kit, product number 34094, Thermofisher Scientific, Massachusetts, USA). The membrane was incubated in the dark for 5 minutes prior to imaging. Excess working solution was washed off and images taken at 10-s intervals for 2 to 10 minutes in a Bio-Rad Molecular Imager® Gel Doc™ XR+ System (Bio-Rad, California, USA) using Image Lab 5.2.1 build 11 (Bio-Rad Laboratories, California, USA). The

same membranes were re-probed for β-actin (Abgent A0125a. Abgent Inc, California, USA) diluted 1:1000 and visualised as described above.

2.2 RNA Procedures

2.2.1 RNA extraction using the acid guanidinium thiocyanate–phenol–chloroform method

RNA was isolated from cell lysates using TRIzol, a commercial reagent derived from the method of Chomczynski and Sacchi (1987). Cells were washed with room temperature 1 × PBS and lysed using the volume of TRIzol (Thermofisher, USA) recommended for flasks or culture plates. The lysates were scraped and transferred to microcentrifuge tubes. After incubation for 5 minutes at room temperature, chloroform was added and the mixture shaken by hand for 15 seconds. Following a 3-minute incubation at room temperature, the mixture was centrifuged at 12,000 × *g* for 15 minutes at 4°C. The aqueous phase was transferred to a new tube and centrifuged as above. In a new tube, RNA was precipitated using 100% w/w isopropanol, and pelleted by centrifugation at 12,000 × *g* for 10 minutes at 4°C. The RNA pellet was washed with 75% w/w ethanol and spun at 7,500 × *g* for 10 minutes at 4°C two or three times. RNA was resuspended in RNase-free water and stored at -80°C.

2.2.2 Reverse transcription reactions

Between 2 µg and 5 µg of RNA was used for standard reverse transcription reactions. The reaction mixture was set up to contain 1 × cDNA first strand buffer (50 mM Tris-HCl (pH 8.3), 75 mM KCl, 3 mM $MgCl_2$, 5 mM

dithiothreitol), 2U/µl RNaseOUT™ RNAse inhibitor, 0.5 mM dNTPs, 2.5 ng/µl random hexamers, and 10U/µl of Superscript II or Superscript III reverse transcriptase (RT) (Thermofisher Scientific, Massachusetts, USA), in RNase-free water. First, the RNA, random hexamer primers and dNTPs were mixed and incubated at 65°C for 5 minutes and cooled on ice for 2 minutes. The RNase inhibitor, dithiothreitol, reaction buffer and RNase-free water were then added, and the mixture pre-heated to 25°C for 2 minutes before adding the Superscript II RT. This pre-heating step was not required for the Superscript III RT.

The reaction was then incubated at 25°C for 10 minutes, followed by 42°C (Superscript II RT) or 55°C (Superscript III RT) for 60 minutes, and 70°C for 15 minutes. 2 U/µl of RNAse H was added to remove RNA template and the reaction incubated at 37°C for 20 minutes.

2.2.3 Preparation of cDNA for the RNA ligase-mediated rapid amplification of 5′-cDNA ends (RLM-RACE)

Total RNA was firstly dephosphorylated to prevent the downstream reaction of non-mRNA species, followed by removal of the 5′ mRNA cap and the ligation of the GeneRacer oligomer to the exposed 5′ mRNA ends prior to generation of cDNA. 4.55 µg (Caco-2) and 4.05 µg (LoVo) total RNA was used at the start of the procedure.

The dephosphorylation reaction contained 1 × calf intestinal phosphatase (CIP) buffer (50 mM Tris-HCl (pH8.5), 0.1 mM EDTA), 1U/µl CIP, 4U/µl RNaseOUT™ RNAse inhibitor) and was incubated at 50°C for 1 hour.

Following phenol:chloroform extraction, the RNA was precipitated with the addition of 20 mg mussel glycogen, 10 µl 3M sodium acetate and 95% w/w ethanol. The RNA pellet was washed with 70% w/w ethanol and resuspended in 8 µl DEPC-treated water for the next reaction. 1 µl of the RNA was run on a denaturing formaldehyde agarose gel to check for RNA degradation.

The decapping reaction contained 1 × tobacco acid pyrophosphatase (TAP) buffer (50 mM sodium acetate (pH6.0), 0.1 mM EDTA, 0.1% w/w β-mercaptoethanol, 0.01% w/w Triton X-100), 0.05 U/µl tobacco acid pyrophosphatase, and 4 U/µl RNaseOUT™ RNAse inhibitor**.** The reaction was incubated at 37°C for 1 hour, and RNA precipitated as described above.

The 7 µl of resuspended RNA was added to the 250 ng of lyophilised GeneRacer RNA oligomer. The ligation reaction was set up in 1 × ligase buffer (33 mM Tris-acetate, 66 nM potassium acetate, 10 mM magnesium acetate, 0.5 mM dithiothreitol), 1 mM ATP, 4 U/µl RNaseOUT™ RNAse inhibitor and 0.5 U/µl T4 DNA ligase. The reaction was incubated at 37°C for 1 hour, RNA precipitated as described above, and resuspended in 11 µl of DEPC-treated water.

Due to the GC-rich nature of the *HPGD* and *SLCO2A1* 5′-UTRs, Thermoscript RT was used for the reverse transcription reaction in place of the Superscript RT III to ensure effective cDNA generation. The final reaction mixture contained 1 × cDNA synthesis buffer (50 mM Tris acetate (pH 8.4), 75 mM potassium acetate, 8 mM magnesium acetate), 5 mM dithiothreitol, 2.5 ng/µl random hexamer primers, 0.5 mM dNTP, 2 U/µl RNaseOUT™ RNAse inhibitor and 0.75 U/µl Thermoscript RT. Random hexamer primers, dNTPs and DEPC-treated water were added to 10 µl of the RNA from the oligomer ligation reaction. These were incubated at 65°C for 5 minutes, followed immediately by

incubation on ice for a further 2 minutes. To this mixture, the cDNA synthesis buffer, dithiothreitol, RNAse inhibitor and ThermoScript RT were added, at the final concentrations described above. The reaction was incubated at 25°C for 10 minutes, followed by 60°C for 60 minutes and 85°C for 5 minutes. 2 U/µl of RNAse H, in the final reaction volume, was added to remove RNA template and the reaction incubated at 37°C for 20 minutes.

2.3 DNA procedures

2.3.1 PCR primer design

All primers (Table 1) were designed using the Primer-BLAST program (Ye, et al, 2012), to check for possible off-target products.

2.3.2 Polymerase chain reaction (PCR)

Standard PCRs were set up in 1 × GoTaq Flexi buffer (M8901, Promega), or 1 × GoTaq Flexi buffer (green) (M8911, Promega, Wisconsin, USA) with 1.5 mM $MgCl_2$, 200 µM dNTPs, 0.2 µM each forward and reverse primer, in-house *Taq* polymerase and 10–40 pg/µl of template DNA in the final reaction volume (Table 2). All PCR reactions were carried out on a MJ Research DNA Engine Dyad Peltier Thermocycler (Bio-Rad, California, USA).

For applications where proof-reading capability was needed, the Platinum *Pfx* DNA polymerase and protocol were used (ThermoFisher Scientific, Massachusetts, USA) (Table 2). The final reaction mixture contained 1 × *Pfx* amplification buffer, 1 mM $MgSO_4$, 300 µM dNTPs, 0.3 µM each forward and reverse primer, 1U/µl Platinum *Pfx* DNA Polymerase and 10–40 pg/µl of

template DNA. A variation of this setup was followed for the RLM-RACE reactions.

2.3.3 RNA ligase-mediated rapid amplification of cDNA 5′-ends (RLM-RACE) and nested PCR

For the first PCR step, the generic GeneRacer Oligomer forward primer and a gene-specific reverse primer were used in a ratio of 3:1, given the ligation of the oligomer to all mRNA sequences, and the reliance on the reverse primer for target gene specificity. The PCR reactions to amplify specific cDNA products for *HPGD*, *SLCO2A1* and *ACTB* were set up according to the GeneRacer manual, including the recommended single-primer controls and no-DNA template (negative) controls. “Touchdown” PCR was carried out for the first PCR step (Table 5 and Table 6), and the subsequent nested PCR was a conventional reaction using the Platinum *Pfx* DNA polymerase, as described above (section 2.3.2).

2.3.4 DNA purification

Shrimp alkaline phosphatase (SAP) and exonuclease I were used to remove residual primers from PCR reactions prior to the RLM-RACE or sequencing. 5 µl of PCR reaction was treated with 2 µl SAP and exonuclease I (ExoSAP-IT), and incubated at 37°C for 15 min, followed by 80°C for 15 min, to remove dNTPs and primers.

Where PCR products needed to be purified, a column-based kit system was used, derived from the methods of Hamaguchi and Geiduschek (1962) and Vogelstein and Gillespie (1979) (GeneElute, Sigma, Missouri, USA). If gel

extraction was carried out for PCR products or restriction fragments, the DNA was run on an agarose gel, 0.5% w/v to 2% w/v, depending on the DNA fragment sizes, alongside a 100-bp+ or 1-kb ladder. Ethidium bromide solution was added to a final concentration of 0.33 µg/ml in the agarose gel. Where crystal violet was used instead, the concentration in gel and 1 × TAE buffer was 10 µg/ml. A clean scalpel was used to excise the bands of interest, and the Qiagen (Germany) or Sigma gel extraction kits were used to purify the DNA; sodium iodide solution was used to dissolve the agarose gel, and the DNA isolated using silica columns. The purified PCR products were eluted in autoclaved distilled water to facilitate use in downstream reactions.

2.3.5 Estimation of nucleic acid concentrations

Spectrophotometry (Nanodrop-1000, Thermofisher Scientific, Massachusetts, USA) was used for routine DNA and RNA concentrations. The PicoGreen and Qbit colorimetric assay systems were used as per the manufacturers' instructions to estimate plasmid DNA concentration. These concentrations was used to adjust the volumes of luciferase expression vector and pUC19 to 50 ng/µl total DNA, with equivalent molar amounts of the expression vectors (section 2.3.15).

2.3.6 Agarose Gel Electrophoresis

Agarose gels (0.5–2% w/v) were prepared in 1 × TAE buffer; 0.33 µg/ml of ethidium bromide was added before pouring. Gels were generally run for 1 hour, at 60 V (for 30 ml), 90 V (100 ml) or 120 V (200 ml and 300 ml, depending on gel mould size). 10 µg/ml of crystal violet was added to both the 1 × TAE

buffer and the agarose gel instead of ethidium bromide, if excision of specific bands from the gel was necessary.

For denaturing gel electrophoresis, 1.3% w/v agarose, 6.67% w/v formaldehyde gels were prepared in 1 × MOPS buffer (20 mM MOPS, 1 mM EDTA, 13.4 mM sodium acetate, pH 7.0). RNA was added to loading buffer (60% w/w formamide, 19% w/w formaldehyde, 8% w/w glycerol, 1 × MOPS buffer, 4 µg/ml ethidium bromide and bromophenol blue) to prevent degradation and to increase sample volume for loading onto the gel (Chomczynski, 1992). All glassware and gel tanks were pre-treated with 3% w/w H_2O_2 in DEPC-treated water for 10 minutes and washed with DEPC-treated water prior to buffer and gel preparation. For RNA formaldehyde gel running buffer, see Chomczynski, 1992.

2.3.7 Dye termination (Sanger) sequencing

Dye termination (Sanger) sequencing was carried out using the BigDye Terminator v3.1 Cycle Sequencing Kit (Applied Biosystems, California, USA). Reactions were setup as in Table 3, terminated with 125 mM EDTA and the reaction products precipitated with 100% w/w ethanol. Following a 70% w/w ethanol wash step, the reaction products were resuspended in 10 µl Hi-Di™ formamide (Applied Biosystems, California, USA) and capillary electrophoresis carried out on an ABI 3130 Genetic Analyser (Applied Biosystems, California, USA). Analysis and base-calling of sequencing electropherograms were carried out using ABI Sequencing Analysis v5.2.

2.3.8 Semi-quantitative gene expression by PCR band intensity

Relative expression of *SLCO2A1* and *GAPDH* was measured by PCR. Owing to the low baseline expression of *SLCO2A1* in A549 cells, 5 µg of total RNA was used in the reverse transcription reactions to generate cDNA for the PCR reactions. ImageLab 5.2.1 (Bio-Rad Laboratories, California, USA) was used to quantify PCR band intensity from the gel images. Band intensities were measured as the volume intensity. This is a value derived from the number of pixels and their brightness within each PCR band. The volume intensity ratio between *SLCO2A1* and *GAPDH* was used to normalise *SLCO2A1* band intensity to that of *GAPDH*.

2.3.9 Generation of the *SLCO2A1* and *HPGD* promoter deletion series

The human *HPGD* and *SLCO2A1* promoter sequences were obtained from bacterial artificial chromosomes (BACs), RPCI-11 511O14 and RPCI-11 252L8 for *HPGD*, and, RPCI-11 974M1 and RPCI-11 1063N7 for *SLCO2A1.* The pGL4.10[luc2] (catalogue number E6651, Promega. WI, USA) promoterless firefly luciferase vector was used as the backbone to construct all *HPGD* and *SLCO2A1* promoter constructs. For both genes, the promoter was inserted in such a way that the −1 positions relative to the genes' translational start sites preceded the +1 of the luciferase ATG start codon. For *HPGD*, AvrII and NruI/Bsp68I sites were introduced into the vector's multiple cloning region, prior to the two-stage process of inserting the *HPGD* promoter fragment. Double restriction digests with single-cutting enzymes, and where not possible, proof-

reading PCR, were used to generate the promoter deletion series for each gene.

Colonies were screened by *PCR* and the correct ligation confirmed by sequencing. The constructs were named with a letter designating the gene (H or S), followed by a number denoting the 5′ position of the promoter fragment: Thus, the full length *HPGD* construct, which contained the −3082 to −1 region of the *HPGD* promoter was “H-3082”, and the full-length *SLCO2A1* construct “S-3198”.

2.3.10 Site-directed mutagenesis of EGR, SP and CDX transcription factor binding sites on the −364 to −1 *SLCO2A1* promoter

The two EGR, one SP and one CDX2 putative transcription factor binding sites chosen for investigation in the −364 to −1 region of the *SLCO2A1* promoter were mutated using the Quikchange II site-directed mutagenesis kit, using as template the S-364 deletion construct containing this proximal segment of the promoter. Based on the consensus sequences in the footprint-db and JASPAR databases, two of the most conserved bases were chosen for mutation. Two complementary primers with two adjacent point mutations in the same position were used for each transcription factor to amplify the entire plasmid. After DpnI treatment to digest the methylated template, the reaction was transformed into chemically competent *E. coli.* Colonies for each transcription factor binding site were screened by PCR (Table 1 and Table 2) and sequenced to verify the presence of the mutations.

To avoid unwanted mutations on the plasmid backbone due to DNA polymerase errors, the 364-bp *SLCO2A1* promoter fragment was digested, and ligated into the pGL4.10[luc2] backbone from the same starting plasmid. The resulting colonies were screened by PCR and sequencing to confirm the presence of the promoter and point mutations, and plasmid DNA was prepared for subsequent transfections.

2.3.11 Linker scanning mutagenesis of the proximal 364 bp of the *SLCO2A1* promoter

Linker scanning mutagenesis (Dykxhoorn, et al., 1997) uses the random insertion of small insert within a region of DNA in order to disrupt the function of regulatory elements or introduce mutations in a target protein. The procedure, based on (Haapa, et al, 1999) and since developed into a commercial kit, utilises an engineered transposable element comprising a kanamycin resistance gene (*npt*), and NotI restriction sites near the 5′ and 3′ ends. MuA transposase is used to mediate integration into the target plasmid. The integration event causes a 5-bp duplication of the target sequence adjacent to the insertion site. Digestion with NotI excises the transposon and kanamycin resistance gene, resulting in a 15-bp insertion (transposon ends encompassing NotI site, and the duplicated region). This results in a pool of insert-containing plasmids.

The *SLCO2A1* deletion construct containing the −364 to −1 segment of the *SLCO2A1* promoter (S-364) already possessed an existing NotI restriction site. This was removed by restriction digestion followed by blunting and religation. Linker scanning mutagenesis was carried out on the resulting S-364-NotI(x) plasmid, using the Mutation Generation System kit (Thermofisher Scientific).

Transposition reactions were set up using 182 ng of S-364-NotI(x), in 1 × MuA transposase buffer, 10 ng of kanamycin resistance transposon (M1-Kan^R) and 220 ng MuA transposase, in a 20-µl final volume. The reaction was incubated at 30°C for 1 hour, followed by 75°C for 10 minutes. 5 µl of the reaction was used to transform competent *E. coli*. Plasmid DNA was isolated from the resulting pooled colonies.

In order to exclude unwanted insertions in the plasmid backbone, the pooled plasmids were digested with Acc65I and MreI to isolate and gel-purify the *SLCO2A1* promoter sequence containing the transposon. This was then ligated to intact backbone from the original S-364-NotI(x) template. Digestion with NotI was used to remove the transposon to retain the 15-bp insertion after plasmid recircularization. Colonies were screened by PCR and sequencing to identify the positions of the inserts.

2.3.12 Restriction endonuclease digestion of DNA

All restriction enzymes used were purchased from New England Biolabs or Thermofisher Scientific (Table 7). Reaction volumes for single- and double-digest reactions were set up as recommended, between 20 µl and 100 µl depending on the required yield of digestion products. All reactions (except for SfiI and BssHII, which required a reaction temperature of 50°C) were carried out at 37°C for 1 hour or overnight. Restriction endonucleases were denatured at 65°C or 80°C for 20 minutes; otherwise the digestion products were isolated by column purification prior to dephosphorylation with shrimp alkaline phosphatase at 37°C for 1 hour followed by 65°C for 20 minutes, where necessary. Blunting of cohesive ends, where needed, was carried out using *Pfx* DNA polymerase (set up for as for PCR, but without primers) (Greenland et al., 2000), or by using

the Klenow fragment of DNA Polymerase I. The restriction fragments were purified either directly using spin columns, or by gel extraction of specific bands following electrophoresis on a crystal violet gel.

2.3.13 Ligation Reactions

Reactions were set up in 20 µl final reaction volume, in 1 × reaction buffer (50 mM Tris-HCl (pH 7.6), 10mM $MgCl_2$, 1 mM ATP, 1 mM dithiothreitol, 5% w/v polyethylene glycol-8000), and with 1 unit of T4 DNA ligase (Thermofisher Scientific, Massachusetts, USA). Reactions were carried out at 16°C for 16 hours (overnight).

2.3.14 Library Generation using the Zero-Blunt TOPO vector

Blunt-ended PCR products were ligated to the Zero-Blunt TOPO vector, set up as per the manual and incubated at room temperature for 30 minutes. The ligation products were then transformed into One Shot Top 10 DH10B or Library Efficiency DH5α *E. coli* as described below. Colonies were screened by PCR (Table 1 and Table 2) and the PCR products sequenced to identify the transcriptional start sites.

2.3.15 Preparation of 50 ng/µl equimolar dilutions of deletion series constructs

A spreadsheet (Microsoft, USA) was used to calculate the molar mass of each plasmid, and the volume of deletion construct plasmid, water and pUC19 (makeweight) to be added in the equimolar mixture. Total DNA concentration,

by mass, was 50 ng/µl. Prior to the deletion series transfection, the equimolar dilutions of each construct were linearized and run on an agarose gel to check for equivalence.

2.4 Microbiology

2.4.1 Transformation of chemically competent *Escherichia coli* cells

Transformation of plasmid DNA was carried out in chemically competent *E. coli* cells. Plasmid DNA or ligation product (2–5 ng of DNA) was added to 50 µl or 100 µl of the competent cells, and incubated on ice for 30 min. This was followed by heat shock at 42°C for 20–45 s, and incubation on ice for 2 minutes. Pre-warmed (37°C) S.O.C. medium was added as per the specific protocols. The transformed cells were incubated for 1 hour on a shaking 37°C incubator at 200 RPM. The transformation reactions were plated on LB agar plates with ampicillin at a final concentration of 100 µg/ml, and incubated overnight for at 37°C for 16 hours. Where blue-white screening was carried out, X-Gal was also added to the agar prior to pouring, to a final concentration of 50 µg/ml. Where used, kanamycin concentration was 60 µg/ml.

2.4.2 Alkaline lysis of *E. coli* cells and plasmid DNA isolation

Starter cultures were set up, in 3 ml LB medium with 100 µg/ml ampicillin, for 8 hours at 37°C, 200 RPM. A 1:1000 dilution was made in a larger volume (5–500 ml, depending on plasmid copy number and required DNA yield) for the overnight culture (37°C for 16 hours at 200 RPM) in LB medium + 100 µg/ml ampicillin. The Qiagen Mini-Prep, Midi-Prep, Maxi-Prep, and Sigma

GenElute plasmid preparation kits were used to isolate DNA, according to the culture volume used and yield of plasmid DNA that was needed. Additionally, two aliquots from the overnight culture were used to make glycerol stocks (25% w/w glycerol in final volume) of all plasmids.

2.5 Cell culture

2.5.1 Culture of colorectal cancer cell lines and the A549 lung cancer cell line

Six colorectal adenocarcinoma cell lines and one lung adenocarcinoma cell line were used. RPMI 1640 medium + GlutaMAX (Gibco) + 10% w/w fetal calf serum (FCS, Thermo Fisher Scientific) was used for CaCo-2, HT-29, HT-116, SW480 and SW620 cell lines. F12 nutrient mix + GlutaMAX + 10% w/w FCS was used for LoVo cells, and Dulbecco's Modified Eagle Medium (Thermo Fisher Scientific) for the A549 lung adenocarcinoma cell line. The cells were maintained in a 37°C incubator, at 5% CO_2 and 100% humidity. Cells were checked daily under a light microscope, and medium changed every two days.

The cells were passaged at 70% to 80% confluency, in ratios of 1:10 to 1:2. Medium was removed, and the cells washed with 1 × PBS. Cells were dissociated by treating with 1 × PBS + 1 × trypsin-EDTA (0.05% w/v) solution for 5 minutes. Trypsin was inactivated by the addition of complete cell medium. The suspended cells were pelleted by centrifugation at 400 × *g* at 20°C for 5 minutes. After removing the supernatant, the cells were resuspended in cell medium, and aliquoted to new tissue culture flasks at the required split ratio. A haemocytometer was used to calculate cell density prior to seeding cells in well plates for experiments.

2.5.2 Cell line verification

Short tandem repeat analysis was carried out to verify the above cell lines every six months, and to identify any genetic drift from the accepted standards.

2.5.3 Transfection of cultured cells using Lipofectamine 2000

On day 1, cells were seeded, at densities adjusted to obtain between 60% and 70% confluence after 24 hours, depending on the plate format used. On day 2, cell media were changed and the transfection carried out. Lipofectamine 2000 and plasmid DNA were prepared in Opti-MEM medium in the order and incubation times recommended in the manual (Table 8).The resulting solution was added to cells. The dual luciferase assay was carried out on day 3, after 24 hours of treatment.

2.5.4 Estimation of transfection efficiency using yellow fluorescent protein-tagged tubulin alpha 1B

Caco-2 and LoVo cells were transfected using the YFP-TUBA1B plasmid, in a 24-well format. Transfection efficiency was estimated by the ratio of fluorescent to total cells in three fields of view per well after 24 and 48 hours, with medium being changed 24 hours after the transfection.

2.5.5 Quantification of promoter activity using the dual luciferase assay

The dual luciferase assay kit (catalogue number E1910, Promega) was used to quantify promoter activity on a Mithras LB940 multimode microplate reader (Berthold Technologies GmbH & Co. KG, Germany). The reagents were prepared as described in the manual. The only modification to the protocol was to reduce reagent volumes from 100 µl to 50 µl.

Medium containing the transfection reaction was removed, and the cells washed in 100 µl 1 × PBS at room temperature. The cells were then lysed in 22 µl 1 × passive lysis buffer (Promega) and incubated at room temperature on a shaker for 30 minutes. 20 µl of the lysates were transferred to a white-walled, flat-bottom 96-well plate (Lumitrac 200, item number 655075, Greiner Bio One International GmbH, Germany). The plate reader was programmed to run as recommended in the protocol, except for the dispensed reagent volume (50 µl).

2.5.6 Treatment of cells with TGF-β2 and smoothened agonist (SAG)

Caco-2, LoVo and A549 cells were seeded on two 6-well plates at a density of 1×10^5 cells/well (day 1), to be treated for 24 and 48 hours. Activated TGF-β2 (product number GTX48351-PRO, Genetex, Taiwan) was reconstituted in 1 × PBS (pH 7.4) + 0.1% w/v BSA to a stock concentration of 10 µg/ml and serial dilutions made in the same solvent were added to cell medium. Serial dilutions were made ranging from 200 ng/ml to 1.5625 ng/ml and 0 ng/ml. Smoothened agonist (product number SML1314, Sigma-Aldrich, USA) was reconstituted in filter-sterilised distilled water to a stock concentration of 1 mM;

serial dilutions were prepared in filter-sterilised water, and added to cell medium to a final concentrations of 10 nM to 0.625 nM, and 0 nM.

On day 2, 24 hours after seeding, the medium was changed and replaced on both plates with the TGF-β2- or SAG-containing medium. On day 3, RNA was extracted from the 24-hour plate, and the medium changed on the 48-hour plate. Next, on day 4, RNA was extracted from the 48-hour plate.

A total of three (TGF-β2) and four (SAG) independent experiments were carried out at the 24- and 48-hour time points. All three cell lines were treated with TGF-β2, and the SAG treatments were carried out on A549 cells. Three independent experiments were carried out for A549 cells transfected with the *SLCO2A1* promoter deletion series in the presence or absence of TGF-β2 for 24 hours. There were three replicates within each experiment for each construct, with or without TGF-β2.

2.6 Statistics

The Student's *t*-test was used for determining statistical significance when comparing experimental results for the firefly:Renilla luminescence ratios in the transfection experiments, and for RT-PCR band intensity ratios for *SLCO2A1* and *GAPDH*. The calculations were set up and carried out on a spreadsheet (Microsoft Excel).

Chapter 3 Identification of the Transcriptional Start Sites of HPGD and SLCO2A1 in colorectal cancer cell lines

3.1 Introduction

The role of PGE_2 signalling in facilitating cancer development, and the utility of NSAIDs in colorectal cancer prophylaxis have been established in the literature (section 1.2.4 and 1.2.5) (Bennett et al., 1987; Kune et al., 1988; Eberhart et al., 1994; Sano et al., 1995; Gustafson-Svard et al., 1996). More recently, the degradation component of the PGE_2 pathway, involving *HPGD* (Yan et al., 2004; Backlund et al., 2005), and *SLCO2A1* (Holla et al., 2008), has also been implicated in exacerbating increased PGE_2 signalling alongside the known upregulation of *PTGS2* (Sano et al., 1995; Gustafson-Svard et al., 1996). Elucidating the mechanisms of *HPGD* and *SLCO2A1* regulation in relation to known signalling pathways that are perturbed in colorectal cancer would enable the pharmacologically reactivation *HPGD* expression to counteract excessive PGE_2 signalling as an alternative or adjunct to PTGS2 inhibition by NSAIDs (Seira et al., 2017; Na et al., 2011). However, relatively little is known about how *HPGD* and *SLCO2A1* transcription is regulated in the colon.

The transcriptional start sites (TSS's) delineate the start of the gene's first exon from the upstream promoter sequence. Identifying the positions of a gene's TSS is one of the first steps to elucidate its regulation at the transcriptional level (Bansal et al., 2014). It can help identify the key regulatory DNA regions in the core promoter, allowing potential insight into the transcription factors involved. Knowledge of the TSS positions is important for the design of a promoter deletion series experiment, so that deletion constructs do not encroach within exon 1, and experimental results can be interpreted correctly (Beliveau et al., 1999).

In the literature, only one publication has characterised the *HPGD* TSSs. The study by Greenland et al, (2000) found positions -34 and -36 (relative to the *HPGD* first exon ATG translational start site), to be *HPGD*'s TSS. However, their source of RNA (placenta) meant that their observations may not directly applicable to other organs or cell lines, as alternative isoforms can be generated by using different TSS's, particularly in a tissue specific manner (Reyes and Huber, 2018). In addition, the method of choice used by Greenland et al, (2000), the Ribonuclease Protection Assay, lacked the sensitivity of alternative PCR-based techniques, such as the RNA Ligase-Mediated Rapid Amplification of 5'-cDNA Ends (RLM-RACE).

For *SLCO2A1,* no comparable experiments have been published in the literature. However, initial characterisation of the gene has been undertaken in the rat (Kanai et al., 1995) and human (Lu et al., 1996; Lu and Schuster, 1998), and a consensus transcriptional initiator sequence identified, indicating a possible human TSS at position -123. Therefore, the relative lack of data specifically for the colon or colorectal cancer cell lines meant that TSS's had to be determined experimentally for *HPGD* and *SLCO2A1*.

In order to experimentally determine *HPGD* and *SLCO2A1* TSS's, mRNA transcripts from colorectal cancer cell lines needed to be isolated from the other RNA species, reverse-transcribed and sequenced (Volloch et al., 1994). RLM-RACE is an established procedure that streamlines this process, was thus chosen. RLM-RACE has been used for determining TSSs, and applied successfully in large-scale mRNA sequencing studies (Chi et al., 2006; Olivarius et al., 2009). Unlike the ribonuclease protection assay used in the original Greenland et al, (2000) study for *HPGD,* RLM-RACE requires much lower quantities of RNA, owing to two PCR amplification steps in the procedure.

Moreover, this procedure is more sensitive, and allows for the detection of less common transcripts within a particular sample (Schaefer, 1995; Chi et al., 2006).

3.2 Aims

Identify Colorectal Cancer cell lines that express both *HPGD* and *SLCO2A1*

Determine experimentally the TSS of both *HPGD* and *SLCO2A1* in the chosen colorectal cancer cell line models

3.3 Methods

3.3.1 RT-PCR to determine expression of HPGD and SLCO2A1 in colorectal cancer cell lines

Reverse-Transcriptase Polymerase Chain Reaction (RT-PCR) (sections 2.2.1, 2.2.2, 2.2.3) was used on a panel of colorectal cancer cell lines to qualitatively identify which expressed both *HPGD* and *SLCO2A1*. Exon-spanning primers were used to amplify gene-specific cDNA for *HPGD*, *SLCO2A1* and *GAPDH* in six colorectal cell lines (Caco-2, HT-29, HCT-116, LoVo, SW480 and SW620) and one lung adenocarcinoma cell line (A549).

3.3.2 RLM-RACE for HPGD and SLCO2A1 using the Caco-2 and LoVo cell lines

RLM-RACE (Figure 3.1) was carried out using Caco-2 and LoVo total RNA (sections 2.2.3 and 2.3.3). This procedure required 5'-capped mRNAs with at least the first two exons, given that the region of interest was the 5'-Untanslated Region (5'- UTR) of exon 1 (Figure 3.1). Total RNA from cell lysates was dephosphorylated to prevent downstream reactions, whilst the 7-methylguanosine cap in mRNAs conferred protection of the 5' phosphate groups. Next, Tobacco acid pyrophosphatase was used to remove the 5'-cap on the mRNAs to expose the 5'-phosphate group, to which the GeneRacer RNA oligomer then ligated.

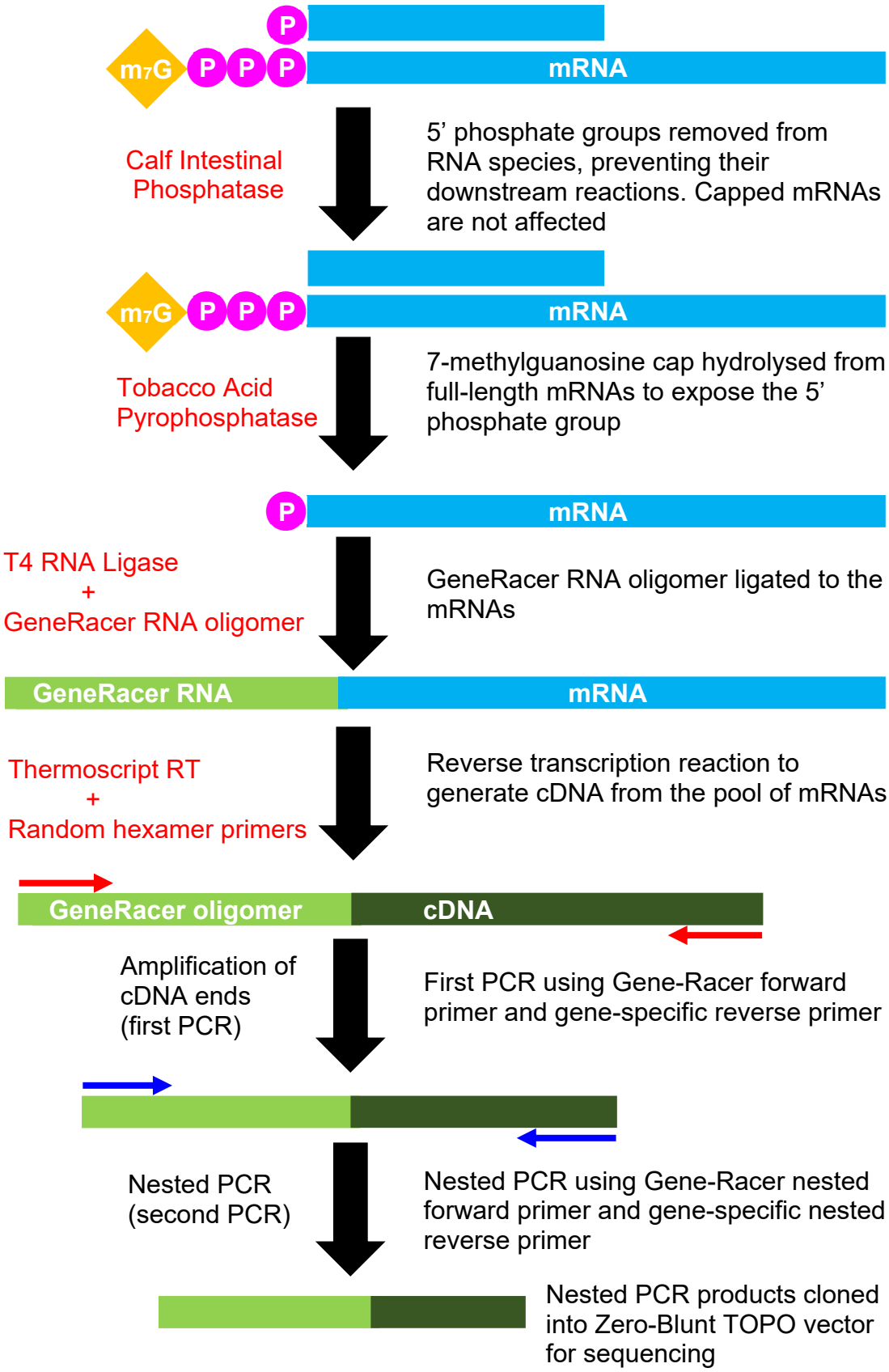
P
m7G
P P P
mRNA
Calf Intestinal Phosphatase
5’ phosphate groups removed from RNA species, preventing their downstream reactions. Capped mRNAs are not affected
m7G
P P P
mRNA
Tobacco Acid Pyrophosphatase
7-methylguanosine cap hydrolysed from full-length mRNAs to expose the 5’ phosphate group
P
mRNA
T4 RNA Ligase
+
GeneRacer RNA oligomer
GeneRacer RNA oligomer ligated to the mRNAs
GeneRacer RNA
mRNA
Thermoscript RT
+
Random hexamer primers
Reverse transcription reaction to generate cDNA from the pool of mRNAs
GeneRacer oligomer
cDNA
Amplification of cDNA ends (first PCR)
First PCR using Gene-Racer forward primer and gene-specific reverse primer
Nested PCR (second PCR)
Nested PCR using Gene-Racer nested forward primer and gene-specific nested reverse primer
Nested PCR products cloned into Zero-Blunt TOPO vector for sequencing

Figure 3.1: Outline of RLM-RACE procedure

The different steps of the RLM-RACE procedure is shown in the figure. The RNA-processing steps isolate capped mRNAs which are reverse-transcribed after the ligation of an RNA oligomer at the 5'-end, which corresponds to the start of the transcript and therefore, the TSS. Two PCR reactions are needed to selectively amplify the gene of interest's transcripts from the resulting cDNA pool. The resulting pool of PCR products is then cloned and sequenced.

Random hexamer primers were used for the reverse transcription reaction step (section 2.2.3) to provide a common cDNA pool for each cell line which could be used at the template for the subsequent PCR reactions. Two PCR reactions (Figure 3.1) were used to selectively amplify *HPGD* and *SLCO2A1* because gene specificity was conferred only by the reverse primer. The forward primers were complementary to the Gene-Racer oligomer. Therefore, the first PCR reaction was carried out on the cDNA template, and the second, nested PCR used a 1/1000 dilution of the first PCR reaction products, after excess dNTPs and primers were removed using exonuclease I/Shrimp Alkaline Phosphatase (section 2.3.4). For both PCR reactions, a proofreading DNA polymerase (Pfx Platinum) was used to reduce the chance of mutations due to PCR error.

The PCR products for *HPGD* and *SLCO2A1* were column-purified (section 2.3.4), instead of agarose gel electrophoresis followed by gel extraction in order to capture a greater range of the amplified transcript sequences, and due to the relative inefficiency of extracting DNA from agarose gels. These PCR products were then cloned into the ZERO-Blunt TOPO vector (section 2.3.14). Following transformation into chemically competent *E. coli* cells (Section 2.4.1), colonies were picked, and the ligated *HPGD* or *SLCO2A1* inserts amplified by PCR using M13 forward and reverse primers in order to ensure that both the 5' oligomer sequence and the spliced junction between exon 1 and exon 2 of each gene were visible during the subsequent sequencing (section 2.3.7).

These sequences were aligned with BLAST to the *HPGD* and *SLCO2A1* genomic sequences (GRCh38/hg38, 2013 assembly), and manually inspected to delineate splicing between exon 1 and exon 2 of either gene, the vector sequence at the ends of the reads, and the GeneRacer oligomer's sequence

(Altschul et al., 1990; Kent et al., 2002). Given the correct alignments to the human genome, TSS was taken as the base immediately adjacent to the last base of the GeneRacer oligomer, as inferred in similar studies where amplified transcripts are aligned to the genome sequence, and any vector or restriction-site containing oligomer sequence is excluded (Shiraki et al., 2003; Hashimoto et al., 2004; Tosetto et al., 2014)

3.4 Results

3.4.1 Expression of HPGD and SLCO2A1 mRNA in six colorectal cancer cell lines and one lung adenocarcinoma cell line

A panel of colorectal cell lines was assessed for *HPGD* and *SLCO2A1* expression in order to determine which cell lines express both *HPGD* and *SLCO2A1* at appreciable levels to generate sufficient mRNA for the RLM-RACE. The A549 lung cancer cell line was included as an additional control because it is known to express *HPGD* at relatively high levels, and no or very little *SLCO2A1* (Uhlen et al., 2005; Tong et al., 2006a). Across the seven cell lines, Caco-2, HT-29, LoVo, and SW480 were found to express both *HPGD* and *SLCO2A1* (Figure 3.2). HCT-116 appeared to have *SLCO2A1* expression, but did not express *HPGD* at detectable levels (Figure 3.2). Caco-2 and LoVo both showed modest *HPGD* expression, relative to the other four colorectal cancer cell lines. As expected, the lung cancer cell line A549 was found to show a relatively high expression of *HPGD*, but with no detectable *SLCO2A1* expression.

LoVo has been shown to express *SLCO2A1* mRNA and protein at higher levels compared to HT-29, HT-116, SW480 and SW620 in the literature, which

is in agreement to this observation (Holla et al., 2008; Smartt et al., 2012a). Furthermore, a higher expression of *SLCO2A1* mRNA by LoVo relative to Caco-2 has been shown quantitatively in the literature, and lends support to RT-PCR results (Figure 3.2) (Kasai et al., 2016). The HCT-116's expression of *SLCO2A1*, however, did not match the low expression reported in other studies (Holla et al., 2008; Smartt et al., 2012a). Therefore, based on the experimental results and the additional evidence from the literature, the Caco-2 and LoVo cell lines were thus selected for use in the RLM-RACE.

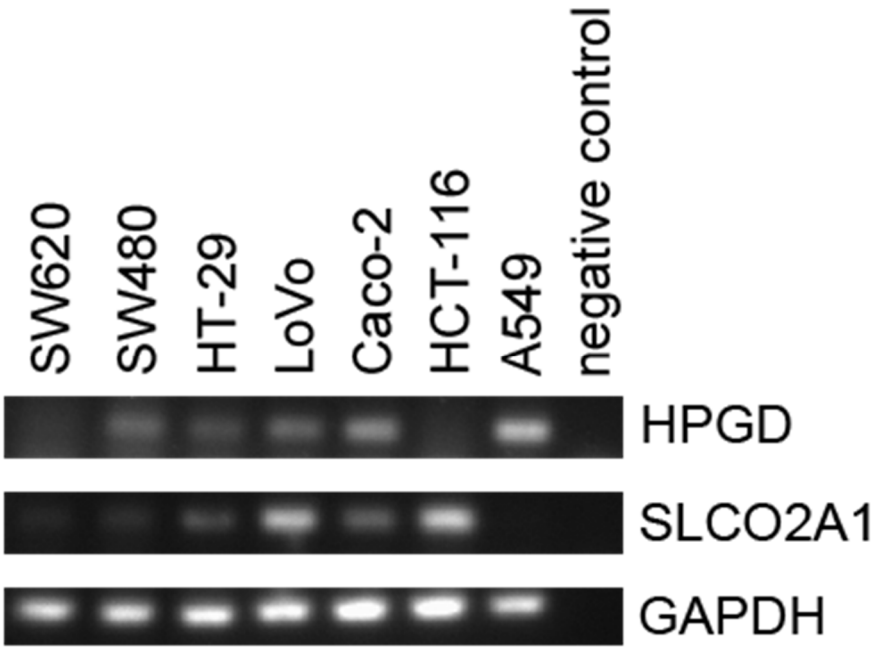

Figure 3.2: RT-PCR to visualise gene expression in the seven cell lines
HPGD and *SLCO2A1* expression was assessed by comparison to the level of the housekeeping gene *GAPDH*. *HPGD* expression was not detectable in SW620 and HCT116 cells, and *SLCO2A1* expression was absent in SW620. Four colon cell lines (Caco-2, HT-29, LoVo, and SW480) expressed both genes. The *GAPDH* on the positive control, expressed by all seven cell lines, and no bands are visible on the negative water control. The PCR product sizes are 191 bp for *HPGD*, 232 bp for *SLCO2A1*, and 310 bp for *GAPDH*

3.4.2 Determination of HPGD and SLCO2A1 TSSs in Caco-2 and LoVo cell lines using RLM-RACE

After establishing that the Caco-2 and LoVo cells expressed both *HPGD* and *SLCOA1* to at least a moderate level relative to the other cell lines, these were used in RLM-RACE. The first PCR, the amplification of the cDNA ends (Figure 3.1) yielded a number of product bands (Figure 3.3 and Figure 3.4). For *SLCO2A1*, in Caco-2 two predominant bands at approximately 190 bp and 350 bp were visible (Figure 3.4), while in the LoVo cell line, the 350 bp band was predominant, as well as several weaker, larger bands. For *HPGD,* the main PCR product band for Caco-2 and LoVo was at 210 bp (Figure 3.4) while a number of larger but weaker bands were also present.

In the subsequent nested PCR the number of bands decreased (Figure 3.4 and Figure 3.5) as the more specific products were amplified more efficiently. For *SLCO2A1*, Caco-2 had one visible band at 310 bp, while for LoVo, additional bands were seen in addition to the predominant one at 310 bp (Figure 3.5). In *HPGD,* the number of weaker bands decreased for both cell lines, with 210 bp and 350 bp predominating in both cell lines (Figure 3.4). The presence of many bands was not unexpected, given that gene specificity was determined only by the reverse primer. The 250 bp (first PCR) and 210 bp (nested PCR) bands for *HPGD* were near the product size for the -36 or -34 TSSs reported in Greenland et al, (2000). Similarly, for *SLCO2A1*, the 350 bp band would correspond to the PCR product based on the predicted TSS at -123 (Lu and Schuster, 1998).

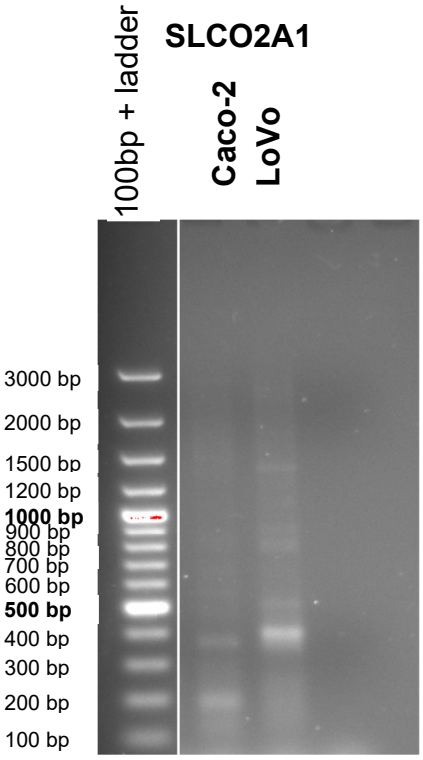

Figure 3.3: First PCR (amplification of cDNA ends) for *SLCO2A1*
The first PCR in the RLM-RACE yielded a number of bands. For Caco-2 (lane 1) and LoVo (lane 2) the band patterns are distinct, suggesting different transcripts and off-target products that were amplified in the PCR reaction. Bands at ~190 bp and ~350 bp predominate in Caco-2, while the strongest band appears at ~350 bp for Lovo. The agarose gel has been cropped (white vertical line) for increased clarity between the 100bp plus ladder, and the *SLCO2A1* PCR product bands

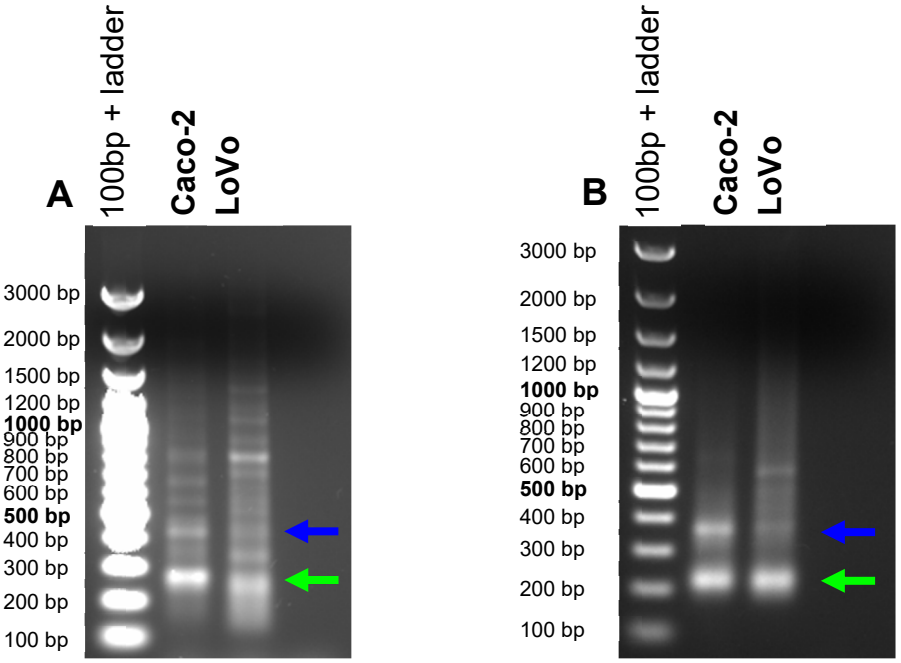

Figure 3.4: First PCR (A) and nested PCR (B) for *HPGD*
For Caco-2 the first PCR revealed a number of bands, of which those at~210 bp (green arrow) and ~350 bp (blue arrow) persisted in the nested PCR. Although the ~210 bp band was also the strongest in the LoVo cDNA, a greater number of bands was discernible on the Nested PCR, suggesting a greater number of transcripts.

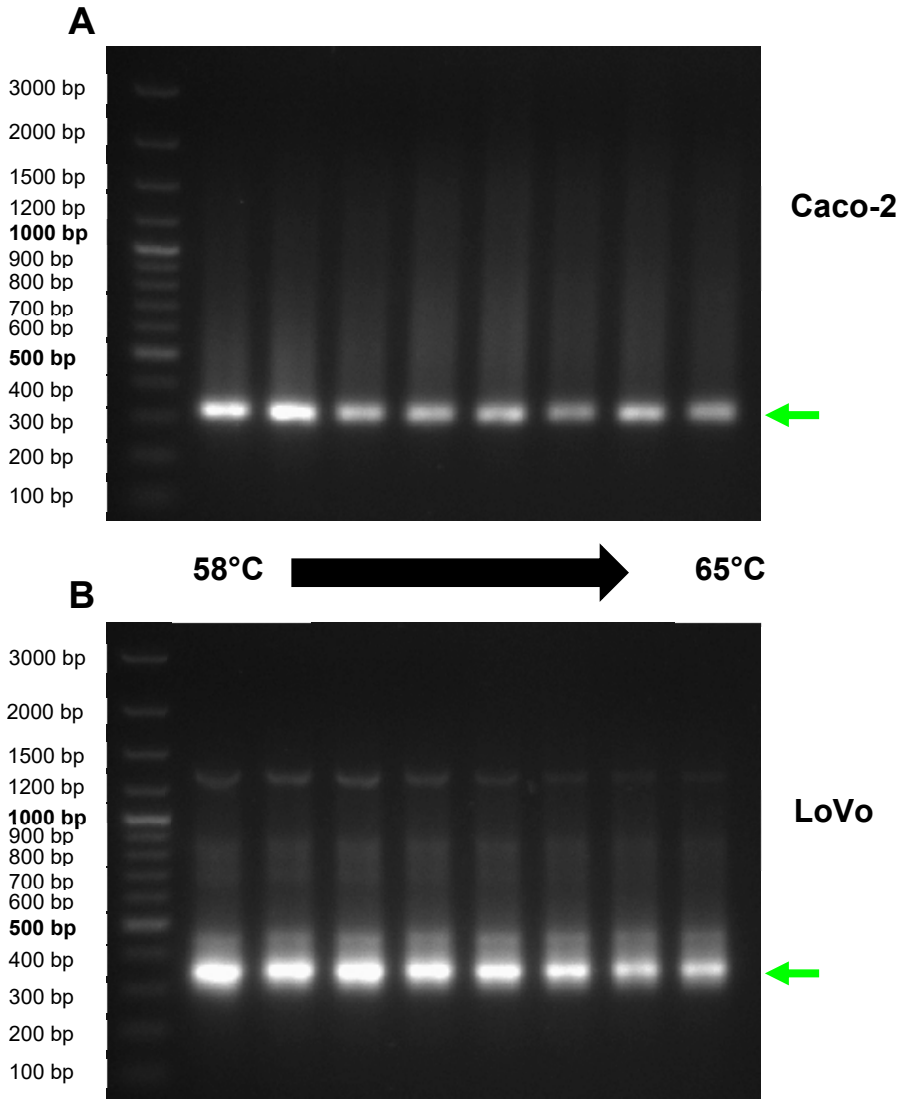

Figure 3.5: Second PCR (nested PCR) for *SLCO2A1*
Gradient PCRs were carried out and the products at the highest annealing temperature (65°C) were purified and cloned to sequence the PCR products. (A) Caco-2 showed a single predominant band at ~310 bp (green arrow), and no other discernible bands. (B) LoVo, on the other hand had a predominant band at the same ~310 bp position (green arrow), although brighter smearing or other bands were visible from 350 bp to 450 bp, and 700 bp to 900 bp, as well as 1200 bp.

The nested PCR products for *HPGD* and *SLCO2A1* were subsequently cloned for sequencing. A total of 55 and 65 for Caco-2 and LoVo cells respectively for *HPGD*, and 55 and 56 clones for *SLCO2A1* were obtained for analysis. These clones excluded the occasional detection of off-target cDNA sequences that persisted to be amplified in the nested PCR, or instances of GeneRacer oligomer concatamers. As shown in Figure 3.6, the TSS was taken as the first base in exon 1 immediately after the end of the GeneRacer oligomer sequence, and its position was taken relative to the translational start site ATG.

Overall, the results suggested that the -65 position is the predominant TSS for *HPGD* in Caco-2 and LoVo cells, with the -37 or -36 positions showing the second-highest frequency, contrary to the observed consensus that is suggested in the spliced EST data (Figure 3.7 and Figure 3.8). For *SLCO2A1* in contrast, Caco-2 and LoVo cells showed differing TSS profiles. Caco-2 transcripts terminated at 5 bases upstream of the spliced EST consensus at -127 (Figure 3.8), rather than the predicted -123 TSS (Lu and Schuster, 1998), while the LoVo cells showed a more distributed pattern with -159 being the most frequent TSS after -123.

A

>Caco2_SLCO2A1-02B[M13F]
CAGCCACAATCTGTGTCTGAGTTTAGCGGCCGCGATTCGCCCTTGGACACTGACATGGACTGAAG
GAGTAGAAATCTCAGTCTCCGCTCCGCGAATCTCCTCCGGCCACTGCCGCCGCGGTCGCCTCTCA
CCCGCCCGGCCGCTCCAGCCCGAGGCGCCCCGACCCCGCGCCACTCCGCGCCCGGCCAGCCGCCC
GCAGCCATGGGGCTCCTGCCCAAGCTCGGCGCGTCCCAGGGCAGCGACACCTCTACTAGCCGAGC
CGGCCGCTGTGCCCGCTCGGTCTTCGGCAACATTAAGGTGTTTGTGCTCTGCCAAGGCCTCCTGC
AGCTCTGCCAACTCCTGTACAGCGCCTACTTCAAGAGAAGGGCGAATTCGTTTAAACCTGCAGGA
CTAGTCCCTTTAGTGAGGGTTAATTCTGAGCTTGGCGTAATCATGGTCATAGTTGTTTCCTG

>Caco2_SLCO2A1-02B[M13R]
GCTTTCCTGGGTGATCGCTCTCGCAGGGACTAGTCCTGCAGGTTTAAACGAATTCGCCCTTCTCT
TGAAGTAGGCGCTGTACAGGAGTTGGCAGAGCTGCAGGAGGCCTTGGCAGAGCACAAACACCTTA
ATGTTGCCGAAGACCGAGCGGGCACAGCGGCCGGCTCGGCTAGTAGAGGTGTCGCTGCCCTGGGA
CGCGCCGAGCTTGGGCAGGAGCCCCATGGCTGCGGGCGGCTGGCCGGGCGCGGAGTGGCGCGGGG
TCGGGGCGCCTCGGGCTGGAGCGGCCGGGCGGGTGAGAGGCGACCGCGGCGGCAGTGGCCGGAGG
AGATTCGCGGAGCGGAGACTGAGATTTCTACTCCTTCAGTCCATGTCAGTGTCCAAGGGCGAATT
CGCGGCCGCTAAATTCAATTCGCCCTATAGTGAGTCGTATTACAATTCACTGGCCGTCGTTTTAC
-127

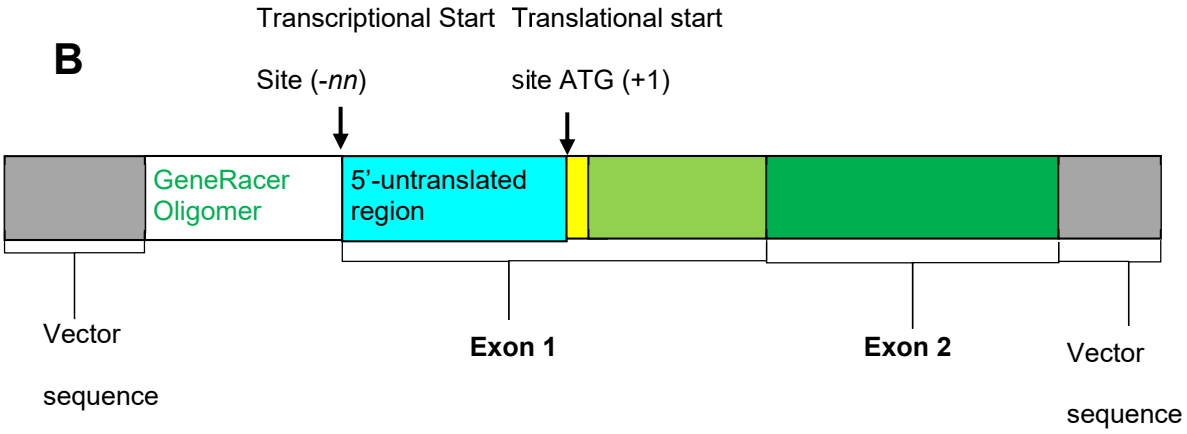

Figure 3.6: Representative sequencing reads of SLCO2A1 nested PCR products
Following the cloning and transformation reactions, colonies were picked and the inserted nested PCR products amplified using M13 forward and reverse primers on the flanking vector sequence. These PCR products were sequenced in both directions. (A) An example of a Caco-2 *SLCO2A1* read that terminates at -127 is shown. (B) Schematic representation of the above sequence. GeneRacer oligomer sequence (green text), exon 1 (5'-UTR (light blue), translated region (green), with ATG start codon (yellow), exon 2 (dark green), vector sequence (grey).

3.4.3 Spliced EST sequences terminating within the 5' UTR of HPGD and *SLCO2A1*

Expressed Sequence Tags (ESTs) are single-pass sequencing reads from cDNA that represents a segment of the mRNA sequence (Adams et al., 1991; Boguski et al., 1993). EST data is available through tools such as the UCSC Genome Browser (Kent et al., 2002), which align the raw sequencing reads to the genome and remove flanking vector sequences. Spliced ESTs are a subset of ESTs that only map to the gene of interest's exons, thereby representing mRNA sequence rather than sequence from genomic DNA or pre-mRNA (Kent et al., 2002; Nagaraj et al., 2007).

In spite of the caution with which EST data needs to be viewed, and the limitations inherent to the generation of these sequences, the spliced ESTs aligning to exon 1 and exon 2 of *HPGD* and *SLCO2A1* can provide an indication for the position of the TSSs (Boguski et al., 1993; Nagaraj et al., 2007). The spliced EST data could show whether the Caco-2 and LoVo TSS for *HPGD* and *SLCO2A1* were similar to the consensus, or to normal colon, if a sufficient subset of the spliced EST sequences originated from that organ.

Spliced ESTs encompassing the 5'-UTR and splicing between exon 1 and exon 2 of both *HPGD* and *SLCO2A1* were compared alongside the RLM-RACE results. The spliced EST data suggested that the most common TSS for *HPGD* was -37, and for *SLCO2A1* -123 (Figure 3.7 and Figure 3.8). For *HPGD* this was similar to published work by Greenland et al, (2000), but contrasted with both Caco-2 and LoVo cell lines where although -36 or -37 were minor TSS's, the predominant position for both cell lines was -65. The major EST TSS for *SLCO2A1* was also different from the two colon cell lines.

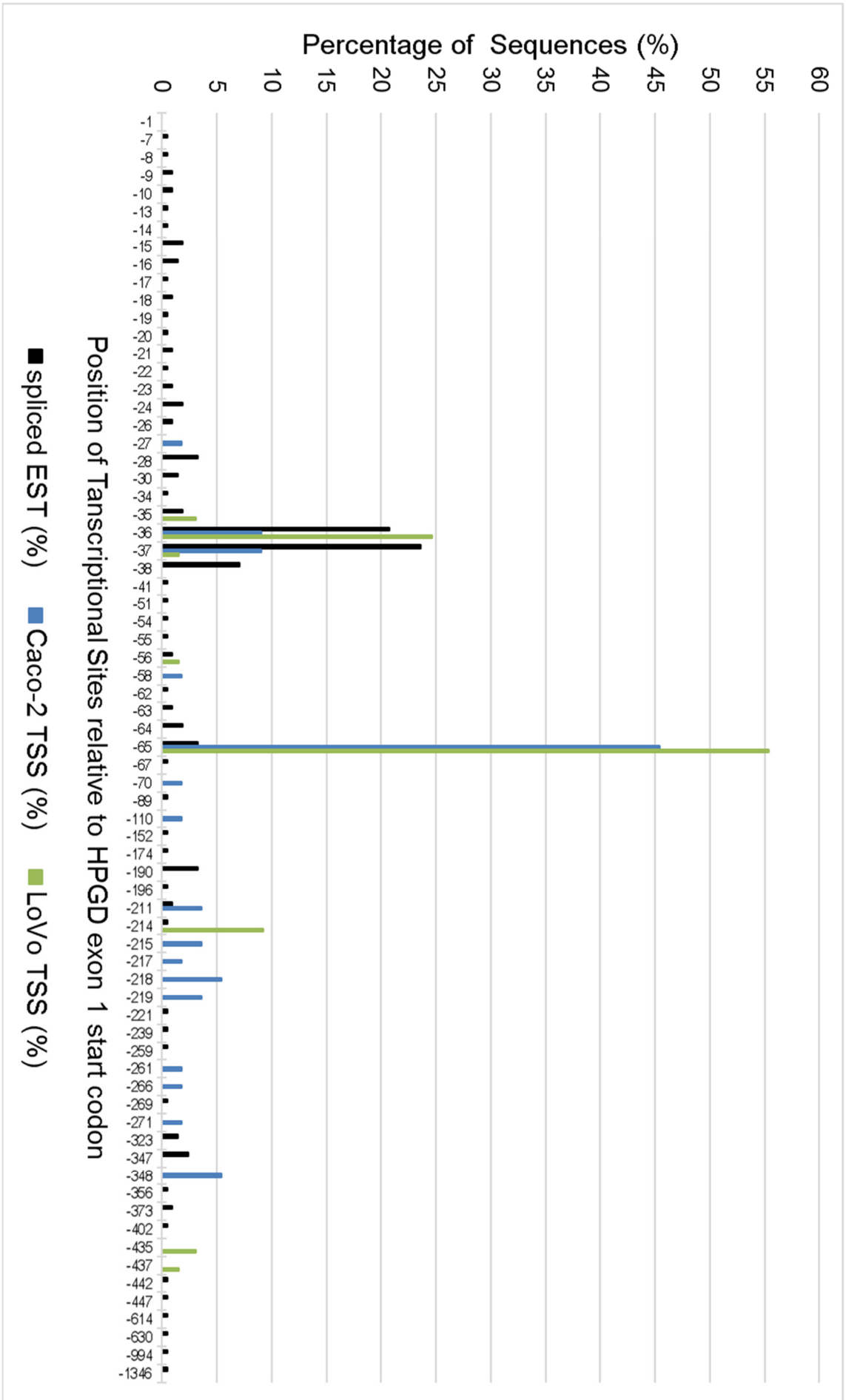
Percentage of Sequences (%)
0
5
10
15
20
25
30
35
40
45
50
55
60
Position of Tanscriptional Sites relative to HPGD exon 1 start codon
-1
-7
-8
-9
-10
-13
-14
-15
-16
-17
-18
-19
-20
-21
-22
-23
-24
-26
-27
-28
-30
-34
-35
-36
-37
-38
-41
-51
-54
-55
-56
-58
-62
-63
-64
-65
-67
-70
-89
-110
-152
-174
-190
-196
-211
-214
-215
-217
-218
-219
-221
-239
-259
-261
-266
-269
-271
-323
-347
-348
-356
-373
-402
-435
-437
-442
-447
-614
-630
-994
-1346
spliced EST (%)
Caco-2 TSS (%)
LoVo TSS (%)

Figure 3.7: Percentage of transcriptional start sites for *HPGD* from experimental data and spliced expressed Sequence tag data

Following the RLM-Race a total of 55 clones for Caco-2 and 65 for LoVo were sequenced. In the Caco-2 cell line, the -65 position appears to be the predominant transcriptional start site in 45.5% (25/55) of clones. The -36 and -37 sites are the second-most common, with 9.1% (5/55) of clones each. In addition, between 1 and 3 clones occur in other positions, with the largest detectable transcript for Caco-2 terminating at -348. In the LoVo cell line 55.4% (36/65) of clones occur at the -65 position, with 24.6% (16/65) at -36 and 9.2% (6/65) at -214. 1 or 2 clones are found at few other positions. The largest observed transcripts for LoVo terminated at -435 and -437. The -36, -37, -56, -65, -211, -214 transcriptional start sites observed experimentally were also seen in the spliced EST data. In addition a number of novel transcriptional start sites were observed, predominantly for Caco-2 at -58, -70, -110, -215, -217, -218m -219, -261, -266, -271 and -348. Likewise, the -435 and -437 positions were observed in Lovo. 25% of spliced ESTs terminating at -37. Spliced ESTs (black), Caco-2 (blue), Lovo (green).

Figure 3.8: Percentage of transcriptional start sites for *SLCO2A1* from experimental data and spliced expressed sequence tag data

The numbers transcriptional start site positions from 60 Spliced ESTs, 55 sequenced Caco-2 clones and 56 sequenced LoVo clones are represented as percentages of each set. For clarity, the -1 position and all other positions at which any of the sequences terminated are shown on the graph. 60% of the spliced EST peaks occurred at the -123 position. In contrast the -127 position predominates in 87.2% (48/55) of Caco-2 clones, while LoVo shows a more distributed pattern with 33.9% (19/56) of TSS at -159 and 19.6% (11/56) at -123. 58% of spliced ESTs terminated at -123. However no ESTs originated from the colon, and 60% are from lung samples. Spliced ESTs (black), Caco-2 (blue), Lovo (green).

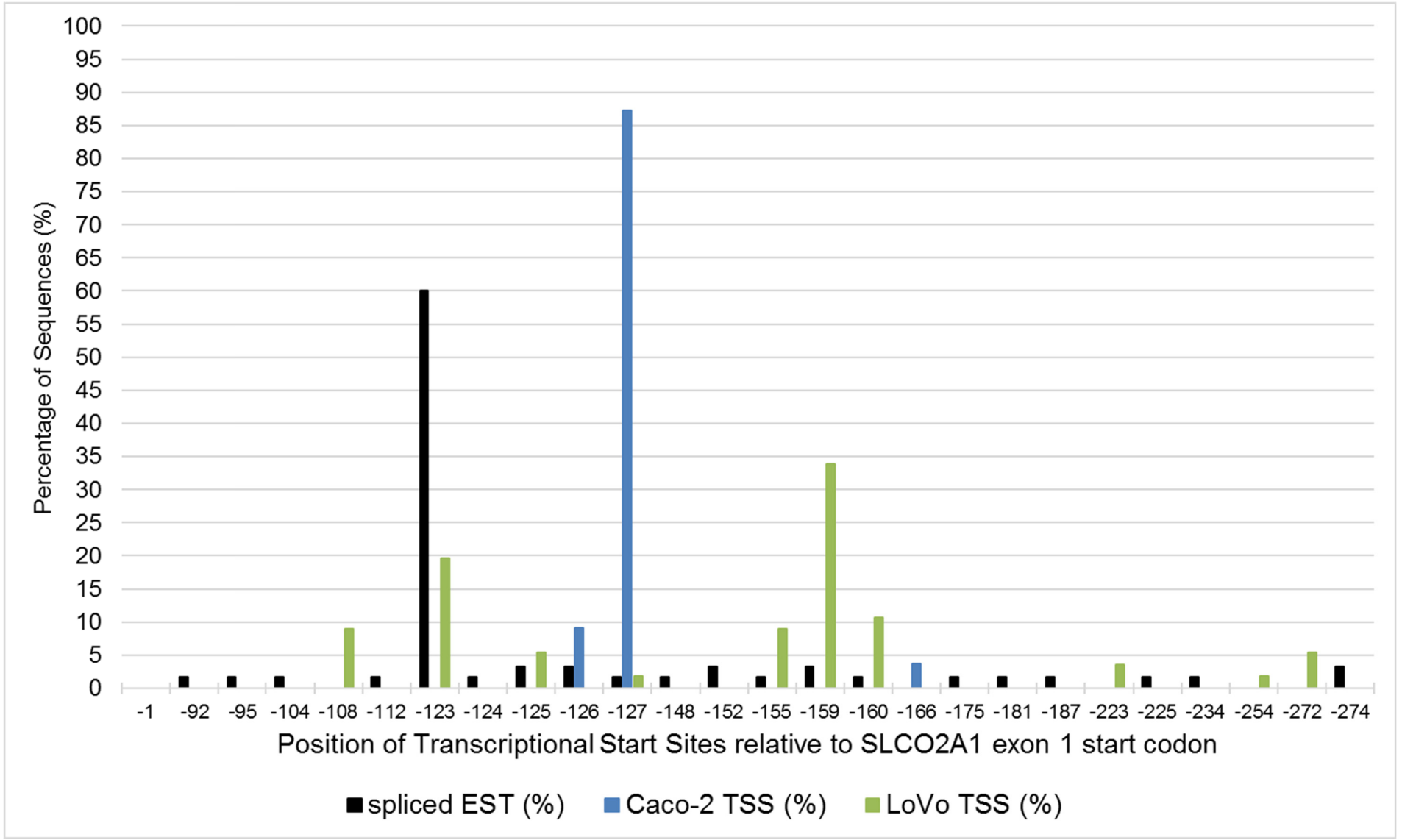
100
95
90
85
80
75
70
65
60
55
50
45
40
35
30
25
20
15
10
5
0
Percentage of Sequences (%)
-1
-92
-95
-104
-108
-112
-123
-124
-125
-126
-127
-148
-152
-155
-159
-160
-166
-175
-181
-187
-223
-225
-234
-254
-272
-274
Position of Transcriptional Start Sites relative to SLCO2A1 exon 1 start codon
spliced EST (%)
Caco-2 TSS (%)
LoVo TSS (%)

3.5 Discussion

The RT-PCR results, while not quantitative, appeared to generally agree with *HPGD* and *SLCO2A1* expression seen previously in Caco-2 and LoVo cells (Uhlen et al., 2005). A moderate or high expression at the mRNA level would imply modest promoter activity, and therefore both cell lines were deemed suitable candidates for subsequent functional transcriptional analysis studies, such as promoter deletion series experiments, because decreases in promoter activity would likely be greater in magnitude and more likely to be detected. The Caco-2 and LoVo cell lines were thus chosen for the RLM-RACE. Using two cell lines also allowed for a comparison to be made in TSSs between the different cell lines.

The comparison of the TSSs observed in the RLM-RACE to existing spliced EST data was prompted by the similarities and differences observed in the results for Caco-2 and LoVo's main TSS, and those identified or predicted in previous publications. Both cell lines' predominant *HPGD* TSS was at -65, contrary to the -36 and -34 positions which were identified in Greenland et al, 2000. Similarly, for *SLCO2A1*, the predominant TSS for Caco-2 was found to be at -127, and for LoVo, -159 and across a range of positions, in contrast to the prediction made at -123 based on sequence motifs only (Lu and Schuster, 1998). The use of algorithms was a limitation recognised by the authors, although despite recommending validating this prediction, they did not pursue this course in their future publications (Lu and Schuster, 1998; Chan et al., 1999; Chan et al., 2002a; Chi et al., 2006).

It is known that that the raw sequences from ESTs suffer from poor quality at the start and end of the read, as well as contamination with vector ends at the end of the read (Boguski et al., 1993). However, bioinformatics tools

mitigate these issues in a number of ways (Nagaraj et al., 2007). Sequence alignment algorithms identify the ESTs that align to a particular gene of interest, while ancillary programs filter out any contaminating vector sequences at the ends of the ESTs. Moreover, spliced ESTs are aligned to a gene's exons, in addition to the above filtering steps in order to show alignments that have originated from spliced mRNA sequences which have greater than 96% homology (Boguski et al., 1993; Kent et al., 2002; Nagaraj et al., 2007). The ESTs analysed in this study were selected to be spliced, so eliminating many of these contamination issues, and so this was not the cause for the differences in TSS found.

One of the main reasons for the differences in TSS between the *HPGD* EST and colon cell lines could be that the overall pattern is not representative of the colon, as the EST data represented an average across samples from different tissues, not all of which may be represented in similar proportions (Kent et al., 2002). Indeed, only 5% (11/212) of all spliced *HPGD* ESTs originated from the colon, and approximately 60% of the *SLCO2A1* spliced ESTs originated from lung samples, and none were from the colon. Given the tissue specific variability in gene TSS choice, which may allow for finer control of gene and protein function, this was not a wholly unexpected result (Reyes and Huber, 2018). However these discrepancies could have resulted from differences in the cDNA preparation. Given the CG-rich nature of the *HPGD* and *SLCO2A1* first exon, it was also possible that the RNA secondary structure could have impeded the reverse transcriptase's progression, and resulted in fewer transcripts upstream of -37 (Romeo et al., 1997; Kent et al., 2002). For the cDNA generation step of the RLM-RACE, a reverse transcriptase with a higher optimal reaction temperature was used in order to account for the CG-

rich nature of the *HPGD* and *SLCO2A1* first exons and promoter, and an RNA oligomer had been ligated to the mRNAs, providing a clear demarcation of the 5'-end (Volloch et al., 1994). Under more standard RT conditions, the reverse transcriptase could stall due to persisting RNA secondary structure in lower reaction temperatures (Schaefer, 1995). Therefore, the Spliced EST data, whilst providing an overall distribution of TSSs for *HPGD* and *SLCO2A1*, had to be viewed with caution. Therefore an experimental approach taken to determine the TSSs in the cell line systems to be used was considered prudent, given that a procedure such as RLM-RACE had been specifically developed to identify 5'- and 3'- cDNA ends (Schaefer, 1995).

An interesting finding was the difference in *SLCO2A1* TSSs between Caco-2 and LoVo, but not in *HPGD*. The Caco-2 cell line appeared to have one predominant TSS, while in the LoVo transcripts were found to originate in a range of positions. It may be the case that discrepancy arose from different regulatory mechanisms between these cell lines, or the fact that the *SLCO2A1* promoter has intermediate features that allowed for flexibility between the broad promoters (characterised by CpG rich content), and single peak promoter classes (characterised by presence of a TATA box) (Carninci et al., 2006). *SLCO2A1'*s exon 1, part of intron 1, and the proximal promoter lie within a CpG island, yet the gene does have a TATA box sequence (Lu and Schuster, 1998).The difference in the colon cell lines TSSs may suggest that due to different accumulated chromosomal changes and gene mutations, these could have contributed to choice of TSS (Knutsen et al., 2010; Ahmed et al., 2013). It is possible that somatic changes may influence the mechanism of TSS selection.

The differences in the TSS between Caco-2 and LoVo, particularly for *SLCO2A1,* highlighted the caution needed when interpreting results from immortalised *in vitro* cell line model systems. What was observed in an immortalised cell line could not be directly extrapolated to the normal colon mucosa, or to primary cells within the colon adenocarcinoma. It may be true the some of the TSSs could be present in the normal epithelial cells, but this would need to be verified using primary cells to reflect the normal expression in the body (Roche, 2001).

However, for the purpose of designing and interpreting downstream experiments, such as a promoter deletion series, the TSS information generated from the two colon cell lines was crucial. It allowed the setting of lower limits to the smallest constructs when generating a full deletion series, and indicated at what positions loss of promoter activity would result from the loss of TSS.

In conclusion, the TSSs identified for *HPGD* and *SLCO2A1* using RLM-RACE were the first to be reported in the Caco-2 and LoVo cell lines. Reliance only on the in-silico spliced EST data, or the *HPGD* publications would have led to potentially erroneous conclusions, given that the transcription start site distribution and the limitations of EST data when contrasted to RLM-RACE (Greenland et al., 2000; Nandy et al., 2003; Kent et al., 2002). This data will allow the appropriate design and interpretation of further transcriptional studies, including promoter deletion constructs.

Chapter 4 Promoter deletion series to identify *HPGD* and *SLCO2A1* regulatory regions

4.1 Introduction

After determining the *HPGD* and *SLCO2A1* transcriptional start sites using RLM-RACE, it was possible to design a promoter deletion series, in order to identify regions important for transcriptional regulation. Prior knowledge of the transcriptional start site locations was necessary in order to ensure that these could be included in the reporter constructs. Intervals associated with an increase or reduction in promoter activity on deletion are then likely to contain binding sites for transcriptional repressors and activators, respectively. These could, in turn, be studied in more detail to determine which transcriptional activators or repressors bind and regulate *HPGD* and *SLCO2A1*. This information could shed light on the mechanisms by which the expression of these two genes is lost in colorectal cancer, and hence suggest ways to reactivate their expression. As discussed earlier, reactivation of these two genes, by reducing the effects of PGE_2 overproduction in colorectal cancer, could supplement or replace in place of or in combination with conventional NSAIDs that inhibit PG synthesis (Kune et al., 1988; Sano et al., 1995; Gustafson-Svard et al., 1996).

To date, only two publications have characterised the transcriptional regulation of the HPGD promoter (Greenland et al., 2000; Nandy et al., 2003), and similar work has not been done on SLCO2A1. Greenland et al. (2000) were the first to carry out an HPGD promoter deletion series. They suggested that Ets and AP-1 transcription factors, and the progesterone receptor, were able drive HPGD promoter activity through a proximal and a distal region. The second study analysed these two regions further, utilising a combination of

binding site mutations on the promoter, and electrophoretic mobility shift assays (EMSA), to provide strong evidence of direct promoter control by AP-1 and Ets (Nandy et al., 2003). However, AP-1 factors are upregulated in colorectal cancer (Zhang et al., 2005), and so are unlikely to be a main driver of HPGD expression in colorectal epithelial cells, given the downregulation of HPGD observed in the neoplastic cells (Yan et al., 2004; Backlund et al., 2005).

In both the above studies, the authors' research aims were to characterise *HPGD* regulation in the uterus and the placenta, including whether mineralocorticoids or other steroid hormones affect its expression (Greenland et al., 2000) and its role in parturition (Nandy et al., 2003). Although relevant to the function of *HPGD*, these results may not be extrapolatable to colon and how *HPGD* is downregulated in colorectal cancer. Similarly, although Lu and Schuster (1998) showed that a proximal 3.5-kb *SLCO2A1* promoter fragment was sufficient to drive a luciferase reporter construct, they did not characterise this further. The present studies were therefore undertaken in order to identify which regions of the *HPGD* and *SLCO2A1* promoters were important for driving expression in the context of colorectal cancer.

4.2 Aims

Characterise the activity of the *HPGD* and *SLCO2A1* proximal 3-kb promoter regions.

Identify regulatory regions within the *HPGD* and *SLCO2A1* promoters for more detailed analysis.

4.3 Methods

4.3.1 Design of *HPGD* and *SLCO2A1* promoter luciferase reporter constructs

In a promoter deletion series experiment, a gene's promoter region is cloned upstream of a reporter gene (such as firefly luciferase or β-galactosidase) in a promoterless plasmid. The promoter region in this initial "full-length" construct is then progressively truncated to generate a panel of shortened constructs, each of which is transfected into cultured cells to assess the promoter activity, as indicated by an enzymatic reaction driven by the reporter gene product. A second reporter plasmid (usually encoding *Renilla* luciferase) driven by a constitutive promoter is used as a transfection control (Shifera and Hardin, 2010).

The 3-kb regions of the *HPGD* and *SLCO2A1* promoters were isolated by restriction digestion from BAC DNA (section 2.3.9) and cloned into the pGL4.10[luc2] firefly luciferase reporter plasmid to generate the "full-length" constructs H-3082 and S-3198 respectively. These regions were chosen based on the presence of a CpG island in both each gene within this interval, and chromatin immunoprecipitation sequencing (ChIPseq) data suggesting that a proximal 3-kb region may be important for regulation of gene expression (Kent et al., 2002).

Each construct was named by the first letter of the gene, followed by the position of its 5′-end relative to the exon 1 start codon. The *HPGD* construct required a two-step process and the use of an adaptor sequence in pGL4.10[luc2] to clone the −3082 to −206 region of the *HPGD* promoter, followed by PCR (with a proofreading DNA polymerase) to insert the −206 to −1

segment. All promoter deletion series constructs were sequence-verified (section 2.3.7) to exclude unwanted mutations.

4.3.2 Design of the *HPGD* and *SLCO2A1* promoter deletion series

The H-3082 and S-3198 constructs were used as the starting points to generate a further eight deletion constructs at approximately 300-bp intervals, through double restriction digestion, where possible, or else through the use of proofreading PCR to introduce restriction sites into the product prior to cloning. Also, a further four constructs were generated using PCR and restriction enzyme digestion at S-266, S-209 and S-140, to study the proximal part of the *SLCO2A1* promoter with greater resolution.

4.3.3 Luciferase reporter assays

The transfection efficiency of Caco-2 and LoVo cells was determined as described in section 2.5.4 and the optimum Lipofectamine 2000 concentrations were determined. The activities of the full-length *HPGD* and *SLCO2A1* constructs were also verified in these two cell lines prior to the construction of the promoter deletion series.

Transfections of Caco-2, LoVo, HT-29 and A549 cells were carried out as described in the methods sections 2.5.3 and 2.5.5. 50 ng/μl equimolar *HPGD* or *SLCO2A1* deletion construct (with pUC19 DNA to equalise total DNA mass), and 0.84 ng/μl pRL-CMV *Renilla* luciferase transfection control were added to the cultured cells in 96-well plates. Two or three repeats of each transfection experiment was carried out, each with three replicate wells for each deletion construct.

4.4 Results

4.4.1 Transfection efficiencies of Caco-2 and LoVo cells

The suitability of Caco-2 and LoVo cells for transfection with the *HPGD* and *SLCO2A1* promoter deletion constructs was assessed by measuring the proportion of YFP-positive cells after transfection with a YFP-expressing plasmid. Low transfection efficiency would reduce the sensitivity of the deletion series experiments to detect real differences in promoter activity (Shifera and Hardin, 2010). A transfection efficiency of 10% was chosen as the minimum for the cell lines to be used in the dual luciferase assay.

LoVo cells showed transfection efficiencies ranging from 25% to 44%, with no appreciable difference between 24 and 48 hours, or the amount of Lipofectamine 2000 used (Figure 4.1). Caco-2 transfection ranged from 15% to 25%. In both cell lines, transfection efficiency rose only slightly after increasing Lipofectamine 2000 to 5 µl in 100 µl. The greatest observed transfection efficiency for Caco-2 was 24.5%, and for LoVo at 44.4% with 5 µl Lipofectamine 2000. Across the range of Lipofectamine 2000 concentrations, LoVo cells were transfected at approximately twice the efficiency of Caco-2 cells.

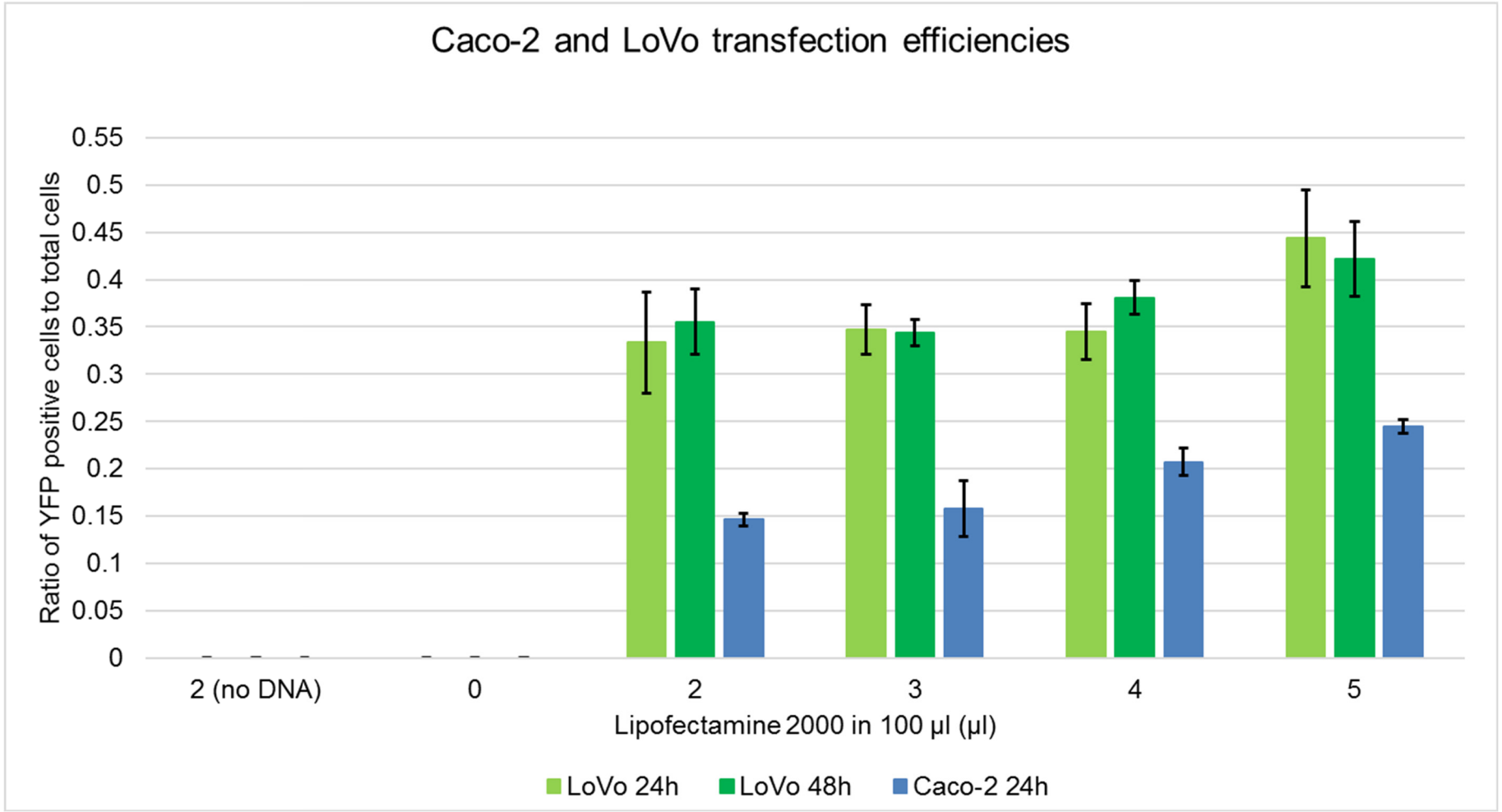
Caco-2 and LoVo transfection efficiencies
Ratio of YFP positive cells to total cells
0.55
0.5
0.45
0.4
0.35
0.3
0.25
0.2
0.15
0.1
0.05
0
2 (no DNA)
0
2
3
4
5
Lipofectamine 2000 in 100 µl (µl)
LoVo 24h
LoVo 48h
Caco-2 24h

Figure 4.1: Transfection efficiency of Caco-2 and LoVo cells as the proportion of YFP-positive cells
Caco-2 and LoVo cells were transfected with 10 ng/µl YFP-TUBA1B plasmid in 100 µl of Opti-MEM medium containing 2 µl, 3 µl, 4 µl, or 5 µl of Lipofectamine 2000. Two controls, one omitting plasmid DNA, and the other Lipofectamine 2000 were also included. The bar graphs represent the average proportion of YFP-positive cells in six random 10 × objective fields of view between two duplicate wells. The error bars represent the standard deviation.

Figure 4.2: Maps of the H-3082 and S-3198 full-length firefly luciferase expression plasmids
The *HPGD* promoter from −3082 to −1, and the *SLCO2A*1 promoter from −3198 to −1 were ligated at the −1 position relative to the firefly luciferase gene (luc2) start codon, resulting in a 7.3-kb and 7.4-kb plasmid, respectively. The pGL4.10[luc2] backbone also contains a β-lactamase (AmpR) gene for plasmid selection during *E. coli* culture. All regions indicated on the plasmid are shown to scale. The plasmid maps were designed using PlasMapper (Dong et al., 2004)

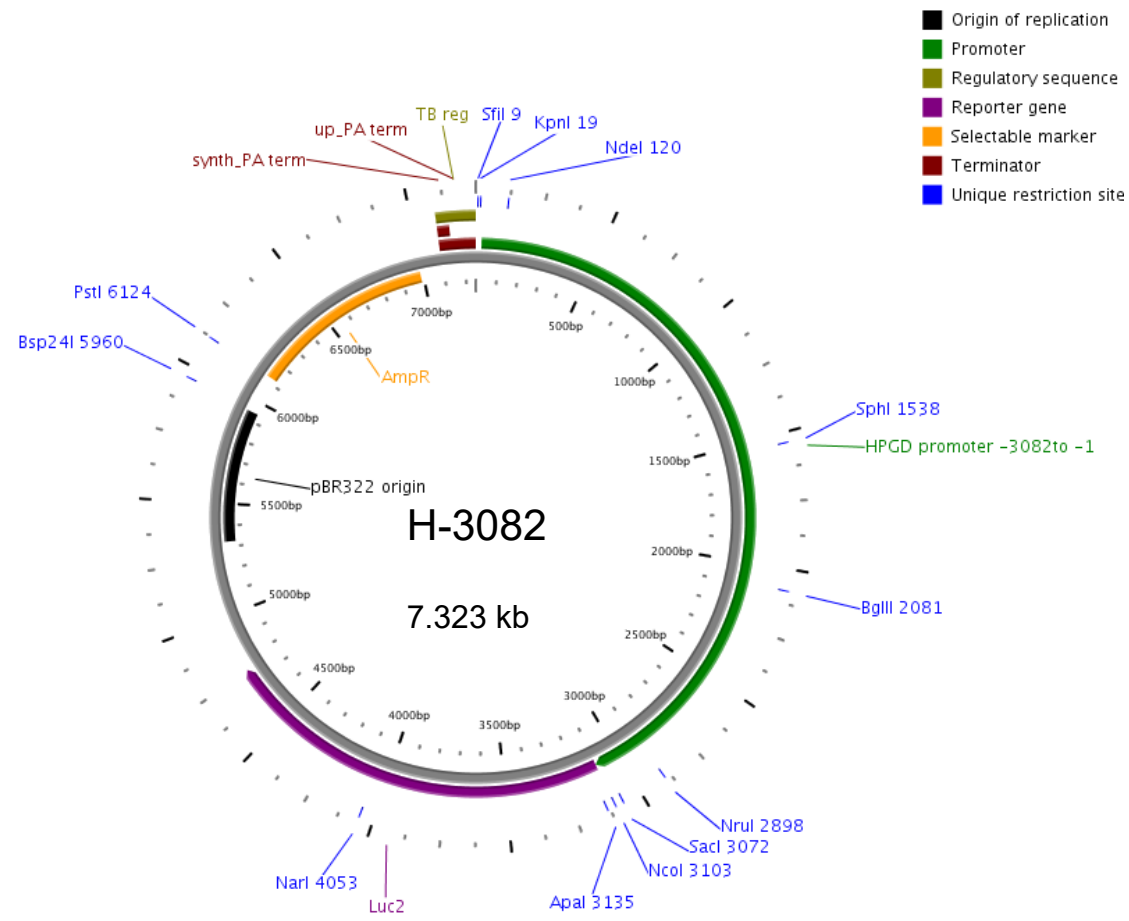
Origin of replication
Promoter
Regulatory sequence
Reporter gene
Selectable marker
Terminator
Unique restriction site
up_PA term
TB reg
SfiI 9
KpnI 19
NdeI 120
synth_PA term
PstI 6124
Bsp24I 5960
AmpR
pBR322 origin
H-3082
7.323 kb
SphI 1538
HPGD promoter -3082to -1
BglII 2081
NruI 2898
SacI 3072
NcoI 3103
ApaI 3135
NarI 4053
Luc2
7000bp
500bp
6500bp
1000bp
6000bp
1500bp
5500bp
2000bp
5000bp
2500bp
4500bp
3000bp
4000bp
3500bp

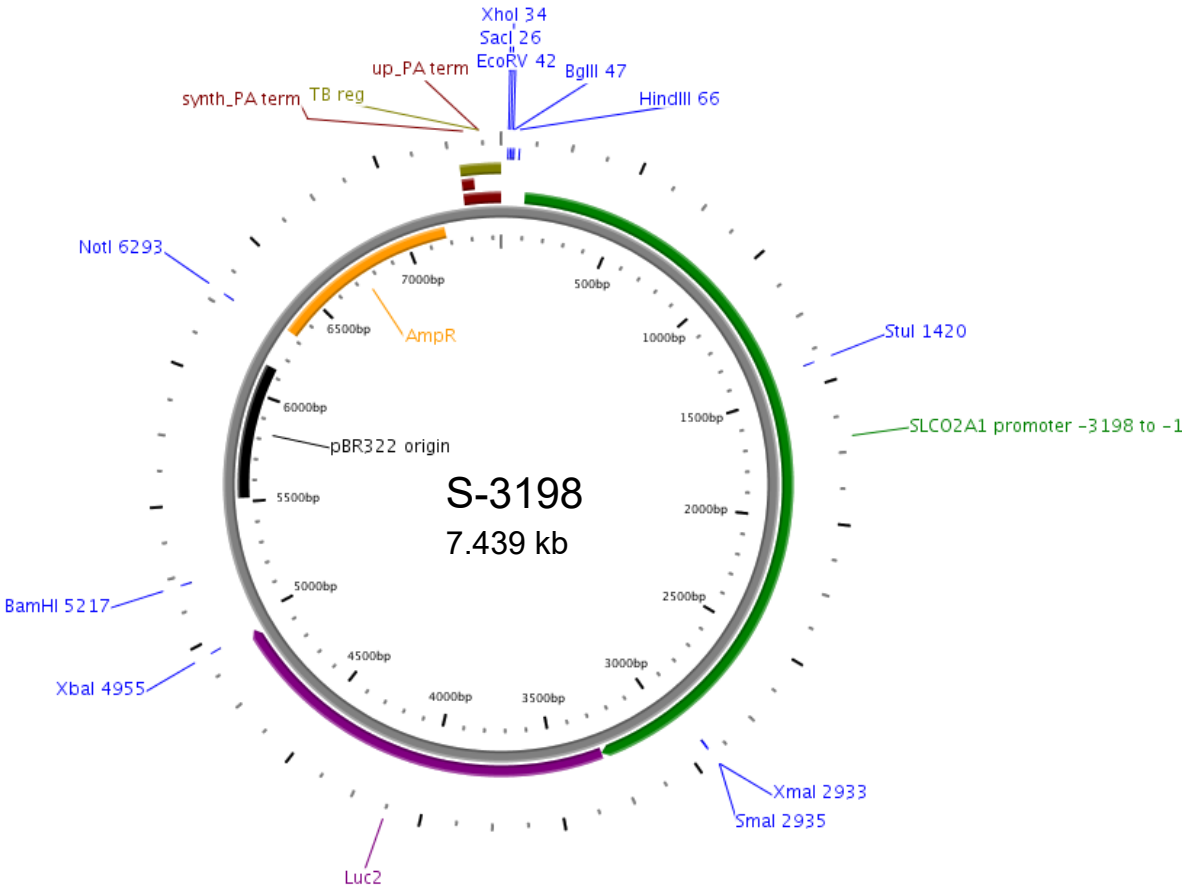
XhoI 34
SacI 26
EcoRV 42
BglII 47
up_PA term
HindIII 66
synth_PA term
TB reg
NotI 6293
StuI 1420
AmpR
SLCO2A1 promoter -3198 to -1
pBR322 origin
S-3198
7.439 kb
BamHI 5217
XbaI 4955
XmaI 2933
SmaI 2935
Luc2
7000bp
500bp
6500bp
1000bp
6000bp
1500bp
5500bp
2000bp
5000bp
2500bp
4500bp
3000bp
4000bp
3500bp

4.4.2 Promoter deletion series of *HPGD* and *SLCO2A1*

The full-length *HPGD* and *SLCO2A1* constructs H-3082 and S-3198 were designed to address the limitations of those used in Greenland et al (2000), and, Lu and Schuster (1998). In these studies, the promoter fragments were ligated upstream of the luciferase reporter gene using only available restriction sites, which in both cases resulted in loss of a promoter fragment close to the −1 position, and the inclusion of vector sequences between the 3′ end of the promoter and the luciferase gene.

As shown in the plasmid maps (Figure 4.2) and in Figures 4.3 and 4.4, the H-3082 and S-3198 constructs positioned the *HPGD* and *SLCO2A1* −1 position directly adjacent to the luciferase gene's ATG start codon. Therefore, the −3082 to −1 promoter region from *HPGD*, and −3198 to −1 in *SLCO2A1*, were positioned as in their native genes, modelling the native promoters more accurately than the earlier studies (Greenland et al., 2000; Nandy et al., 2003; Lu and Schuster, 1998).

Including the "full-length" H-3082 and S-3198, two series of nine promoter constructs each were initially generated both for *HPGD* (Figure 4.3) and *SLCO2A1* (Figure 4.4). These two figures show the lengths of the promoters in the deletion series to scale, with the number representing the length of the construct from the −1 position (section 2.3.9).The sizes of the smallest constructs were chosen to avoid the loss of transcriptional start sites observed in the RLM-RACE in the Caco-2 and LoVo cell lines.

Transfection of the deletion series was first carried out in the Caco-2 and LoVo cell lines. This was later expanded to include the SW480 and HT-29 cell lines, which retain expression of *HPGD* and *SLCO2A1* at the mRNA level. The A549 cell line was also transfected with both genes' deletion series, in the

expectation that its high *HPGD* expression (observed both here by RT-PCR and in the literature) would result in stronger activity (Chi et al., 2009), and due to the reported activity of the *SLCO2A1* promoter in A549 cells (Lu and Schuster, 1998). Prior to transfection, equimolar dilutions of the plasmids were prepared, and assayed using spectrophotometry with confirmation by agarose gel electrophoresis. Figures 4.5, 4.6 and 4.7 show the linearized *HPGD* and *SLCO2A1* deletion series constructs, in equimolar dilution with pUC19, prior to the transfection; the progressive truncation of the promoters is observed as a reduction of the linearized plasmid's length.

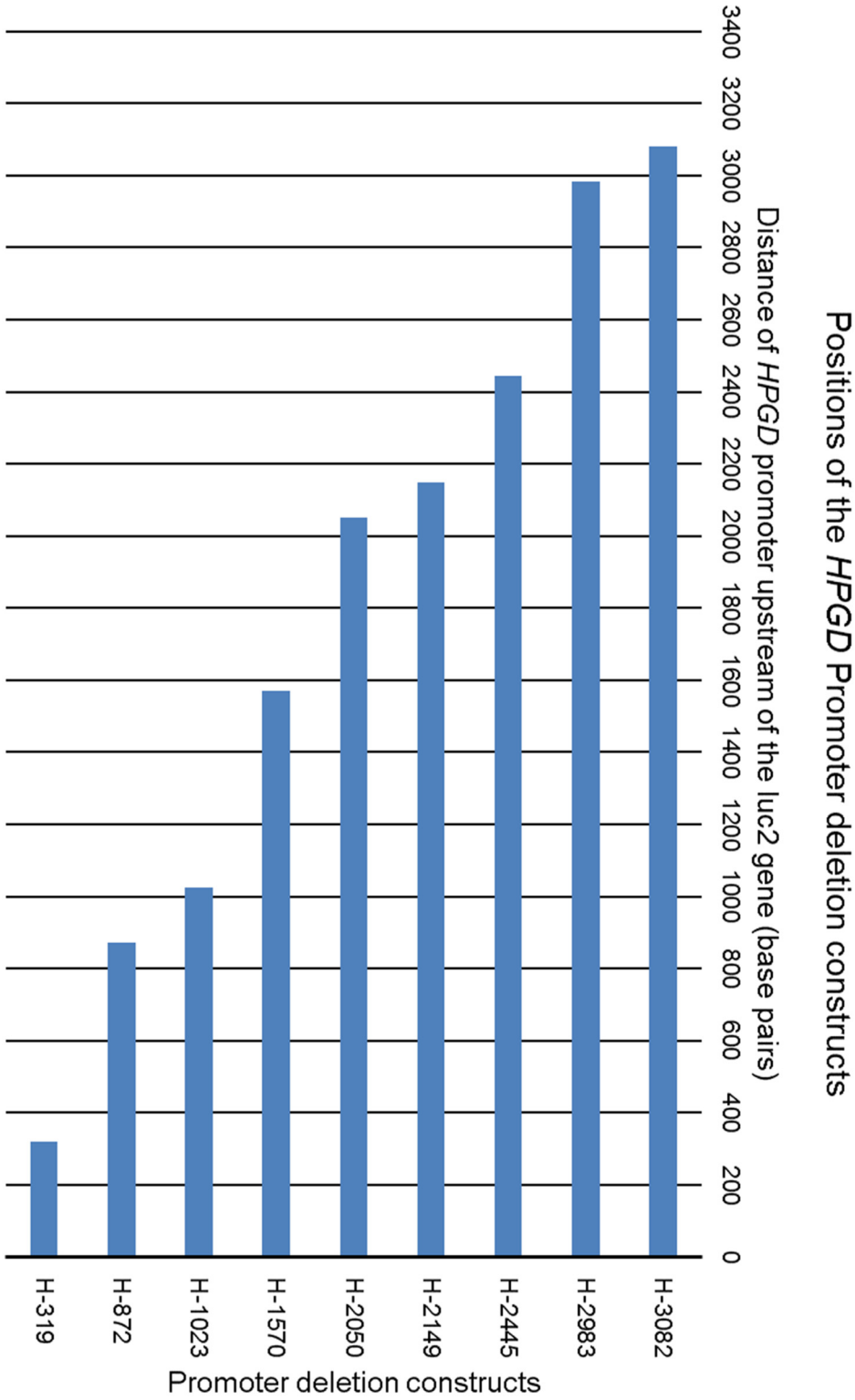

Figure 4.3: The 3-kb *HPGD* promoter region deletion series constructs
The full-length 3082-bp *HPGD* promoter construct was truncated at different positions to generate a total of 9 promoter constructs. The size of each promoter is shown to scale.

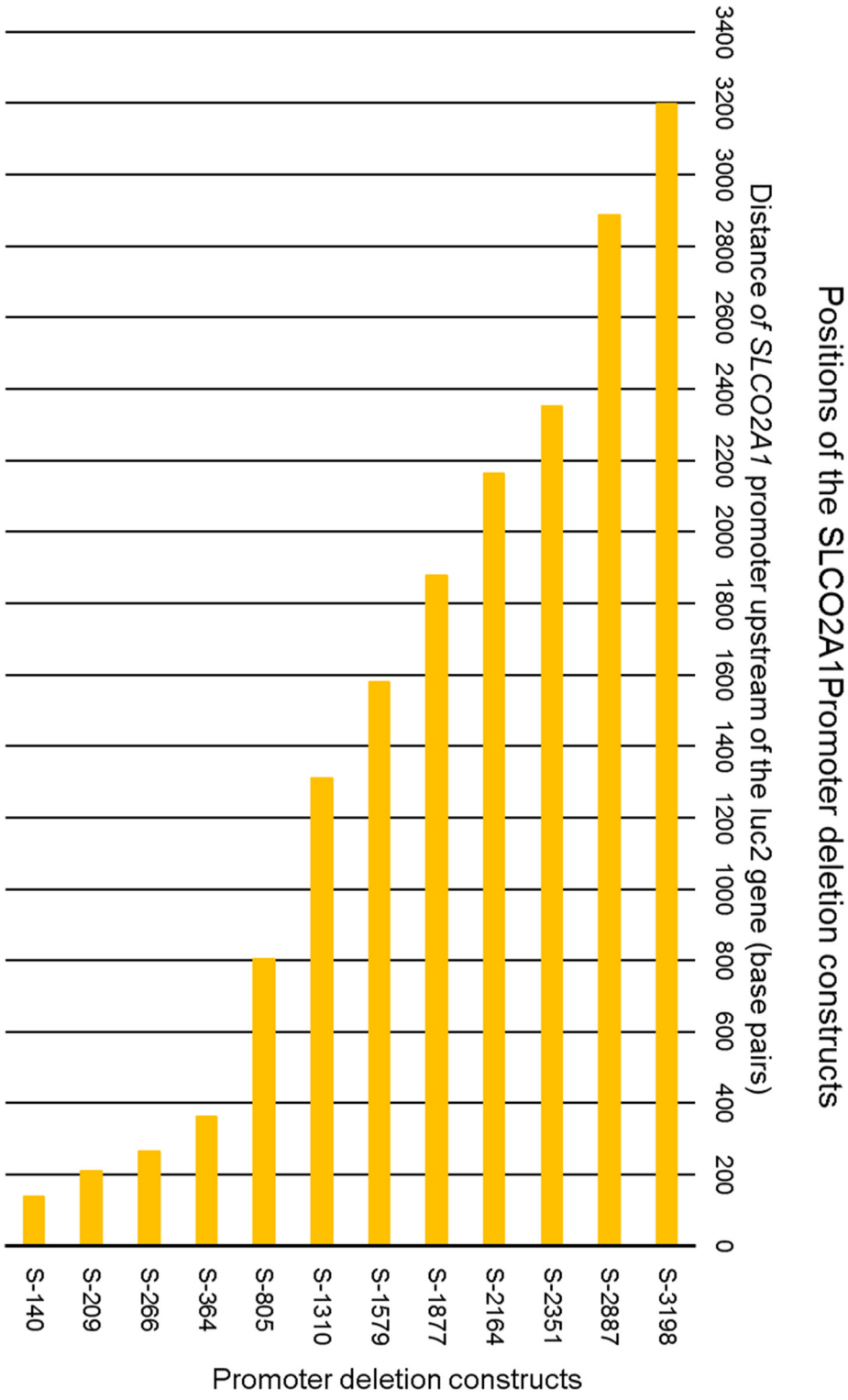

Figure 4.4: The 3-kb *SLCO2A1* promoter region deletion series constructs
The full-length 3198-bp *SLCO2A1* promoter construct was truncated at different positions to generate the initial panel of 9 promoter constructs (S-3198 to S-364). The S-266 to S-140 constructs were used to study the proximal 364 bp in more detail. Two constructs with an internal deletion were also made following the initial *SLCO2A1* deletion series results. The length of each promoter is shown to scale.

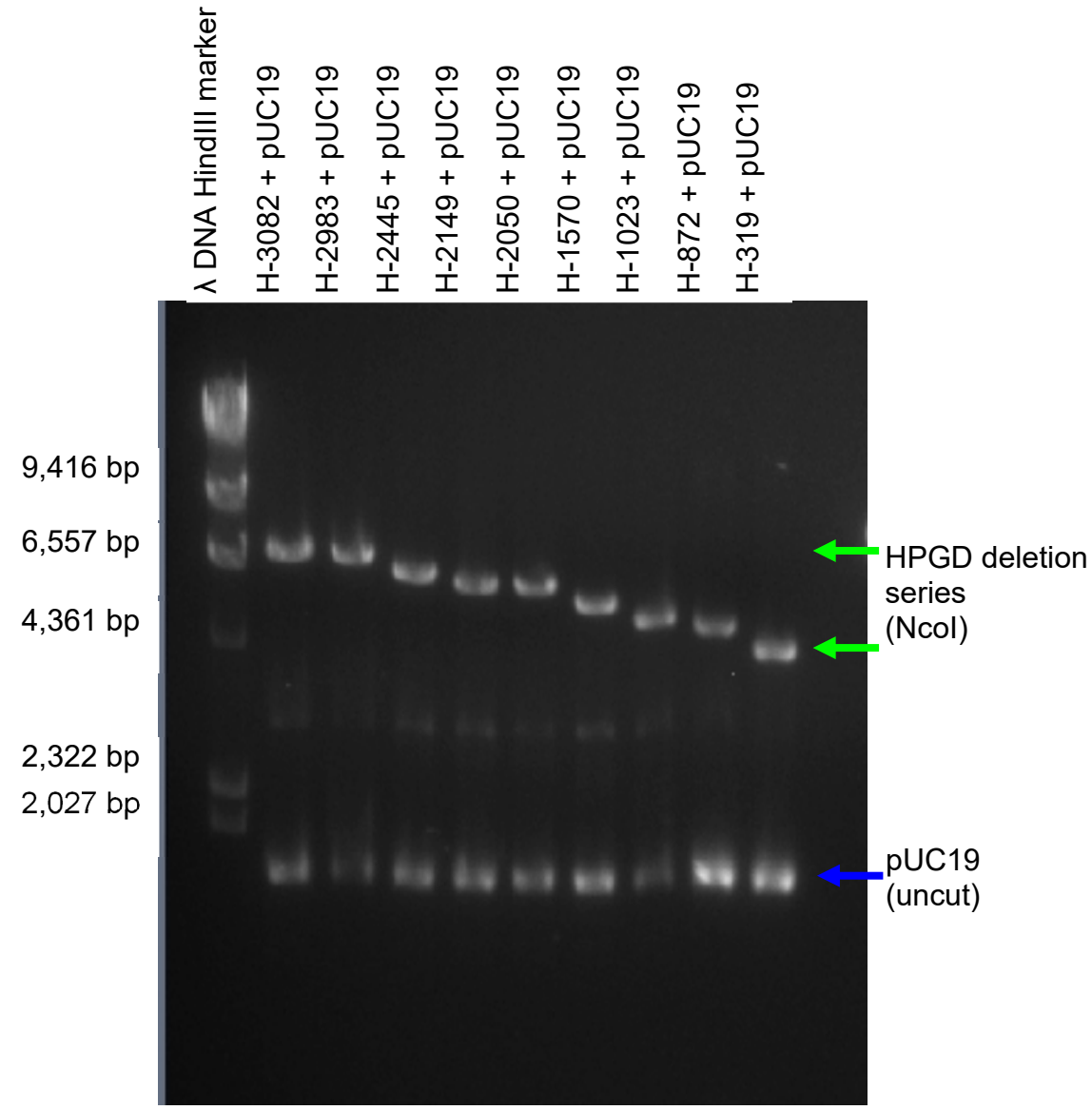

Figure 4.5: *HPGD* promoter deletion constructs, in equimolar solution with pUC19 DNA
The nine *HPGD* promoter deletion series constructs have been linearized by digesting with NcoI, and appear as the top bands (green arrows) that progressively decrease in size as the *HPGD* promoter is truncated. The weaker bands below 2,027 bp (blue arrow) represent uncut pUC19 plasmid. The faint band at ~3000 bp is pUC19 that was linearized during the purification of stock plasmid DNA.

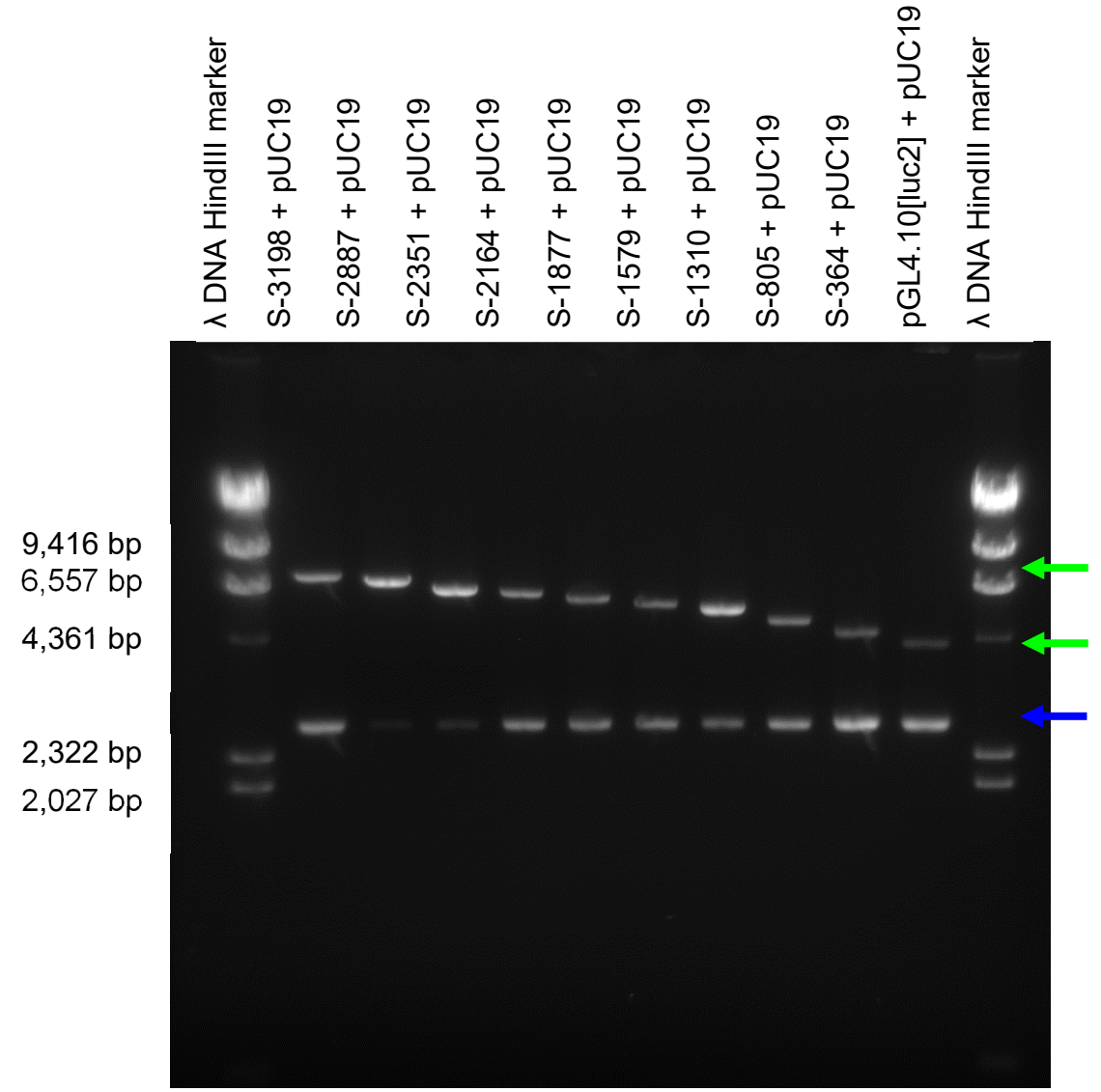

Figure 4.6: *SLCO2A1* promoter deletion constructs, in equimolar solution with pUC19 DNA
The nine *SLCO2A1* promoter deletion series constructs have been linearized by digesting with XhoI (green arrows), and appear as the top bands that progressively decrease in size as the promoter is truncated. The weaker bands below 2,027 bp (blue arrow) represent pUC19 linearized by digestion with NdeI.

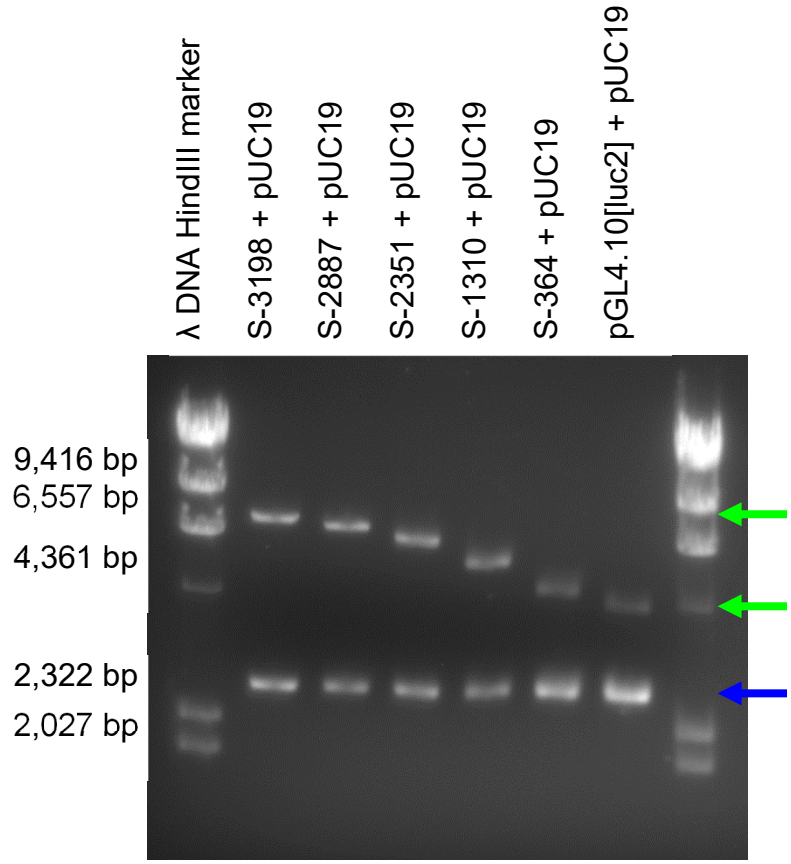

Figure 4.7: Equimolar dilutions of *SLCO2A1* constructs
The equimolar dilutions for S-2887, S-2351 and S-1310 were repeated (green arrows). The smaller bands (blue arrows) represent linearized pUC19

All constructs in the *HPGD* and S*LCO2A1* promoter deletion series demonstrated significantly higher activity than the promoterless pGL4.10[luc2] in the Caco-2, LoVo, HT-29 and SW480 cell lines, and (for *HPGD*) the A549 cell line. This was true even for the smallest of the constructs, H-319 and S-364, indicating that these two proximal regions were sufficient to drive expression of the luciferase gene in all of the cell lines.

For *HPGD* (Figure 4.8), the greatest luciferase activity was obtained in Caco-2 cells. Pairwise comparisons between successive truncations of the HPGD promoter revealed decrease in promoter activity between H-872 and H-319, which was, however, statistically significant only in the Caco-2 cells. This implies the presence of transcriptional activator binding sites in that region. This region contained an AP-1 binding site (−829 to −820) identified by Greenland et al (2000) and Nandy et al (2003), but not further tested in their experiments. Given that AP-1 transcription factors were shown to be able to drive *HPGD* expression (Nandy et al., 2003), it could be that the loss of this AP-1 site accounts for the reduction of promoter activity seen in H-319 (Figure 4.8).

Other changes in *HPGD* promoter activity, though statistically significant, were not consistent among the cell lines. The loss of the −1570 to −1023 region led to an increase in promoter activity in Caco-2 and SW480 cells, but a decrease in A549 cells. Given that A549 is a lung cancer cell line, this difference may reflect tissue of origin. An increase in promoter activity between −2445 and −2149, and −2050 to −1570, was observed in Caco-2 and SW480, but not the other three cell lines. These two regions encompass the “distal element” identified by (Nandy et al., 2003), whose loss increases, rather than decreases promoter activity in Caco-2 and LoVo cells.

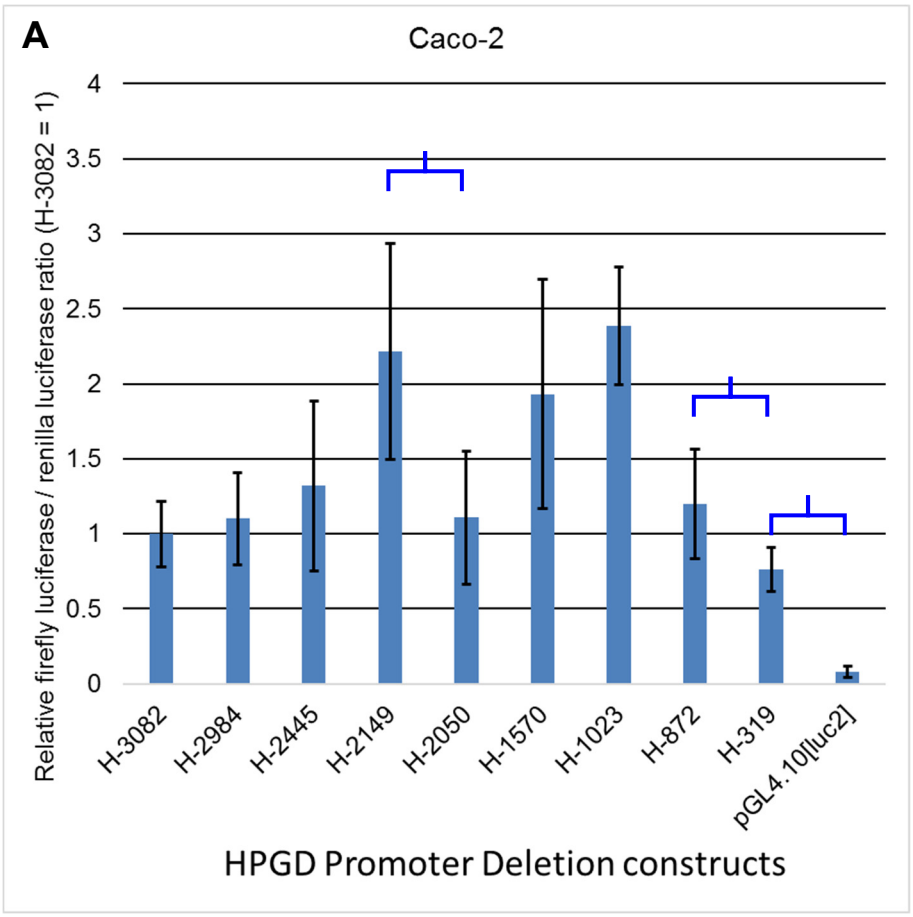
A
Caco-2
Relative firefly luciferase / renilla luciferase ratio (H-3082 = 1)
4
3.5
3
2.5
2
1.5
1
0.5
0
H-3082
H-2984
H-2445
H-2149
H-2050
H-1570
H-1023
H-872
H-319
pGL4.10[luc2]
HPGD Promoter Deletion constructs

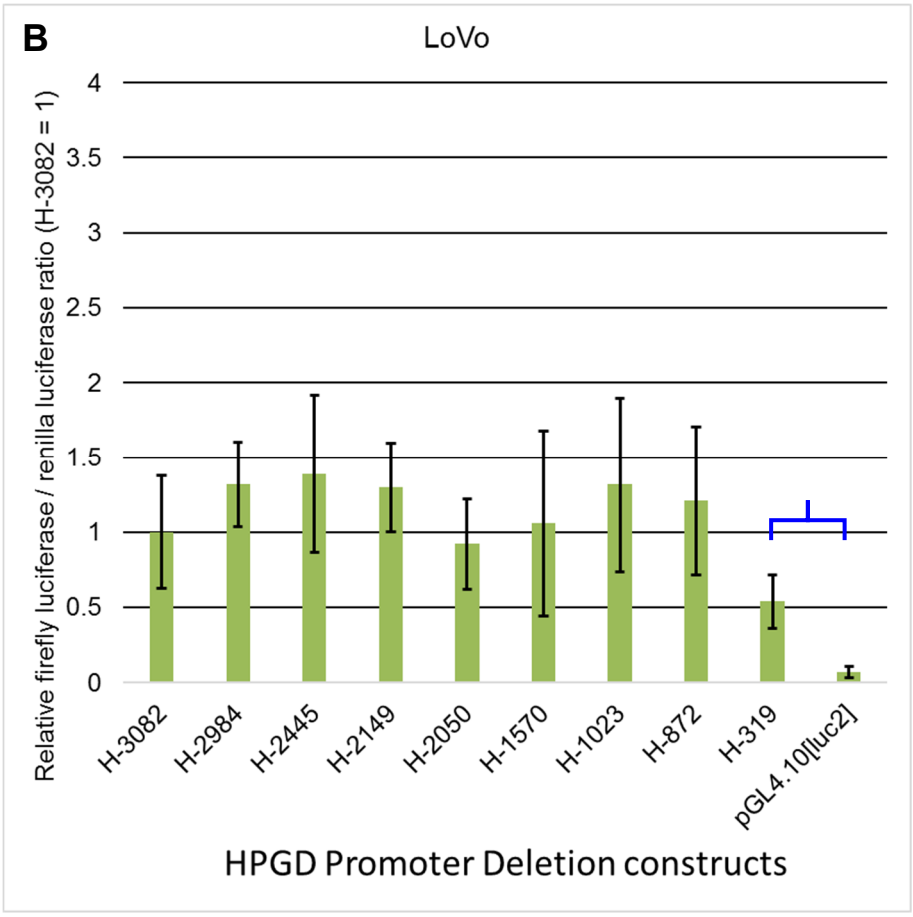
B
LoVo
Relative firefly luciferase / renilla luciferase ratio (H-3082 = 1)
4
3.5
3
2.5
2
1.5
1
0.5
0
H-3082
H-2984
H-2445
H-2149
H-2050
H-1570
H-1023
H-872
H-319
pGL4.10[luc2]
HPGD Promoter Deletion constructs

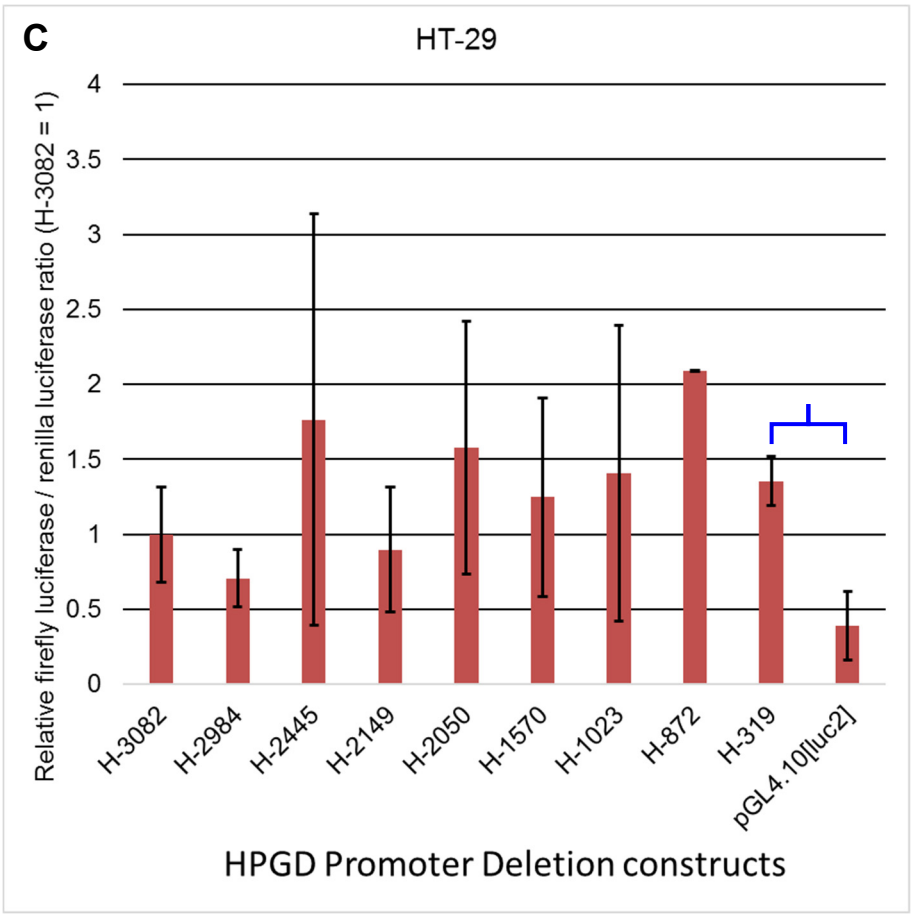
C
HT-29
Relative firefly luciferase / renilla luciferase ratio (H-3082 = 1)
4
3.5
3
2.5
2
1.5
1
0.5
0
H-3082
H-2984
H-2445
H-2149
H-2050
H-1570
H-1023
H-872
H-319
pGL4.10[luc2]
HPGD Promoter Deletion constructs

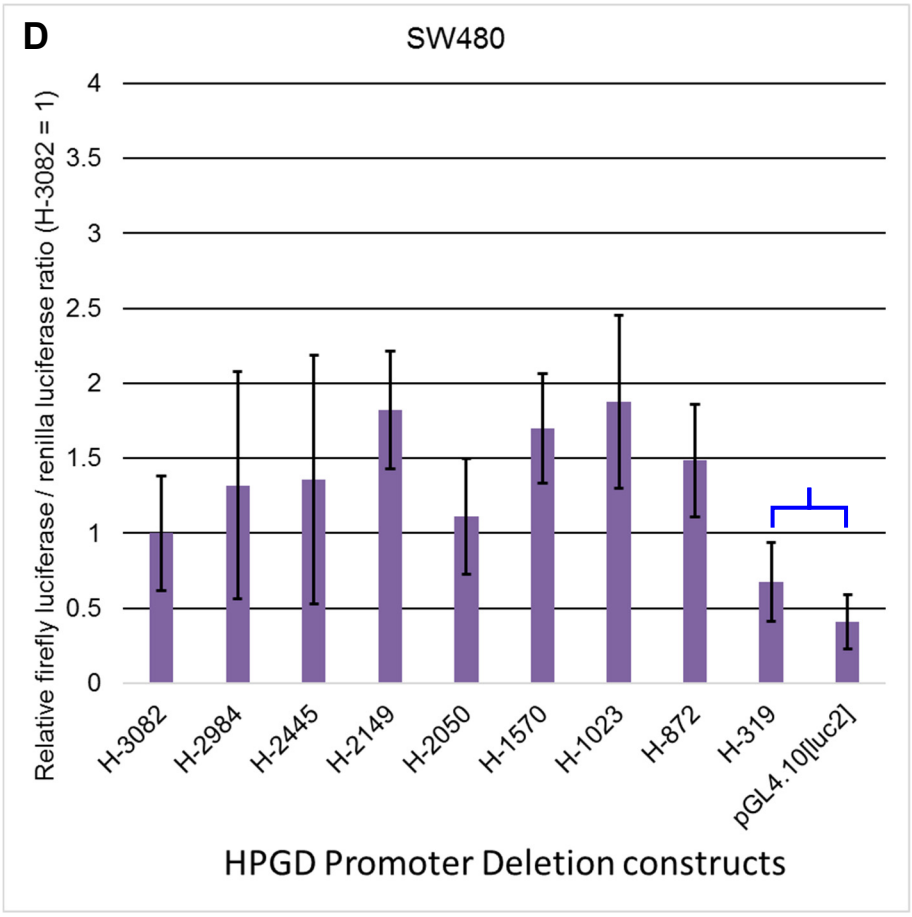
D
SW480
Relative firefly luciferase / renilla luciferase ratio (H-3082 = 1)
4
3.5
3
2.5
2
1.5
1
0.5
0
H-3082
H-2984
H-2445
H-2149
H-2050
H-1570
H-1023
H-872
H-319
pGL4.10[luc2]
HPGD Promoter Deletion constructs

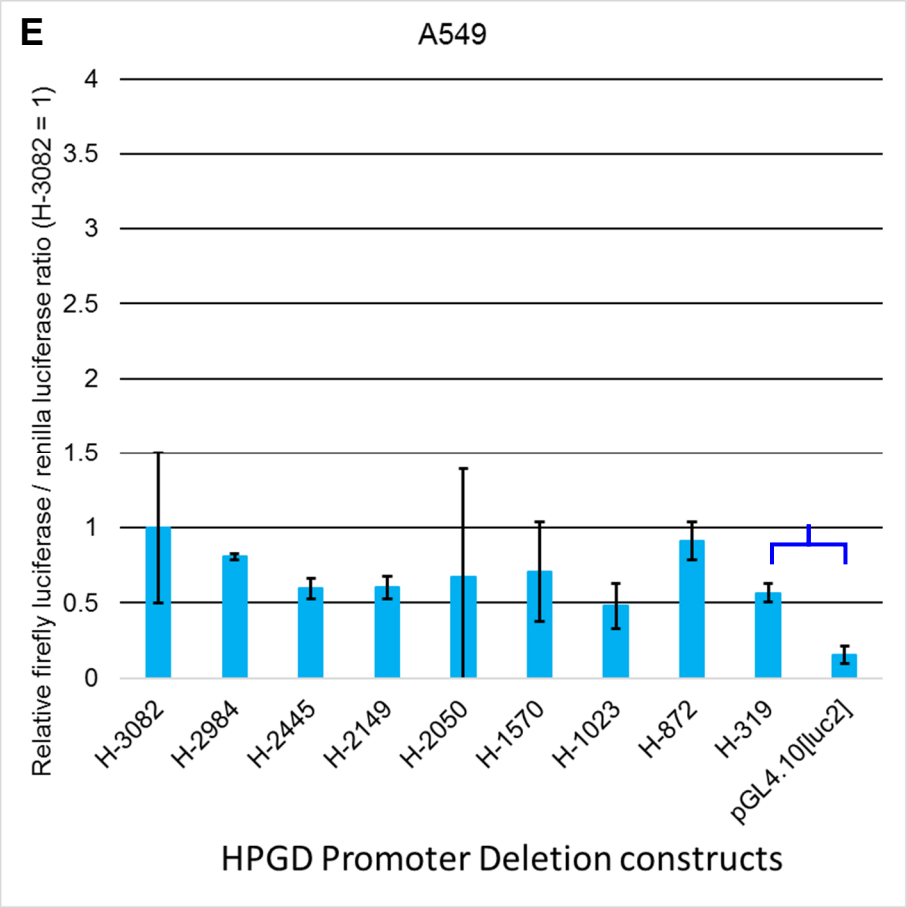

Figure 4.8: *HPGD* promoter activity in Caco-2 (A), LoVo (B), HT-29 (C), SW480 (D) and A549 (E) cells
The nine *HPGD* promoter deletion series constructs were transfected into four colorectal cancer cell lines and one lung adenocarcinoma cell line that had been found to express both *HPGD* and *SLCO2A1* mRNA. The absolute ratio of firefly luciferase to *Renilla* luciferase was normalised to the full-length H-3082 to allow comparison of changes in promoter activity across the four cell lines. These results represent three (Caco-2 and LoVo) and two (HT-29, SW480 and A549) independent experiments, with three replicates within each experiment. Statistics were carried out using the averages of each experiment's replicates. Student's *t*-test was used to determine significant changes in activity between adjacent deletion constructs (blue brackets), with $p \leq 0.05$ taken as significant. All constructs also showed significantly greater expression when compared to the promoterless vector, using Student's *t*-test. The error bars represent one standard deviation.

Unlike *HPGD*, no deletional analysis of the *SLCO2A1* promoter has been previously described. Across all four colorectal cancer cell lines (Figure 4.9), the smallest of the deletion constructs, S-364, appeared to be responsible for most of the observed *SLCO2A1* promoter activity. There initially appeared to be an increase in promoter activity when the 217-bp region between −2351 and −2164 was lost, across the Caco-2, LoVo, HT-29 and SW480 cell lines (Figure 4.9). However, this apparent change was found to be due to an error in preparing the S-2164 construct. When the transfections were repeated to address this, the activity of the S-2164 construct was lower than previously observed, and no significant decrease in promoter activity was found between −2164 and −1877, as shown in Figure 4.10. The key finding, that the proximal 364-bp region of the *SLCO2A1* promoter appeared to drive expression comparable to the full-length S-3198 construct, prompted further analysis of this region.

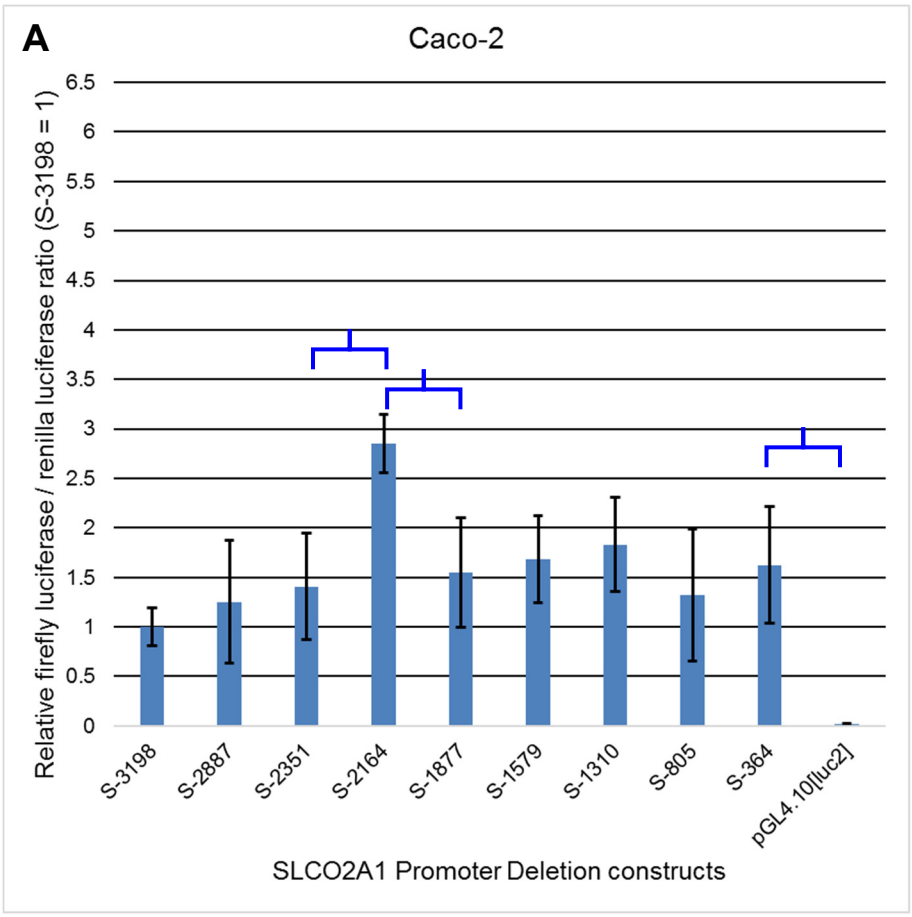
A
Caco-2
Relative firefly luciferase / renilla luciferase ratio (S-3198 = 1)
6.5
6
5.5
5
4.5
4
3.5
3
2.5
2
1.5
1
0.5
0
S-3198
S-2887
S-2351
S-2164
S-1877
S-1579
S-1310
S-805
S-364
pGL4.10[luc2]
SLCO2A1 Promoter Deletion constructs

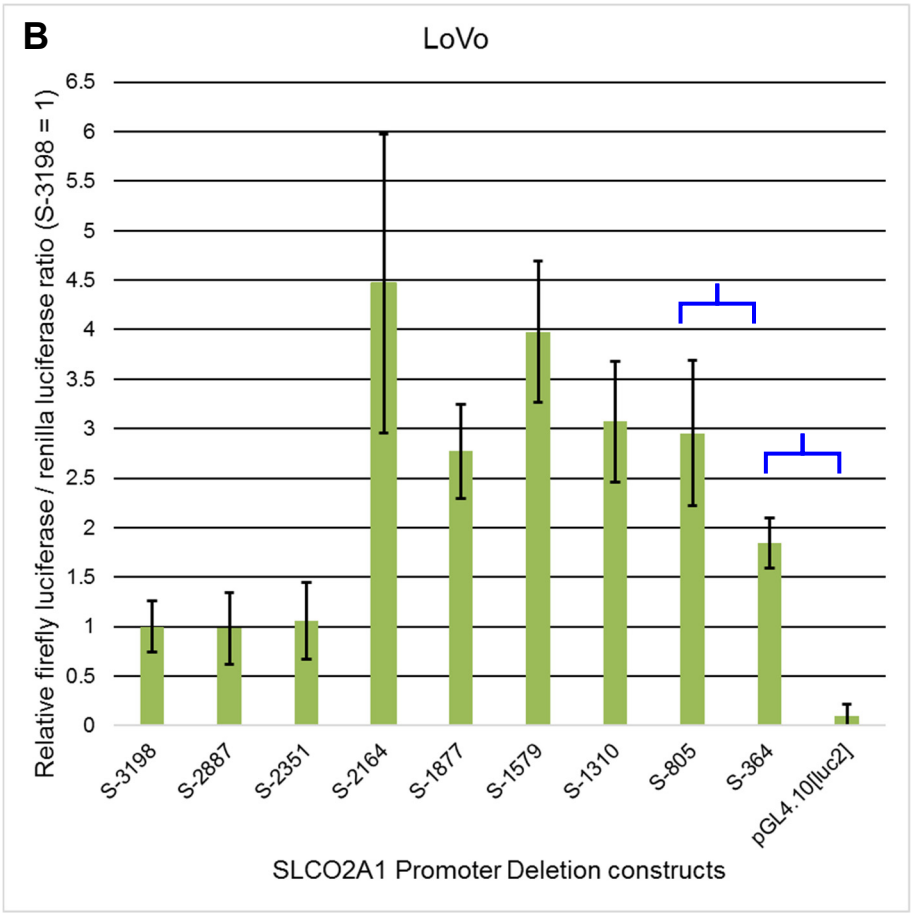
B
LoVo
Relative firefly luciferase / renilla luciferase ratio (S-3198 = 1)
6.5
6
5.5
5
4.5
4
3.5
3
2.5
2
1.5
1
0.5
0
S-3198
S-2887
S-2351
S-2164
S-1877
S-1579
S-1310
S-805
S-364
pGL4.10[luc2]
SLCO2A1 Promoter Deletion constructs

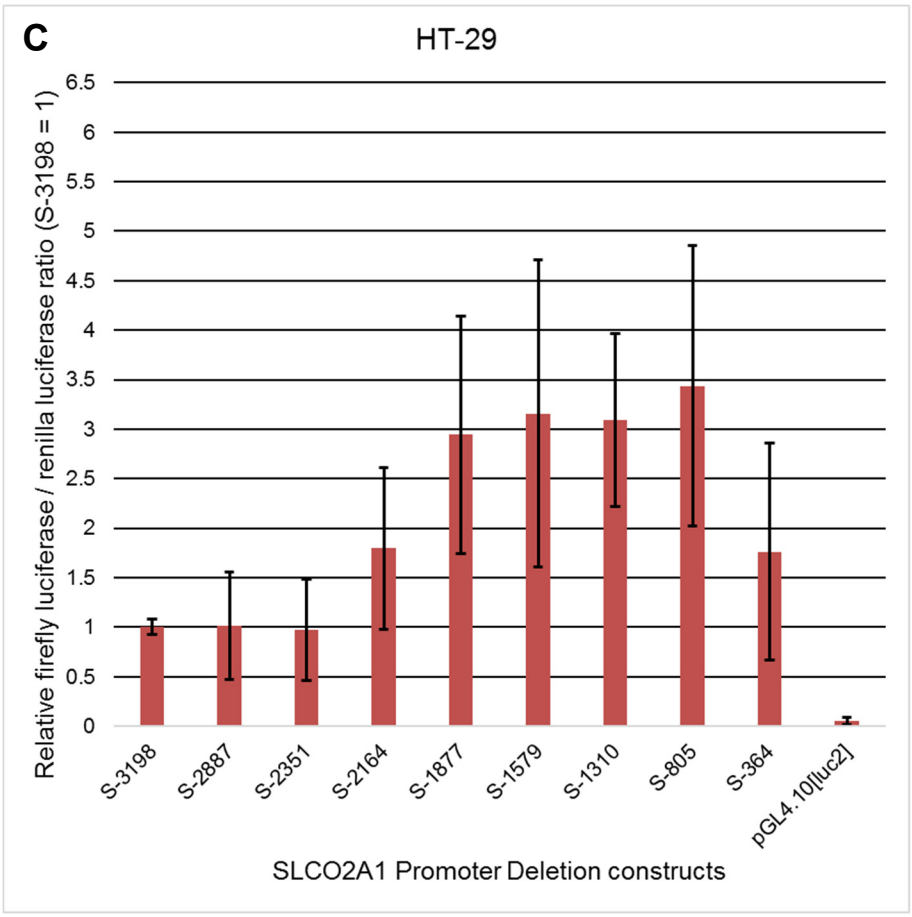
C
HT-29
Relative firefly luciferase / renilla luciferase ratio (S-3198 = 1)
6.5
6
5.5
5
4.5
4
3.5
3
2.5
2
1.5
1
0.5
0
S-3198
S-2887
S-2351
S-2164
S-1877
S-1579
S-1310
S-805
S-364
pGL4.10[luc2]
SLCO2A1 Promoter Deletion constructs

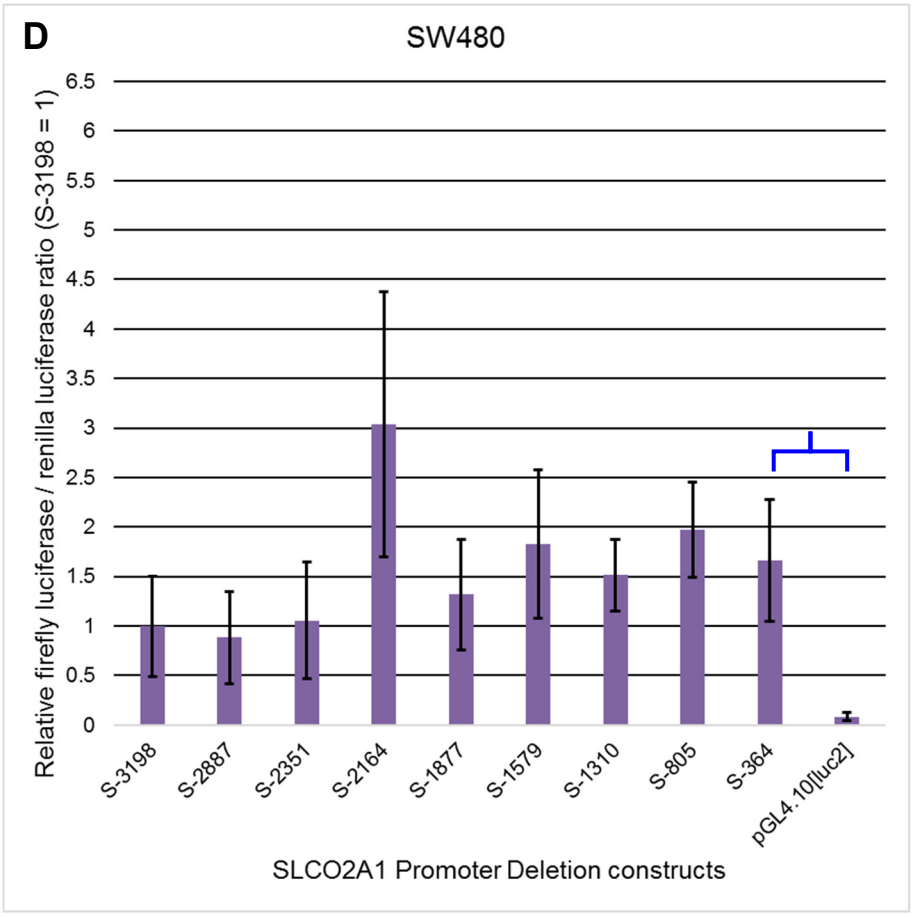
D
SW480
Relative firefly luciferase / renilla luciferase ratio (S-3198 = 1)
6.5
6
5.5
5
4.5
4
3.5
3
2.5
2
1.5
1
0.5
0
S-3198
S-2887
S-2351
S-2164
S-1877
S-1579
S-1310
S-805
S-364
pGL4.10[luc2]
SLCO2A1 Promoter Deletion constructs

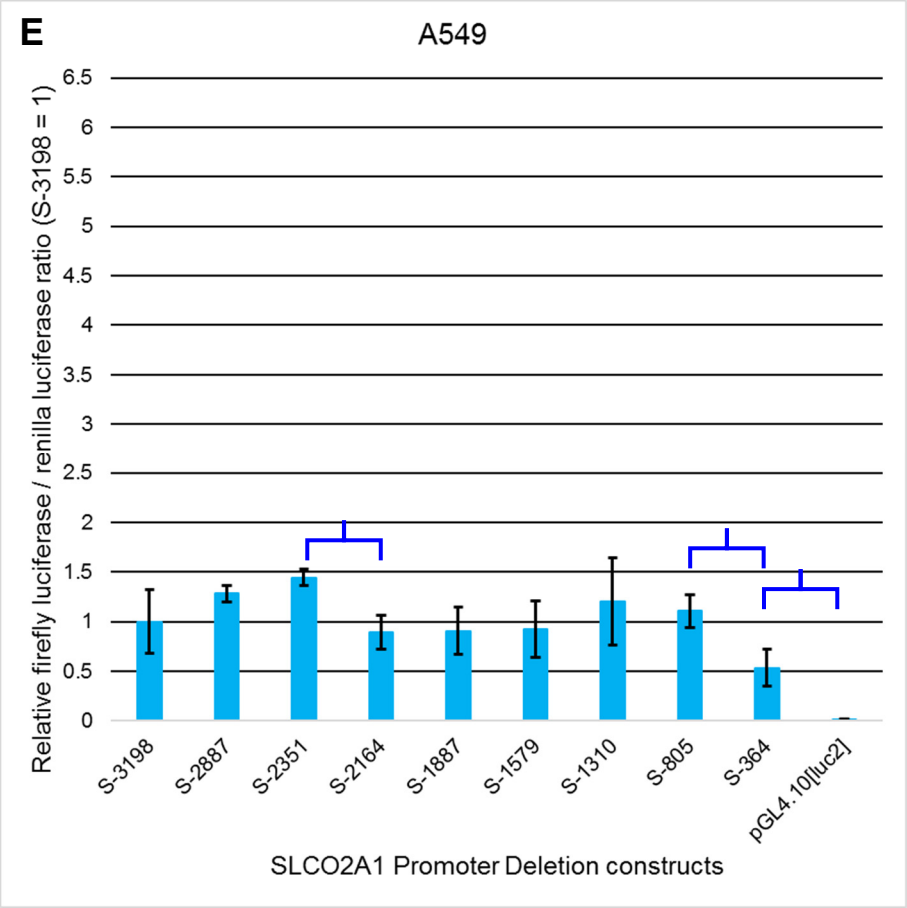

Figure 4.9: *SLCO2A1* promoter activity in Caco-2 (A), LoVo (B), HT-29 (C), SW480 (D) and A549 (E) cells
The nine *SLCO2A1* promoter deletion series constructs were transfected into four colorectal cancer cell lines that were found to express both HPGD and SLCO2A1 mRNA. The absolute firefly luciferase to *Renilla* luciferase ratio was normalised to the full-length S-3198 to compare any changes in promoter activity across the five cell lines. These results represent three (Caco-2, LoVo and A549) and two (HT-29 and SW480) independent experiments, with three replicates within each experiment. Statistics were carried out using the averages of each experiment's replicates. Student's *t*-test was used to determine the statistical significance of differences in promoter activity between adjacent constructs (blue brackets). The error bars represent one standard deviation.

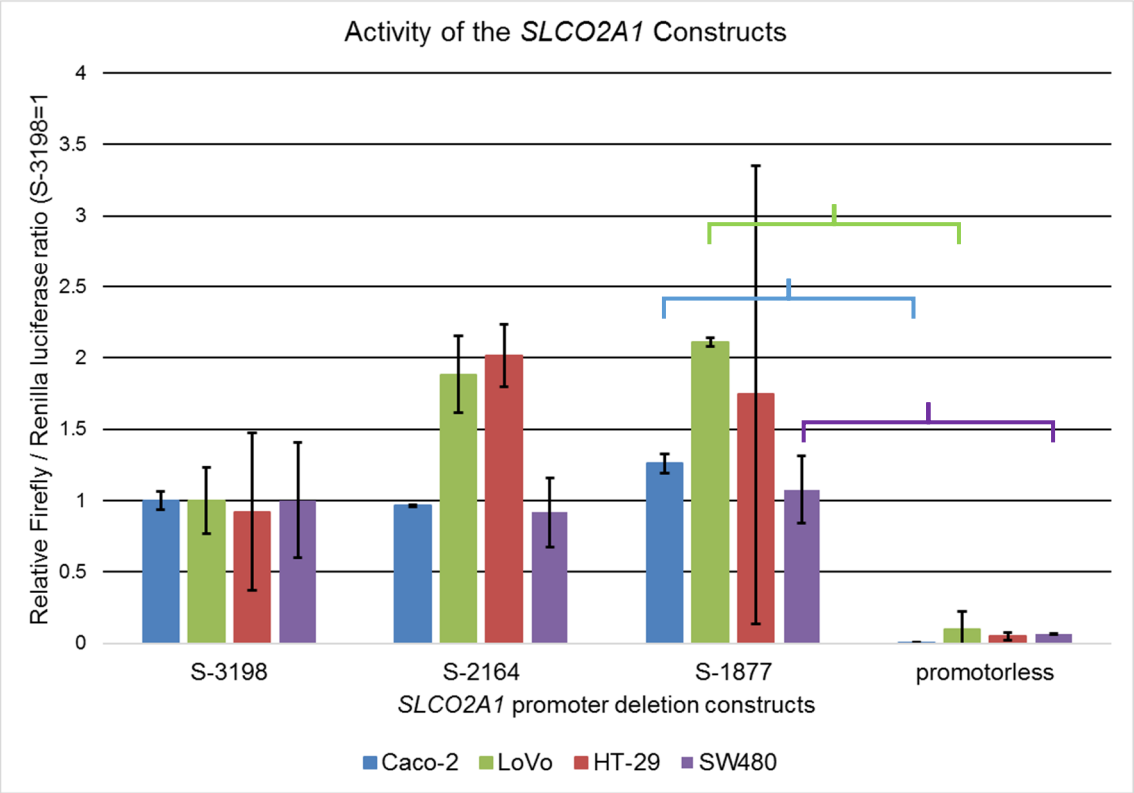

Figure 4.10: *SLCO2A1* promoter constructs S-3198, S-2164 and S-1877 activity in Caco-2, LoVo, HT-29, and SW480 cells

These results represent two independent experiments for each cell line, with three replicates within each experiment. Statistics were carried out using the averages of each experiment's replicates. Student's *t*-test was used to determine the significance of differences in promoter activity between adjacent constructs, with $p \leq 0.05$ (coloured brackets) taken as significant. One standard deviation is indicated by the error bars.

4.4.3 Fine deletion series for the *SLCO2A1* promoter (−364 to −140)

The transcriptional start sites (TSS) identified by RLM-RACE in Caco-2 and LoVo cells were used to define the minimum size of the new deletion constructs for the proximal 364-bp *SLCO2A1* promoter region. Caco-2 had one predominant TSS at −127 bp, while LoVo displayed a range of TSS from −159 to −108. The smallest construct was chosen to be at position −140. This means that for the LoVo cell line, a decrease in activity in the S-140 construct might be attributable to loss of the most downstream TSS. However, at least in Caco-2, and likely the SW480 cell lines, any loss of activity would indicate loss of transcription factor binding sites.

In Caco-2, there was a progressive reduction in activity as the SLCO2A1 promoter was truncated from −364 to −140 bp (Figure 4.11). A similar pattern was seen in SW480, in which reduction of promoter activity was statistically significant between successive constructs from S-364, except −364 and −266. In all three cell lines, there was a decrease in promoter activity from −266 to −209, and from −209 to −140, which was statistically significant for two of three cell ines. Although, as mentioned above, for the LoVo cell line, part of the reduction between −209 to −140 may be attributable to the loss of the −159 TSS, the similar observation in Caco-2 suggests that it may nonetheless reflect loss of transcriptional activator binding sites. Overall, these results suggested that the −364 to −140 region of the *SLCO2A1* promoter was essential for transcriptional activation, and is likely to contain transcription factor binding sites necessary for driving *SLCO2A1* expression.

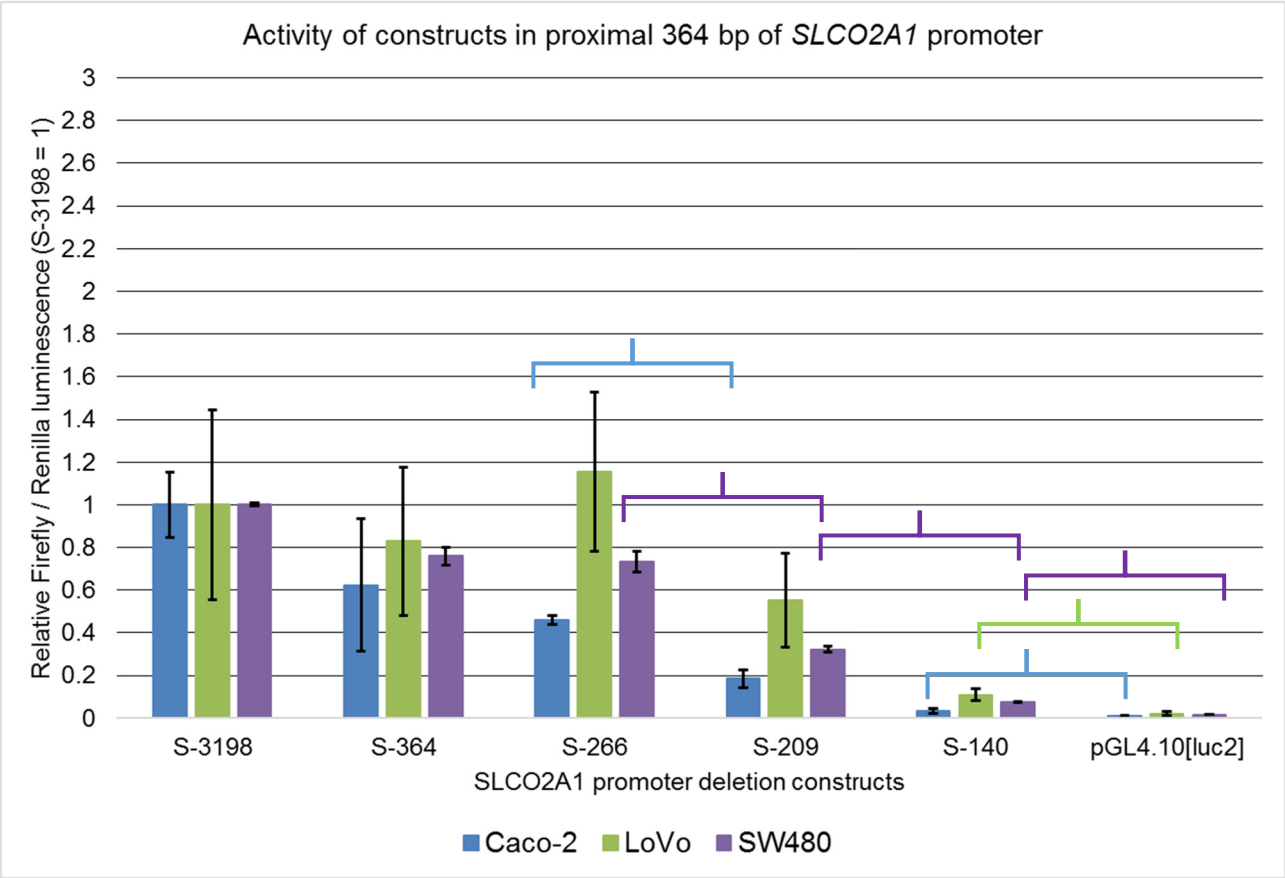

Figure 4.11: Activity of the proximal 364-bp *SLCO2A1* promoter region in Caco-2, LoVo, HT-29 and SW480
Two additional constructs at −266 and −140 were generated and transfected into the four colorectal cancer cell lines. The absolute firefly luciferase to *Renilla* luciferase luminescence ratio was normalised to the full-length construct S-3198 to detect changes in promoter activity. Significant differences are indicated by the coloured brackets. The error bars represent one standard deviation.

4.5 Discussion

The two promoter deletion series allowed characterization of the proximal 3-kb regions of the *HPGD* and *SLCO2A1* promoters in four colorectal cancer cell lines, and the A549 lung carcinoma cell line. The A549 line was included because of its known high expression of *HPGD* (Tong et al., 2006b; Uhlen et al., 2005), and evidence of *SLCO2A1* promoter activity (Lu and Schuster, 1998), despite its low levels of *SLCO2A1* mRNA and protein expression (Zhu et al., 2015; Shirasaka et al., 2013; Uhlen et al., 2005). The luciferase constructs were designed to approximate the native genomic context, without omitting sequences abutting the ATG start codon, or introducing foreign vector sequence between the promoter and luciferase reporter gene. In this way, they address some of the design limitations seen in previous reporter constructs (Lu and Schuster, 1998; Greenland et al., 2000). The H-3082 and S-3198 constructs and their derivatives might therefore prove to be useful, more up-to-date tools for studying *HPGD* and *SLCO2A1* regulation in a range of cell types. For example, a number of recent publications have continued to rely on the original Greenland et al (2000) *HPGD* constructs (Kim et al., 2014; Mehdawi et al., 2017; Smartt et al., 2012b), for which H-3082 and its derivatives could be a better alternative.

An interesting finding from the *HPGD* deletion series was that in the colorectal cancer cell lines, loss of the −2152 to −1944 region identified by Greenland et al, (2000) did not lead to a large reduction in promoter activity, and indeed, actually led to an increase in Caco-2 and SW480 cells. This highlights the importance of using model systems appropriate to the biological question being addressed, and adequate controls. (In the Greenland et al,

(2000) study, only the four cell lines derived from the placenta, uterus or myometrial smooth muscle showed a decrease in promoter activity.)

Likewise, the latter authors demonstrated a difference between a myometrial smooth muscle cell line (SKN) and primary cells from the same tissue type; the latter showed an increase in activity when the −2152 to −1944 region is lost. This observation highlights the caution needed when using a cell line system to model a normal tissue, since cell lines undergo physical and epigenetic changes (such as DNA methylation) that may not reflect the source cell type (Zolk et al., 2013).

Considering these various results, it appears that the “distal element” identified by Greenland et al. (2000) may, at least in some cell types, including Caco-2 and SW480, function to recruit transcriptional repressors rather than transcriptional activators. The AP-1 family of transcription factors suggested to drive HPGD expression in cell lines of uterine and placental tissue origin (Greenland et al., 2000; Nandy et al., 2003) may therefore not have a similar role in the colon. Other aspects of the earlier studies make interpretation difficult; the authors ligated the “distal element” upstream of their smallest construct, in effect deleting the intervening promoter sequence (Nandy et al., 2003). Having done so, they did not subsequently test whether their artificial set-up’s responsiveness to these transcription factors was retained in the native full-length promoter construct.

The AP-1 transcription factors, which include FOS, FOSB and JUN, generally act as transcriptional activators (Ashida et al., 2005; Trop-Steinberg and Azar, 2017). Some members of this family are overexpressed in colorectal cancer (Zhang et al., 2005), but their role in driving *HPGD* expression is probably limited, because *HPGD* is downregulated in colorectal cancer, despite

upregulation of c-Jun, Fra-1 or Fra-2 (Yan et al., 2004; Backlund et al., 2005; Kang et al., 2014). It may therefore be that other transcriptional repressors act on this region to reduce *HPGD* transcription.

The analysis of the *SLCO2A1* promoter was of particular interest because, unlike *HPGD*, it has not been characterised previously in the literature. The proximal −364 to −140 region of the *SLCO2A1* promoter was found to be contribute more than 80% of the observed activity of the full-length 3198 bp, in contrast to the H-319 *HPGD* construct. This suggests that key transcription factor binding sites for driving the *SLCO2A1* promoter are likely to be found within this proximal 224-bp region. This observation prompted the decision to focus further on *SLCO2A1*, and use a series of smaller deletion constructs to achieve greater resolution across this region.

The progressive decrease in promoter activity seen in Caco-2, HT-29 and SW480 between S-364, S-266, S-209 and S-140 supports this promoter region's importance, and suggests the sequential loss of multiple binding sites for transcription factors that induce gene expression, rather than the existence of a single dominant effector site. In the LoVo cell line, however, there was a small increase in activity between S-364 and S-266, which might suggest that in this cell line a repressor binds to this region. Overall, these results support the observation that in the cell lines employed here, the −364 to −140 region of the *SLCO2A1* promoter appeared to be the key driver for promoter activation, and should therefore be the focus for further study to understand how *SLCO2A1* is regulated at the transcriptional level.

One limitation of the present study is that the experimental approach has restricted analysis to the proximal 3 kb of the promoter. While promoter regions immediately upstream of the start site are essential for the binding of

transcription factors to drive expression, plasmid reporter systems cannot perfectly model the influence of enhancers or repressors that could be located tens of kilobases upstream (or downstream) of the promoter; these may interact with the promoter and its bound transcription factors through the 3-D organisation of the genomic DNA (Ptashne, 1988; Amano et al., 2009; Thurman et al., 2012; Olsen et al., 2013). Enhancer elements are typically identifiable as DNase I hypersensitive sites within in the genome (Sabo et al., 2004; Thurman et al., 2012). In the vicinity of *SLCO2A1*, such DNase I hypersensitive clusters can be seen approximately 30 kb and 60 kb from the transcriptional start sites. In addition to this limitation, a promoter deletion series cannot model the effects of DNA methylation, or of histone modifications that influence chromatin packing and the accessibility of the promoter sequence to transcription factors and the RNA polymerase II complex (Soboleva et al., 2014; Boudreau et al., 2017). For this reason, it cannot be assumed that the activity of a transfected promoter will always reflect the level of endogenous gene expression in the recipient cell line; the A549 cell line is an example of this, given the relatively strong promoter activity it displayed in the deletion series, contrasting with its very low levels of native *SLCO2A1* mRNA and protein (Uhlen et al., 2005; Shirasaka et al., 2013).

Despite these caveats, given that *SLCO2A1* transcriptional regulation has not been characterised before, scrutinizing the promoter for transcriptional control regions was an essential first step in understanding the expression of this gene, including the mechanism by which it becomes downregulated in colorectal cancer. Very few published studies have attempted to link *SLCO2A1* regulation in colorectal cancer with known pathways (such as Wnt/β-catenin) (Smartt et al., 2012a) that are known to be perturbed in colorectal cancer, even though it has been shown that like *HPGD*, *SLCO2A1* expression is reduced or

lost in adenocarcinomas relative to normal colonic mucosal epithelium (Smartt et al., 2012a; Smartt et al., 2012b; Takeda et al., 2015; Tootle, 2013; Holla et al., 2008). In this regard, when compared to *HPGD, PTGS2* and other enzymes in the PGE_2 synthesis and degradation pathway, *SLCO2A1* has remained understudied in this context. There remains a need to link upstream signalling pathways with transcription factors that exert their effect directly on the *SLCO2A1* promoter, in order to understand the mechanism of this dysregulation.

Chapter 5 Transcriptional Regulation of the proximal 364 bp *SLCO2A1* promoter

5.1 Introduction

A large component of the 3198 bp *SLCO2A1* promoter's activity in colorectal cancer cell lines was found to be driven by the -364 to -140 bp region of the gene (Chapter 4). As this 224 bp was likely to contain important transcription factor binding sites to drive transcription, it was investigated further. Eukaryotic transcription factor binding sites are on average approximately 10 bp in size, but can range between 5 to 22 bp (Stewart et al., 2012). Therefore, this ~200bp region was expected to contain a large number of transcription factor binding sites, both for different transcription factors but also multiple sites for certain transcription factors. Searching for potential transcription factor binding sites within this region of the *SLCO2A1* promoter was therefore deemed to be the next logical step. The approach where following the determination of a gene's transcriptional start sites, a promoter deletion series is used to reveal which specific areas of a promoter should be subjected to further analysis for their role in transcriptional regulation, has proved successful previously (Sirois et al., 1993; Yang et al., 2008). For *HPGD*, Greenland et al (2000), and Nandy et al (2003) represented an example of this methodology.

Two approaches were selected to help determine sites on the *SLCO2A1* promoter that could bind transcription factors. A targeted approach utilised publicly available data from chromatin immunoprecipitation and sequencing (ChIP-seq) experiments. This allows selection of transcription factors likely to act at the gene locus of interest, and whose binding sites can be found on the DNA sequence with a reasonably high similarity to the predicted or

experimentally determined consensus sequence (Messeguer et al., 2002; Matys et al., 2003). With this approach, prior knowledge could be used to then mutate the chosen transcription factor binding sites, and in the first instance, test for an increase or decrease in promoter activity. The obvious demerit is that this method can only test the action of the transcription factor binding sites that have previously been identified and characterised. Another limitation is that the output from such analysis shows the probable specificity of the transcription factor to a DNA sequence, but not its actual affinity to it.

On the other hand, a hypothesis-free approach where DNA sequences in a region of interest are disrupted by introducing short DNA inserts at random, offers the ability to detect novel transcription factor binding sites which a targeted approach would not. Linker Scanning Mutagenesis is an established technique that, from its inception, continues to be used for this purpose (McKnight and Kingsbury, 1982; Montero-Conde et al., 2017). Mutations are introduced randomly in a region of interest within a gene promoter, with or without inserting additional DNA, to identify positons where these lead to a disruption in the transcriptional expression (or, protein function when applied to coding regions) (McKnight and Kingsbury, 1982; Dykxhoorn et al., 1997; Montero-Conde et al., 2017). Therefore, there was merit in considering both approaches to study *SLCO2A1*, given the complementary information they could yield.

5.2 Aims

Identify transcription factor binding sites that could modulate the activity of *SLCO2A1* within the -364 to -140 region of its promoter.

5.3 Methods

5.3.1 Bioinformatic search for transcription factor binding sites in the *SLCO2A1* promoter sequence

Potential transcription factor binding sites within the -364 to -140 positions of the *SLCO2A1* promoter were identified following a bioinformatics search using the ALGGEN-PROMO (Messeguer et al., 2002), CIS-BP (Weirauch et al., 2014) and footprint-db (Sebastian and Contreras-Moreira, 2014) databases. Potential transcription factor binding sites that were common across two or more databases were considered for further analysis (Mathelier et al., 2016).

RT-PCR was used to assay for the expression of transcription factors in Caco-2, LoVo, HT-29 and SW480 cells, whose binding sites were found on the -364 to -140 region of the *SLCO2A1* promoter. Any binding sites for transcription factors not expressed by these cells could be thus excluded.

5.3.2 Site-Directed Mutagenesis

Site-Directed mutagenesis was carried out using the S-364 deletion construct as the wild-type template, to introduce adjacent substitutions in the two most highly conserved bases within the transcription factors' binding site consensus. This strategy was informed based on similar work carried in other publications that utilised this method to mutate predicted transcription factor binding sites (Saunders et al., 2016; Sabui et al., 2014; Abbas et al., 2014). The introduced mutations were confirmed by sequencing (section 2.3.7) the 364 bp *SLCO2A1* promoter region cloned into the pGL4.10[luc2] plasmid backbone.

5.3.3 Linker Scanning Mutagenesis

Linker-scanning mutagenesis (section 2.3.11) was used to introduce random 15 bp insertions within the same -364 to -140 region of the *SLCO2A1* promoter to disrupt potential transcription factor binding sites (Stewart et al., 2012; Wilkins et al., 1953; Xu et al., 1996). Initially, this required mutating the pGL4.10[luc] backbone's native NotI restriction site to prevent it from interfering with the subsequent digestion steps. The key steps in this procedure are outline in Figure 5.1. The constructs were sequenced across the ligation sites and insert in order to confirm the presence of the 15 bp insertion within the *SLCO2A1* promoter, and to exclude any generated reagents where the insertion occurred within the short length of plasmid backbone or firefly luciferase gene.

5.3.4 Dual Luciferase assay

Colorectal cancer cell line cells were transfected with the S-364 derived constructs from the site-directed mutagenesis and linker-scanning mutagenesis in order to assess the activity of the *SLCO2A1* promoter through its induction of the firefly luciferase reporter gene relative to the wild-type S-364 (sections 2.5.3 and 2.5.5)

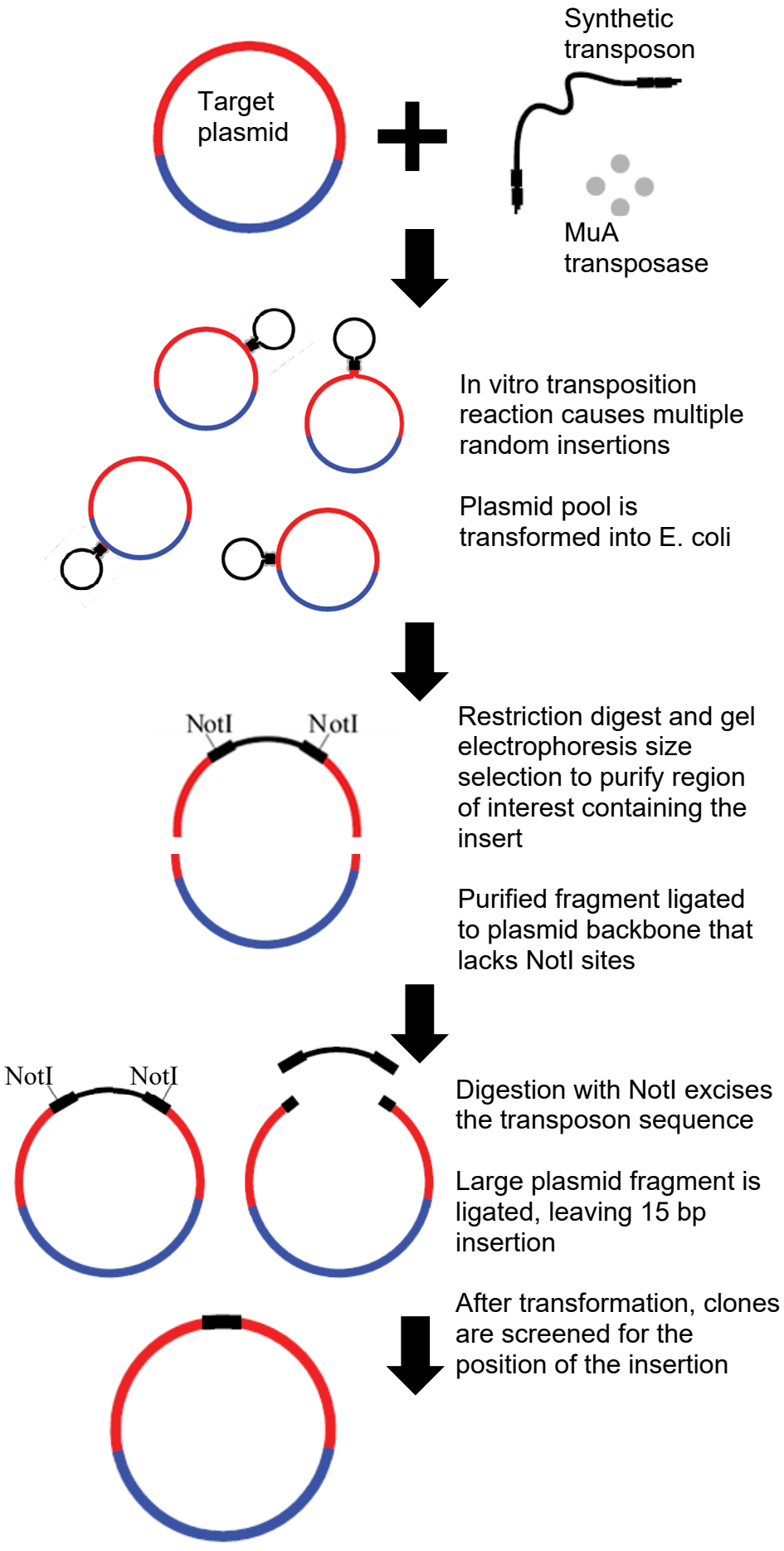
Target plasmid
Synthetic transposon
MuA transposase
In vitro transposition reaction causes multiple random insertions
Plasmid pool is transformed into E. coli
NotI
NotI
Restriction digest and gel electrophoresis size selection to purify region of interest containing the insert
Purified fragment ligated to plasmid backbone that lacks NotI sites
NotI
NotI
Digestion with NotI excises the transposon sequence
Large plasmid fragment is ligated, leaving 15 bp insertion
After transformation, clones are screened for the position of the insertion

Figure 5.1: General overview of the linker scanning mutagenesis procedure

The transposon's integration into the plasmid DNA is mediated by the MuA transposase. This can occur within the cloned promoter region of interest (red), or in the plasmid backbone (blue). NotI digestion was then used to excise the transposon and leave a 15 bp insertion. This mechanism results in a pool of plasmids with random insertions. Images adapted from Thermo Fisher Scientific Inc (2012) Mutation Generation System Kit Technical Manual F-701 v2_2012. (Thermo Fisher Scientific, 2017)

5.4 Results

5.4.1 Bioinformatic identification of potential transcription factor binding sites

The CIS-BP database (Weirauch et al., 2014) predicts transcription factor binding sites based on Protein Binding Microarray data (Weirauch et al., 2014), and the ALGGEN-PROMO (Messeguer et al., 2002) and footprint-db (Sebastian and Contreras-Moreira, 2014) databases predict transcription factor binding sites using curated data, predominantly from ChIP experiments. As each of these databases uses different datasets and prediction algorithms, transcription factors binding sites that were common between two or more datasets were considered to be more likely to correctly identify functional elements in the *SLCO2A1* promoter sequence. However, greater weight was given to concordance with or between overlapping binding sites from ALGGEN-PROMO and footprint-db, where the transcription factor binding site consensus sequences have been validated.

CIS-BP uses three different algorithms to predict transcription factor binding sites (Weirauch et al., 2014). These are the archetypical log-odds position weight matrix (PWM) algorithm (Stormo, 1990), a binding energy-based algorithm (Zhao and Stormo, 2011), and an octamer-based algorithm specific to Protein Binding Microarray data (Berger et al., 2006). Individually the databases identified a large number of potential transcription factor binding sites, which was expected given the short consensus sequence size for transcription factors. Figure 5.2 shows the overlap of three transcription factors selected for further study, as a number of the databases and algorithms had a high level of agreement in the position of the binding sites

SLCO2A1 promoter sequence -364 bp to -140

CCGGGCCCGCCACCTCCTTCCCTCCCTCTCCGCCTCCCGGCAGGCGGGATCTTCTCGGGGCAGTCAAGCCTCGCGGGTCGCTGCGGCGTCACACCTGTCTGAGGGGGCGGCGGCGGCGGCGGCGGCGGGGCGGGGGCTCGTAGCG
CCTTTGACACCCGAGGAAAAGAGGGAGGAGGGAGAGCGCGTTTCATCATCGGCGGCGGCCACTTATAAAAACTTCTAGGC

SLCO2A1 promoter sequence -284 bp to -140 bp (first 80 bp (blue) removed for clarity to show the alignments below)

CTGCGGCGTCACACCTGTCTGAGGGGGCGGCGGCGGCGGCGGCGGCGGGGCGGGGGCTCGTAGCGCCTTTGACACCCGAGGAAAAGAGGGAGGAGGGAGAGCGCGTTTCATCATCGGCGGCGGCCACTTATAAAAACTTCTAGGC

Cis-BP (log-odds PWM) SP GGGGCGGCGGCGGCGGCGGCGG

Cis-BP (energy PWM) **SP** GGGGGCGGC

ALGGEN-PROMO **SP** GGGGCGGCGG GGGGCGGGGG

Footprint-db **SP** CGGCGGCG CGGCGGCG

TGAGGGGGCGGCGGCGGCGG GGCGGCGGGGC Cis-BP (log-odds PWM) **EGR**

TGAGGGGGCG GGCGGCGGGGC Cis-BP (energy PWM) **EGR**

GTCACACC Cis-BP (octamer) **EGR**

GGCGGCGG GGCGGCGG Footprint-db **EGR**

Cis-BP (energy PWM) **CDX2** TTATAAAA

Cis-BP (octamer) **CDX2** TTATAAAA

Footprint-db **CDX2** ATAAA

Figure 5.2: Predicted transcription factor binding sites in the −364 bp to −140 bp region of the *SLCO2A1* promoter

The different algorithms identified binding sites for transcription factors of the SP family (highlighted in yellow), EGR family (highlighted in light blue), and CDX2 (highlighted in pink). A GC-rich region between -265 and -228 (highlighted in light grey) contained most of the EGR sites, and all of the SP sites, whilst a region identified between -157 and -150 (light grey) contained all the sites identified for CDX2.

SP site for Cis-BP (log- odds) extended from -261 to -238.
SP site for Cis-BP (energy) extended from -262 to -254.
SP sites for ALGGEN-PROM extended from -261 to -252, and -238 to -229.
SP sites for Footprint-db extended from -257 to -250, and -248 to -241.
EGR sites for Cis-BP (log- odds) extended from -265 to -246, and -244 to -234.
EGR sites for Cis-BP (energy) extended from -265 to -256, and -244 to -234.
EGR sites for Cis-BP (octamer) extended from –277 to -270.
EGR sites for Footprint-db extended from –259 to -252, and -250 to -243.
CDX2 site for Cis-BP (energy) extended from -157 to -150.
CDX2 site for Cis-BP (octamer) extended from -157 to -150.
CDX2 site for Footprint-db extended from -155 to -151.

A single CDX2 binding site was identified by footprint-db and two of the CIS-BP algorithms (Figure 5.2). It was not identified by ALGGEN-PROMO, as it was absent from this database, however, the overlap between the sequences identified by the algorithms was high. The region between -265 bp and -228 bp was GC-rich and contained binding sites for the SP and the majority of the EGR family of transcription factors (Figure 5.2). Although some of the regions identified had good overlap between algorithms, other regions were identified only by a single method. There was also some overlap in the sites for SP and EGR, due to the similarity in their consensus sequences, which made differentiating the two, and subsequent selection of appropriate bases to mutate challenging (Mathelier et al., 2016; Van Poucke et al., 2009)

5.4.2 Expression of *SP*, *EGR* and *CDX* transcription factors by colorectal cancer cell lines

RT-PCR was used to determine if members of these transcription factor families were natively expressed in the Caco-2, LoVo, HT-29 and SW480 cell lines. Expression of these transcription factors should, if they bind to the *SLCO2A1* promoter, drive expression of luciferase constructs, and mutation at the consensus binding site would be expected to reduce promoter activity

As shown in Figure 5.3, *EGR1* and *EGR4* appeared to be expressed across all four of the cell lines, though expression levels were variable between cell lines as judged by comparison to the *GAPDH* control. *EGR3* appeared to be expressed only in the LoVo cell line. *EGR2* yielded no visible bands, which in the absence of a known positive control, cannot be attributed to lack of expression by all four cell lines. However, overall, these results indicated that a

number of the *EGR* family transcription factors were expressed, at least at the mRNA level, by all four of the colon cancer cell lines.

Expression of the SP family members was assessed in the same cell lines. All four colorectal cancer cell lines showed expression of the widely expressed *SP1*, *SP2*, *SP3* and *SP4*, though expression was considerably weaker for *SP2* (Figure 5.4). The remaining family members have a more tissue specific restricted expression pattern, and where detected were restricted to one (*SP5),* or two (*SP9*) of the colon cell lines. All of the *SP8* amplicons were of the incorrect size, and were likely to be off target products. However, several members of the SP family transcription factors were expressed in each colon cell line indicating they could be possible activators for *SLCO2A1* transcription. (Schuster et al., 1997; Lu et al., 1996; Bao et al., 2002; Kang et al., 2005).

As shown in Figure 5.5, *CDX2* was expressed in Caco-2, LoVo, and SW480 cells, but not in HT-29 cells. The MDA-MB231 breast cancer cell line, on the other hand, showed no *CDX2* expression, which was consistent to the observed specificity of *CDX2* to cells derived from the intestinal and colonic epithelium with very low or undetectable expression in other organs (Hryniuk et al., 2014; Dalerba et al., 2016; Qualtrough et al., 2002). Taken together, the RT-PCR data indicated that the four cell lines expressed a number of the *SP*, *EGR* family members, and Caco-2, LoVo and SW480 expressed *CDX2,* consequently these factors could bind to the sites identified in the *SLCO2A1* promoter sequence, and may be responsible for the activity observed in the deletion series.

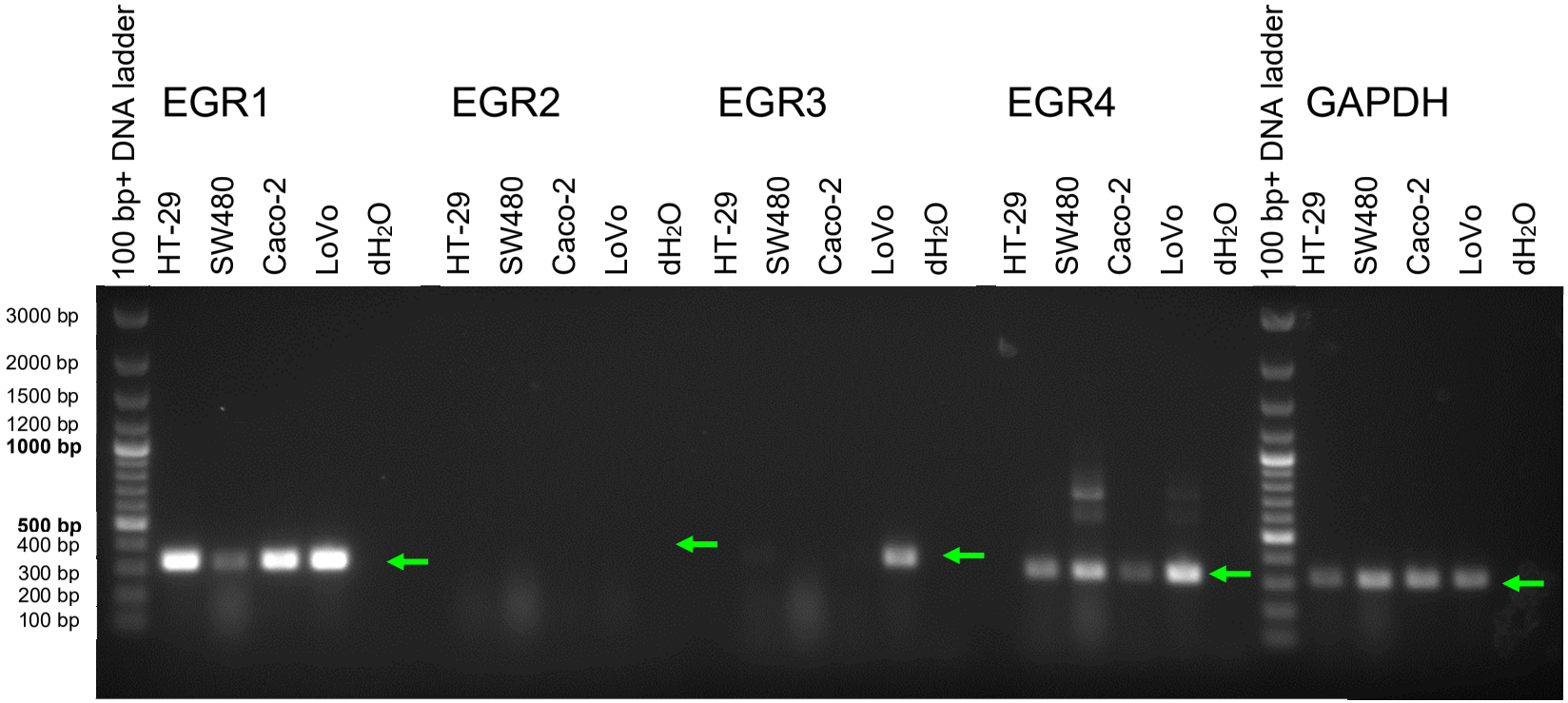

Figure 5.3: RT-PCR of *EGR* transcription factors and *GAPDH* in Caco-2, LoVo, HT-29 and SW480 cell lines

PCR products of the correct size (green arrows) were amplified and sequence verified. All four colorectal cancer cell lines natively express *EGR1* and EGR4 mRNA, with only LoVo showing expression of *EGR3*. The secondary, weaker bands visible in *EGR4* for SW480 and LoVo may be alternative mRNA transcripts or gDNA. The same batch of cell RNA was used for the SP, EGR, CDX2 and GAPDH RT-PCR reactions

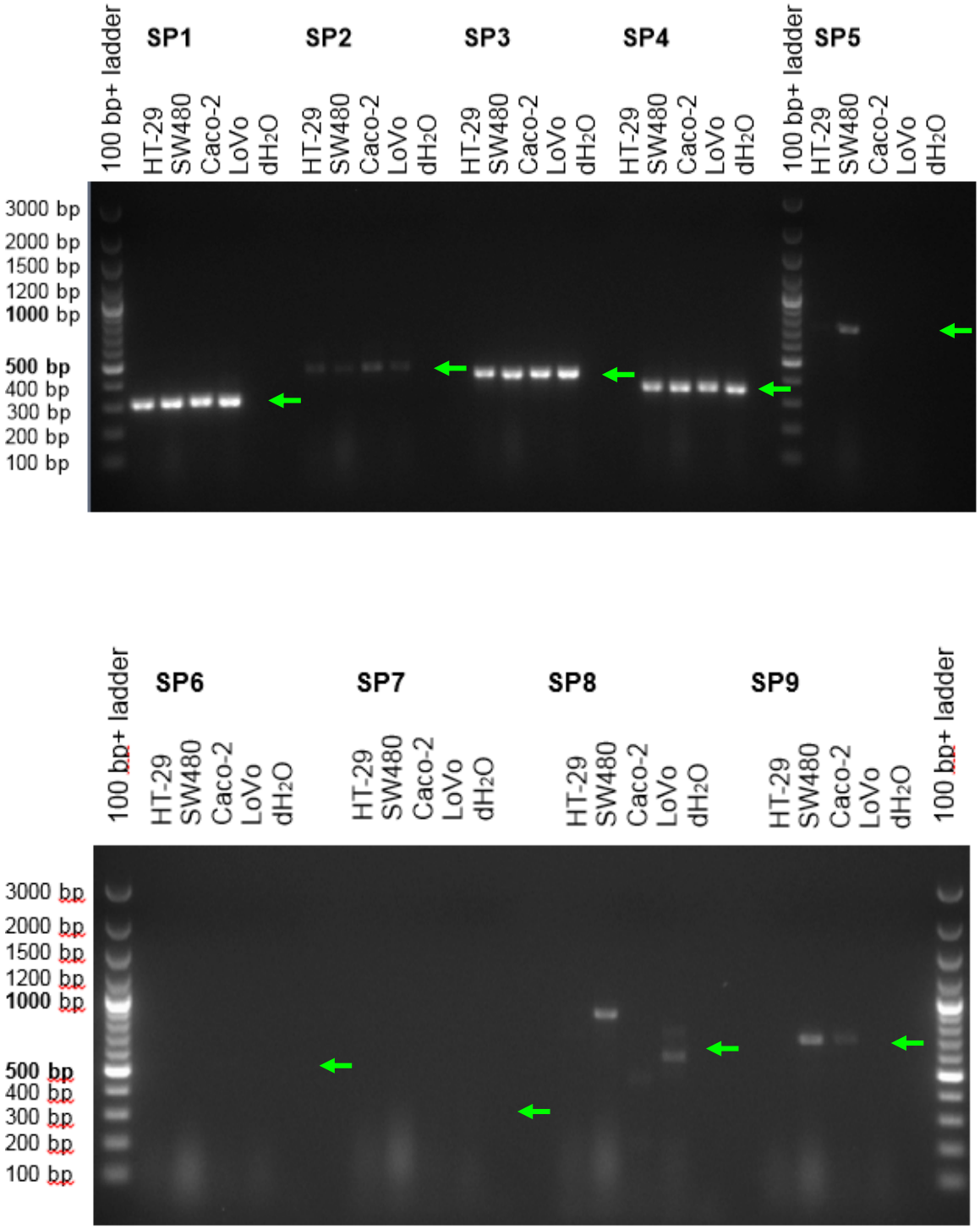

Figure 5.4: RT PCR of *SP* transcription factors and in Caco-2, LoVo, HT-29 and SW480 cell lines

The expected sizes for (green arrows) *SP1* through to *SP9* were 307, 446, 414, 347, 721, 506, 300, 675, 667 bps respectively. The same batch of cell RNA was used for the SP, EGR, CDX2 and GAPDH RT-PCR reactions

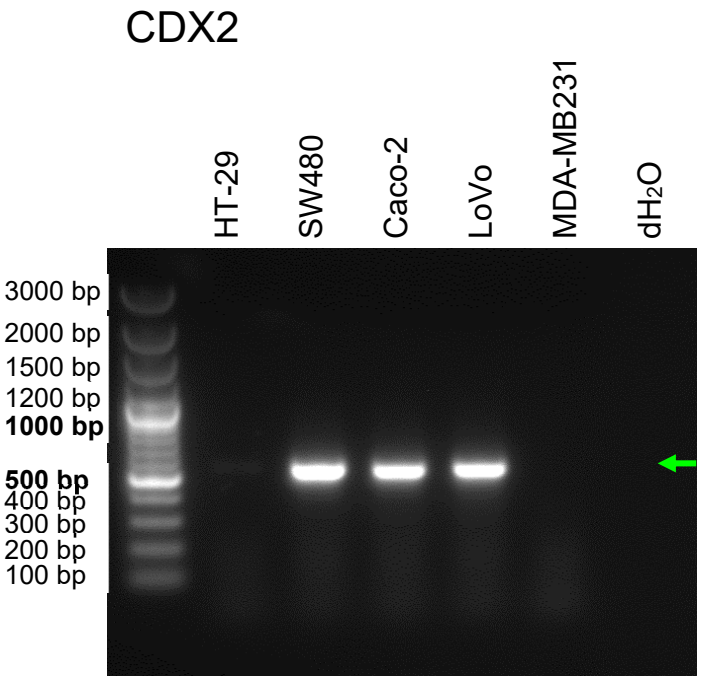

Figure 5.5: RT-PCR of *CDX2* in Caco-2, LoVo, HT-29 and SW480 cell lines
CDX2 expression was observed in the colorectal cancer cell lines SW480, Caco-2 and LoVo cells, while a very weak band was seen on the HT-29 cell line. MDA-MB231, which is a breast cancer cell line, did not express *CDX2*. The same batch of cell RNA was used for the SP, EGR, CDX2 and GAPDH RT-PCR reactions

5.4.3 Generation of S-364-derived constructs with transcription factor binding site mutations

Following on from the identification of potential transcription factor binding regions and the knowledge that appropriate transcription factors were indeed expressed in the cells of interest, mutations were inserted into selected binding sites. This would determine if removal of these binding sites could affect the promoter's activity in driving Firefly luciferase expression, and so the functional importance of the sites.

Footprint-db and the JASPAR database were used to identify the most highly conserved bases in the EGR, SP and CDX2 binding site consensus sequences for targeted mutagenesis (Mathelier et al., 2016). Figure 5.6 shows the mutations inserted within the consensus sequence, and their overall position in the promoter sequence. For the regions identified previously (Figure 5.2), a single CDX2 consensus site was mutated. For the EGR region, two consensus binding sites were mutated, both were in regions with high overlap between two different algorithms. A single SP consensus sequence was mutated within the region identified by ALGGEN-PROMO. Although other consensus sites were present in the SP region, they had a larger overlap with the EGR sites, so the site with least EGR overlap was selected.

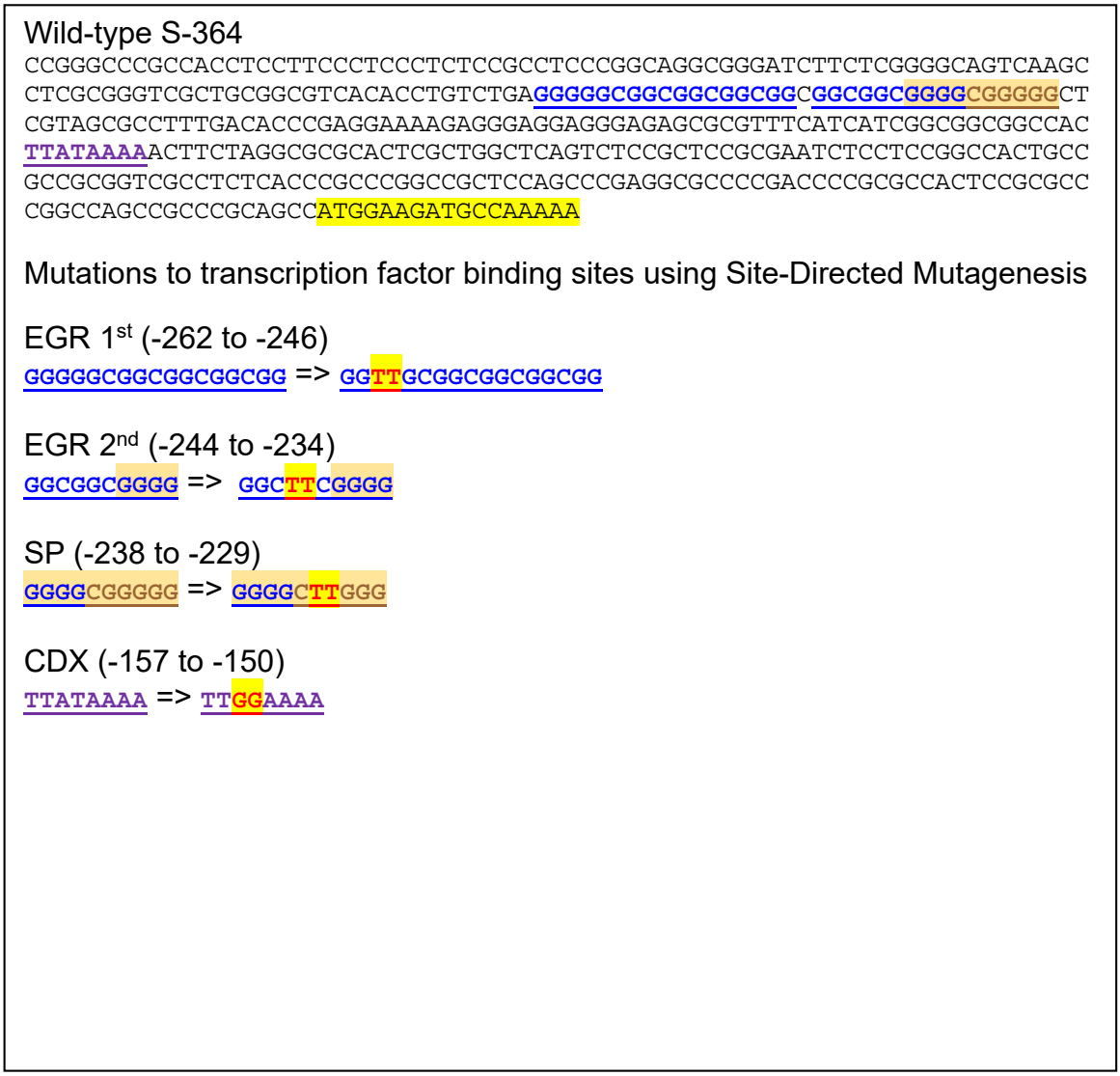

Figure 5.6: Point mutations introduced in the predicted EGR, SP and CDX2 binding sites
The wild-type S-364 sequence shows the -364 bp to -1 *SLCO2A1* promoter region, with the start of the vector's luciferase gene highlighted in yellow. The underlined blue text shows the position of the two EGR regions that were selected for mutagenesis. The sequence highlighted in orange indicates the SP target region, and has some overlap with the EGR region. The purple underlined text shows the CDX2 binding site region. Site Directed Mutagenesis was used to mutate two highly conserved bases in the predicted transcription factor binding sites. The inserted bases are in red text.

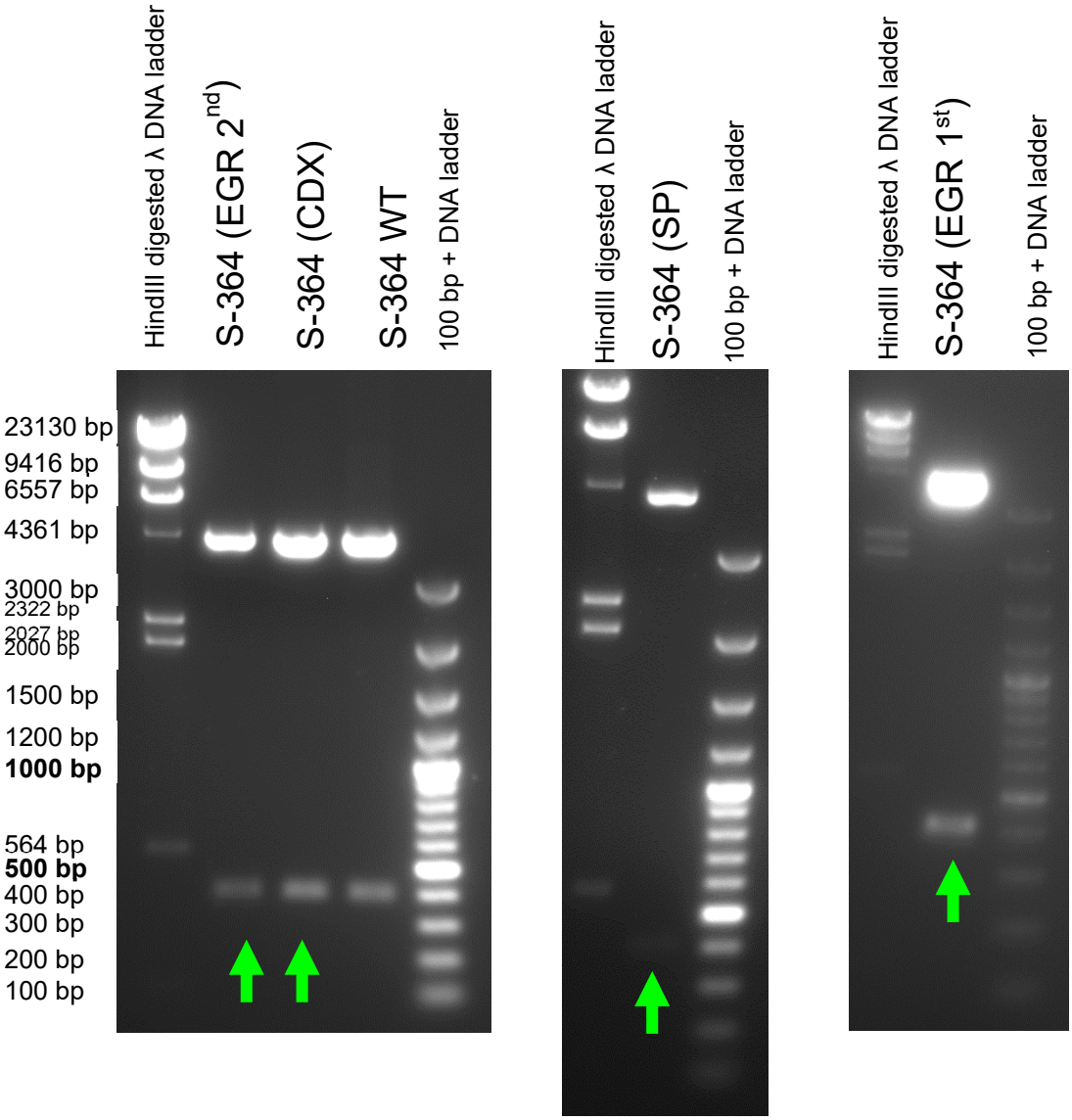

Figure 5.7: Digestion of the 364 bp *SLCO2A1* promoter from the site-directed mutagenesis products

The above gel images show the digestion of the S-364-derived plasmids containing mutations to the potential transcription factor binding sites. NcoI and XhoI were used to excise the 364 bp *SLCO2A1* promoter fragment (~400 bp, green arrows).The same reaction products were separated on a crystal violet gel, the 400 bp fragments extracted from the gel and ligated to pGL4.10[luc2] backbone digested by the same restriction enzymes.

The S-364 was taken as the “wild-type” control, and the template on which these mutations were introduced. To avoid any unintended mutations within the plasmid backbone, the *SLCO2A1* promoter was excised using restriction enzymes Figure 5.7 and ligated to pGL4.10[luc2] that was not subjected to PCR through the site-directed mutagenesis reaction. These plasmids were subsequently diluted to equimolar concentrations Figure 4.9 and transfected into Caco-2, LoVo and SW480 cells.

5.4.4 Effects of Predicted Transcription Factor Binding Site Mutations on the activity of the proximal -364 bp *SLCO2A1* promoter

The S-364-derived constructs containing mutations to the two EGR, and single SP and CDX predicted transcription factor binding sites were transfected into Caco-2, LoVo and SW480 cells to assess the effect on promoter activity through firefly luciferase expression. As seen on Figure 5.8, all constructs showed higher luciferase activity relative to the promoterless control. No statistically significant difference was observed between the wild-type S-364 and the S-364 constructs containing mutations in any of the three cell lines. However, in the Caco-2 and SW480 cell lines, mutation of the CDX2 binding site led to an approximately 50% decrease in average promoter activity relative to the control. The SP mutated construct also appeared to have a reduction in average promoter activity in Caco-2 and SW480 cell lines, though this was much less pronounced than seen for CDX2. The data suggests that CDX2 and also possibly an SP family member, may have a role in driving *SLCO2A1* expression.

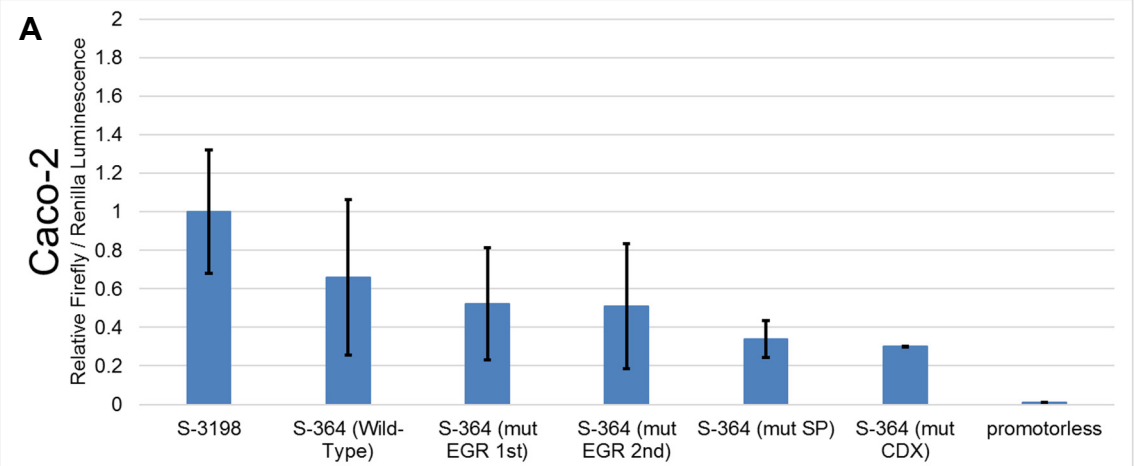

Construct name	S-364 (Wild-Type)	S-364 (mut EGR 1st)	S-364 (mut EGR 2nd)	S-364 (mut SP)	S-364 (mut CDX)	promoterless
***t*-Test p-values**	N/A	0.73545059	0.722051359	0.455197713	0.426099966	**0.026240813**

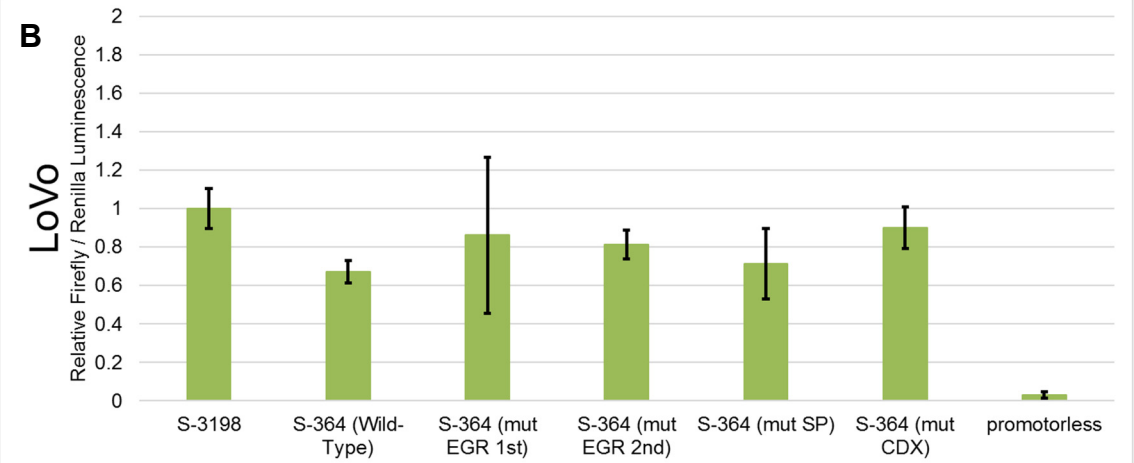

Construct name	S-364 (Wild-Type)	S-364 (mut EGR 1st)	S-364 (mut EGR 2nd)	S-364 (mut SP)	S-364 (mut CDX)	promoterless
***t*-Test p-values**	N/A	0.625415282	0.171648064	0.802012692	0.156199033	**0.029944894**

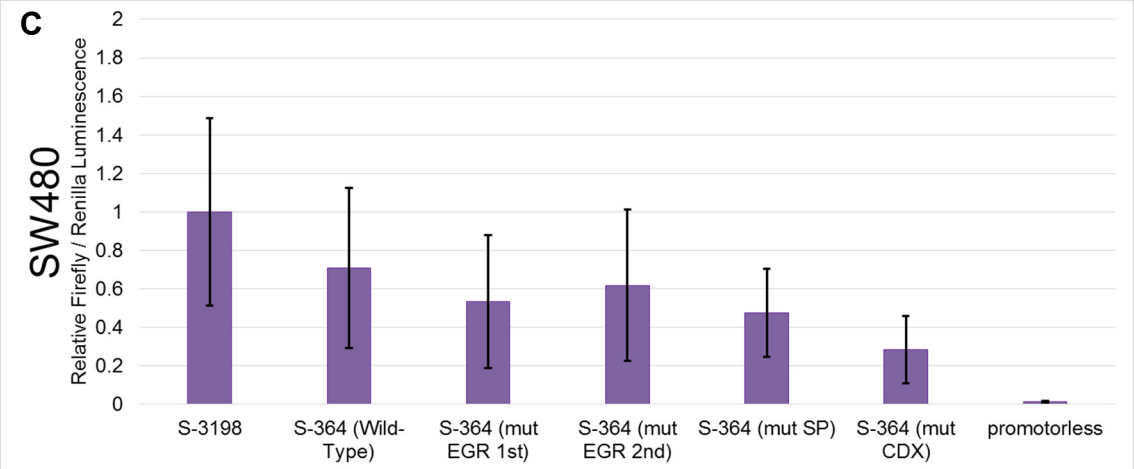

t-Test p-values	S-364 (Wild-Type)	S-364 (mut EGR 1st)	S-364 (mut EGR 2nd)	S-364 (mut SP)	S-364 (mut CDX)	promoterless
Relative to S-364 (WT)	N/A	0.4500679	0.710947	0.2643690	0.0564672	**0.0094341**

Figure 5.8: Activity of the S-364 derived constructs containing transcription factor binding site mutations in Caco-2 (A), LoVo (B), and SW480 (C) cell lines

Caco-2, LoVo and SW480 cell lines were transfected with S-3198, wild-type S-364 and S-364 derivative constructs with mutations to the predicted two EGR, SP and CDX consensus binding sites, and the pRL-CMV Renilla luciferase transfection control. Promoter activity was measured as the ratio of firefly luciferase luminescence to Renilla luciferase luminescence. For each cell line, luminescence ratios and standard deviations were normalised to the average for S-3198. Activity is displayed as average with one standard deviation. The table below each graph shows p-values of two-tailed t-tests carried out relative to the wild-type S-364 to determine the statistical significance of any observed differences. Two experiments were carried out for each cell line, each with three replicates. The averages of each experiment's replicates were used for statistical analysis. The HT-29 cell line was not included in the analysis as it did not express CDX2, and had previously been shown to have a much wider spread of data from transfection experiments (Figure 4.9), indicating it was less likely to generate data of statistical significance.

5.4.5 Generation of random insertions in the −364 to −140region of the *SLCO2A1* promoter using Linker-Scanning Mutagenesis

A random mutagenesis approach was followed in order to identify regions in the sequence that may contain important transcription factor binding sites whose disruption affects the *SLCO2A1* promoter activity. First, the existing NotI site, within the plasmid backbone, was mutated in order to prevent digestion of the plasmid during the subsequent reaction (Figure 5.1 and Figure 5.9). The transposition reaction generated a pool of plasmids with random insertions. Digestion with Acc65I and MreI allowed for the isolation of the ~1600 bp fragment containing the 364 bp *SLCO2A1* promoter and the 1131 bp transposon insert (Figure 5.10).

During the initial transposition reaction (Figure 5.1), a five base pair duplication of the plasmid sequence was created adjacent to the ligation site. Digestion with NotI removed the transposon sequence, leaving a 10 bp fragment, which together with the adjacent duplication, create the 15 bp insertion. After transforming the resulting plasmid pool, 240 of the resultant clones were screened by PCR and sequencing. Any constructs with the 15 bp inserts located in the ~50 bp vector sequence upstream of the -364 bp *SLCO2A1* promoter, or within the ~60 bp of luciferase gene were excluded. A number of constructs were isolated more than once, leading to the use of five different insertion constructs for the transfection experiment. Equimolar dilutions of these constructs were prepared (Figure 5.11) for transfection into Caco-2 and LoVo cells. The 15 bp insertions were at positions -347, -310 -271, -209 and -169, occurring at approximately every 40 bp as shown in Figure 5.12.

Figure 5.9: Mutation of the native NotI restriction site in the S-364 construct's pGL4.10[luc2] backbone
The pGL4.10[luc2] plasmid's native NotI site was mutated prior to carrying out the linker scanning mutagenesis reaction. S-364 was digested with NotI, blunted using Klenow DNA polymerase I fragment, and the blunt ends ligated prior to transformation into competent cells. Colonies were screened by digesting plasmid DNA with NotI. Colonies 1 to 6 (green arrow) contain the S-364-NotI(x) which is uncut, while the linearized colony 7 (blue arrow) indicates that it is native S-364. Sequencing was used to confirm the four-base insertion at the NotI site.

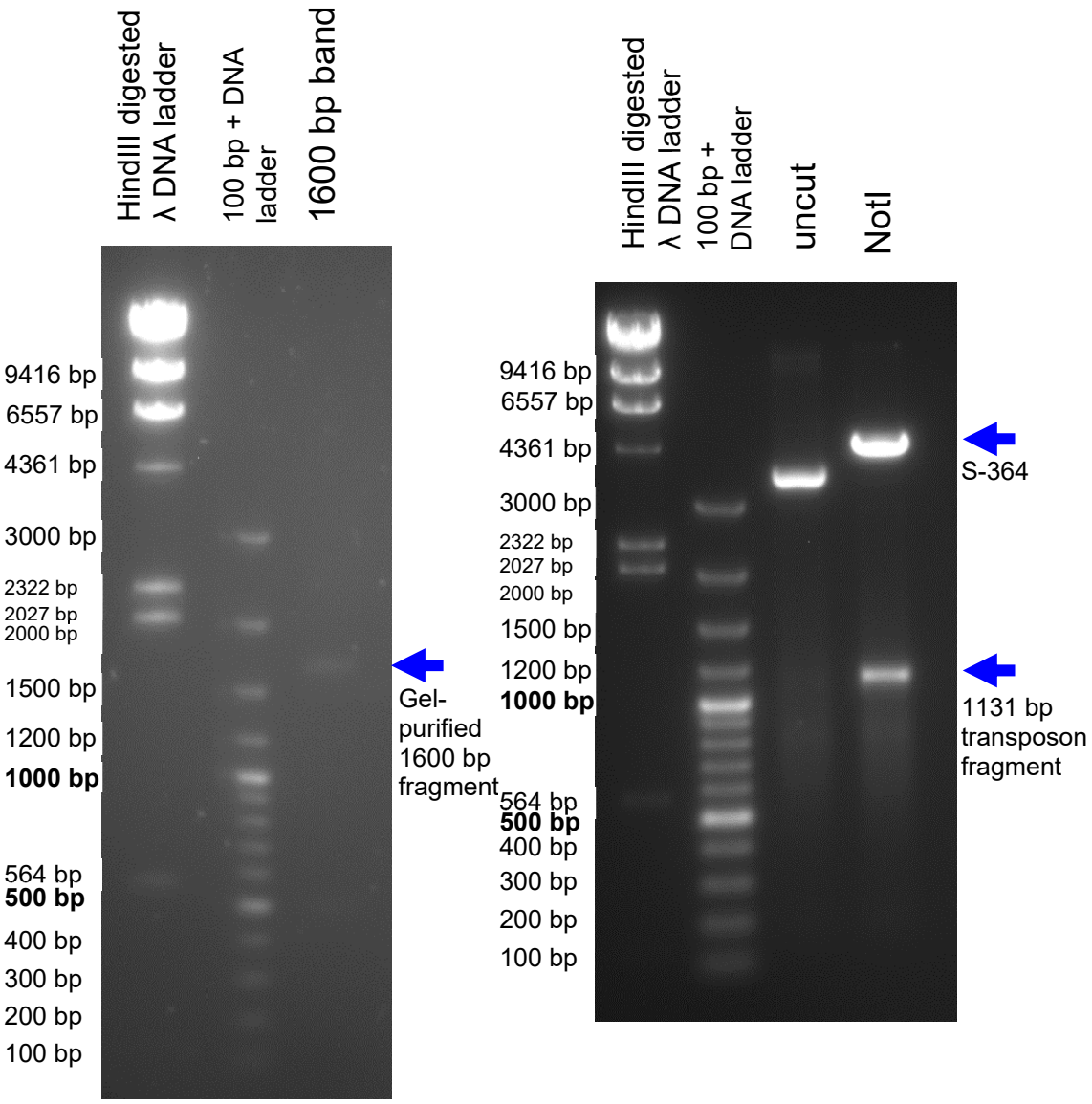

Figure 5.10: Isolation of the 364-bp *SLCO2A1* promoter containing transposon insertion, and excision of the transposon sequence to generate the 15-bp insertions

Following the transposition reaction, S-364 was digested with Acc65I and MreI. As shown in the left image, the 1600 bp fragment containing the *SLCO2A1* promoter with the inserted transposon was gel purified and ligated to pGL4.10[luc2] backbone containing the NotI site mutation. In the right image, subsequent digestion with NotI removed the transposon sequence and ligation of the linearized plasmids yielded a pool of S-364 containing 15 bp insertions

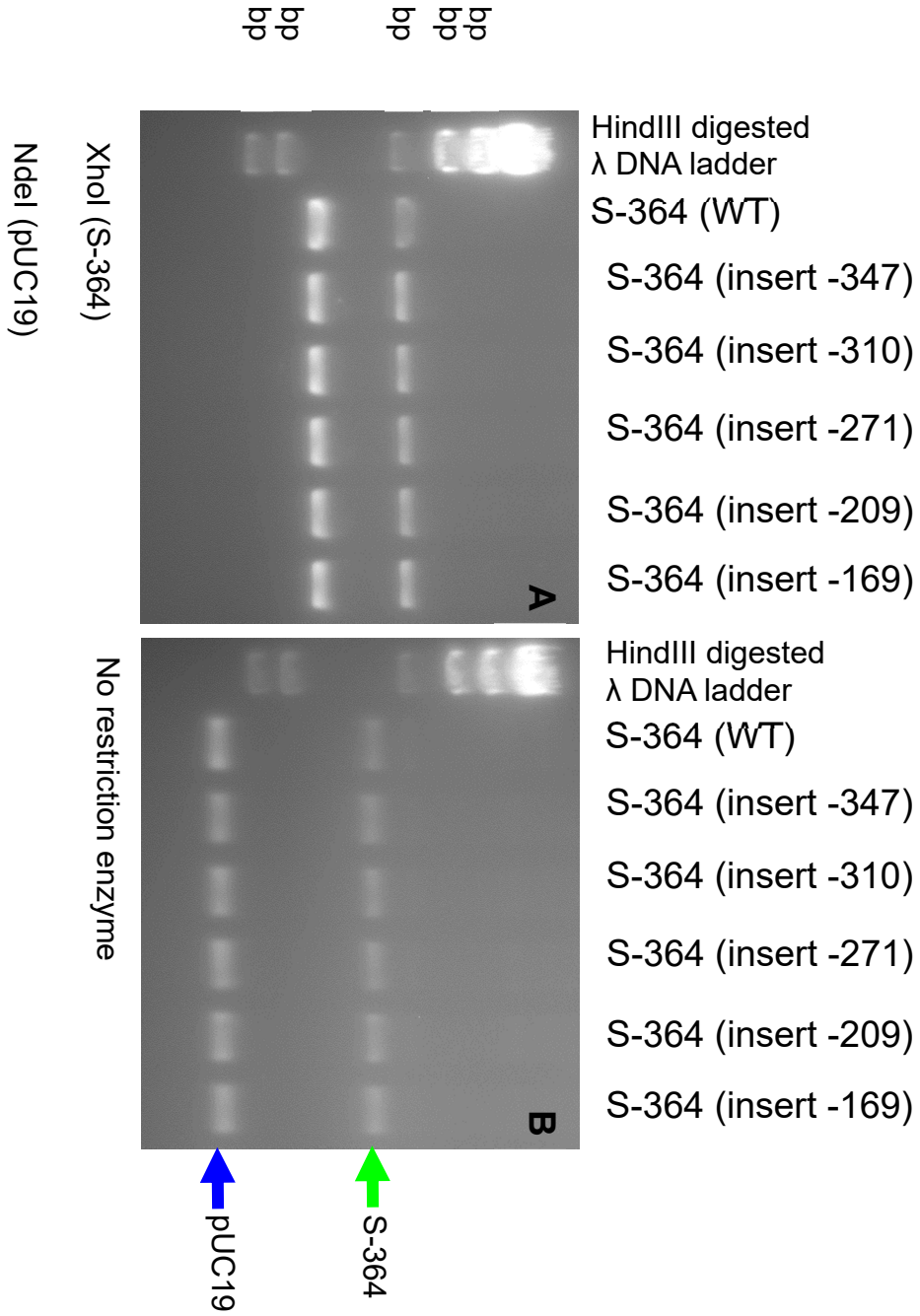

Figure 5.11: Equimolar dilutions of the S-364 derived constructs containing 15-bp insertions
Prior to transfection, the equimolar dilutions of the wild-type S-364 and the insertion constructs were run to confirm that their concentrations were effectively the same. (A) S-364 and pUC19 plasmids linearized with single-cutting enzymes, where they appear at their expected sizes (pUC19: 2686 bp, S-364 (WT) 4605 bp, S-364 (insert): 4620 bp). (B) S-364 and pUC19 uncut plasmids.

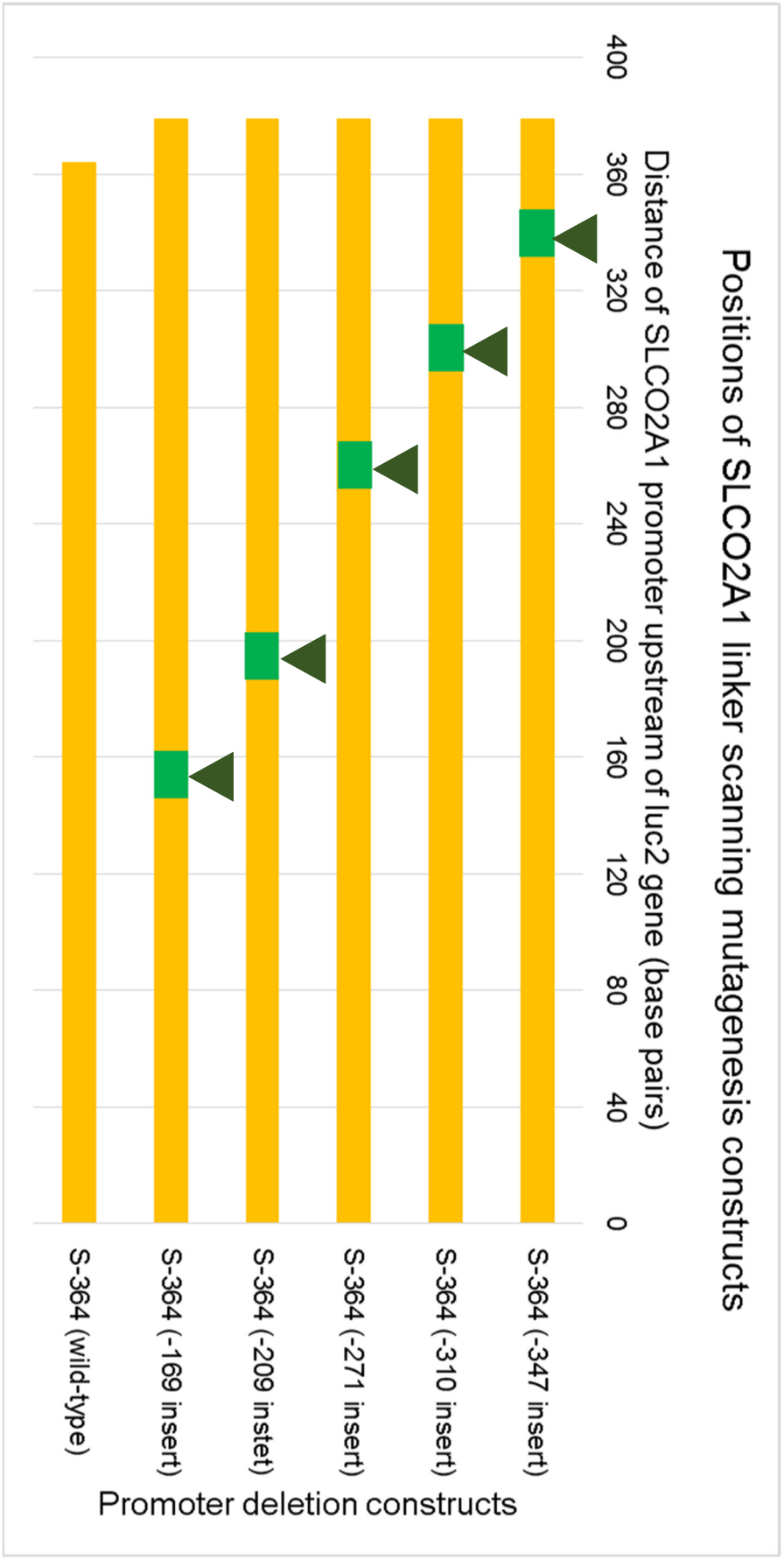
Positions of SLCO2A1 linker scanning mutagenesis constructs
Distance of SLCO2A1 promoter upstream of luc2 gene (base pairs)
400
360
320
280
240
200
160
120
80
40
0
S-364 (-347 insert)
S-364 (-310 insert)
S-364 (-271 insert)
S-364 (-209 instet)
S-364 (-169 insert)
S-364 (wild-type)
Promoter deletion constructs

Figure 5.12: Positions of the 15-bp insertions in the S-364 derived linker-scanning mutagenesis constructs
This diagram shows the positions of the five 15 bp insertions (green rectangles) within the proximal 364 bp of the *SLCO2A1* promoter. The insertions are relatively evenly spaced between the -364 and -140 region, at approximately every 40 bp

5.4.6 Effects of random 15 bp insertions on the activity of the proximal -364 bp *SLCO2A1* promoter

Caco-2 and LoVo cells were transfected with the five *SLCO2A1* promoter constructs containing 15 bp deletions (Figure 5.13). All of the S-364 derived constructs showed higher activity than the promoterless control. Although there was some variation in mean relative luminescence ratio this was less than a two-fold change, and given the spread of data, no significant difference was observed between the wild-type S-364 and the constructs containing the 15 bp insertions.

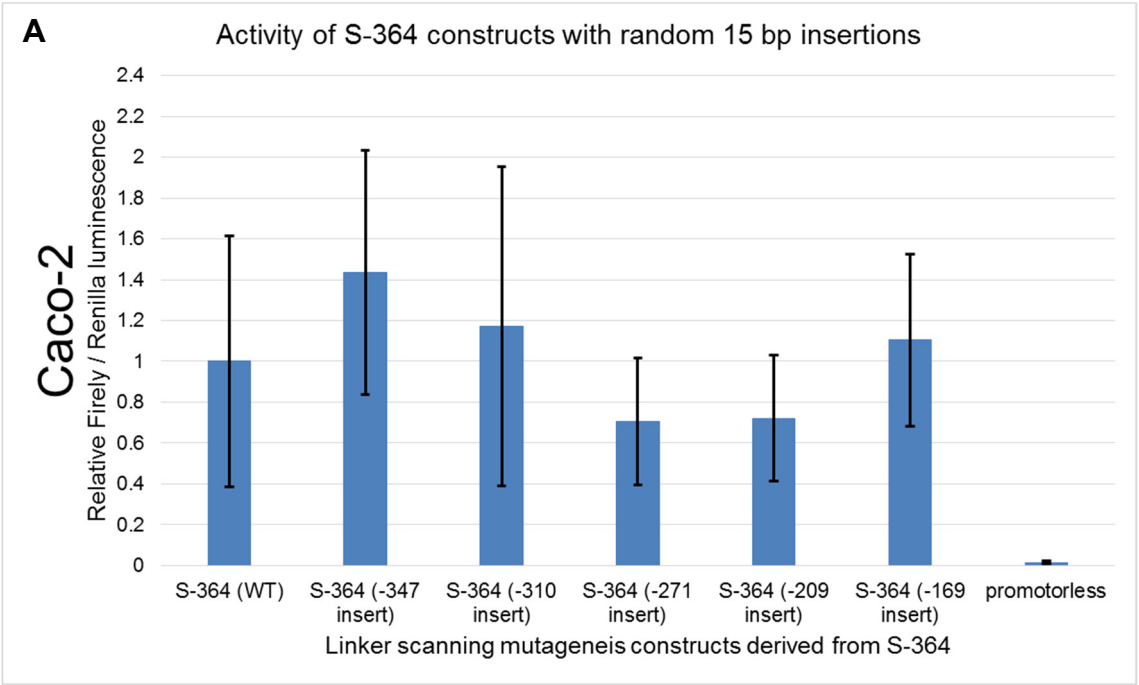

Construct name	S-364 (-347 insert)	S-364 (-310 insert)	S-364 (-271 insert)	S-364 (-209 insert)	S-364 (-169 insert)	promoterless
***t*-Test p- values**	0.1481177	0.6138622	0.2242372	0.2461441	0.6804508	0.1055995

Construct name	S-364 (-347 insert)	S-364 (-310 insert)	S-364 (-271 insert)	S-364 (-209 insert)	S-364 (-169 insert)	promoterless
***t*-Test p- values**	0.5295593	0.3600031	0.6726378	0.635886	0.2437462	0.6467893

Figure 5.13: Activity of the S-364 derived constructs containing random insertions in the -364 to -140 region of the *SLCO2A1* promoter in Caco-2 (A) and LoVo (B) cells

The Caco-2 and LoVo cell lines were transfected with wild-type S-364 and S-364 derivative constructs with random 15 bp insertions in the *SLCO2A1* promoter sequence, and the pRL-CMV Renilla luciferase transfection control. Promoter activity was measured as the ratio of firefly luciferase luminescence to Renilla luciferase luminescence. For each cell line, luminescence ratios and standard deviations were normalised to the average for S-364. The table below each graph shows p-values of two-tailed t-tests carried out relative to the wild-type S-364. Three independent experiments were carried out for each cell line, each with three replicates.

5.5 Discussion

Two approaches were used in order to identify transcription factor binding sites within the proximal promoter responsible for the change in *SLCO2A1* activity. Although the linker scanning mutagenesis approach has been used successfully previously, no sites were identified in this study. While 10 bp is the average length of eukaryotic promoter transcription factor binding sites (Stewart et al., 2012), this is also the period of DNA's helical structure (Wilkins et al., 1953). Therefore, a 15 bp insertion was expected to be potentially more disruptive because sequences on each side of the insertion would be rotated 180°, and spatial orientation of the binding sites altered, in addition to the sequence itself. This would prevent the binding of transcription factors that bind cooperatively to closely-spaced sites (Xu et al., 1996). The lack of any positive findings here may be due to the small number of constructs analysed. Generation of a much larger number of reagents would be required to assess the region completely.

The targeted approach with site directed mutagenesis was more successful. A consensus sequence for the CDX2 binding site was previously described as conserved between human, mouse, rat, cow and pig *SLCO2A1* homologues, however no functional evaluation was performed (Van Poucke et al., 2009). The experimental results presented here suggest that CDX2 may indeed have a role in regulating *SLCO2A1* expression, and further replicates of the experiment to increase the statistical power may help demonstrate this with more certainty.

CDX, compared to the SP or EGR transcription factors, may be more functionally relevant. CDX2 is a transcription factor specific to the small intestine and colon, where it is expressed in the epithelial cells. In the mouse it has been

found to be essential for colon development at the embryonic stage, and essential for the maintenance and renewal of the intestinal and colonic epithelium (Freund et al., 2015; Hryniuk et al., 2014). Loss of *Cdx2* function in the mouse has also been shown to exacerbate the tumour formation in the small intestine and colon of $Apc^{+/min}$ mice (Hryniuk et al., 2014; Bae et al., 2015; Ee et al., 1995). Its loss in colorectal adenocarcinomas is associated with a poorer differentiation phenotype and prognosis (Dawson et al., 2013; Olsen et al., 2016), and increased invasiveness (Mallo et al., 1997; Bae et al., 2015; Coskun et al., 2014).

Although CDX2 expression is lost in less than 10% of colorectal adenocarcinomas (Olsen et al., 2016), closer inspection has revealed that loss of expression occurs at the invasive front of the tumour, where it facilitates invasion, even if expression is maintained in the rest of the tumour (Coskun et al., 2014). Furthermore, CDX2 can stimulate expression of *APC*, *AXIN2* and *GSK3β*, through binding to their respective promoters and enhancers (Olsen et al., 2013). This implies a mechanism to suppress the Wnt/β-catenin pathway in the presence of functional APC protein, and further suggests a second, indirect mechanism by which CDX2 could drive *SLCO2A1* expression (Smartt et al., 2012a). However, unlike SLCO2A1, CDX2 does not show an increasing expression gradient from the crypt to the colon lumen (Qualtrough et al., 2002), which suggests that its role may be to maintain rather than initiate differential *SLCO2A1* expression. Interestingly CDX2 has been found to regulate the expression of another prostaglandin pathway component, PTGS2, where it reduces transcriptional activity (Kim et al., 2004). However, as CDX2 is not frequently reduced in early stage cancer samples, it is not likely to be a main factor in the decrease of either *PTGS2* or *SLCO2A1* in early stage disease.

There is limited information on the EGR family members for all but EGR1 in the colon. EGR1 has been implicated in colorectal cancer development, however the evidence is not as compelling as that for CDX2. EGR1 is expressed in adenocarcinomas, with little to no expression in normal colonic epithelium, suggesting that it promotes tumour growth (Myung et al., 2014; Ongen et al., 2014). EGR1 is known to upregulate *PTGS2* expression in colorectal cancer with a suggested role in potentiating PGE_2 synthesis by inducing *PTGES* in the presence of $PGE_{2\alpha}$ and PGE_2 (Kim et al., 2004; Stamatakis et al., 2015). Its role as a transcriptional activator for *SLCO2A1* would therefore be in functional opposition, regarding their roles in PGE_2 production and removal. EGR1 can also act as a repressor via the same binding site (Gashler et al 1993), however as the two altered consensus binding sites showed no clear effect on transcriptional activity, this suggests they are not likely to be functional sites within the *SLCO2A1* promoter.

SP binding sites were found on the *SLCO2A1* promoter in the original study that characterised the gene (Lu and Schuster, 1998). One of these sites was also conserved in the rodent, pig and cow *Slco2a1,* and was the site selected here for mutation (Van Poucke et al., 2009). Many of the SP transcription factors are generally considered to be ubiquitously expressed and function as transcriptional activators (Wilson et al., 2010; Hedrick et al., 2016). *SLCO2A1* expression similarly occurs in a number of cell types and tissues, so SP transcription factors could have a role in driving baseline expression (Bao et al., 2002; Kang et al., 2005; Schuster et al., 1997). Given the similar consensus transcription factor binding site for the SP family, a number of them have a potential to control transcription in the cell lines used. They do not all act as activators, as SP5 is known to function as a transcriptional repressor that

downregulates genes driven by SP1 (Fujimura et al., 2007). While SP5 expression can be stimulated by activation of the Wnt/β-catenin pathway, any effect or competition with endogenously expressed SP1 could potentially make it difficult to interpret its role in regulating target genes unless specific SP factors are upregulated or knocked down. However, establishing that the modest decrease in *SLCO2A1* promoter activity through mutation of the single SP site can be reproduced, needs to be demonstrated first.

The consensus binding site sequences for both EGR and SP transcription factors are GC rich, and there was overlap in the initial site identification. It is possible they may have a level of redundancy, and therefore mutating one site would be insufficient to appreciably alter expression. This is one limitation of the transfection experiments, and may have contributed to the lack of response seen with the EGR and SP binding site mutations. This could be assessed by generating constructs containing mutations to more than one of the different EGR and SP sites (Xu et al., 2016; Xu et al., 2012). This has been demonstrated in SP binding sites, where mutation of two out of four SP sites led to a large reduction in promoter activity compared to the individual mutations (Xu et al., 2012). Alternatively, these transcription factors could be transiently knocked down using RNAi to test the effect on *SLCO2A1* mRNA expression and promoter activity. This would reveal whether a transcription factor does influence the expression level of the target gene, although the disadvantage would be the inability to discriminate between direct and indirect actions (for example, inducing an activator or repressor that then acts on the target gene).

To conclude, a CDX2 and an SP binding site were identified in the *SLCO2A1* promoter that reduced transcriptional activity, albeit to less than statistical significance, but still merit further investigation.

Chapter 6 Actions of TGF-β and Hedgehog Pathways on *SLCO2A1* Expression

6.1 Introduction

The effects of mutating predicted transcription factor binding sites on *SLCO2A1* promoter activity helped to identify potential factors acting at the gene locus (Chapter 5). Transcription factors represent the effectors at the confluence of several signalling pathways, however, regulation of *SLCO2A1* can also be investigated by identifying compounds that act closer to the start of these pathways.

The Wnt/β-catenin pathway is one of the first to be dysregulated in colorectal carcinogenesis (Munemitsu et al., 1995; Takayama et al., 1996; Rubinfeld et al., 1993; Fearon, 2011) and demonstrates where upstream events effect transcription factor recruitment to promoters and the subsequent expression of a wide range of genes (Mohammed et al., 2016). For example, *APC* mutation releases bound β-catenin which can translocate to the nucleus and allow interaction with transcription factors. β-catenin typically activates transcription by recruiting TCF4 to the promoters and displacing repressors like TCF3 (Morin et al., 1997; Wray et al., 2011). Both β-catenin and TCF4 can bind to the *HPGD* promoter, which contains a non-classical TCF binding site (Smartt et al., 2012b). Although the exact events at the *SLCO2A1* promoter are not known, that modulation of β-catenin can alter activity at promoters, including *HPGD* and *SLCO2A1,* is clear. Similarly, changes further upstream would be expected to also alter gene transcription for these genes.

Exposure to NSAIDs can also upregulate *HPGD* and *SLCO2A1*, for example the COX-2 selective antagonist Apricoxib increases *HPGD* and *SLCO2A1* expression (St John et al., 2012). The downstream mechanism for

this effect is most likely due to the disruption of the positive feedback of PGE_2 acting on the EP2 and EP4 receptors that typically acts to upregulate *PTGS2* and to repress expression of the degradation enzyme (Zhu et al., 2015; Steinert et al., 2009; Nishimura et al., 2013). The precise events occurring at the promoters have yet to be well defined.

Transforming Growth Factor-β (TGF-β) is a cytokine that can activate a series of downstream events in its signalling pathway (Figure 1.6). It is one of the tumour suppressor pathways that is also inactivated in colorectal cancer (MacKay et al., 1995; Samowitz and Slattery, 1997; Hoosein et al., 1987; Engle et al., 1999).

TGF-β affects the expression of multiple enzymes in the PGE_2 metabolic pathway. It suppresses PGE_2 signalling by downregulating the inducible *PTGS2*, and at the same time upregulating *HPGD*, therefore reducing PGE_2 synthesis and accelerating its degradation (Takai et al., 2013; Yan et al., 2004). TGF-β has also been shown to co-regulate *PTGS2* and *PGES* in the kidney, which further emphasises it can exert opposite effects on the PGE_2 synthesis and degradation parts of the prostaglandin pathway (Takai et al., 2013; Kang et al., 2015; Harding et al., 2006). As TGF-β can regulate at least three components of the PGE_2 synthesis and degradation pathway, it is plausible that it could also stimulate *SLCO2A1*. Given that TGF-β expression displays a gradient from base of the colonic crypt towards the mucosal surface (Avery et al., 1993), which follows that observed for both *HPGD* (Smartt et al., 2012b) and *SLCO2A1* (Smartt et al., 2012a), this provides additional biological relevance to the potential transcriptional control relationship between TGF-β and *SLCO2A1*.

While the literature can provide evidence to suggest that TGF-β or other agents may positively regulate *SLCO2A1*, publicly available data from

microarray and high-throughput sequencing experiments could reveal stronger associations between treatments or signalling pathways and their effect on *SLCO2A1* expression (Kolesnikov et al., 2015). Unlike the inferences drawn from associated patterns of protein expression on tissue sections, microarray studies measure the effects of a test condition on gene transcription relative to an untreated control (Barrett et al., 2013). Therefore, this provides stronger evidence of transcriptional regulation, and given the large number of datasets that are available, it was likely that data on *SLCO2A1* was captured across a number of studies as part of the panel of genes that were tested.

6.2 Aims

Use bioinformatic data to identify genes, signalling factors and drugs that can modulate *SLCO2A1* expression.

Test whether the gene products or drugs exert an effect on *SLCO2A1* mRNA expression, and *SLCO2A1* promoter activity

6.3 Methods

6.3.1 Bioinformatics Search to identify drugs or signalling pathways that affect *SLCO2A1* expression

A bioinformatics search was carried out using the NCBI Gene Ontology Omnibus database (Barrett et al., 2013) and the EBI Expression Atlas (Petryszak et al., 2016) using *SLCO2A1* as the search term to identify experimental conditions or treatments that increased or decreased *SLCO2A1* activity. This search was focused on human tissues or cell lines. DNA demethylation or deacetylation treatments were excluded because *SLCO2A1* possesses CpG islands, which in the expression constructs described in section 4.4 above, do not reflect the endogenous epigenetic status.

6.3.2 Treatment of cultured cells with TGF-β2 and Smoothened Agonist (SAG)

The colorectal cancer cell lines Caco-2 and LoVo were used in the treatments and RT-PCR experiments. The A549 cell line, which originated from the malignant transformation of the secretory Type II alveolar epithelial cells in the lung alveoli, was also included (Lieber et al., 1976). This cell line is known to express low levels of *SLCO2A1*, as was observed in Figure 3.2, so any increase in expression caused through the activation of signalling pathways would in theory be more readily detectable (Uhlen et al., 2015).

Caco-2, LoVo and A549 cells were cultured and treated with activated TGF-β2 and SAG as described in in sections 2.5.1 and 2.5.6 above. Images of

the cells were also taken under a light microscope at 24 hours and 48 hours. RNA was extracted from the cells for RT-PCR (sections 2.2.1, 2.2.2 and 2.3.2)

PCR band intensity for *SLCO2A1* and *GAPDH* was quantified using ImageLab 5.2.1 (section 2.3.8). The concentration ranges for TGF-β2 and SAGs were inferred from information in the literature where they were used in similar cell culture experiments (Bragina et al., 2010; Kang et al., 2015; Wu et al., 2014; Takai et al., 2013; Zhou et al., 2008).

6.3.3 TGF-β2 Treatment of A549 Cells Transfected with *SLCO2A1* deletion series

Cultured A549 cells were transfected with the first nine *SLCO2A1* promoter deletion series constructs S-3198 to S-364 (section 2.5.3). One set of transfected cells was treated with 25 ng/ml TGF-β2 for 48 hours, and the control set with 1 × PBS), after which promoter activity was measured using the dual luciferase assay (section 2.5.5). Foetal calf serum at the 10% dilution used in cell culture media is known to contain 1 – 2 ng/ml TGF-β2 (Oida and Weiner, 2010). However, this TGF-β2 is predominantly the immature latent form that is unable to bind the TGF-β2 receptor complex (*TGFBR1, TGFBR2, TGFBR3*), so the baseline concentration of mature, active TGF-β2 in the serum-enriched medium was considered to be negligible for the purpose of the experiments (Oida and Weiner, 2010; Poniatowski et al., 2015).

6.4 Results

6.4.1 Bioinformatics search

The activation TGF-β pathway was found to increase *SLCO2A1* expression by a factor of nine for TGF-β1 and by a factor of eleven for TGF-β2 in an ovarian fibroblast cell line treated with 5 ng/ml of active ligand (ArrayExpress ID: E-GEOD-40266 (Yeung et al., 2013) in Expression Atlas (Petryszak et al., 2016). The action of TGF-β2 appeared to be more pronounced, and given the lack of similar experiments on *SLCO2A1* in the literature, TGF-β2 was chosen as the ligand to test. While this activation was not in a colon cell line, TGF-β's possible role is supported by the facts that TGF-β signalling can upregulate *HPGD* (Yan et al., 2004), and shows a similar expression gradient to both *HPGD* and *SLCO2A1* in the colonic epithelium (Smartt et al., 2012a; Smartt et al., 2012b; Avery et al., 1993). Therefore, it would be reasonable to hypothesise that *SLCO2A1* expression may be directly upregulated by the TGF-β pathway and TGF-β2.

Inhibition of the hedgehog signalling pathway was found to reduce *SLCO2A1* expression in human umbilical vein endothelial cells (GEO accession: GDS4482 (Rivron et al., 2012). This was mediated by the drug cyclopamine, which binds to Smoothened to inhibit its function (Chen et al., 2002). Hedgehog signalling has been implicated in colorectal cancer, its role to drive or repress tumorigenesis is unclear (Wu et al., 2017; Gerling et al., 2016), and little data exists on any role for Hedgehog signalling in PGE_2 regulation. However, the possibility of *SLCO2A1* expression in the colon being driven by the Hedgehog pathway was considered for further investigation.

6.4.2 TGF-β2 induces morphological changes to A549 cells, but not Caco-2 or Lovo cells

TGF-β2 induced a change in the A549 cell's morphology, which appeared to be associated with TGF-β2 concentration (Figure 6.2). A549 cells are typically compact and polygonal epithelioid cells, with a prominent nucleus (Lieber et al., 1976). Exposure to TGF-β2 caused the A549 cells to elongate and adopt a spindle-like shape. This effect was more pronounced after 48 hours (Figure 6.3), and at the higher TGF-β2 concentrations, 12.5 ng/ml and 25 ng/ml used in the experiment. TGF-β signalling is known to be a trigger for epithelial-to-mesenchymal transition (EMT) in a number of cancers, and it has been shown in the literature that A549 cells can be induced to undergo EMT through this mechanism (Liu, 2008; Albo et al., 1994; Tirino et al., 2013). In contrast, no such change in the appearance of LoVo (Figure 6.4) and Caco-2 cells (Figure 6.5) was observed when these cell lines were treated with TGF-β2 under the same conditions.

TGF-β2 24 h 0 ng/ml

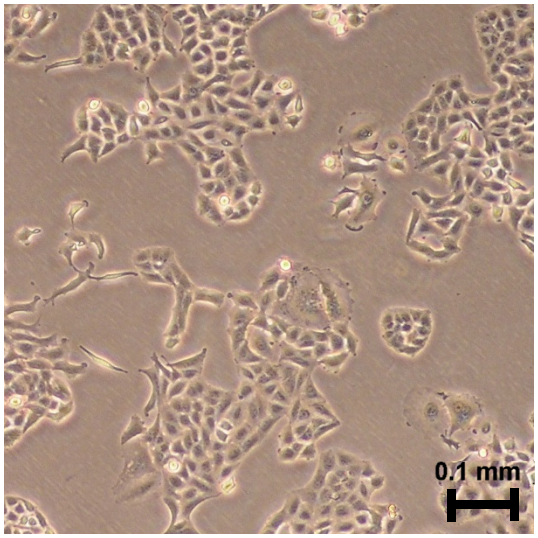

TGF-β2 24 h 1.5625 ng/ml

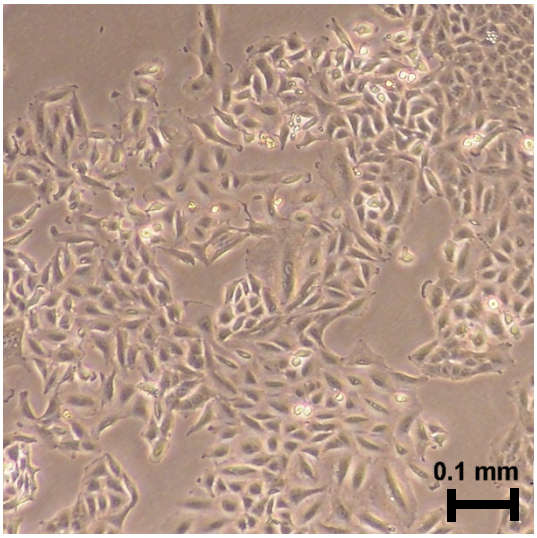

TGF-β2 24 h 3.125 ng/ml

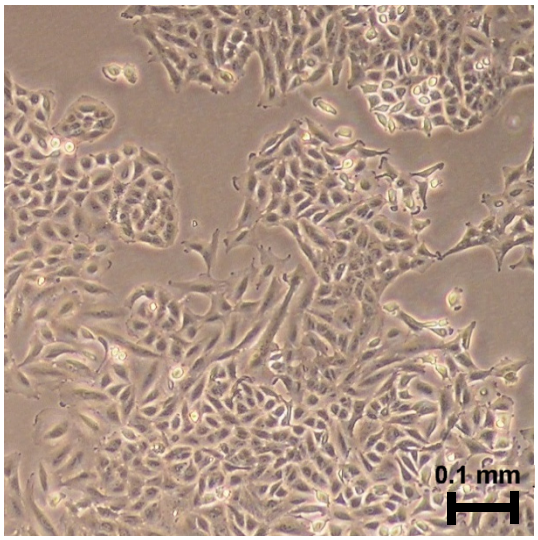

TGF-β2 24 h 6.25 ng/ml

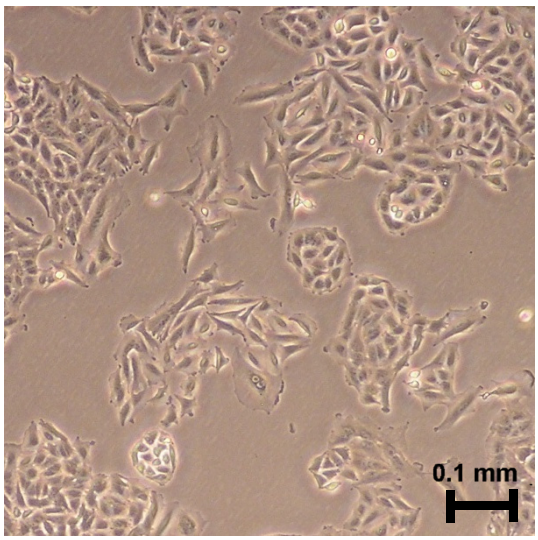

TGF-β2 24 h 12.5 ng/ml

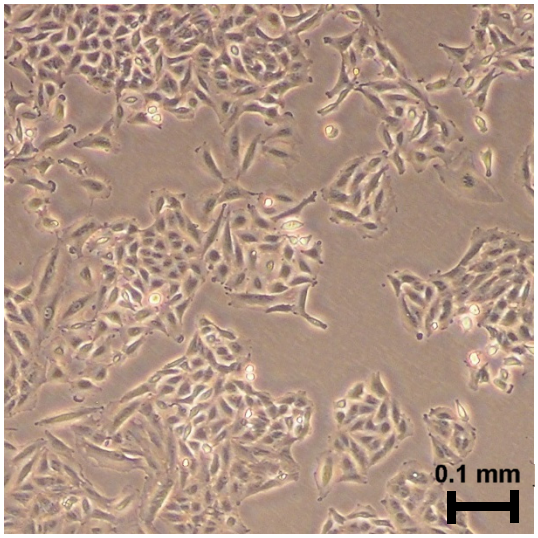

TGF-β2 24 h 25ng/ml

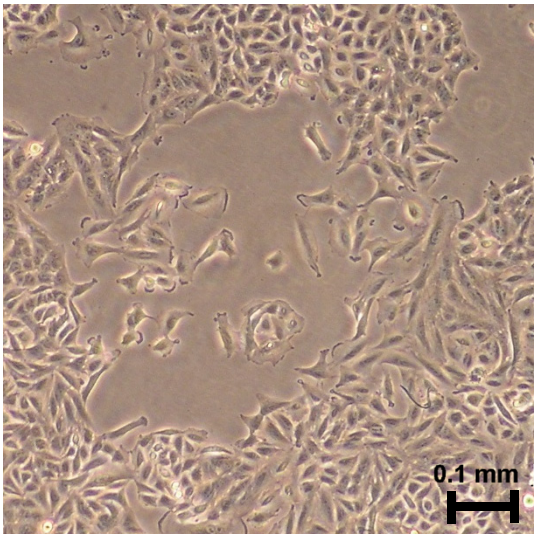

Figure 6.1: A549 cells treated with TGF-β2 for 24 hours
After 24 hours of TGF-β2 treatment, the A549 do not appear to show a change in morphology relative to the untreated control, as viewed under a light microscope. Total magnification × 100

TGF-β2 48 h 0 ng/ml

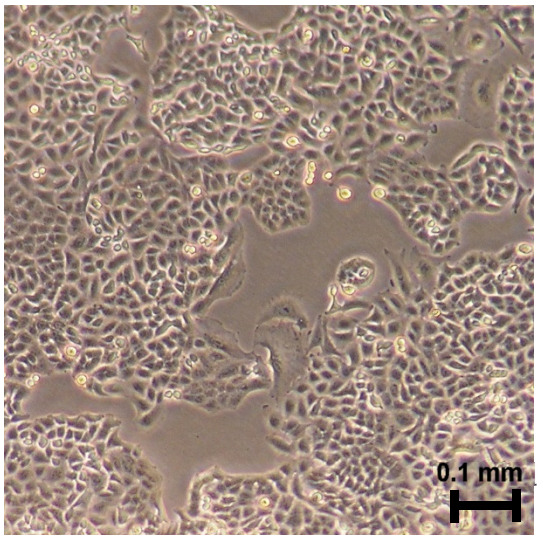

TGF-β2 48 h 1.5625 ng/ml

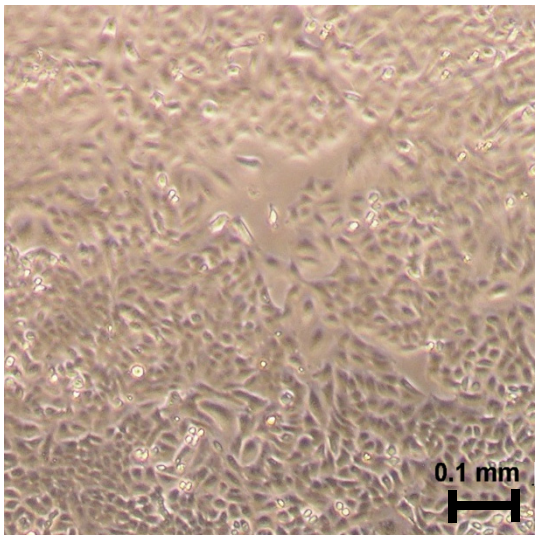

TGF-β2 48 h 3.125 ng/ml

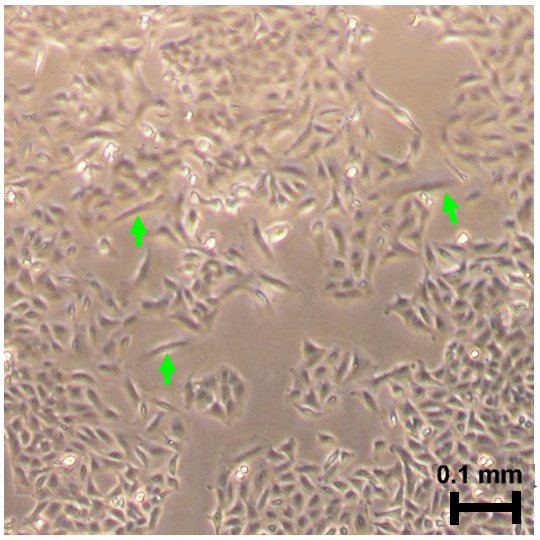

TGF-β2 48 h 6.25 ng/ml

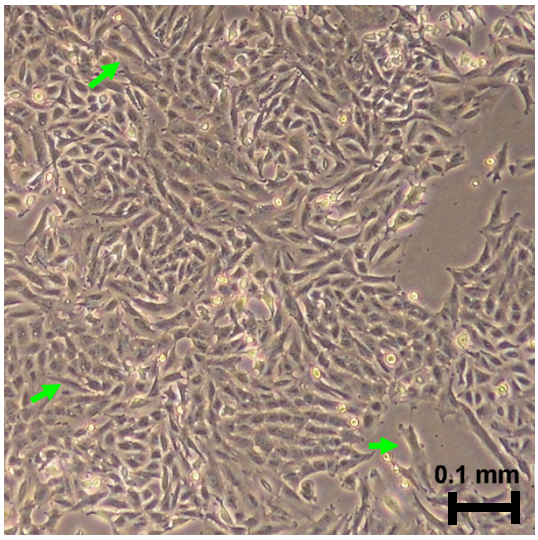

TGF-β2 48 h 12.5 ng/ml

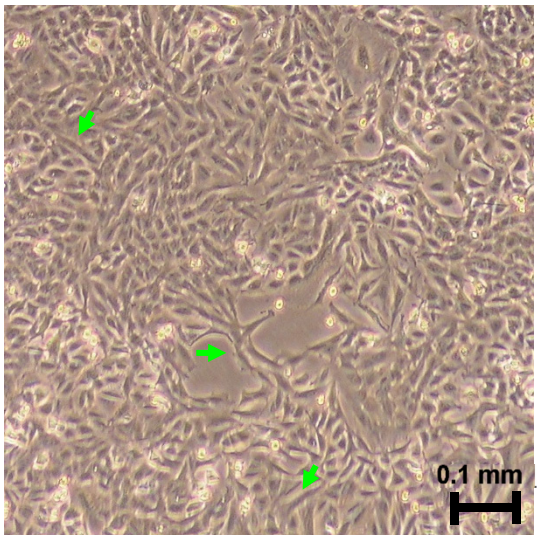

TGF-β2 48 h 25 ng/ml

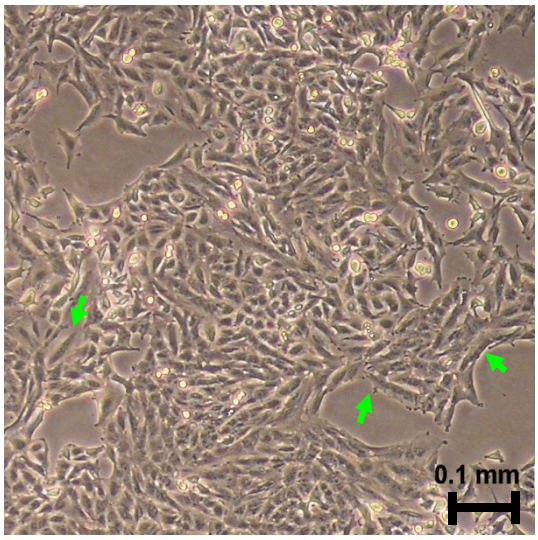

Figure 6.2: A549 cells treated with TGF-β2 for 48 hours
Exposure of A549 cells to TGF-β2 for 48 hours led to a more pronounced elongated phenotype (green arrows) compared to the untreated controls. Total Magnification × 100

TGF-β2 24 h 0 ng/ml

TGF-β2 24 h 25 ng/ml

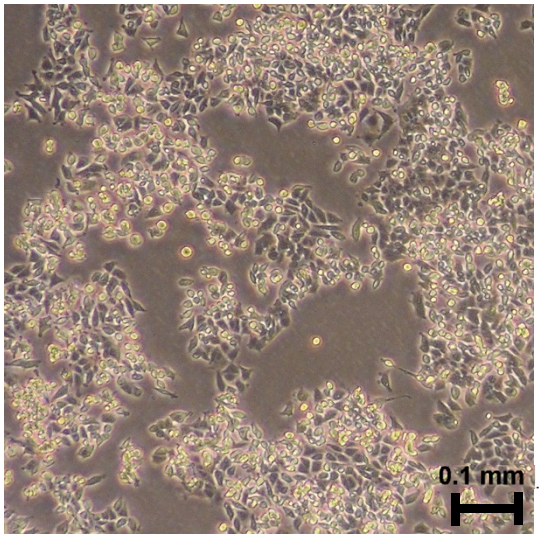

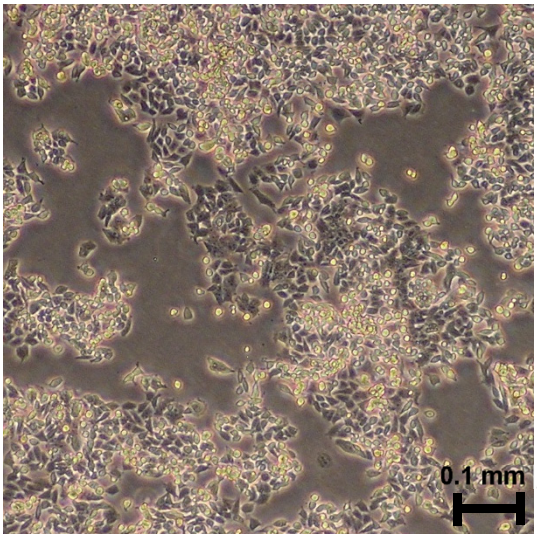

TGF-β2 48 h 0 ng/ml

TGF-β2 48 h 25 ng/ml

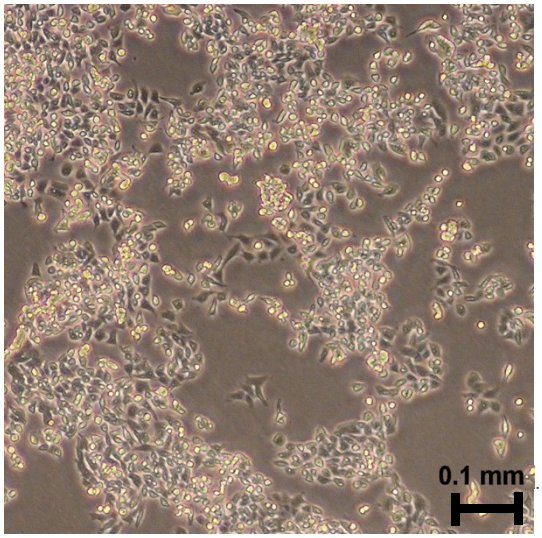

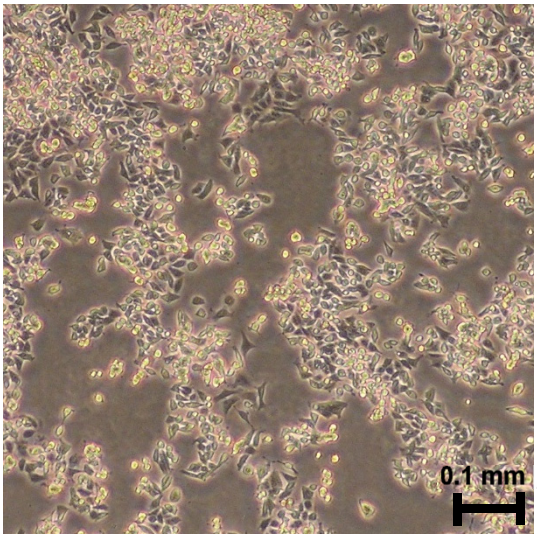

Figure 6.3: LoVo cells treated with TGF-β2 for 24 and 48 hours
Exposure of LoVo cells to TGF-β2 caused no change in the cells' morphology, even after 48 hours. Total Magnification × 100

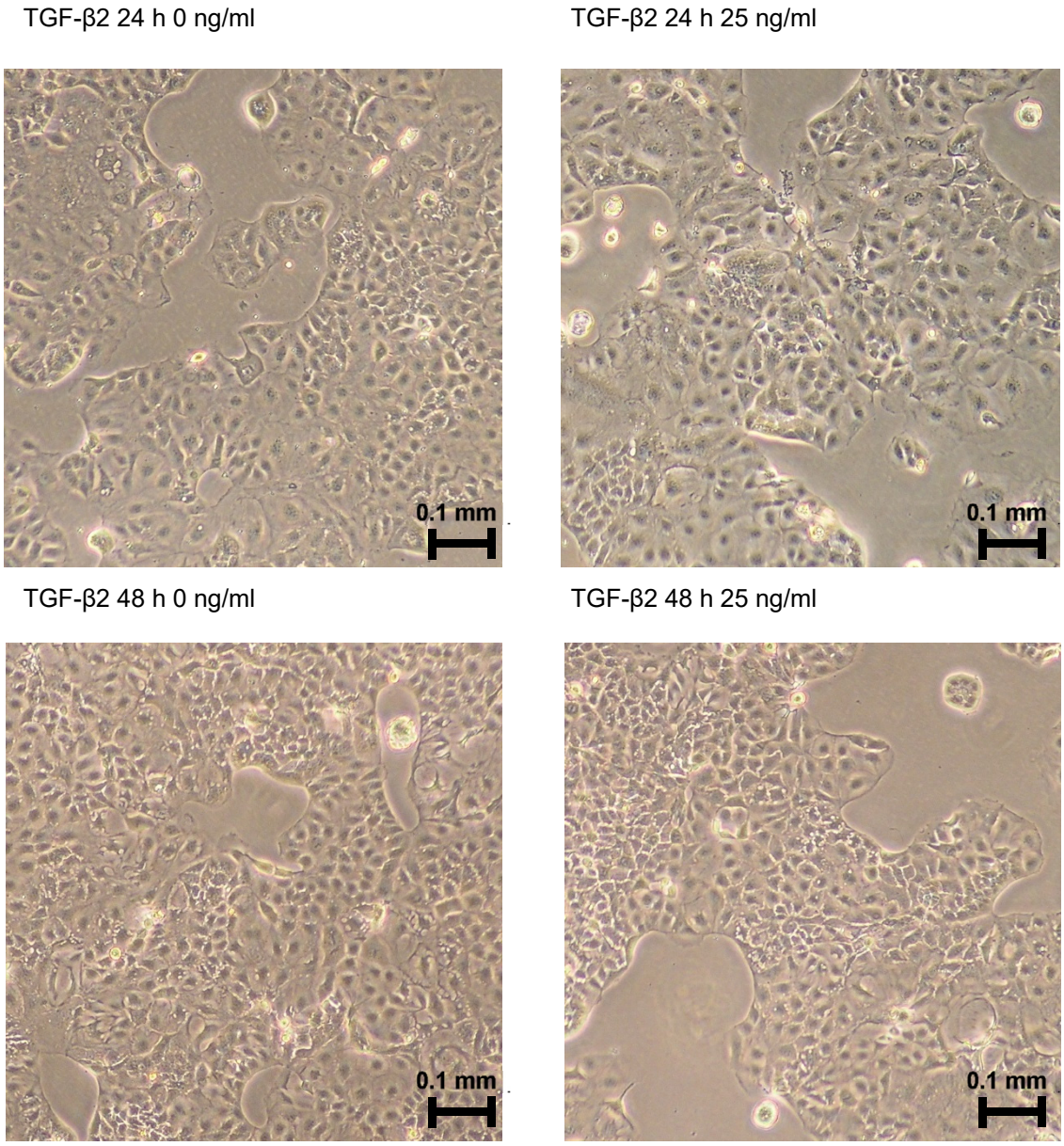

Figure 6.4: Caco-2 cells treated with TGF-β2 for 24 and 48 hours
No change in Caco-2 cell morphology was seen under light microscopy after TGF-β2 treatment, even after 48 hours. Total Magnification × 100

6.4.3 TGF-β2 effect on *SLCO2A1* expression

A549, LoVo and Caco-2 cells were treated with a range of concentrations of TGF-β2 for 24 hours and 48 hours. In A549 cells, an increase in the average *SLCO2A1* to *GAPDH* amplicon band intensity ratio was seen at all TGF-β2 concentrations (Figure 6.6), though the increase at 12.5 ng/ml and 25 ng/ml TGF-β2 appeared more pronounced at 48 hours (Figure 6.7). Although this trend was not found to differ significantly relative to the untreated control, or between the two time points, only the A549 cell line demonstrated this trend. In contrast, LoVo (Figure 6.8) and Caco-2 (Figure 6.9) did not show any appreciable change in *SLCO2A1* expression across the TGF-β2 concentrations used, even after 48 hours of treatment. Likewise, there was little change from 24 hours to 48 hours in these cell lines.

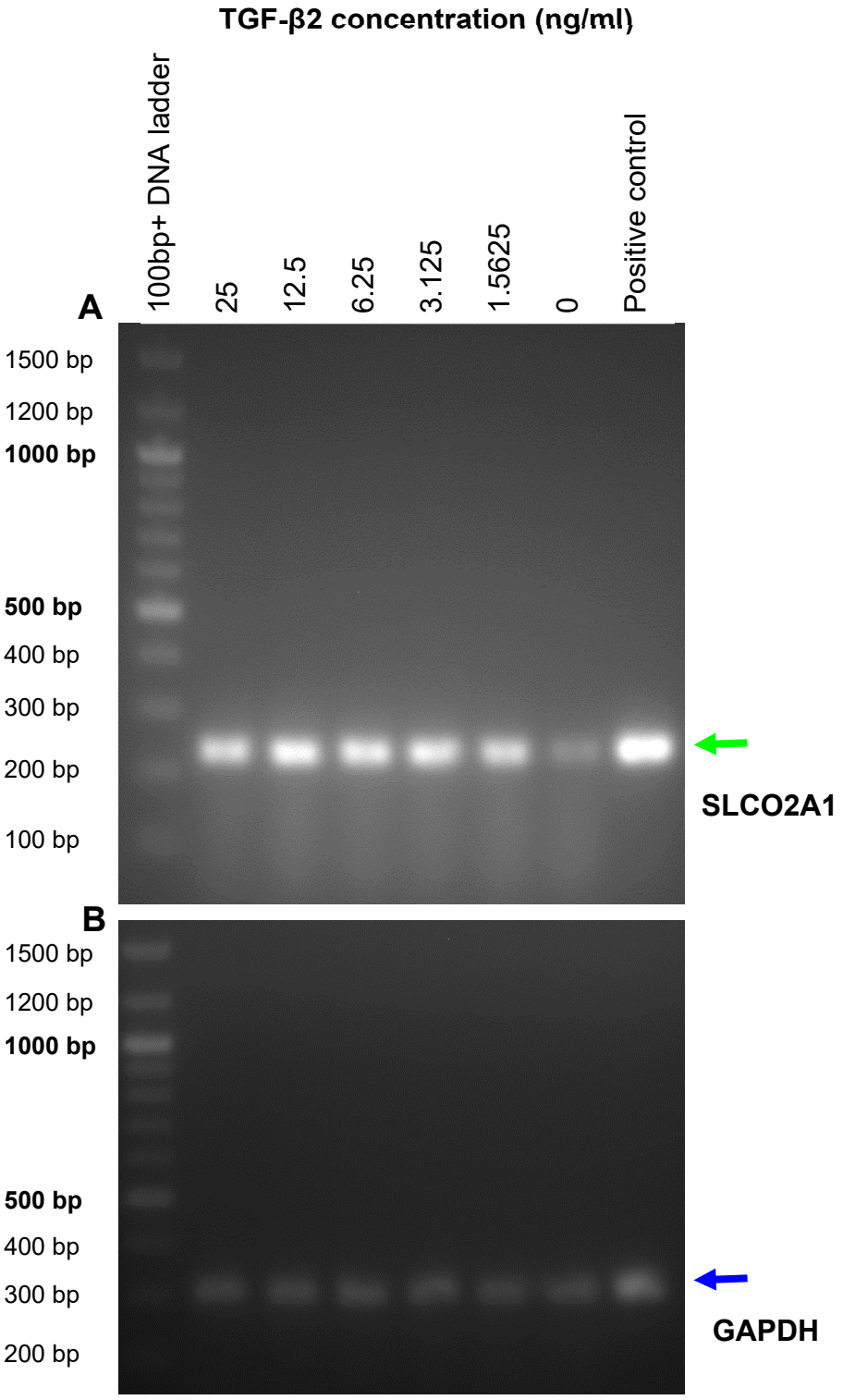

Figure 6.5: Representative agarose gels for A549 cells treated with TGF-β2 for 24 hours

The above gels represent one of the three *SLCO2A1* (A) (green arrow) and GAPDH (B) (blue arrow) PCR reactions for the 24 hour treatment whose band intensities were quantified to give the *SLCO2A1*/GAPDH volume intensity ratio. The same exposure time was used for *SLCO2A1* and GAPDH, and the same principle was used in all gel images for SAG, *SLCO2A1* and GAPDH at the 24 hour and 48 hour time points

A

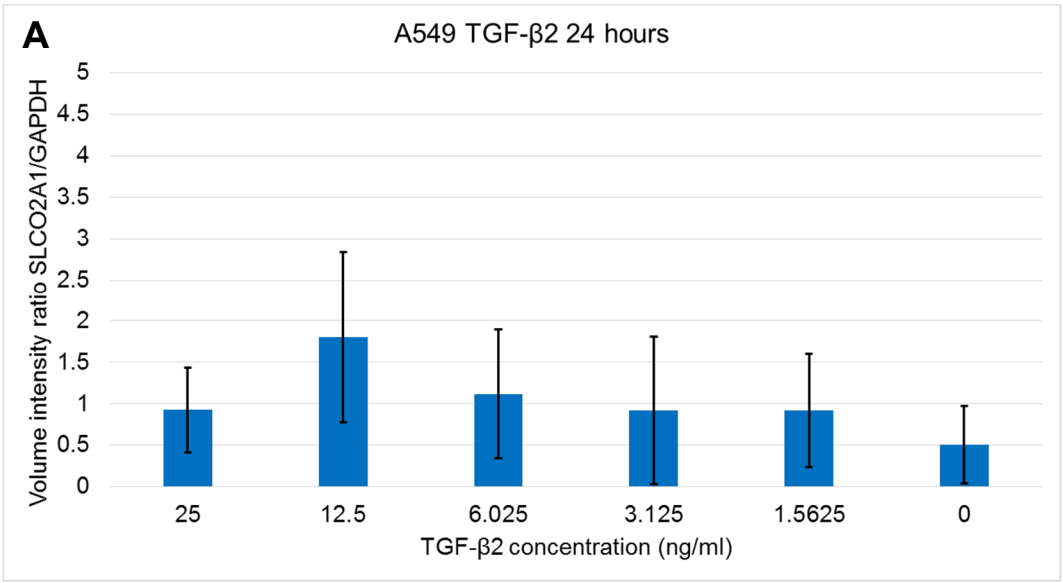

t-test p-values relative to 0 ng/ml TGF-β2				
25 ng/ml	12.5 ng/ml	6.25 ng/ml	3.125 ng/ml	1.5625 ng/ml
0.3564	0.1486	0.3208	0.5264	0.4432

B

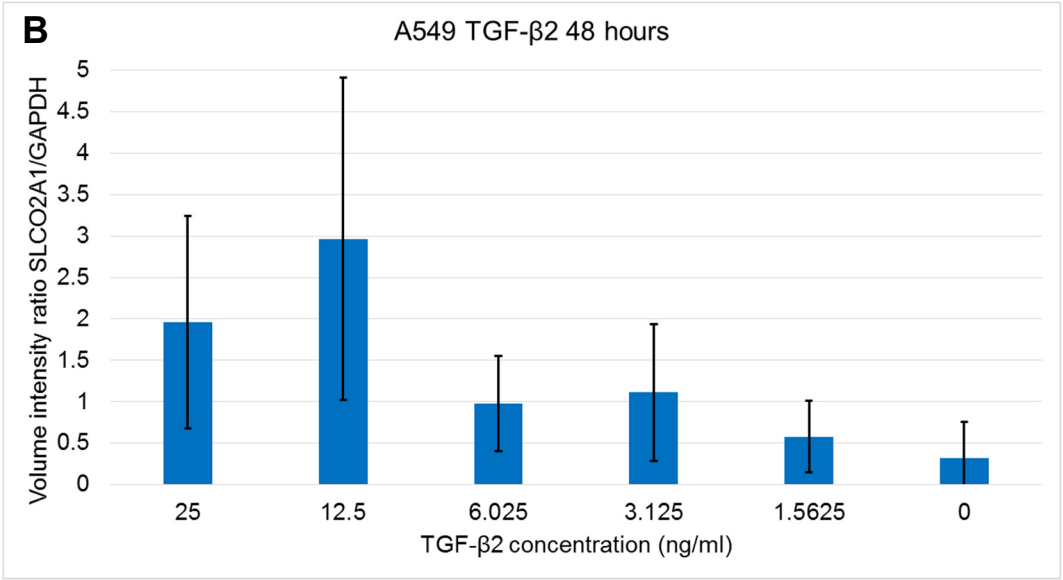

t-test p-values relative to 0 ng/ml TGF-β2				
25 ng/ml	12.5 ng/ml	6.25 ng/ml	3.125 ng/ml	1.5625 ng/ml
0.1469	0.1366	0.1920	0.2379	0.5062

C

t-test p-values for each concentration between 48 hours and 24 hours					
25 ng/ml	12.5 ng/ml	6.25 ng/ml	3.125 ng/ml	1.5625 ng/ml	0 ng/ml
0.2966	0.4286	0.8156	0.8004	0.5113	0.6350

Figure 6.6: Ratio of *SLCO2A1/GAPDH* expression in A549 cells treated with TGF-β2

The volume intensity ratio between *SLCO2A1* and *GAPDH* PCR band intensity was used as an indicator of *SLCO2A1* expression after 24 hours (A) and 48 hours (B). The results represent the average of three independent experiments and one standard deviation. Statistical significance was measured using a two-tailed Student's t-test. The p-value for each TGF-β2 concentration relative to the untreated control is shown in the table beneath each graph. (C) The table shows the p-value for any difference between 24h and 48h of treatment at each TGF-β2 concentration.

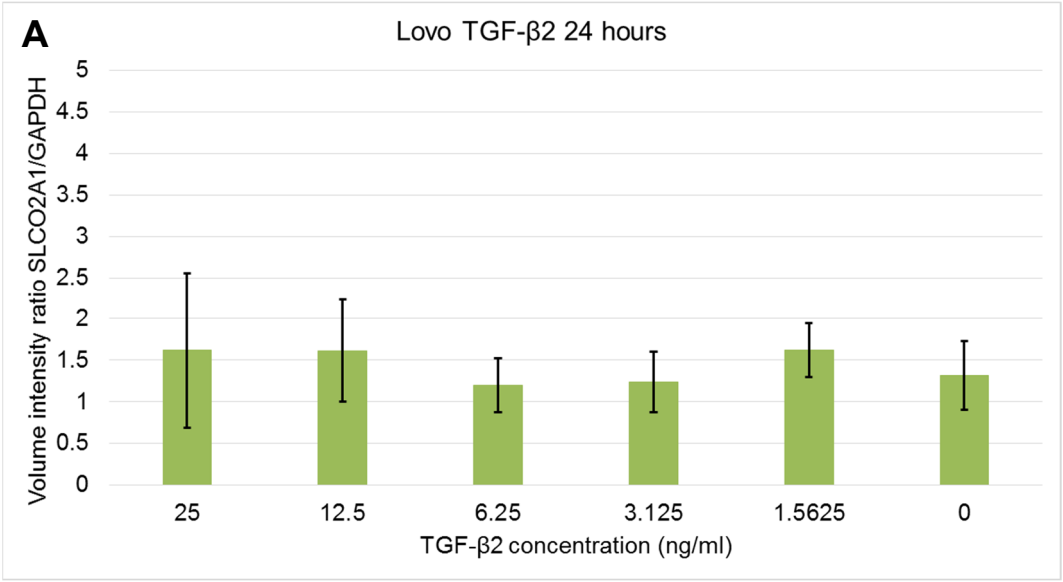

t-test p-values relative to 0 ng/ml TGF-β2				
25 ng/ml	12.5 ng/ml	6.25 ng/ml	3.125 ng/ml	1.5625 ng/ml
0.6458	0.5285	0.7147	0.8150	0.3723

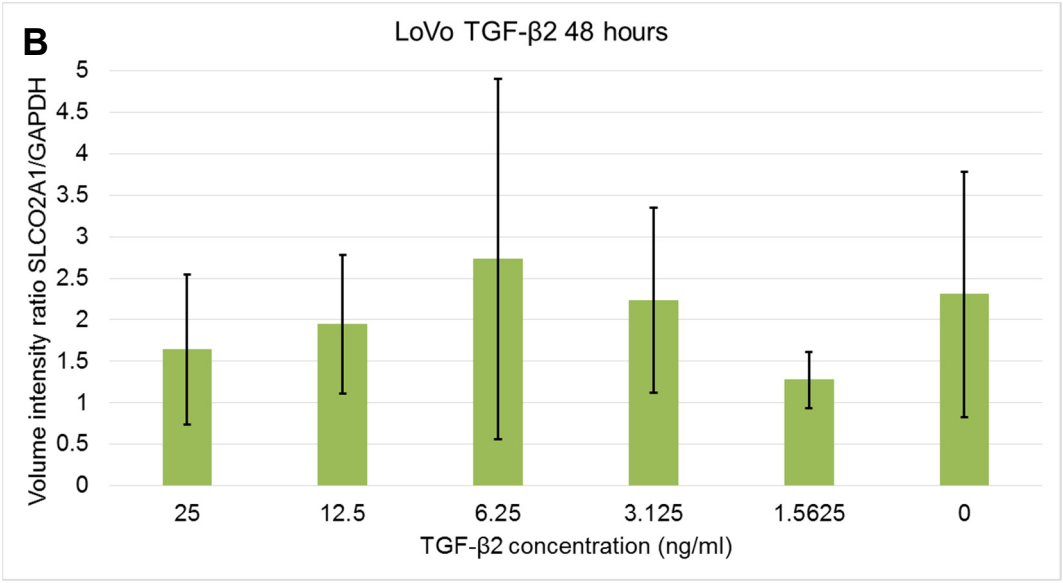

t-test p-values relative to 0 ng/ml TGF-β2				
25 ng/ml	12.5 ng/ml	6.25 ng/ml	3.125 ng/ml	1.5625 ng/ml
0.5478	0.7364	0.7934	0.9481	0.3496

C

t-test p-values between 48 hours and 24 hours					
25 ng/ml	12.5 ng/ml	6.25 ng/ml	3.125 ng/ml	1.5625 ng/ml	0 ng/ml
0.9814	0.6138	0.3442	0.2583	0.2689	0.3667

Figure 6.7: Ratio of SLCO2A1/GAPDH expression in LoVo cells treated with TGF-β2
Graphs show the average with one standard deviation in relative expression at (A) 24 hours and (B) 48 hours of treatment.

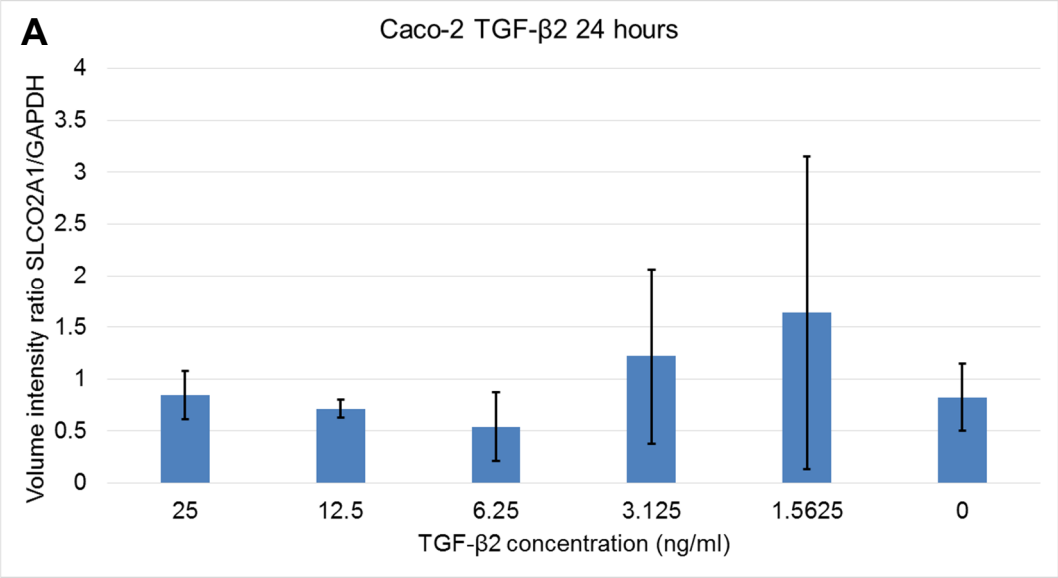

t-test p-values relative to 0 ng/ml TGF-β2				
25 ng/ml	12.5 ng/ml	6.25 ng/ml	3.125 ng/ml	1.5625 ng/ml
0.9358	0.6257	0.3483	0.5090	0.4474

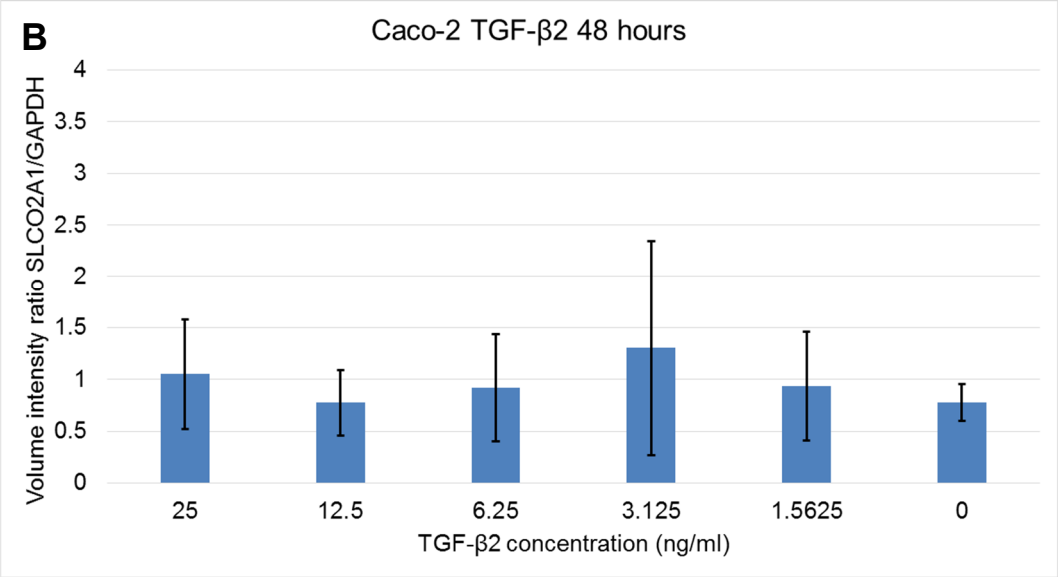

t-test p-values relative to 0 ng/ml TGF-β2				
25 ng/ml	12.5 ng/ml	6.25 ng/ml	3.125 ng/ml	1.5625 ng/ml
0.4696	0.9959	0.6891	0.4701	0.6595

C

t-test p-values between 48 hours and 24 hours					
25 ng/ml	12.5 ng/ml	6.25 ng/ml	3.125 ng/ml	1.5625 ng/ml	0 ng/ml
0.5802	0.7729	0.3553	0.9144	0.5103	0.8434

Figure 6.8: Ratio of SLCO2A1/GAPDH expression in Caco-2 cells treated with TGF-β2

Graphs show the average with one standard deviation in relative expression at (A) 24 hours and (B) 48 hours treatment.

6.4.4 Effect of TGF-β2 on *SLCO2A1* promoter deletion series

In the RT-PCR experiments, endogenous *SLCO2A1* expression showed an increase in A549 cells across the all of the TGF-β2 concentrations, unlike Caco-2 and LoVo. The promoter deletion constructs could identify regions within the 3198 bp of the *SLCO2A1* proximal promoter which could be important in mediating the downstream effects of TGF-β signalling.

As was also seen in the original deletion series transfections (section 4.4.2, Figures 4.3 and 4.4) all of the promoter constructs showed significantly greater activity compared to the promoterless control. For the S-3198, and S-1579 constructs, treatment with TGF-β2 for 48 hours appeared to increase the activity of the luciferase reporter constructs by approximately 30%, although these changes were not statistically significant (Figure 6.10). This level of change was however much less than the 400% to 600% increase in the endogenous SLCO2A1 mRNA expression (Figure 6.3).

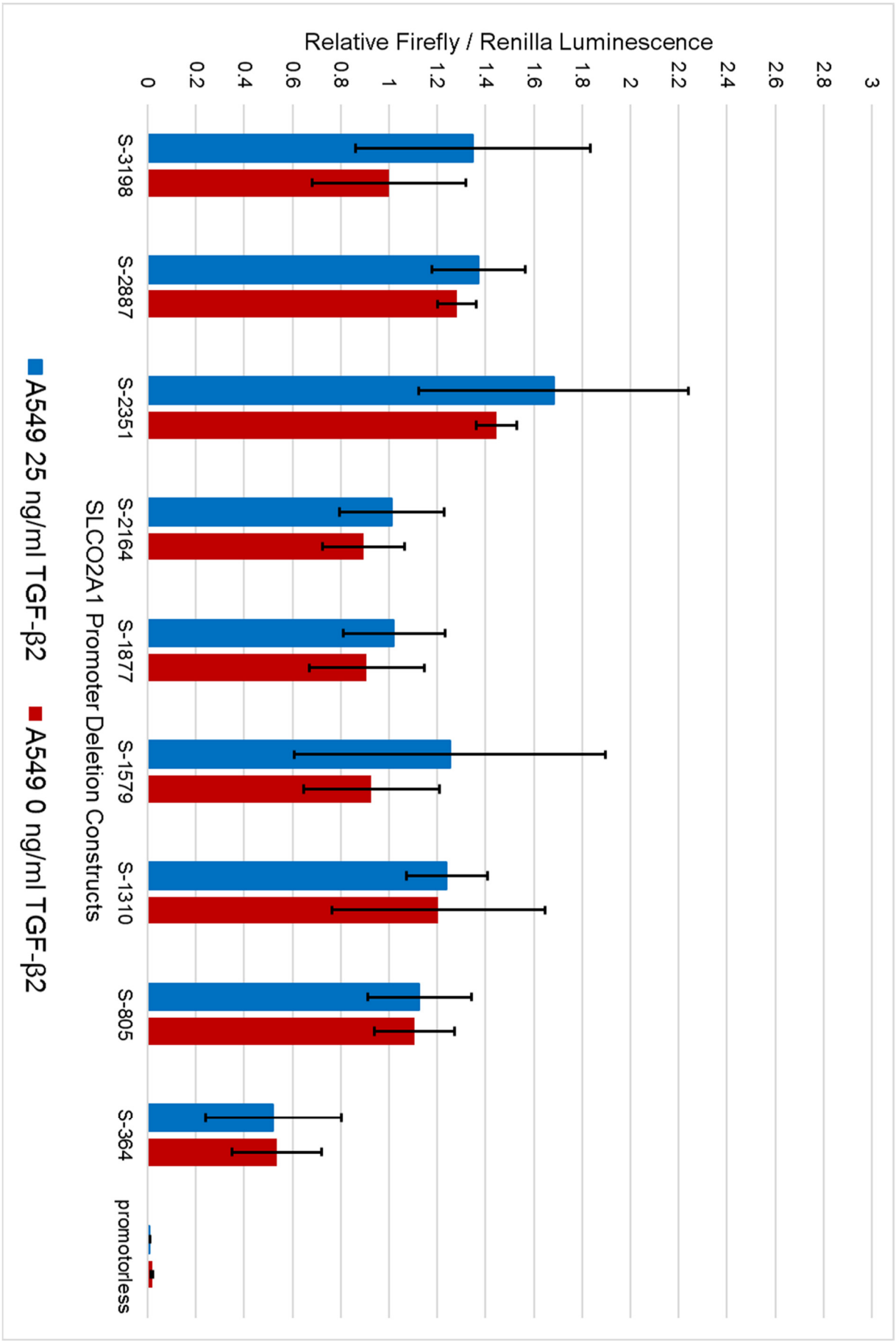
Relative Firefly / Renilla Luminescence
0
0.2
0.4
0.6
0.8
1
1.2
1.4
1.6
1.8
2
2.2
2.4
2.6
2.8
3
S-3198
S-2887
S-2351
S-2164
S-1877
S-1579
S-1310
S-805
S-364
promotorless
SLCO2A1 Promoter Deletion Constructs
A549 25 ng/ml TGF-β2
A549 0 ng/ml TGF-β2

Figure 6.9: Treatment of A549 cells transfected with the SLCO2A1 promoter deletion series for TGF-β2 for 48 hours
A549 cells were transfected with the nine *SLCO2A1* promoter deletion constructs from S-3198 to S-3164. In each experiment, one set was treated with 25 ng/ml TGF-β2, and the other with diluent solution lacking TGF-β2. A total of three experiments were carried out, each with three replicates for the treated and untreated groups. All luminescence ratios were normalised to the average of the untreated S-3198. The error bars represent the standard deviation.

6.4.5 Effect of Hedgehog Pathway activation on *SLCO2A1* expression

As inhibition of the hedgehog pathway had decreased *SLCO2A1* expression (Rivron et al 2012), it was expected that the Smoothened agonist (SAG), would lead to an increase in *SLCO2A1* transcript levels. As shown in Figure 6.11, the A549 cellular morphology showed no change in the presence of SAG, even after 48 hours of treatment at the highest dose of 10 nM. The A549 cells retained their usual polygonal appearance, and did not undergo epithelial to mesenchymal transition as when treated with TGF-β2 (Figure 6.3).

The volume intensity ratios of *SLCO2A1* to *GAPDH* showed no overall change across the concentration range of SAG used (Figure 6.12) at 24 hours. At 48 hours, a slight increase of approximately 30% in *SLCO2A1* expression was seen at 10 nM and 5 nM relative to the untreated A549 cells, although this change was not statistically significant. Also, at 10 ng and 5 ng, expression increased by approximately 30% between 24 and 48 hours, although this change was not statistically significant.

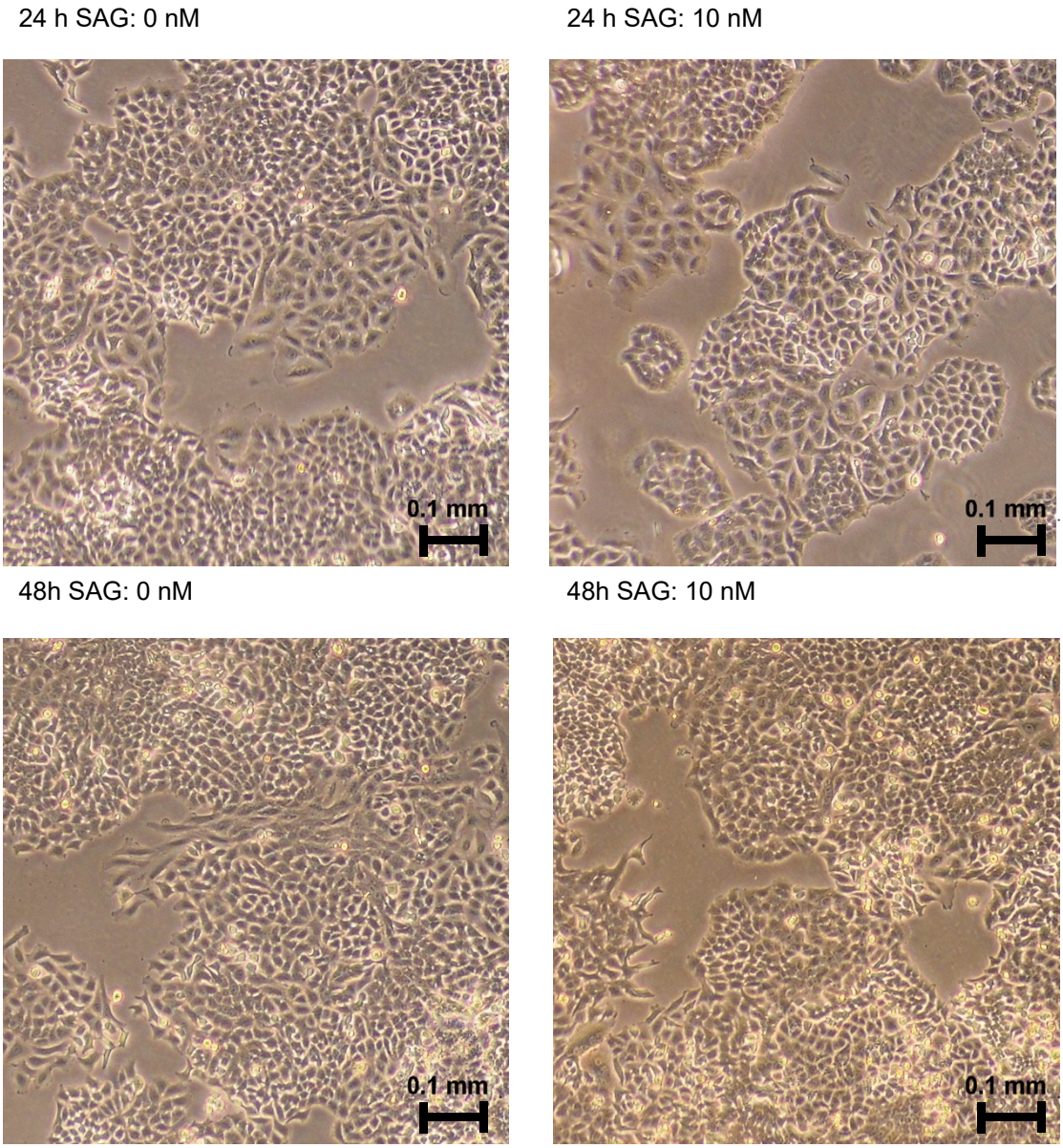

Figure 6.10: A549 cells treated with smoothened agonist (SAG) for 24 and 48 hours
A549 cells were either untreated or exposed to 10 nM SAG for 24 and 48 hours. Total Magnification × 100

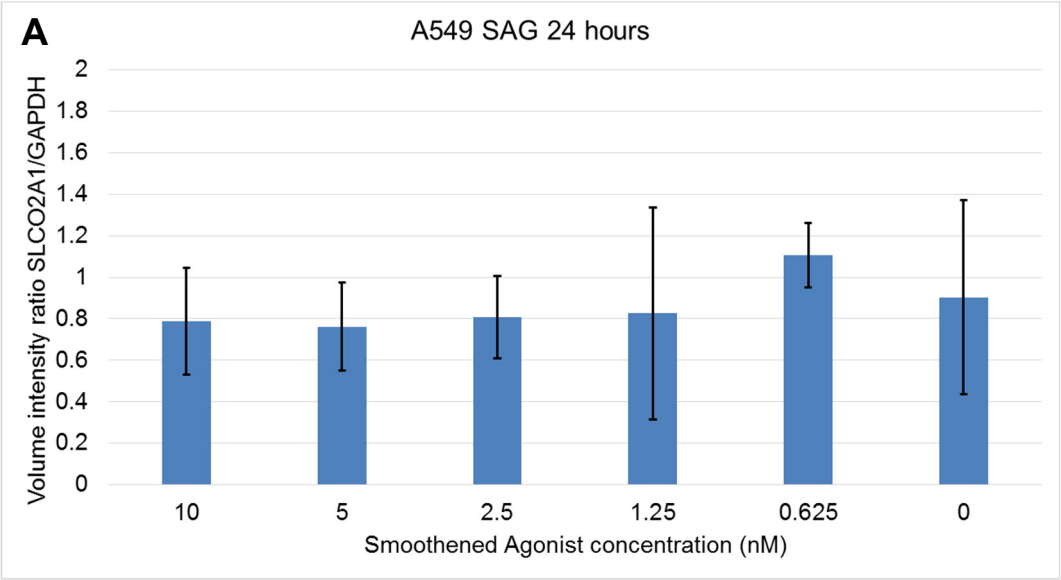

t-test p-values relative to 0 nM SAG				
10 nM	5 nM	2.5 nM	1.25 nM	0.625 nM
0.6847	0.6154	0.7221	0.8291	0.4800

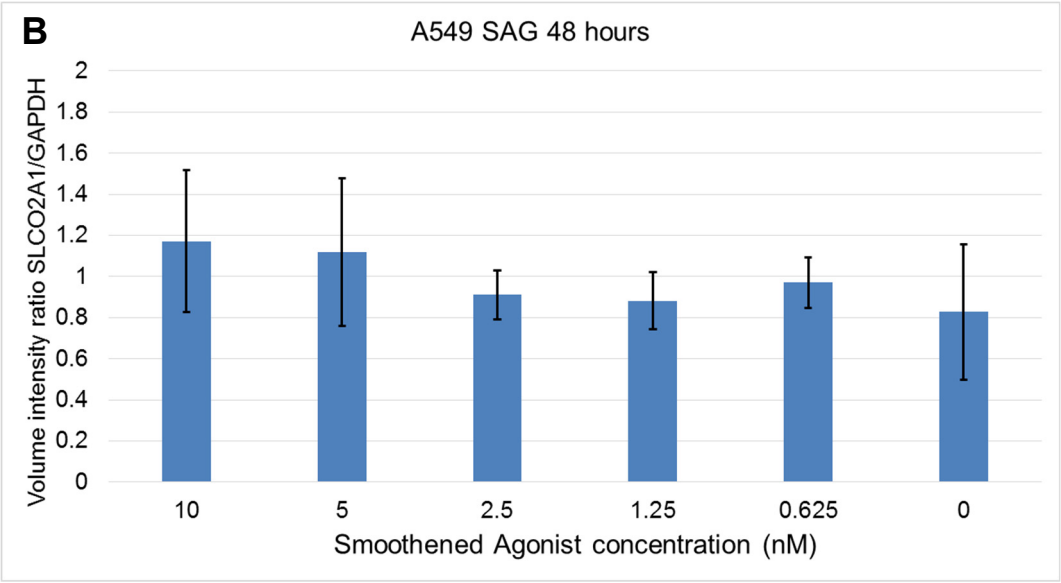

t.0-test p-values relative to 0 nM SAG				
10 nM	5 nM	2.5 nM	1.25 nM	0.625 nM
0.1989	0.2762	0.6603	0.7742	0.4689

C

t-test p-values between 48 hours and 24 hours					
10 nM	5 nM	2.5 nM	1.25 nM	0.625 nM	0 nM
0.1300	0.1619	0.4135	0.8434	0.4167	0.7992

Figure 6.11: Volume intensity ratios of *SLCO2A1* and *GAPDH* RT-PCR bands in A549 cells treated with SAG for 24 and 48 hours:
The volume intensity ratio between *SLCO2A1* and *GAPDH* PCR band intensity was used as an indicator of *SLCO2A1* expression. Overall no statistically significant difference was seen in A549 cells treated with SAG relative to the untreated control. The averages represent four independent experiments. The error bars represent the standard deviation

6.5 Discussion

The objective in these experiments was to assess whether the agents identified through bioinformatics analysis, TGF-β2 and SAG, could stimulate *SLCO2A1* expression in the A549, Caco-2 and LoVo cell lines. TGF-β2 was able to increase average *SLCO2A1* expression, though the variability of the data did not generate statistical significance. Alternative, more sensitive and accurate approaches could be used to detect and quantify changes in gene expression. Real-time PCR, for example can quantify the amount of PCR product through the course of the reaction (Arezi et al., 2003). Interestingly, TGF-β2 generated larger average transcriptional changes at the endogenous locus rather than the cloned 3 kb promoter construct. This may imply that the proximal *SLCO2A1* promoter only made a small contribution to the downstream effects transcriptional effects.

The TGF-β signalling pathway has been described as having a tumour suppression role in colorectal cancer (Markowitz et al., 1995; Samowitz and Slattery, 1997; Engle et al., 1999). Mutation or deletion of genes in the pathway occur in at least 70% of sporadic colorectal cancers (Fearon, 2011). Loss of homozygosity usually accounts for the loss of *SMAD2* and *SMAD4* alleles, while mutations in *TGFBR2* are also relatively common. (Yan et al., 2004; Huang et al., 1994).

The Caco-2 and LoVo colorectal cancer cell lines showed no change in *SLCO2A1* expression following TGF-β2 treatment, though as mutations in the TGF-β2 pathway are common in colon cancer, this may be due to genetic alterations in these cell lines inactivating the functional pathway. Caco-2 expresses wild-type *TGFBR2*, while LoVo carries a single and two base deletion in each allele (Ilyas et al., 1999). Yet, TGF-β1 had a functional effect on

LoVo, with a 10% reduction in growth rate, whereas no growth changes were seen in Caco-2 (Ilyas et al., 1999). Therefore, it is possible that TGF-β ligands could activate downstream SMAD2, SMAD3 and SMAD4 proteins via an alternate type V receptor (O'Grady et al., 1992; Ilyas et al., 1999). LoVo retains functional *SMAD4*, whilst Caco-2 carries a missense mutation in that gene (Woodford-Richens et al., 2001), which would explain the observations made by Ilyas et al (1999). Therefore, this may account for the lack of response observed in the Caco-2 cell line. Both Caco-2 and Lovo showed much higher expression of *SLCO2A1* compared to the A549 cell line, consequently the lack of a visible effect on LoVo could be explained by the inability to detect a small increase in mRNA relative to the higher baseline *SLCO2A1* expression.

That TGF-β pathway operates to repress PGE_2 signalling in the differentiated colon epithelial cells by upregulating *HPGD* (Yan et al., 2004), and repressing *PTGS2* (Harding et al., 2006; Takai et al., 2013), and as suggested here upregulating *SLCO2A1*, could represent one of the mechanisms by which PGE_2 signalling is normally supressed in the differentiated colonic epithelial. This supports the beneficial role of TGF-β in countering tumour progression. Although TGF-β signalling generally reduces growth of colorectal cancer cell lines (MacKay et al., 1995; Ilyas et al., 1999), its role as a tumour suppressor is however controversial. Evidence from cultures of primary colorectal cancer cells suggests that TGF-β signalling represses growth of early-stage colorectal cancer, while on the other hand, it accelerates growth, of more advanced disease (Huang et al., 1994).

The induction of epithelial-to-mesenchymal transition has been previously described in A549 cells (Miettinen et al., 1994; Kasai et al., 2005; Liu, 2008). This ability of TGF-β to trigger EMT (Tirino et al., 2013; Portella et al.,

1998) is of particular concern because it increases cell motility and invasiveness, and thus promotes metastasis. A more recent study has also implicated the TGF-β pathway in promoting colorectal cancer survival at metastatic sites by local immunosuppression in the tumour microenvironment (Tauriello et al., 2018). Activation of the TGF-β pathway, chiefly by TGF-β1, has been correlated with poorer prognosis in colorectal cancer patients (Friedman et al., 1995), later-stage adenocarcinomas, and lymph node metastasis (Lampropoulos et al., 2012).

Therefore, any theoretical benefit of activating the TGF-β pathway as prophylactic or therapeutic measure against colorectal cancer by suppressing PGE_2 signalling, is heavily offset by the dangers of promoting metastasis, and preferentially accelerating the growth of any cells within the tumour which in which the deregulated TGF-β pathway stimulates cell division and metastatic potential. Careful consideration of its potential use as a therapeutic agent would therefore depend on the nature of the individual tumour, the mutations it contains and the stage of disease.

Inhibition of the hedgehog pathway decreased expression of *SLCO2A1* in endothelial cells (Rivron et al., 2012), however it did not appear to influence transcriptional response in the low *SLCO2A1* expressing A549 cell line. It is not known whether genes encoding the Hedgehog pathway's components are mutated or lost in this cell line, in colorectal cancer, or colorectal cancer cell lines, which as with the lack of TGF-β response in Caco-2 and LoVo, may account for the absence of *SLCO2A1* transcriptional upregulation (Ilyas et al., 1999; Woodford-Richens et al., 2001). Plasmids expressing a downstream pathway component (such as SMAD2 or GLI1) could be used to bypass any unknown mutations that could exist in the natively expressed genes, upstream

mediators or surface receptors, in order to test the effect of activating a particular signalling pathway.

To conclude, whilst TGF-β was able to increase average *SLCO2A1* transcript levels in the low expressing A549 cell line, SAG had no measurable effect.

Chapter 7 Investigation into the co-expression of HPGD and SLCO2A1 in the colon

7.1 Introduction

The presence of HPGD and SLCO2A1 in both the human and rodent colon has been demonstrated by immunohistochemistry (Yan et al., 2004; Lejeune et al., 2010; Smartt et al., 2012a; Smartt et al., 2012b). Both proteins are normally localised to the columnar epithelial cells on the luminal surface of the mucosa. Moreover, a gradient of expression of both genes has been observed, increasing from the base of the colonic crypts to the lumen, as the migrating cells transiently divide and terminally differentiate (Smartt et al., 2012a; Smartt et al., 2012b). From a functional viewpoint, since SLCO2A1 and HPGD cooperate to reduce the levels of prostaglandins available for extracellular receptor activation, their patterns of expression might be expected to be similar.

The germline loss of *Hpgd* has been shown to exacerbate colon tumorigenesis in mice, but only in the presence of a carcinogen (azoxymethane) or a predisposing germline mutation in an established tumour suppressor gene ($Apc^{Min/+}$) (Myung et al., 2006). Both *HPGD* and *SLCO2A1* are downregulated in colorectal cancer (Yan et al., 2004; Backlund et al., 2005; Myung et al., 2006; Holla et al., 2008), and at least for *HPGD*, this occurs at an early stage of the disease (Backlund et al., 2005; Myung et al., 2006). It is not yet known if *SLCO2A1* dysregulation plays a mechanistic role in the development of polyps and adenomas. However, manipulation of the Wnt signalling pathway, by increasing β-catenin, reduces expression of both genes (Smartt et al., 2012a; Smartt et al., 2012b). Since Wnt pathway deregulation, with loss of functional APC and subsequent altered β-catenin expression, is one of the earliest events

in colorectal carcinogenesis (Powell et al., 1992; Munemitsu et al., 1995), it seems likely that SLCO2A1, as well as HPGD, could be reduced in early stage disease.

In both human and mouse tissues, gene expression levels can be examined and compared both at the RNA and protein levels (Myung et al., 2006; Holstege et al., 2010). Although protein detection is more straightforward experimentally, interpretation of results can be difficult, as it is highly reliant on good quality and specific detection reagents (Bordeaux et al., 2010; Algenas et al., 2014). Initial validation of reagents is therefore required, which is time-consuming, and may not provide a definitive answer (Fitzgibbons et al., 2014). However, protein analysis is the only option for detection of specific protein modifications, such as phosphorylation, that can have functional consequences (Brumbaugh et al., 2017).

Immunohistochemistry (IHC), in particular, can provide information on cell type and localisation of expression within tissues that may, for example, be required in order to understand cell-to-cell interactions in a microenvironment (Hofman and Taylor, 2013). IHC is, however, at best a semi-quantitative method, and requires expertise in assessment. RNA analysis can be easier to quantify, but does not give information on the actual location of cell type constituents (and only indirectly suggests their relative expression levels) (Hofman and Taylor, 2013).

7.2 Aims

To investigate the patterns of HPGD and SLCO2A1 expression (including the extent to which they are correlated) within the colon.

7.3 Methods

Immunohistochemistry was carried out to assess the efficacy of various antibodies to detect HPGD and SLCO2A1 protein in human and mouse FFPE tissue (sections 2.1.1, 2.1.2, and 2.1.3). Three antibodies against HPGD (Novus Biologicals NBP1-87061, and NBP1-87062, and Cayman Chemicals 160615) were used, and three for SLCO2A1 (Abcam ab150788, Bioss Antibodies bs-4710R, and Cayman Chemicals 11860) (Table 9). To better discriminate background from specific labelling, the antibody assessment included antibody titration, isotype IgG controls, and comparison with tissue from a second organ (kidney). (The kidney was used for additional assessment as mouse kidney has been shown to express both HPGD and SLCO2A1 (Bao et al., 2002; Nomura et al., 2005; Chi et al., 2008; Yao et al., 2008; Shiraya et al., 2010; Liu et al., 2014)).

Further validation was performed by western blotting on lysates of cells transfected with a *SLCO2A1* expression construct (sections 2.1.5, 2.1.6, 2.1.7 and 2.1.8)

7.4 Results

Antibodies were initially selected for their potential for use on both mouse and human tissue. This was judged by analysis of the sequence similarity between the human and mouse proteins at the target epitope sites (Figure 7.1 and Figure 7.2), and evidence of their previous application.

The HPGD antibodies were all raised against the human sequence, but their target epitopes did show a high levels of similarity to the mouse sequence (Figure 7.1). The Novus NBP1-87062 (Novus 62) epitope was 96.5% identical to the mouse protein, whilst the Cayman, which had the smallest epitope at 14

amino acids, and the Novus 61, had 93% and 81% identity respectively. Although there was a lower sequence identity for the latter antibody, it detected a non-overlapping epitope compared to the other two reagents, so offered the potential to provide additional evidence of labelling specificity. All three antibodies were therefore selected for tissue analysis.

For the prostaglandin transporter, three antibodies were selected. The Abcam, Bioss and Cayman antibody epitopes had 84%, 66% and 64% identity with the mouse sequence (Figure 7.2). The epitope sequences of the Cayman and Bioss antibodies overlapped. All three were used in subsequent immunolabelling experiments.

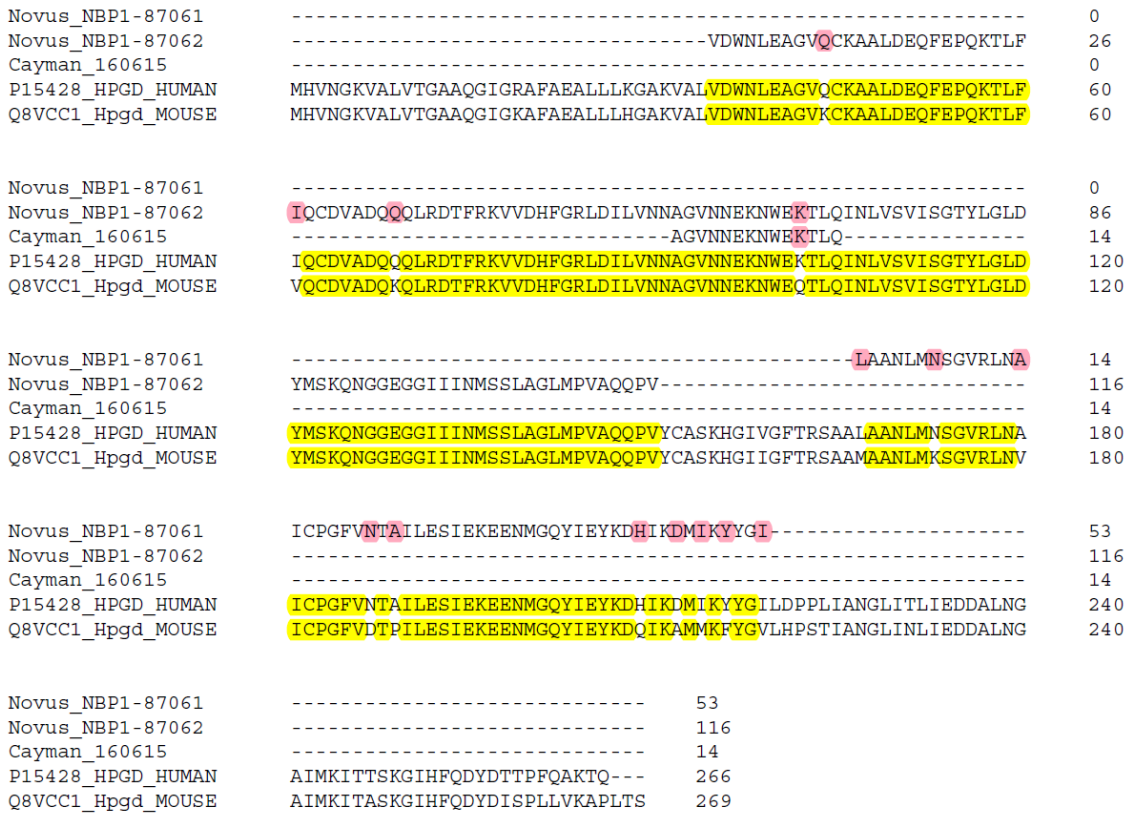

Figure 7.1: Sequence alignment of human and mouse HPGD, and the antibody target epitopes

Human HPGD (UniProt P15428), mouse HPGD (UniProt Q8VCC1), and the antibody epitopes were aligned using Clustal Omega (Goujon et al., 2010; Sievers et al., 2011). Amino acid positions where the mouse differed from the three human epitope sequences are highlighted in light red on the antibody target epitope sequences. Regions within the epitope sequence that were identical in both species are highlighted in yellow. The epitope of Novus NBP1-87061 differs in 10 of 53 amino acid positions, Novus NBP1-87062 differs in 4 of 116 positions, and Cayman 160615 by 1 of 14.

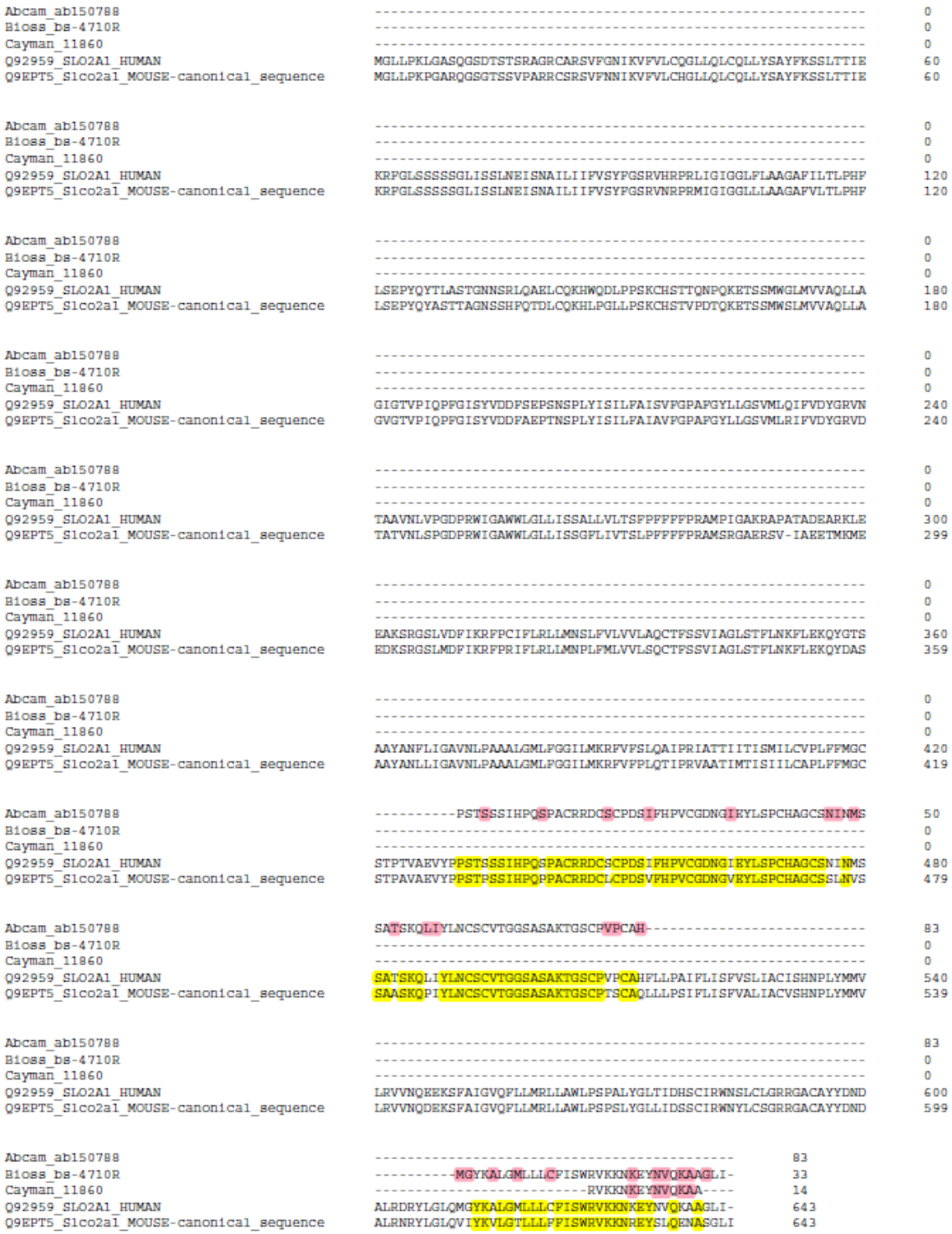

Figure 7.2: Sequence alignments of human and mouse SLCO2A1, and the antibody target epitopes

Differences between the human and mouse are in red and matching residues in yellow. The epitope of the Abcam antibody differs in 13 of 83 amino acid positions, Bioss differs in 11 of 33 positions, and Cayman in 5 of 14 amino acids.

7.4.1 Expression of HPGD in mouse tissue

Using the Novus 61 antibody, HPGD expression appeared to be localised to the goblet cells, rather than the terminally differentiated colonic epithelial cells expected (Figure 7.4). The Novus NBP1-87062 (Novus 62) antibody failed to label any cells, while the Cayman antibody did label the most differentiated columnar epithelium, with staining present to a much lesser extent in other cells within the submucosa. Unfortunately, the corresponding isotype control bound non-specifically throughout the section, making interpretation of specific HPGD labelling difficult.

In the kidney tissue used as a control, none of the antibodies generated any positive staining, which had previously been reported in the proximal convoluted tubules, the thick ascending limb of the loop of Henle, and the collecting duct (Nomura et al., 2005; Yao et al., 2008; Shiraya et al., 2010; Liu et al., 2014).

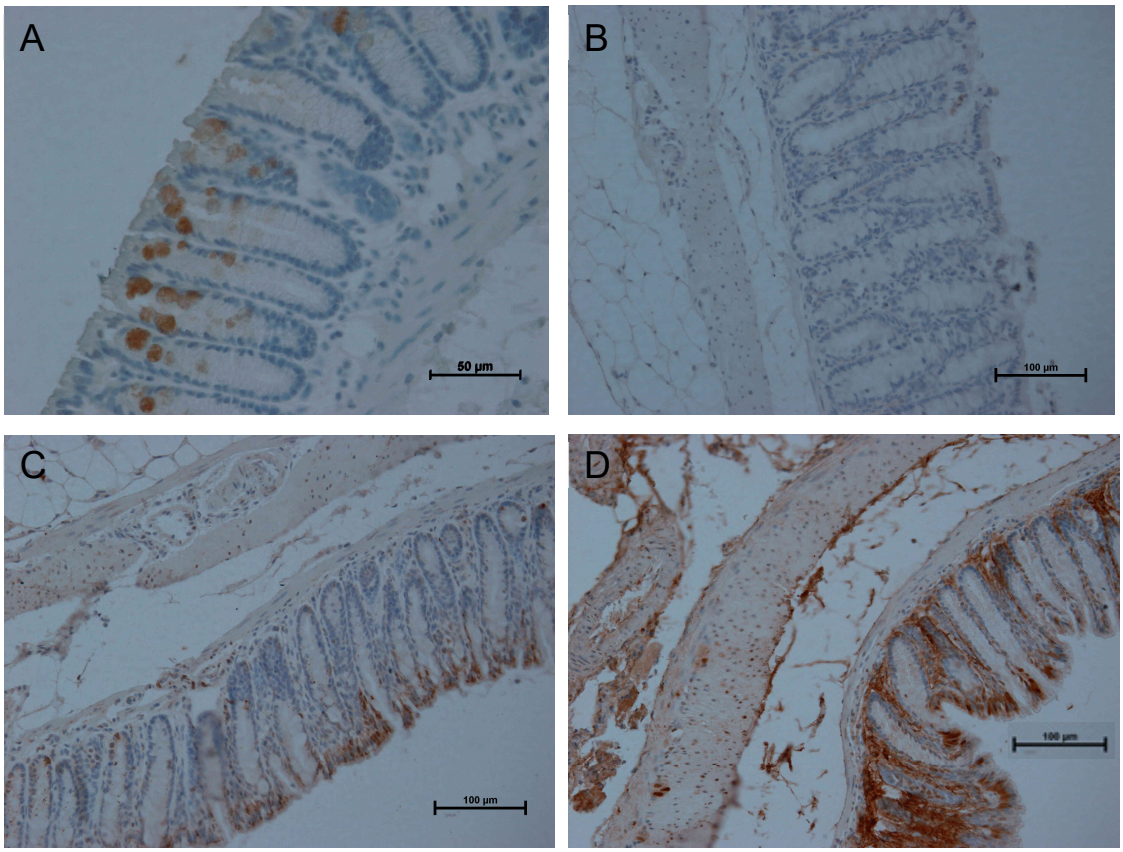

Figure 7.3: HPGD staining on normal colon sections

(A) Novus NBP1-87061 (2 µg/ml), and (B) corresponding isotype control; (C) Cayman 160615 (20 µg/ml), and (D) corresponding isotype control.

7.4.2 Expression of SLCO2A1 in mouse tissues

The Abcam antibody to SLCO2A1 did label vascular endothelial cells within the colon tissue, as expected; however, the labelling in the epithelium was essentially absent, with a very faint brown wash on a minority of the terminally differentiated cells (Figure 7.4). Although the Bioss reagent did identify the differentiated epithelium, with individual cells in the mucosa especially strongly immunolabelled, there was substantial isotype control labelling, that questioned the specificity of the Bioss reagent. The Cayman antibody was the most specific, localising to the terminal epithelium.

In the kidney, the faint Abcam antibody labelling was similar to the isotype control, indicating non-specific reactivity. The Bioss and Cayman antibodies both labelled collecting ducts (Figure 7.5) which was an expected localisation of the prostaglandin transporter (Bao et al 2002, Nomura et al 2005, Chi et al 2008). Overall the Cayman antibody appeared most specific, but further optimisation/validation would be of benefit to increase the signal relative to the non-specific background, before used this as an analytical reagent in mouse tissues.

As all of these antibodies were raised against the human protein sequence, this factor may account at least in part for the variable specificity. It was anticipated that they might show better labelling specificity on human tissues, which were therefore examined next.

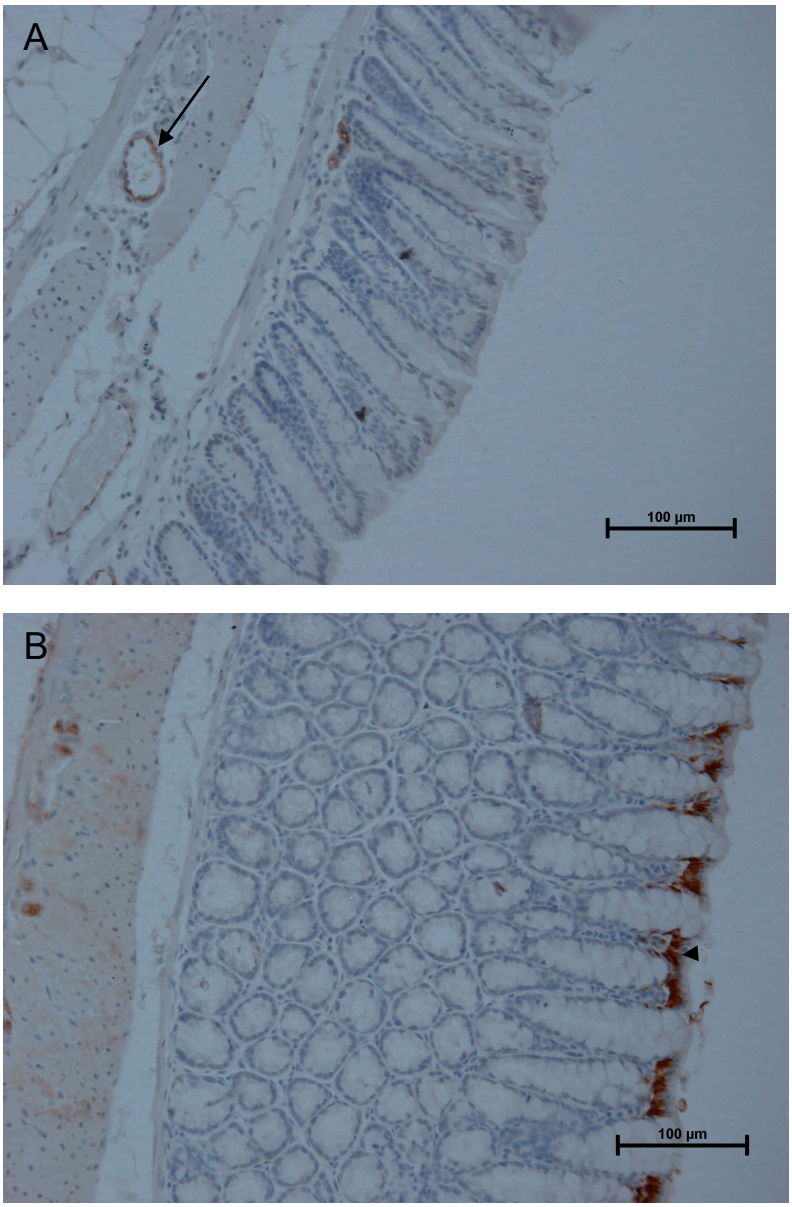

Figure 7.4: SLCO2A1 staining on normal mouse colon sections

(A) Abcam, (2 µg/ml). Endothelial labelling indicated by arrow. (B) Cayman, (2 µg/ml). Epithelial labelling indicated by arrow head.

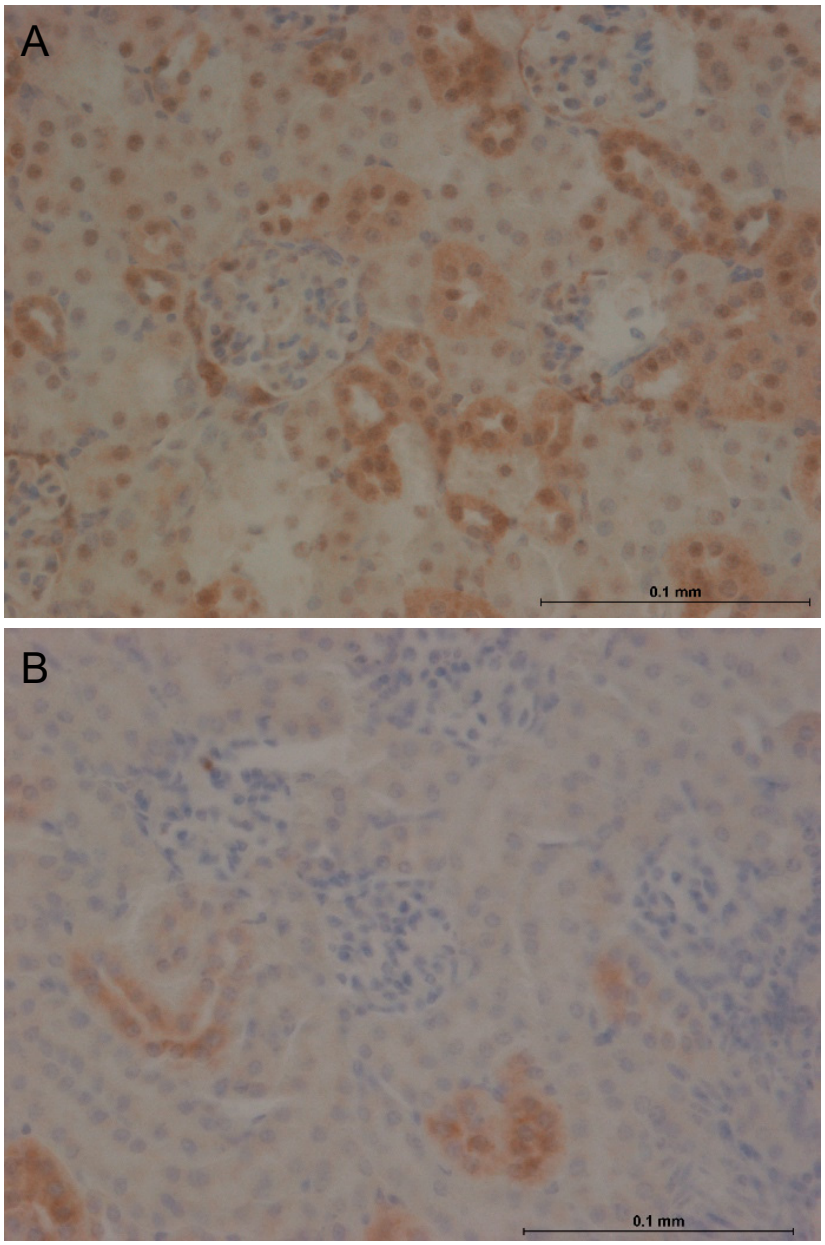

Figure 7.5: SLCO2A1 staining on normal mouse kidney sections

(A) Bioss 1:100 (10 µg/ml). Labelling present in the collecting ducts, both within the cytoplasm and nucleus of the cells. The glomeruli were not labelled, Labelling elsewhere was due to the relatively strong background (B) Cayman 1:200 (1 µg/ml). Labelling in a few collecting ducts.

7.4.3 Expression of HPGD in human tissue

HPGD expression was identified in the colonic epithelial cells (Figure 7.6). The Novus 61 antibody showed the clearest labelling with least background. The columnar epithelial cells on the luminal edge showed a strong labelling pattern that was cytoplasmic with occasional positive nuclei. Isolated additional cells also stained positive for HPGD, predominantly visible in the muscularis propria layer, but also occurring in the submucosa and mucosa between the colonic crypts; these were thought to be immune cells, macrophages or lymphocytes. A similar staining pattern was observed with the Novus 62 antibody, but the background staining was more prevalent. The Cayman reagent showed the weakest staining and greatest background. Although the colonic epithelium was clearly stained, background persisted in the rest of the mucosal layer, reflected in the IgG isotype control also.

In the kidney, the medullary collecting duct epithelium was weakly and non-uniformly labelled with the Novus 61, and was barely detectable with the Novus 62 and Cayman antibodies; this is however likely to be non-specific, as the isotype control also preferentially labelled these cells (Figure 7.7).

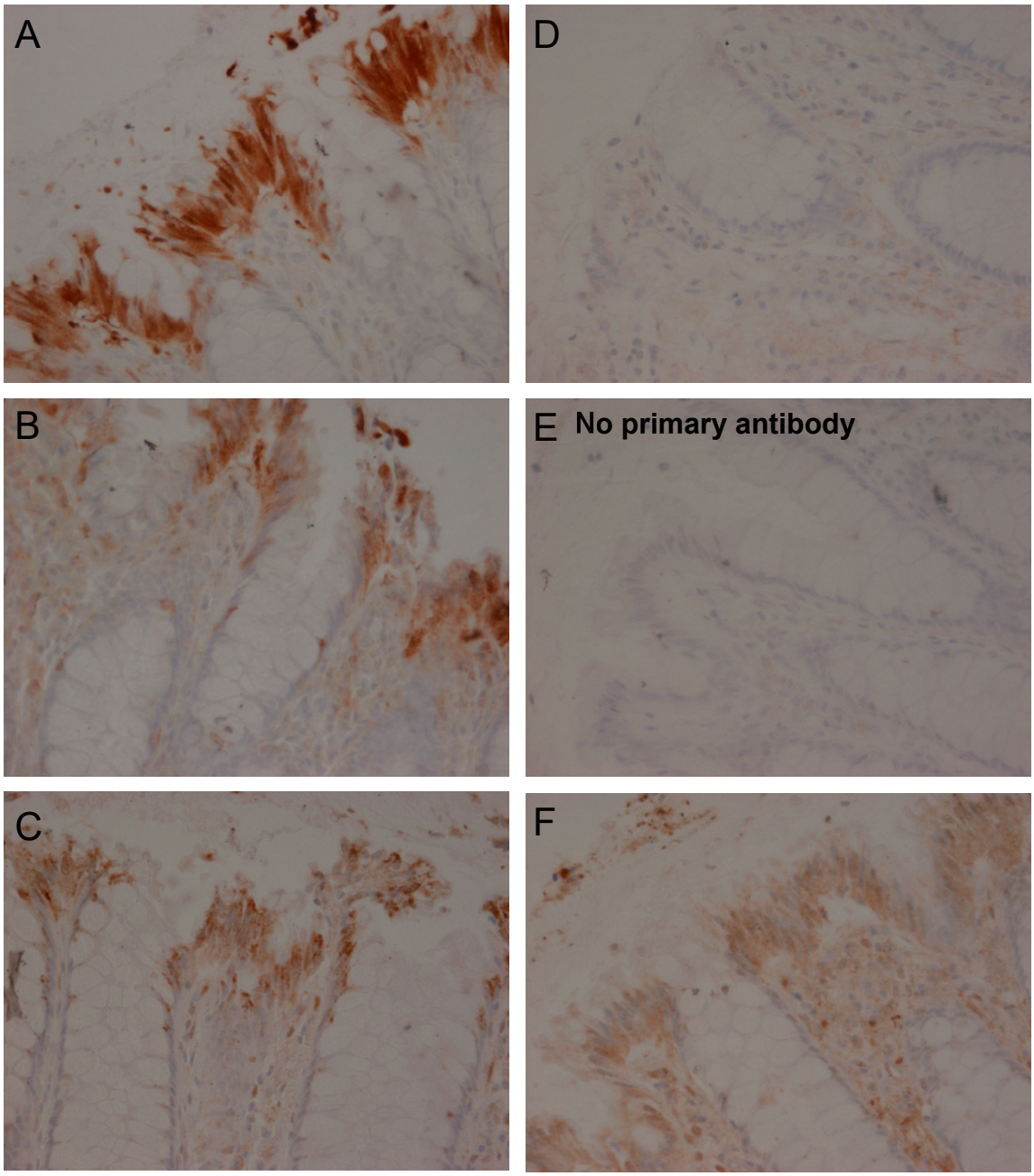

Figure 7.6: HPGD expression in the normal human colon

(A) Novus NBP1-87061 1:50 (2 µg/ml). The colonic epithelial cells show strong staining, both in the cytoplasm and nuclei. A few isolated HPGD-positive cells also occurred within the mucosa, submucosa and muscularis layers. (B) HPGD Novus NBP1-87062 1:25 (2 µg/ml). The staining pattern was very similar to the 87061 antibody, although weaker, and with noticeably stronger background staining. (C) Cayman 160615 1:200 (5.7 µg/ml). Although the colonic epithelium cells stain more intensely than the background, the rest of the section showed comparable background staining to the rabbit IgG control at the same concentration (F). (D) Rabbit IgG 1:1000 (2 µg/ml). (E) No primary antibody. (F) Rabbit IgG 1:351 (5.7 µg/ml)

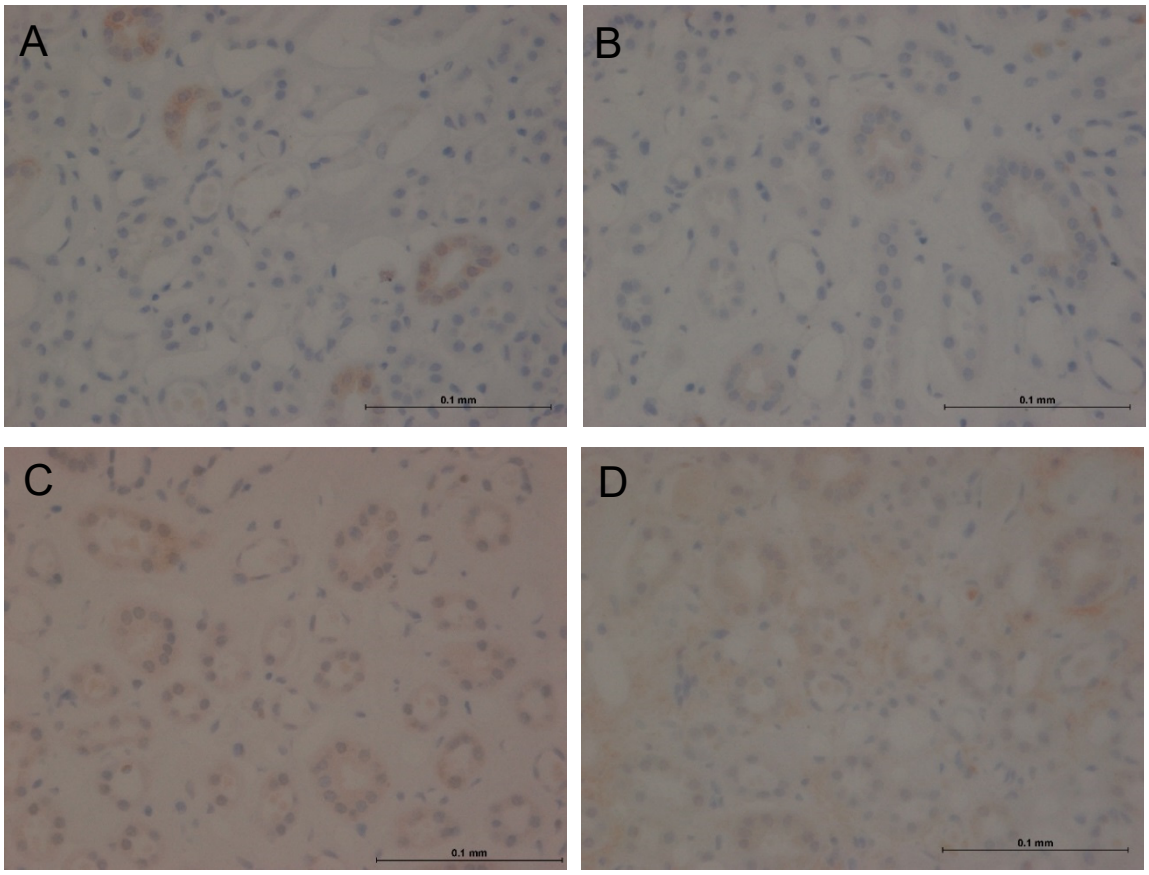

Figure 7.7: HPGD expression in the normal human kidney medulla

(A) Novus NBP1-87061 1:100 (1 µg/ml). (B) Novus NBP1-87062 1:50 (1 µg/ml). (C) Cayman 160615 1:100 (11.4 µg/ml). (D) Rabbit IgG. 1:1000 (2 µg/ml).

7.4.4 Expression of SLCO2A1 in human tissue

Overall, the SLCO2A1 antibodies appeared to show differences in preference for endothelial vs. epithelial labelling. The Abcam antibody weakly labelled the colonic epithelium, while in contrast, endothelial cells in capillaries and other blood vessels stained more strongly (Figure 7.8). The Cayman anti-SLCO2A1 antibody showed comparable labelling intensity on both colonic epithelial cells and endothelial cells in the vasculature, and moderate levels of background. The Bioss antibody labelled both epithelial and endothelial cells, with the epithelial cells more strongly labelled. However, for all the antibodies there was a small degree of non-specific labelling throughout the tissue, as judged by the isotype control.

The three SLCO2A1 antibodies also showed different labelling abilities for the cell types in the kidney (Figure 7.9). Strong labelling in cortical endothelium, with less intensity in the medulla, was detected with the Abcam reagent. The Bioss antibody appeared to more strongly label the collecting ducts in cortex and medulla, with weaker endothelial labelling, particularly of larger vessels in the medulla. The Cayman antibody appeared to label collecting ducts strongly in the medulla, with faint endothelial labelling present in the cortex. Additional cells, some of which appeared to be within the lumen of vessels in the glomerulus, were also labelled.

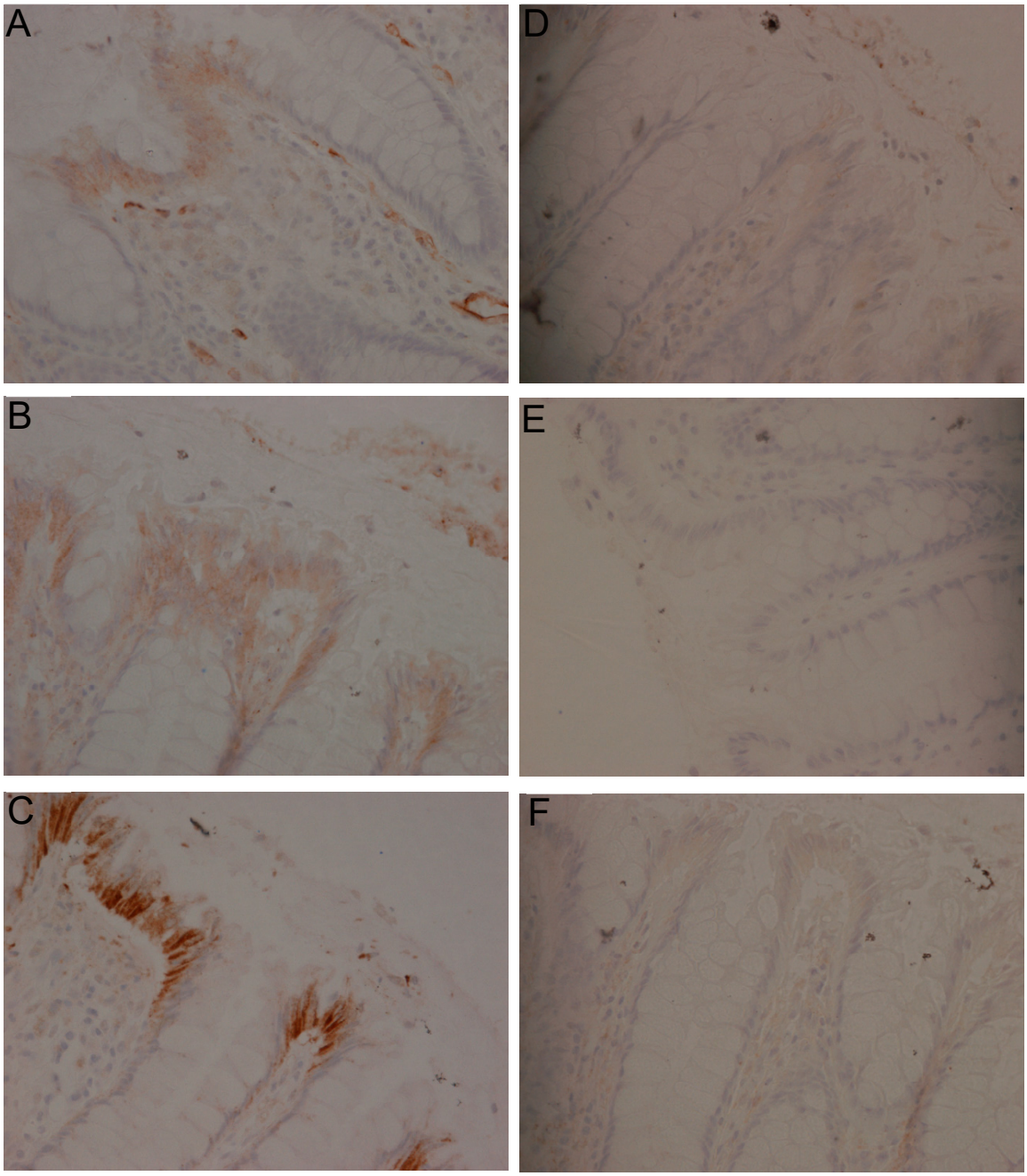

Figure 7.8: SLCO2A1 expression in the normal human colon

(A) Abcam 1:50 (2 µg/ml). Colonic epithelial cells were stained weakly, while as with the kidney, endothelial cells were strongly stained. (B) Cayman 1:100 (2 µg/ml). Colonic epithelium and endothelial cells were both stained. (C) Bioss 1:400 (2.5 µg/ml). Strong staining for colonic epithelial cells, and very weak endothelial cell staining. (D) Rabbit IgG 1:1000 (2 µg/ml). (E) No primary antibody. (F) Rabbit IgG 1:800 (2.5 µg/ml).

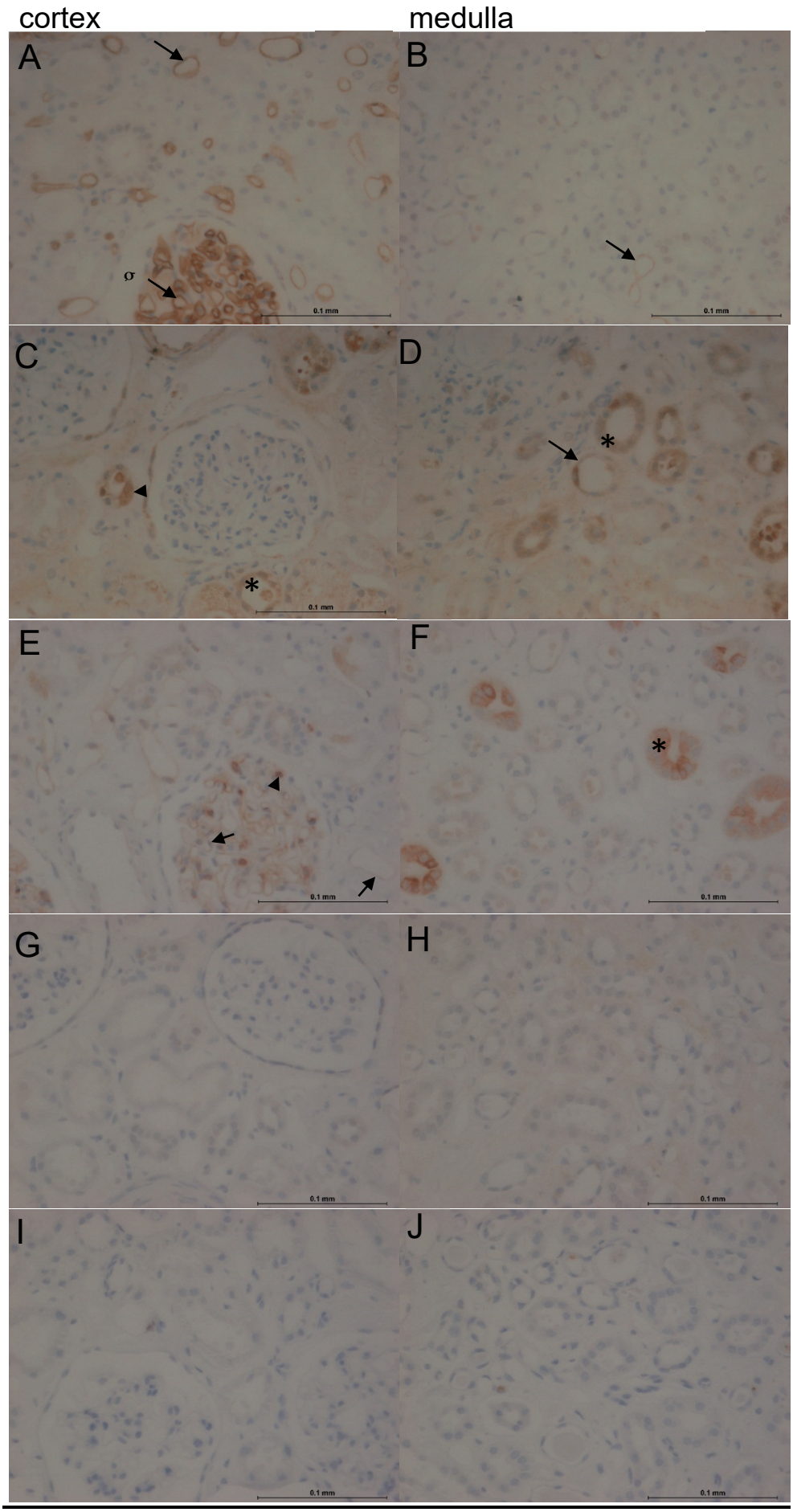
cortex
medulla
A
B
C
D
E
F
G
H
I
J
0.1 mm

Figure 7.9: SLCO2A1 expression in the normal human kidney

(A, B) Abcam 1:200 (0.5 µg/ml). The antibody labelled vascular endothelial cells (arrow). This was in the cortex, both inside and outside of the glomerulus (gl). Endothelial cells, which occur less frequently in the medulla, are also labelled (arrow). (C, D) Bioss 1:100 (10 µg/ml). Labelling of collecting duct epithelial cells within the cortex and medulla (star), with distal tubules (arrow head), and faint medullary endothelial cells (arrow). (E, F) Cayman 1:200 (1 µg/ml). The endothelial cells (arrow), collecting duct cells (star), and additional cells within the glomerulus (arrow head). (G, H) Rabbit IgG 1:1000 (2 µg/ml). (I, J) No primary antibody.

7.4.5 Investigating antibody specificity using western blotting

The antibodies were further assessed for their specificity towards human protein, using western blotting. Previous analysis had been performed on the HPGD antibodies by western blotting of cells containing a HPGD expression construct. The Novus 61 was found to be most specific, as it detected a single band of the correct size. Additional bands were detected with the Novus 62 and Cayman reagents (personal communication, Lisa Allinson, University of Leeds).

Assessment of the SLCO2A1 antibodies on human lysates was performed by transiently over-expressing the prostaglandin transporter in A549 cells, which have undetectable levels as judged by RT- PCR (Figure 3.2). The predicted molecular weight for the protein is 71 kDa, and although a number of bands were detected in all lysates, the dominant bands were not close to this size. No differences in banding were seen between the transfected lysate and control, showing that no specific SLCO2A1 bands were detected by any of the antibodies (Figure 7.10). The commercial antibody datasheets had presented data either from tissues or lysates of cell lines known to express SLCO2A1, and so may have erroneously interpreted the resulting banding patterns as correct. Based on this experience, no additional support for the specificity of any of these antibodies can be obtained from western blotting.

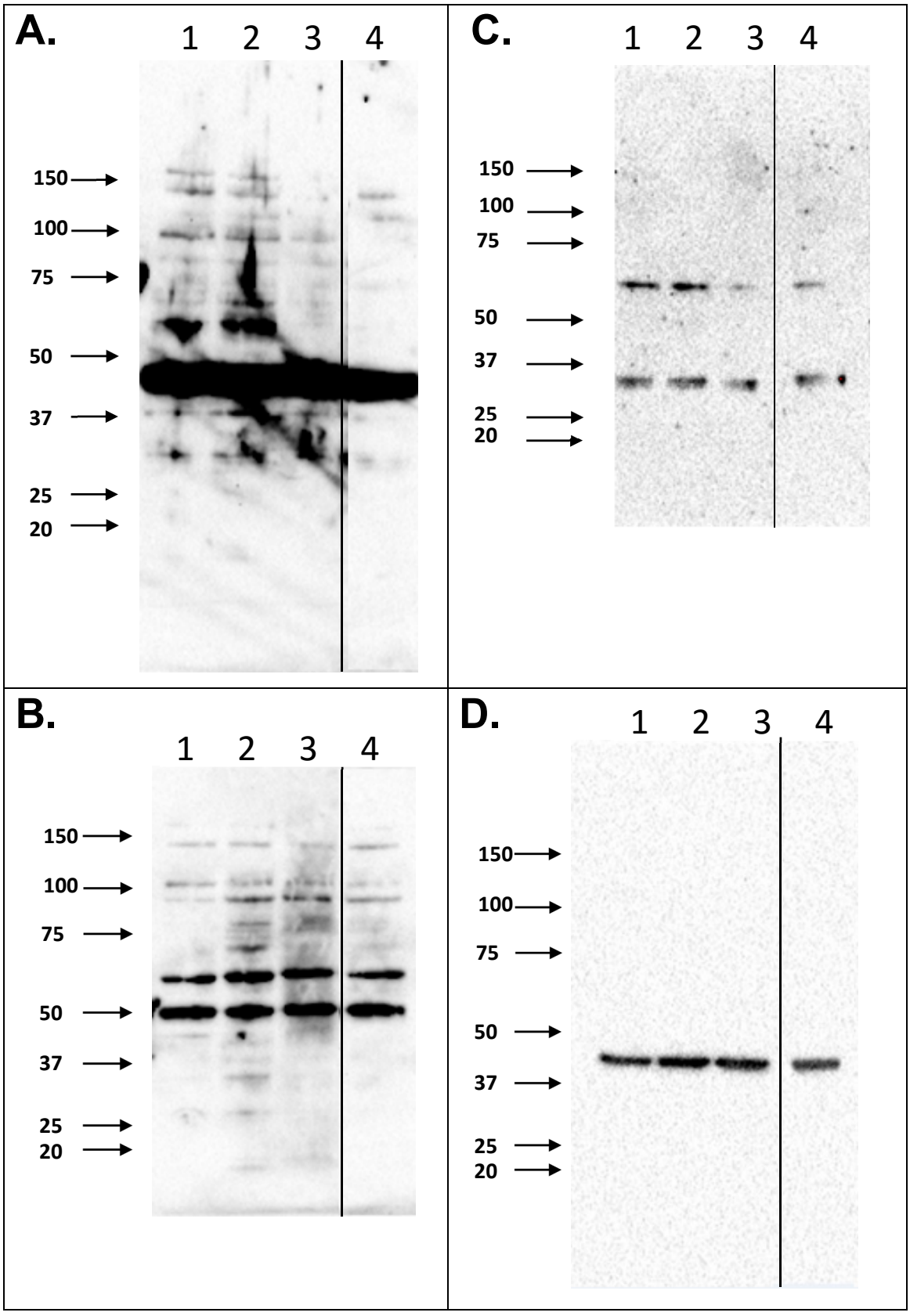

Figure 7.10: Western blotting analysis of SLCO2A1 antibodies

ntibodies used were (A) Bioss 1:500, (B) Cayman 1:200, (C) Abcam 1:400, (D) β-actin control. Lysates were generated from (1) Caco2 cells, (2) LOVO cells, (3) A549 transfected with PGT-pCDNA3, (4) A549 transfected with pCDNA3.

7.5 Discussion

None of the anti-HPGD antibodies were found to be suitable at present for analysis of mouse colon tissue, as the level of immunolabelling was either localised as expected but with additional non-specific background signal, or potentially reacting strongly to something other than HPGD altogether. Furthermore, the lack of HPGD labelling in the kidney was unexpected, as the Cayman antibody has been previously used in this tissue (Shiraya et al 2010, Liu et al 2014, Nomura et al 2005, Yao et al 2008). These published studies did describe some differences in the cell types and structures most strongly labelled, which may have been due to differences in experimental method, such as antigen retrieval. In addition, HPGD expression has been shown to vary according to age, with rat Hpgd highest at 2 weeks of age, and declining into adulthood (Liu et al 2014). This time-dependent expression pattern may also contribute to the different expression patterns seen. The absence of specific labelling in the kidney, and absence or non-specific labelling in the colon suggested that substantial further optimisation/validation would be required for these antibodies, and alternative antibodies might need to be assessed.

One antibody appeared to strongly identify SLCO2A1. However, without a reagent to detect HPGD, at present no further investigations can be performed to determine whether HPGD and SLCO2A1 have an associated decrease in expression in adenomas from for example the *Apc*$^{Min/+}$ mouse model. Protein sequence divergence within the epitopes could have contributed to the poorer specificity in mouse tissues. Another possibility is that the target epitope within the 3-dimensional structure of the protein was not exposed on the protein surface, where it would have been accessible to the antibody. Additional experiments could be performed to assess if the signal to noise ratio could be

further improved. This could be important, as this would allow better discrimination when assessing reduction in expression in tumour samples. Inclusion of further controls, including blocking peptides/proteins, and using tissue from *Hpgd* (Coggins et al., 2002), and *Slco2a1* (Chang et al., 2010) knockout mice would be ideal for validation.

Unsurprisingly, the antibodies for both HPGD and SLCO2A1 showed better specificity on human tissue. The differentiated colon epithelial cells were labelled by all antibodies, albeit with different intensities. The use of antibodies with non-overlapping epitopes does imply that this is the true localisation of these proteins (Hermansen et al., 2011). The localisation of HPGD in the human kidney has not been well established, and the weak labelling that was similar to the isotype control suggested that this may not be relied upon as an accurate reflection of HPGD expression. The SLCO2A1 antibodies did not give concordant kidney labelling patterns, and although endothelial labelling was seen with all reagents, this was not always the strongest localisation. Topper et al. (1998) also reported that the prostaglandin transporter localised to vessels; however, with hindsight, the use of the kidney as a control tissue was not entirely helpful, as it has had limited characterisation itself. Unfortunately, western blotting also proved inconclusive for assessment of specificity, and it appears unlikely that the antibodies were thoroughly validated for this purpose by their originators (Topper et al., 1998).

A usable anti-HPGD antibody, Novus 61, with clear, specific, low-background labelling, was identified for use on the human colon. The Bioss antibody showed the best SLCO2A1 specificity. It would however be necessary to perform additional optimisation and validation to further enhance the labelling before using these reagents to assess expression changes.

Understanding the early events in cancer development is a key goal, as identifying and treating these initial stages is likely to be vital for improving patient outcome. Identifying patterns of co-regulation between related gene products or related pathways can provide insights into the mechanisms at work. *In vitro* analysis has demonstrated reciprocal control of *PTGS2* and *HPGD* in a number of cell lines, including the A549 lung adenocarcinoma and HT-29 colorectal cancer lines (Tong et al., 2006a; Tai et al., 2011). Also, a number of NSAIDs have been found to increase HPGD expression, independently of their inhibition of COX, possibly by reducing the rate of HPGD protein degradation (Chi et al., 2009). However, only analysis of actual patient tumour samples can help to establish the relevance of such observations *in vivo*. That the prostaglandin pathway has a role in the early stages of colon cancer has ample support, especially in regards to PTGS2. More recently, it was found that the efficacy of PTGS2 inhibition on early stages of the disease depended on high level of *HPGD* expression (Fink et al., 2014). With expression levels of HPGD acting as a stratifying biomarker for response, it is plausible that the expression levels of other components of the pathway, such as SLCO2A1, could also influence aspirin response. It would be of interest to investigation the relative importance of these additional components, with the prospect of personalising patient treatment.

Several of the prostaglandin pathway proteins have been localized in the kidney, with PTGS1, HPGD and SLCO2A1 co-expressed in the collecting duct epithelia in rats (Nomura et al., 2005). This may indicate stringent control over local prostaglandin levels. While colonic epithelium also expresses the PGE_2 synthesis and degradation pathway enzymes, prostaglandin signalling has been thought to serve different functions in these two organs. In the kidney, PGE_2

signalling regulates salt reabsorption, while in the colonic mucosa it has been suggested to control epithelial cell proliferation (Myung et al., 2006; Yao et al., 2008; Smartt et al., 2012a; Smartt et al., 2012b). Recently, SLCO2A1 has been ascribed a further function in addition to prostaglandin transport, as an ATP-conductive “maxi-Cl” channel, that influences membrane potential and fluid movements (Sabirov et al., 2017). SLCO2A1 may therefore perform an osmoregulatory function in the kidney as an ion channel, and perhaps in the colon also. The location of both HPGD and SLCO2A1 in the colon indicates that both are markers of terminal differentiation, but the SLCO2A1 may participate directly in water absorption control, as well as its prostaglandin-related function. Since high prostaglandin levels can induce diarrhoea, the prostaglandin pathway may itself be involved in osmoregulation (Rampton and Sladen, 1984; Rivière et al., 1991). However, only a minority of patients with *SLCO2A1* mutations have these symptoms (Zhang et al., 2013; Zhang et al., 2014; Kim et al., 2015), which suggests it is not the main mechanism controlling intestinal ion and water movement. As the balance between the different functions of SLCO2A1 is thought to be dependent on the levels of prostaglandin (Sabirov et al., 2017), this may vary considerably under different physiological conditions and between individuals.

Chapter 8 Discussion

8.1 Introduction

This study represents one of the first attempts to analyse *HPGD* and *SLCO2A1* transcriptional control together in the context of colorectal cancer. This is also the first study to characterise the proximal 3 kb *SLCO2A1* promoter and the transcriptional start sites of this gene, using a colorectal cancer cell line model system. The results suggest that the small intestine- and colon-specific transcription factor CDX2 may have a role in driving *SLCO2A1* expression in the colonic epithelium. In addition, the results suggest that TGF-β signalling could promote *SLCO2A1* upregulation, although further work would be needed to confirm this.

At the protein level, it did not prove possible to compare HPGD and SLCO2A1 expression in normal colon (either mouse or human) and colorectal adenocarcinomas using immunohistochemistry. This was because of poor specificity of the available antibodies. This experience highlighted the limited knowledge of HPGD and SLCO2A1 structure, only human HPGD having been characterised to date (Niesen et al., 2010).

8.2 Regulation and function of *HPGD* and *SLCO2A1*

Published literature indicates that both *HPGD* and *SLCO2A1* are downregulated (but not mutated or lost) in colorectal cancer. At least, *HPGD* does not acquire inactivating mutations and is not lost through chromosomal deletions (Yan et al., 2004). Although a similar study has not strictly verified this

for *SLCO2A1* as well, neither 4q34.1 (*HPGD*) or 3q22.1-22.2 (*SLCO2A1*) is a site where recurrent breakpoints occur in the karyotypes of colorectal cancer cell lines (Knutsen et al., 2010). Consequently, the mechanism by which these genes are down-regulated at the transcriptional level appears more important to understand, particularly since such knowledge could inform how it may be possible to intervene therapeutically, with the aim of suppressing PGE_2-driven tumour growth without relying only on NSAIDs and COX-2 selective inhibitors.

Much published work on the *SLCO2A1* gene product, the prostaglandin transporter, has used cell lines (predominantly renal or fibroblastic in origin), or *Xenopus laevis* oocytes. (Chi et al., 2014; Chi et al., 2011; Chi and Schuster, 2010; Chan et al., 1998). While these studies have illuminated the biochemical function of SLCO2A1 as a PGE_2 transporter, the physiological conclusions drawn cannot necessarily be extrapolated to colorectal cancer, given the diverse range of functions that PGE_2 fulfils in different organs and tissues (Shao et al., 2015; Tootle, 2013; Swan and Breyer, 2011). In addition, results from cell line systems need to be interpreted with a degree of caution, as demonstrated by the study of Zolk, et al, 2013, in which no CpG island methylation was observed in either the normal or tumour tissue samples, implying that the methylation observed in the cell lines was likely an artefact of cell culture (Zolk et al., 2013).

Despite these caveats concerning cell-line systems (demanding caution when extrapolating the results to the *in vivo* cell type, organ, or organism of interest), colorectal cancer cell lines were clearly a more appropriate model with which to study *HPGD* and *SLCO2A1* expression and regulation in the context of colorectal cancer. The identification of transcriptional start sites (TSS) for *HPGD* and *SLCO2A1* in the colorectal cancer cell line system, and the importance of

the proximal 364-bp region in driving *SLCO2A1* expression, represent one of the first steps in characterising the regulation of these genes. A logical next step would be to verify the use of these *HPGD* and *SLCO2A1* TSS in normal colon epithelial cells, and in adenocarcinoma samples. This would reveal any discrepancies between the cell line systems, and would provide information on how these genes are expressed *in vivo*. Data from the normal colon epithelial cells might serve as a reference for baseline *HPGD* and *SLCO2A1* expression, given that despite the extensive public domain cDNA data, very little was found to exist on *HPGD* and *SLCO2A1* in the colon (Boguski et al., 1993; Kent et al., 2002).

In contrast to *HPGD*, few studies have examined the loss of *SLCO2A1* in tumours and normal tissue (Zolk et al., 2013; Takeda et al., 2015) or the loss of both *HPGD* and *SLCO2A1* expression in gastrointestinal adenocarcinomas relative to normal epithelium. This is a gap in knowledge, considering the concerted role that these two gene products play in terminating PGE_2, signalling (Smartt et al., 2012a; Smartt et al., 2012b; Takeda et al., 2015). Addressing this had indeed been one of the original aims of the present work; for example it was planned to compare either wild-type and $Apc^{+/Min}$ mouse colon, or colon and colorectal adenocarcinoma tissue sections from patients, using immunohistochemistry. Given the issues encountered with the HPGD and SLCO2A1 antibodies (section 7.5 above), it may be that RNA-level analysis, using quantitative methods such as qPCR, would prove more informative in assessing the expression levels of these two genes. In addition, procedures have been established to isolate mucosal epithelial cells from both mouse (Booth et al., 1995) and human (Roche, 2001) colon, which would allow the characterization of HPGD and SLCO2A1 expression in the specific cell types of

interest, with less risk of confounding or reduced detection power due to the presence of other cell types (*e.g.* endothelial cells, which do express SLCO2A1 as well).

The potential for *Hpgd* and *Slco2a1* to be co-regulated has been suggested in the mouse, where deregulation of the Wnt signalling pathway resulting in increasing β-catenin expression coincided with a reduction in both Hpgd and Slco2a1 mRNA and protein. (Smartt et al., 2012a; Smartt et al., 2012b). One other study has observed a reduction of both HPGD and SLCO2A1 in gastric adenocarcinomas relative to normal gastric mucosa (Takeda et al., 2015). However, these authors found an association between *SLCO2A1*, but not *HPGD*, expression in the tumour with reduced microvessel density and a more favourable response to adjuvant chemotherapy (Takeda et al., 2015). This was one of the first studies to directly implicate the loss of *SLCO2A1* expression in promoting tumour growth (through prolonging PGE_2 signalling that stimulates VEGF secretion by the tumour cells). Furthermore, given that HPGD's ability to metabolise PGE_2 depends on its influx into the cytoplasm, SLCO2A1 has the capacity to reduce extracellular PGE_2 access to the EP receptors.

However, a mouse *Slco2a1* knockout combined with heterozygous germline *Apc* mutation seems to argue against this view, since mice lacking Slco2a1 survived longer than those with the $Apc^{+/\Delta 716}$ allele and wild-type *Slco2a1* (Nakanishi et al., 2017). This study is not directly comparable to one in which the effect of germline HPGD loss was studied, combined with the $Apc^{+/Min}$ allele or a chemical carcinogen ((Myung et al., 2006)). This is because the phenotype of the $Apc^{+/\Delta 716}$ mouse is not the same as that of $Apc^{+/Min}$(Myung et al., 2006). In the former, polyps from the small intestine are more numerous

and appear to grow within the villi (retaining a layer of epithelium on their surface) (Oshima et al., 1995), which contrasts with the generalised dysplasia in the classical *Apc*$^{+/Min}$ model, considered to be closer to human gastrointestinal adenocarcinoma (Moser et al., 1990). This difference probably influenced the conclusions of Nakanishi *et al.*, 2017, given that PGE_2 and its metabolic pathway enzymes exert their effects on the intestinal and colonic epithelium, and the premalignant lesions that develop from it. Similarly, Nakanishi *et al.*, 2017 observed very little Slco2a1 expression in the epithelium, and did not consider the overexpression of β-catenin downregulating this gene, in the presence of the truncating *Apc* mutations (Smartt et al., 2012a). To explain their observations, Nakanishi *et al.*, 2017 go on to propose that PGE_2 may act via an intracellular mechanism when taken into the cell by *SLCO2A1*(Nakanishi et al., 2017). Surprisingly, they do not refer to their own previous theory of *SLCO2A1* having the potential to export PGE_2 (Kasai et al., 2016; Shirasaka et al., 2013; Shimada et al., 2015). However, patient data (Takeda et al., 2015), and work carried out using mouse small intestine mRNA and IHC both imply a positive correlation between loss of APC function and loss of SLCO2A1 expression (Smartt et al., 2012a); this is consistent with the tumour survival-promoting actions of PGE_2, as discussed in sections 1.2.4 and 1.2.5 above. All in all, though, IHC studies on SLCO2A1 in relation to colorectal cancer, and other cancer types, are few compared to those examining the expression of HPGD, and further investigation is warranted.

Although a reduction in SLCO2A1 has been seen in colorectal cancer and several other malignancies, little is known about the mechanisms by which this downregulation takes place. In the human and mouse ileum, it has been shown that SLCO2A1 gene expression is downregulated following increased β-

catenin activity, secondary to loss of APC function, (Smartt et al., 2012a). However, there is little evidence of other signalling pathways or transcription factors that could regulate SLCO2A1 expression more directly.

Results in this thesis suggest that the cytokine TGF-β2 and the transcription factor CDX2 may positively regulate *SLCO2A1* expression. TGF-β2 was found to increase *SLCO2A1* mRNA, while mutation of the predicted CDX2 binding site reduced promoter activity by 50% (section 6.4.3). CDX2 may therefore bind directly to the *SLCO2A1* promoter to drive transcription, and considering the comparable tissue specificity of both CDX2 and SLCO2A1 protein to the colonic epithelial cells, this may also apply *in vivo* (Olsen et al., 2016; Uhlen et al., 2015). However, further experiments are needed, both to assess CDX2 binding to the promoter and whether it exerts its effects directly on SLCO2A1.

CDX2 expression is known to be lost in colorectal cancer, and transient knockdown increases migration of colorectal cancer cell lines (Coskun et al., 2014). Also, germline mutation of *Cdx2* (but not *Cdx1*) exacerbates the polyposis phenotype in $Apc^{+/min}$ mice (Hryniuk et al., 2014). Loss of CDX2 expression occurs only in a relatively small subset of sporadic colorectal adenocarcinomas, but this has been associated with poor differentiation grade and microsatellite instability due to mutations in the mismatch repair genes (Olsen et al., 2016; Dalerba et al., 2016). While it is not possible at present to say whether loss of CDX2 is an important mechanism by which *SLCO2A1* is downregulated (in contrast to the Wnt/β-catenin signalling pathway (Kikuchi et al., 2012; Mehdawi et al., 2016; Smartt et al., 2012a), this would be worth investigating, given the evidence presented in this thesis.

CDX2 binds predicted sites on the promoters of the genes for *APC*, *AXIN2* and *GSK3β* and drives their transcription, thus repressing the Wnt/β-catenin pathway (Olsen et al., 2013). APC, AXIN2 and GSK3β form a complex that phosphorylates and targets β-catenin for degradation by the proteasome, preventing its accumulation within the cell (Coskun et al., 2014; Chiurillo, 2015; Salomon et al., 1997; Aberle et al., 1997). Therefore, as shown in Figure 8.1, CDX2 may act on both SLCO2A1, and the APC complex to reduce β-catenin, representing a potential feed-forward mechanism that sustains SLCO2A1 expression in the terminally differentiated colonic epithelial cells near the colon lumen.

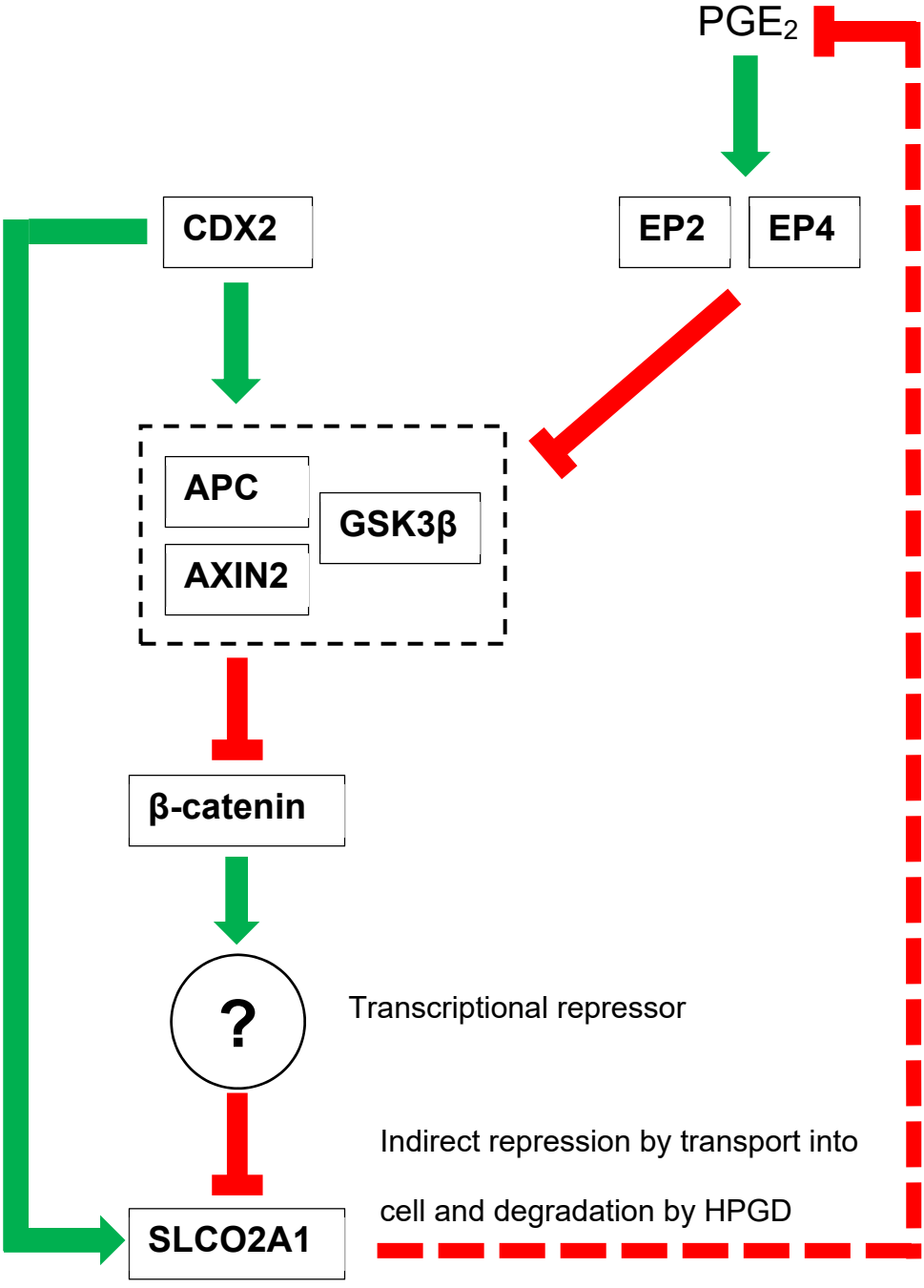
PGE2
CDX2
EP2
EP4
APC
GSK3β
AXIN2
β-catenin
?
Transcriptional repressor
Indirect repression by transport into
cell and degradation by HPGD
SLCO2A1

Figure 8.1: Schematic representation of CDX2 interactions with SLCO2A1

CDX2 could act in a feed-forward loop to induce SLCO2A1 expression, both by acting directly on the *SLCO2A1* promoter to drive transcription, and by counteracting β-catenin's repression through upregulating APC, AXIN2 and GSK3β, which form the complex that ubiquitinates β-catenin and targets it for degradation. β-catenin binds to the TCF family of transcription factors, which are transcriptional activators, so the repression of SLCO2A1 is likely mediated by an as of yet unidentified transcriptional repressor induced by β-catenin. PGE_2, on the other hand, downregulates the APC complex via the activation of the EP2 and EP4 receptors, which leads to a reduction in SLCO2A1 expression, and forms a positive feedback loop that prolongs PGE_2 signalling.

The suggestion that the PGE_2 metabolic pathway, CDX2 and the Wnt signalling pathway (Figure 8.1) may interact has implications for the mechanism by which these pathways contribute to colorectal cancer. Deregulation of the Wnt signalling pathway is one of the earliest events in colorectal cancer development. Furthermore, a key mechanisms by which *APC* mutations can lead to adenoma development is by the disruption of the asymmetrical cell division that maintains the colonic crypt stem cell compartment (Bellis et al., 2012; Boman and Fields, 2013). Wnt and β-catenin display a gradient of decreasing expression from the base of the crypt to the colon lumen, also reflected by a gradient of APC, HPGD and SLCO2A1 in the reverse direction (Boman and Fields, 2013; Smartt et al., 2012a; Smartt et al., 2012b). CDX2, though, does not show such a gradient of expression (Qualtrough et al., 2002), which suggests that its role may be more to do with maintaining baseline levels of SLCO2A1. The Wnt/β-catenin pathway may exert dominant control over *SLCO2A1* expression, because when APC function is lost, CDX2 expression alone appears insufficient to prevent *SLCO2A1* downregulation.

An additional interaction of prostaglandins with the Wnt pathway occurs when PGE_2 phosphorylates and inactivates GSK3β by signalling via the EP2 and EP4 receptors (Figure 8.1) (Fujino, 2016). EP2 receptor activation increases cAMP, which activates PKA to phosphorylate GSK3. EP4 achieves a similar effect through the PI3K pathway (Fujino et al., 2003). In this way, PGE_2 can suppress β-catenin degradation (Castellone et al., 2005). As well as being a route by which PGE_2 promotes cell proliferation and survival, the Wnt pathway can in turn enhance PGE_2 synthesis through the induction of *PTGES* (Fujino, 2016). PGE_2, too, can induce PTGES (Stamatakis et al., 2015), as well as (COX2) PTGS2 (Bradbury et al., 2003; Jabbour et al., 2001) expression through

the EP4 receptor, to set up another positive feedback loop leading to increased PGE_2 production. Therefore, this may form one of the mechanisms by which PGE_2 production is increased early in colorectal carcinogenesis following inactivation or loss of *APC*.

However, how activation of the Wnt pathway downregulates HPGD and SLCO2A1 is not clear, given that β-catenin typically promotes transcriptional activation when it complexes with TCF transcription factors (Smartt et al., 2012a; Smartt et al., 2012b). Although the literature provides examples of *HPGD*'s regulation by signalling pathways (including Wnt/β-catenin), microRNAs (e.g. miR-21 (Lu et al., 2014; Li et al., 2017a)), or feedback from the EP2 receptor, that reduces its expression (Castellone et al., 2005), these studies have not elucidated the mechanism by which these signals are transduced to the *HPGD* promoter (Mehdawi et al., 2016; Smartt et al., 2012b). As mentioned above, since β-catenin typically drives transcription of target genes by binding to TCF in the nucleus, genes that are downregulated as a result of β-catenin activation may be repressed through the induction of transcriptional repressors, or by other indirect routes (MacDonald et al., 2009).

One downstream target of β-catenin, which can function as a transcriptional repressor of genes normally activated by SP1 (Fujimura et al., 2007) is SP5 (Takahashi et al., 2005). Although the *SLCO2A1* promoter was found to contain SP binding sites, and mutation of its consensus sequence did not appear to affect the promoter's activity, it may be that the relative abundance of SP1 and SP5 could still contribute to *SLCO2A1* expression. Moreover, SP5 shows greater target specificity compared to SP1, which would not affect the expression of other more ubiquitous genes whose expression is driven by SP1 (Huggins et al., 2017)

TGF-β was considered to be another likely candidate regulator of *SLCO2A1*, firstly because data in the Expression Atlas (Yeung et al., 2013) indicate that TGF-β1 and TGF-β2 upregulated *SLCO2A1* transcript levels. This pathway is also known to reduce PGE_2 signalling by stimulating *HPGD* expression and downregulating COX-2 (Yan et al., 2004; Takai et al., 2013; Kang et al., 2015). In addition, mutations of the TGF-β2 receptor (TGFBR2), and the downstream SMAD proteins are relatively common early events in sporadic colorectal cancer (Yan et al., 2004). This raised the possibility that *SLCO2A1* might also be regulated by this pathway.

Treating A549 cells with TGF-β2 was found to cause an increase in *SLCO2A1* mRNA as well as *CDX2*; these cells expressed low levels of SLCO2A1 compared to the colorectal cancer cell lines. In contrast, in the two colorectal cell lines that were treated, no change was observed. This could indicate a genuine lack of response to TGF-β2, or that any increase in expression was too small to detect against the baseline levels of SLCO2A1 expressed by Caco-2 and LoVo cells. The former of these could indicate inactivation of the TGFBR/SMAD pathway, and given the lack of data on these genes, in spite of large-scale analyses in the literature (Knutsen et al., 2010; Ahmed et al., 2013; Berg et al., 2017) and publicly available databases (Forbes et al., 2017), this would need to be verified for these cell lines. The latter alternative may imply that TGF-β signalling can stimulate *SLCO2A1* expression, but may not be a major regulator.

8.3 HPGD and SLCO2A1 as possible therapeutic targets

The possibility of using drugs to reactivate and upregulate *HPGD* expression. together with, or instead of NSAIDs or COX2-selective inhibitors to suppress PGE_2 signalling for colorectal cancer prophylaxis, or as an adjunct to chemotherapy, has been put forward (Na et al., 2011; Kaliberova et al., 2009). To date, no compounds that upregulate *SLCO2A1* expression have been identified. SLCO2A1 inhibitors have been identified, such as T26A (Chi et al., 2011) or suramin (Kamo et al., 2017); by potentiating the action of PGE_2, they have been suggested to have potential for improving the healing of diabetic skin ulcers (Liu et al., 2015), or as antihypertensives (Chi et al., 2015).

In contrast, as for *HPGD*, upregulation of *SLCO2A1* could be beneficial instead of or alongside NSAIDS in colorectal cancer prophylaxis, or during treatment as an adjunct to chemotherapy. Furthermore, targeting *HPGD* and *SCO2A1* might reduce the chance of resistance developing. Some COX-2 inhibitors, such as diclofenac, have been found also to impair SLCO2A1's transport function in vitro (Kamo et al., 2017), a further reason why combining upregulation of SLCO2A1 with COX inhibition may be more effective in reducing PGE_2 signalling. In addition, given the wide range of functions that PGE_2 has, drugs should ideally be targeted to the colonic epithelium, in order to avoid adverse effects from suppressing PGE_2 activity across the entire body.

Given that TGF-β signalling can upregulate both *HPGD* (Yan et al., 2004) and *SLCO2A1*, whilst also downregulating *PTGS2* (Takai et al., 2013; Kang et al., 2015), TGF-β pathway agonists could be another way to target multiple enzymes in the PGE_2 metabolic pathway (Kapral et al., 2013). However, as the TGF-β receptors and the downstream SMAD transcription factors can be

mutated in colorectal cancer, the efficacy of such drugs would be limited to adenocarcinomas retaining a functional pathway.

The efficacy of such compounds has been tested in a colorectal cancer cell line model, although exactly how this drug (MW-03) upregulates *HPGD* remained unclear (Seira et al., 2017). The authors found that peroxisome proliferator-activated receptor-γ (PPARγ) may be involved in driving *HPGD* expression during MW-03 treatment, although further work would be needed to confirm whether these nuclear receptors bind directly to the HPGD promoter to exert these effects. Such studies highlight the need for a better understanding of *HPGD* transcriptional regulation.

It should be noted that although increased PGE_2 contributes to the development of colorectal cancer, as well as other malignancies, and although loss of *HPGD* and *SLCO2A1* expression can promote cancer development, these two genes are not, strictly, tumour suppressor genes. PHO patients who have complete germline loss of function of either gene have not shown an increased risk of cancer (Diggle et al., 2012; Uppal et al., 2008) unlike classical tumour suppressor genes involved in hereditary cancer syndromes, such as *SMAD4* in juvenile polyposis syndrome, *MSH2* and *MLH1* in Lynch syndrome, *APC* in familial adenomatous polyposis (Galiatsatos and Foulkes, 2006; Fearon, 2011; Oshima et al., 1995), *BRCA1* and *BRCA2* in breast and ovarian cancer (Cobain et al., 2016), and *RB1* in retinoblastoma (Fabian et al., 2018; Knudson, 1971).

Loss of *HPGD* and *SLCO2A1* expression occurs early in the development of an adenocarcinoma (Yan et al., 2004; Smartt et al., 2012a; Smartt et al., 2012b), and PGE_2 is known to contribute to tumour growth through inflammation and localised suppression of immune responses to the

tumour (Zelenay et al., 2015). Therefore, *HPGD* and *SLCO2A1* downregulation, and the reciprocal COX-2 upregulation alone are not initiating events, even if PGE_2 contributes to an established tumour's growth and survival. Therefore, approaching PGE_2 from its role in supporting cancer development, it appears sensible to reduce its activity through suppressing its production (NSAIDs), or potentially accelerating its degradation (HPGD) and reducing its access to the cell surface receptors (SLCO2A1). However, PGE_2 has a wide range of functions, and there are situations where prolonging its action could be of therapeutic benefit through inhibition of HPGD and SLCO2A1 (Liu et al., 2015; Shao et al., 2015; Sun et al., 2017; Zhang et al., 2015). PGE_2's ability to drive cell proliferation, migration and angiogenesis (mechanisms that are subverted in carcinogenesis) is also useful in tissue regeneration.

In mice, inhibition of HPGD accelerates proliferation of hepatocytes and epithelial cells in the colon crypts of Lieberkühn (Zhang et al., 2015). This led to accelerated liver regeneration following partial surgical resection, and protection against dextran sodium sulphate-induced colitis (Zhang et al., 2015). HPGD inhibition has also been shown to increase cell migration in wound healing assays (Sun et al., 2017), and to facilitate recovery from bone marrow transplantation in mice (Desai et al., 2018).

When intravenously infused in humans, PGE_2 induces systemic vasodilation (Eklund and Carlson, 1980), and prolonging its action by inhibiting SLCO2A1 reduces blood pressure in rodent models of hypertension (Chi et al., 2015). Given the existing range of antihypertensive drugs, it is unlikely that SLCO2A1 inhibitors (such as T26A) would find application for this ability. The same authors have shown that topically applied SLCO2A1 inhibitor led to accelerated wound healing (Liu et al., 2015). A combination of PGE_2 (or a

synthetic analogue) and SLCO2A1 inhibitor could theoretically be more effective in such an application, and would require smaller amounts of either drug to achieve the same effect.

When considering therapeutic targeting of HPGD or SLCO2A1, their substrate specificities, which are not restricted to PGE_2, need to be taken into account. For example, lipoxin A_4 and 15-epimeric lipoxins, which generally function to resolve inflammation, are synthesized by PTGS2, and PTGS2 acetylation by aspirin alters its specificity towards lipoxin production (Serhan, 2002). These lipoxins can likewise be metabolised by HPGD (Na et al., 2011). As a consequence, HPGD upregulation was found to contribute to prolonging inflammation in chronic tendinopathy, therefore, through degradation of these lipoxins, and therefore presenting a paradoxical situation in which HPGD inhibitors would be beneficial (Dakin et al., 2017).

Although this thesis has focused on the regulation of HPGD and SLCO2A1 in the context of cancer, the insights gained are likely to be relevant to understanding other pathologies such as the inflammatory disorders mentioned above. Certainly, the possibility of being able to modulate the expression of these genes is of interest, even if in these other pathological settings, as discussed above, the aim might be to suppress (at least locally) their expression rather than enhance it. Whether modulating a gene's expression is a preferable approach to directly targeting the gene product is a general question, to which the answer is likely to depend on the disease context. Experience shows that sometimes the best pharmacological effect is not obtained by directly aiming at the last component of a pathway. For example, histamine receptor 2 (H_2) antagonists (e.g. ranitidine), which act upstream of the proton pump inhibitors (omeprazole), may be as less effective

at reducing gastric acid secretion, but achieve lower rates of ulcer recurrence, perhaps because of rebound acid hypersecretion when proton pump inhibitors are stopped (Yeomans et al., 1998; Abraham, 2012; Bardhan et al., 1991)

The prominent role played by prostaglandins in many disease states has triggered a high level of interest in the genes that encode components of their metabolic pathway. The two genes studied in this thesis, *HPGD* and *SLCO2A1*, mediate termination of PG signalling. Naturally occurring human genetic disorders (Uppal et al. 2008; Diggle et al. 2012) have offered the insight that failure of these components has wide-ranging physiological effects. However, somatic dysregulation of *HPGD* is an important event accompanying colorectal carcinogenesis, prompting the studies described here to try to understand the regulation of these two genes. Together with evidence from the literature, the results suggest that there may be a complex interaction between the Wnt/β-catenin pathway, the TGF-β pathway, PGE_2 signalling and PGE_2 metabolism regulating the expression of HPGD and SLCO2A1. The transcription factor CDX2 may be involved in *SLCO2A1* expression in colonic epithelial cells. Although evidence is limited, *HPGD* and *SLCO2A1*, are very likely to be co-regulated, considering their inverse relationship with β-catenin expression, and the stimulation of their expression by TGF-β (Smartt et al., 2012a; Smartt et al., 2012b; Takeda et al., 2015). The negative effect of β-catenin on *HPGD* and *SLCO2A1* expression is likely to be indirect, perhaps via the induction of transcriptional repressors that act directly on these genes. CDX2, however, may have a direct role in regulating *SLCO2A1*, and should be explored further to determine whether this transcription factor regulates other components of the PGE_2 metabolic pathway (Freund et al., 2015; Hryniuk et al., 2014).

8.4 Future Work

Many aspects of the present work would benefit from extending the analysis to other sources of biological material. The *HPGD* and *SLCO2A1* transcriptional start sites defined here, should be verified in normal colonic epithelium and fresh tumour material. This would allow exploration of whether all, or particular transcripts are lost when these two genes are downregulated. The epigenetic regulation of *HPGD* and *SLCO2A1* in vivo is also worthy of further study, given evidence that *HPGD* may be downregulated via promoter methylation (Backlund et al., 2008), and that histone deacetylation can upregulate SLCO2A1 expression (Holla et al., 2008). All studies of this type really would need to be validated using an in vivo model (Backlund et al., 2008), given the striking differences that can be observed between cell line models and actual tissue sections (Takeda et al., 2015). Overall, greater emphasis needs to be placed on *SLCO2A1*, about which much less is known genetically, biochemically and physiologically.

CDX2 and its possible direct action on *SLCO2A1* warrants further investigation as well. Its specificity to the colonic epithelium and its interaction with the Wnt pathway suggest that it may have a role in regulating other genes involved in the controlled division and differentiation of colonic epithelial cells (Freund et al., 2015; Olsen et al., 2016). Initial experiments might focus on verifying that CDX2 binds to the *SLCO2A1* promoter in native chromatin, and on testing whether overexpression and knock-down of CDX2 have the predicted effects on *SLCO2A1* expression (as well as that of HPGD, COX2 and PTGES). Further studies would need to be carried out to confirm whether this interaction has physiological relevance *in vivo*. Positive findings would have to be verified

using *ex vivo* colonic epithelial cells, both from mouse (Mahé et al., 2013), and human colon (Roche, 2001), not just cell lines. Further *in vivo* confirmation could be performed using transgenic models to show whether CDX2 can indeed drive *SLCO2A1* expression.

Although this thesis concentrated on transcriptional regulation, mRNA and protein turnover are also key mechanisms that control the activity of proteins in cells (Houseley and Tollervey, 2009). Regulation of β-catenin activity is a classic example of this; phosphorylation by APC/AXIN2/GSK3β and the consequent balance between proteasomal degradation and β-catenin persistence and translocation from cytoplasm to the nucleus are key (Mohammed et al., 2016; MacDonald et al., 2009). The turnover of HPGD and SLCO2A1 proteins could be equally important to their observed loss of expression in colorectal cancer.

In this context, HPGD is believed to have a half-life of approximately 50 minutes in cultured cells (Xun et al., 1991). Therefore, identifying signalling pathways and drugs that could stabilise HPGD mRNA and/or suppress HPGD protein degradation, while perhaps more challenging than upregulating its activity, is another area that could be explored (Lu et al., 2014; Huang et al., 2015; Li et al., 2017a). The same would also obviously apply to SLCO2A1.

As mentioned above, SLCO2A1 itself remains rather under-characterized. The tertiary structure of SLCO2A1, unlike HPGD (Niesen et al., 2010), remains to be experimentally determined; only a very small fragment is published on the Protein Data Bank (Berman et al., 2000), PDB ID 3MRR (Reiser et al., 2014). Historically, X-ray crystallography has been the method of choice to determine protein three-dimensional structures (Glaenzer et al., 2018). Unfortunately, most of the enzymes in the PGE_2 metabolic pathway,

including SLCO2A1, are transmembrane proteins, and are consequently difficult to solubilize and crystallize (Carpenter et al., 2008). Only the structures of the soluble human PGES (Jegerschöld et al., 2008; Sjögren et al., 2013) and HPGD (Niesen et al., 2010) proteins have been determined to date, and of the membrane-bound enzymes, only the structure of the ovine PTGS1 has been characterised (Sidhu et al., 2010; Cingolani et al., 2017). Elucidating the crystal structure of SLCO2A1 would therefore represent an important piece of future work, which would inform the mechanism by which it exchanges anions for the uptake of PGE_2, how pathogenic mutations alter this structure and impede its function in PHO, and where drug inhibitors (such as T26A) bind on the protein, and hence how they exert their action.

A number of hypotheses concerning PGE_2 transport by SLCO2A1 have been proposed, envisaging either unidirectional transport, as observed by the authors who first characterised SLCO2A1 (Nomura et al., 2004; Chi et al., 2011; Schuster et al., 2015), and bidirectional PGE_2 transport, depending on the balance of lactate or other anion concentrations between the cytoplasm and extracellular space (Shirasaka et al., 2013; Kasai et al., 2016). Genetic evidence from mouse knockout (Nakanishi et al., 2017; Nakamura et al., 2018) and from PHO patients (Zhang et al., 2012; Li et al., 2017b) tends to support the original PGE_2 import model, because subjects with SLCO2A1 mutations lose more PGE_2 in urine than either PHO patients with HPGD mutation, or normal subjects. This implies a general inability to clear PGE_2 from the extracellular fluid and blood, into the cytoplasm where it can be metabolised by HPGD. Therefore, if SLCO2A1 does also function to export PGE_2 out of the cell, this function is likely to be a minor one.

Structural analysis of SLCO2A1 would provide the foundations for determining many of the biochemical parameters governing the anions that SLCO2A1 can transport in exchange for PGE_2 (Nakanishi and Tamai, 2017), (For example, co-precipitation in the presence of bound ligand would allow for conformational changes to be modelled to better understand how PGE_2 and large anions are moved across the cell membrane.). Such knowledge would also aid fine-tuning of drug structure to improve specificity or efficacy (Chi et al., 2011).

The dynamics of SLCO2A1 in the cell membrane, including whether it multimerizes or associates with other proteins, remain unknown. In contrast, human HPGD (Niesen et al., 2010) and ovine PTGS1 (Cingolani et al., 2017) are known to exist natively as homodimers, while PGES forms a homotrimer (Sjögren et al., 2013). A recent study using a mouse cell model system has suggested that SLCO2A1 could form part of a chloride channel complex (Sabirov et al., 2017). However, its other components were not identified. All such studies are hampered by the lack of structural data on SLCO2A1.

Another deficiency highlighted in this thesis, which might be mitigated if structural data were available, is the lack of good immunological reagents. Knowledge of SLCO2A1's native structure would allow accessible epitopes to be predicted, for production of synthetic immunogens or recombinant fusion proteins (Yamashita and Okada, 2005). Structural considerations are most likely to be relevant when immunodetecting *in situ* in tissues (since in western blotting, the proteins are fully denatured). Success is difficult to ensure, however, since the usual empirical methods such as heat-induced epitope retrieval are poorly understood, despite their effectiveness in increasing the antigenicity and reducing the background in FFPE tissue sections (Shi et al.,

2011). Antibodies against human SLCO2A1 have been described (Topper et al., 1998; Kang et al., 2005; Breuiller-Fouche et al., 2010; Nakanishi et al., 2015; Kasai et al., 2016; Sabirov et al., 2017). However, no effort has been made to assess their relative specificities for SLCO2A1. Furthermore, there are no available antibodies specific for murine Slco2a1, which limits the scope for exploiting the available HPGD and SLCO2A1 germline knockouts (Chang et al., 2010).

These germline knockout mouse strains for HPGD (Myung et al., 2006) and SLCO2A1 (Nakanishi et al., 2017; Chang et al., 2010) serve as models for the human disease PHO, and have illuminated the physiology of the PGE_2 degradative pathway. However, organ-specific conditional *Hpgd* and *Slco2a1* knockout mice might be more useful for studying colon cancer. To achieve this, the use of Cre recombinase driven by carbonic anhydrase 1 (Car1), which is expressed by the differentiated cells closer to the colon lumen (Tetteh et al., 2016), to delete floxed HPGD or SLCO2A1 in the presence of a germline APC mutant allele, or chemical carcinogen might be an approach worth considering.

Other similar conditional knockout approaches could be applied to the study of other malignancies, in which HPGD and SLCO2A1 are known to be downregulated. For HPGD, this includes gastric (Kang et al., 2014; Li et al., 2017a; Takeda et al., 2015; Hu et al., 2015), breast (Wolf et al., 2006; He et al., 2014; Lehtinen et al., 2012), lung (St John et al., 2012), prostate (Lodygin et al., 2005; Vainio et al., 2011), head and neck squamous cell carcinoma (Zolk et al., 2013), hepatocellular carcinoma (Yang et al., 2014) and cholangiocarcinoma (Lu et al., 2014). Similarly, SLCO2A1 is also lost in lung cancer (Zhu et al., 2015). Conditional knockout systems could also be used to study the wider

roles of PGE_2 signalling in situations where the prolongation of its action would be desirable, such as in applications of tissue regeneration (Zhang et al., 2015).

Returning to the question of PGE_2 signalling in facilitating colonic adenoma and adenocarcinoma growth, a conditional knockout approach could also be used to scrutinize the synthesis components of the PGE_2 pathway. Lgr5 is a marker for stem cells at the base of the colonic crypts, believed to be the site of cancer-initiating events such as loss of *APC* expression (Barker et al., 2007; Mahé et al., 2013). Germline knockout of Ptgs2 reduces polyp number and size in mice carrying mutant *Apc* (Oshima et al., 1996), but these animals suffer developmental abnormalities in the kidneys and ovaries. It would therefore be interesting to use conditional knockout of *Ptgs2* in both the crypt stem cells (Lgr5-Cre (Barker et al., 2008)) and in the differentiated cells (Car1-Cre (Tetteh et al., 2016)) to simulate aberrant Ptgs2 upregulation.

A better understanding of *HPGD* and *SLCO2A1* regulation, and their interactions with other signalling pathways might also help explain the complex phenotypes seen in PHO patients, about which there are several unanswered questions. PHO patients with *SLCO2A1* germline mutations are overwhelmingly male (Zhang et al., 2013; Seifert et al., 2012; Hou et al., 2017), in contrast to those with *HPGD* mutations, where cases were overall equally prevalent in both sexes (Diggle et al., 2010; Uppal et al., 2008). Also, germline *SLCO2A1* mutations can present with chronic multiple small intestinal ulcers, and gastrointestinal haemorrhage in affected patients, a syndrome distinct from PHO in which the typical signs (such as pachydermia, arthralgia, finger clubbing) do not manifest (Umeno et al., 2015; Uchida et al., 2016; Umeno et al., 2018). This lack of systemic symptoms may reflect an inability to rapidly terminate PGE_2 signalling at the cell surface, perhaps resulting from a

disturbance of the complex competitive balance between SLCO2A1, EP receptors, and MRP4 transporter (Chi et al., 2014; Schuster et al., 2015).

There is also no explanation for the fact that unlike PHO subjects, more than a third of the *SLCO2A1*-mutated patients with multiple gastrointestinal ulceration are women.

8.5 Conclusions

This work has characterised the transcriptional start sites of *HPGD* and *SLCO2A1*, and provided evidence suggesting that the TGF-β pathway may regulate *SLCO2A1*, as well as *HPGD* (Yan et al., 2004). Baseline *SLCO2A1* expression may also be regulated by CDX2, a transcription factor expressed in the intestinal and colonic epithelium (Qualtrough et al., 2002), which also interacts with the Wnt signalling pathway by driving expression of APC to suppress β-catenin activity. Although most published work to date has focused on the roles of PTGS2 and HPGD in increasing local PGE_2 concentrations and facilitating carcinogenesis in the colon, SLCO2A1 warrants closer scrutiny for its own role in terminating PGE_2 signalling. Understanding the regulation of both *HPGD* and *SLCO2A1* offers the potential for pharmacologically reactivating their expression in colorectal and other malignancies, where such an approach could be used alongside conventional NSAIDs to reduce PGE_2 signalling.

Chapter 9 References

Abbas, A.K., Le, K., Pimmett, V.L., Bell, D.A., Cairns, E. and Dekoter, R.P. 2014. Negative regulation of the peptidylarginine deiminase type IV promoter by NF-kappaB in human myeloid cells. *Gene.* **533**(1), pp.123-131.

Aberle, H., Bauer, A., Stappert, J., Kispert, A. and Kemler, R. 1997. beta-catenin is a target for the ubiquitin-proteasome pathway. *Embo j.* **16**(13), pp.3797-3804.

Abeywardena, M.Y., McLennan, P.L. and Charnock, J.S. 1987. Long-term saturated fat supplementation in the rat causes an increase in PGI2/TXB2 ratio of platelet and vessel wall compared to n-3 and n-6 dietary fatty acids. *Atherosclerosis.* **66**(3), pp.181-189.

Abraham, N.S. 2012. Proton pump inhibitors: potential adverse effects. *Current Opinion in Gastroenterology.* **28**(6), pp.615-620.

Adams, M.D., Kelley, J.M., Gocayne, J.D., Dubnick, M., Polymeropoulos, M.H., Xiao, H., Merril, C.R., Wu, A., Olde, B., Moreno, R.F. and et al. 1991. Complementary DNA sequencing: expressed sequence tags and human genome project. *Science.* **252**(5013), pp.1651-1656.

Adorno, M., Cordenonsi, M., Montagner, M., Dupont, S., Wong, C., Hann, B., Solari, A., Bobisse, S., Rondina, M.B., Guzzardo, V., Parenti, A.R., Rosato, A., Bicciato, S., Balmain, A. and Piccolo, S. 2009. A Mutant-p53/Smad complex opposes p63 to empower TGFbeta-induced metastasis. *Cell.* **137**(1), pp.87-98.

Ahmed, D., Eide, P.W., Eilertsen, I.A., Danielsen, S.A., Eknaes, M., Hektoen, M., Lind, G.E. and Lothe, R.A. 2013. Epigenetic and genetic features of 24 colon cancer cell lines. *Oncogenesis.* **2**, pe71.

Albo, D., Arnoletti, J.P., Castiglioni, A., Granick, M.S., Solomon, M.P., Rothman, V.L. and Tuszynski, G.P. 1994. Thrombospondin (TSP) and transforming growth factor beta 1 (TGF-beta) promote human A549 lung carcinoma cell plasminogen activator inhibitor type 1 (PAI-1) production and stimulate tumor cell attachment in vitro. *Biochem Biophys Res Commun.* **203**(2), pp.857-865.

Algenas, C., Agaton, C., Fagerberg, L., Asplund, A., Bjorling, L., Bjorling, E., Kampf, C., Lundberg, E., Nilsson, P., Persson, A., Wester, K., Ponten, F., Wernerus, H., Uhlen, M., Ottosson Takanen, J. and Hober, S. 2014. Antibody performance in western blot applications is context-dependent. *Biotechnol J.* **9**(3), pp.435-445.

Altschul, S.F., Gish, W., Miller, W., Myers, E.W. and Lipman, D.J. 1990. Basic local alignment search tool. *J Mol Biol.* **215**(3), pp.403-410.

Amano, T., Sagai, T., Tanabe, H., Mizushina, Y., Nakazawa, H. and Shiroishi, T. 2009. Chromosomal dynamics at the Shh locus: limb bud-specific differential regulation of competence and active transcription. *Dev Cell.* **16**(1), pp.47-57.

Änggård, E. and Samuelsson, B. 1969. [39] A prostaglandin dehydrogenase from pig lung. *Methods in Enzymology.* Academic Press, pp.215-219.

Arezi, B., Xing, W., Sorge, J.A. and Hogrefe, H.H. 2003. Amplification efficiency of thermostable DNA polymerases. *Anal Biochem.* **321**(2), pp.226-235.

Ariel, A., Li, P.L., Wang, W., Tang, W.X., Fredman, G., Hong, S., Gotlinger, K.H. and Serhan, C.N. 2005. The docosatriene protectin D1 is produced by TH2 skewing and promotes human T cell apoptosis via lipid raft clustering. *J Biol Chem.* **280**(52), pp.43079-43086.

Ashida, R., Tominaga, K., Sasaki, E., Watanabe, T., Fujiwara, Y., Oshitani, N., Higuchi, K., Mitsuyama, S., Iwao, H. and Arakawa, T. 2005. AP-1 and colorectal cancer. *Inflammopharmacology.* **13**(1-3), pp.113-125.

Asting, A.G., Caren, H., Andersson, M., Lonnroth, C., Lagerstedt, K. and Lundholm, K. 2011. COX-2 gene expression in colon cancer tissue related to regulating factors and promoter methylation status. *BMC Cancer.* **11**, p238.

Avery, A., Paraskeva, C., Hall, P., Flanders, K.C., Sporn, M. and Moorghen, M. 1993. TGF-beta expression in the human colon: differential immunostaining along crypt epithelium. *Br J Cancer.* **68**(1), pp.137-139.

B Samuelsson, E Granstrom, K Green, M Hamberg, a. and Hammarstrom, S. 1975. Prostaglandins. *Annual Review of Biochemistry.* **44**(1), pp.669-695.

Backlund, M.G., Mann, J.R., Holla, V.R., Buchanan, F.G., Tai, H.H., Musiek, E.S., Milne, G.L., Katkuri, S. and DuBois, R.N. 2005. 15-Hydroxyprostaglandin dehydrogenase is down-regulated in colorectal cancer. *J Biol Chem.* **280**(5), pp.3217-3223.

Backlund, M.G., Mann, J.R., Holla, V.R., Shi, Q., Daikoku, T., Dey, S.K. and DuBois, R.N. 2008. Repression of 15-hydroxyprostaglandin dehydrogenase involves histone deacetylase 2 and snail in colorectal cancer. *Cancer Res.* **68**(22), pp.9331-9337.

Bae, J.A., Yoon, S., Park, S.Y., Lee, J.H., Hwang, J.E., Kim, H., Seo, Y.W., Cha, Y.J., Hong, S.P., Kim, H., Chung, I.J. and Kim, K.K. 2014. An unconventional KITENIN/ErbB4-mediated downstream signal of EGF upregulates c-Jun and the invasiveness of colorectal cancer cells. *Clin Cancer Res.* **20**(15), pp.4115-4128.

Bae, J.M., Lee, T.H., Cho, N.Y., Kim, T.Y. and Kang, G.H. 2015. Loss of CDX2 expression is associated with poor prognosis in colorectal cancer patients. *World J Gastroenterol.* **21**(5), pp.1457-1467.

Bagante, F., Spolverato, G., Beal, E., Merath, K., Chen, Q., Akgul, O., Anders, R.A. and Pawlik, T.M. 2018. Impact of histological subtype on the prognosis of patients undergoing surgery for colon cancer. *J Surg Oncol.* **117**(7), pp.1355-1363.

Baker, N.E. 1988. Transcription of the segment-polarity gene wingless in the imaginal discs of Drosophila, and the phenotype of a pupal-lethal wg mutation. *Development.* **102**(3), pp.489-497.

Bannenberg, G. and Serhan, C.N. 2010. Specialized pro-resolving lipid mediators in the inflammatory response: An update. *Biochimica et Biophysica Acta (BBA) - Molecular and Cell Biology of Lipids.* **1801**(12), pp.1260-1273.

Bansal, M., Kumar, A. and Yella, V.R. 2014. Role of DNA sequence based structural features of promoters in transcription initiation and gene expression. *Curr Opin Struct Biol.* **25**, pp.77-85.

Bao, Y., Pucci, M.L., Chan, B.S., Lu, R., Ito, S. and Schuster, V.L. 2002. Prostaglandin transporter PGT is expressed in cell types that synthesize and release prostanoids. *American Journal of Physiology-Renal Physiology.* **282**(6), pp.F1103-F1110.

Bardhan, K.D., Walker, R., Hinchliffe, R.F., Bose, K., Morris, P., Thompson, M., Miller, J.P., Toivanen, E., Thompson, R.P., Patrier, P. and et al. 1991. Gastric ulcer healing: a comparison of enprostil versus ranitidine. *J Clin Gastroenterol.* **13**(2), pp.157-162.

Barker, N., Ridgway, R.A., van Es, J.H., van de Wetering, M., Begthel, H., van den Born, M., Danenberg, E., Clarke, A.R., Sansom, O.J. and Clevers, H. 2008. Crypt stem cells as the cells-of-origin of intestinal cancer. *Nature.* **457**, p608.

Barker, N., van Es, J.H., Kuipers, J., Kujala, P., van den Born, M., Cozijnsen, M., Haegebarth, A., Korving, J., Begthel, H., Peters, P.J. and Clevers, H. 2007. Identification of stem cells in small intestine and colon by marker gene Lgr5. *Nature.* **449**, p1003.

Barrett, T., Wilhite, S.E., Ledoux, P., Evangelista, C., Kim, I.F., Tomashevsky, M., Marshall, K.A., Phillippy, K.H., Sherman, P.M., Holko, M., Yefanov, A., Lee, H., Zhang, N., Robertson, C.L., Serova, N., Davis, S. and Soboleva, A. 2013. NCBI GEO: archive for functional genomics data sets--update. *Nucleic Acids Res.* **41**(Database issue), pp.D991-995.

Beliveau, A., Leclerc, S., Rouleau, M. and Guerin, S.L. 1999. Multiple cloning sites from mammalian expression vectors interfere with gene promoter studies in vitro. *Eur J Biochem.* **261**(2), pp.585-590.

Bellis, J., Duluc, I., Romagnolo, B., Perret, C., Faux, M.C., Dujardin, D., Formstone, C., Lightowler, S., Ramsay, R.G., Freund, J.N. and De Mey, J.R. 2012. The tumor suppressor Apc controls planar cell polarities central to gut homeostasis. *J Cell Biol.* **198**(3), pp.331-341.

Bennett, A., Civier, A., Hensby, C.N., Melhuish, P.B. and Stamford, I.F. 1987. Measurement of arachidonate and its metabolites extracted from human normal and malignant gastrointestinal tissues. *Gut.* **28**(3), pp.315-318.

Berg, K.C.G., Eide, P.W., Eilertsen, I.A., Johannessen, B., Bruun, J., Danielsen, S.A., Bjornslett, M., Meza-Zepeda, L.A., Eknaes, M., Lind, G.E., Myklebost, O., Skotheim, R.I., Sveen, A. and Lothe, R.A. 2017. Multi-omics of 34 colorectal cancer cell lines - a resource for biomedical studies. *Mol Cancer.* **16**(1), p116.

Berger, M.F., Philippakis, A.A., Qureshi, A.M., He, F.S., Estep Iii, P.W. and Bulyk, M.L. 2006. Compact, universal DNA microarrays to comprehensively determine transcription-factor binding site specificities. *Nature Biotechnology.* **24**, p1429.

Berman, H.M., Westbrook, J., Feng, Z., Gilliland, G., Bhat, T.N., Weissig, H., Shindyalov, I.N. and Bourne, P.E. 2000. The Protein Data Bank. *Nucleic Acids Research.* **28**(1), pp.235-242.

Boguski, M.S., Lowe, T.M. and Tolstoshev, C.M. 1993. dbEST--database for "expressed sequence tags". *Nat Genet.* **4**(4), pp.332-333.

Boman, B.M. and Fields, J.Z. 2013. An APC:WNT Counter-Current-Like Mechanism Regulates Cell Division Along the Human Colonic Crypt Axis: A Mechanism That Explains How APC Mutations Induce Proliferative Abnormalities That Drive Colon Cancer Development. *Front Oncol.* **3**, p244.

Booth, C., Patel, S., Bennion, G.R. and Potten, C.S. 1995. The isolation and culture of adult mouse colonic epithelium. *Epithelial Cell Biol.* **4**(2), pp.76-86.

Bordeaux, J., Welsh, A., Agarwal, S., Killiam, E., Baquero, M., Hanna, J., Anagnostou, V. and Rimm, D. 2010. Antibody validation. *Biotechniques.* **48**(3), pp.197-209.

Boudreau, H.E., Ma, W.F., Korzeniowska, A., Park, J.J., Bhagwat, M.A. and Leto, T.L. 2017. Histone modifications affect differential regulation of TGFbeta-induced NADPH oxidase 4 (NOX4) by wild-type and mutant p53. *Oncotarget.* **8**(27), pp.44379-44397.

Bradbury, D.A., Newton, R., Zhu, Y.M., El-Haroun, H., Corbett, L. and Knox, A.J. 2003. Cyclooxygenase-2 induction by bradykinin in human pulmonary artery smooth muscle cells is mediated by the cyclic AMP response element through a novel autocrine loop involving endogenous prostaglandin E2, E-prostanoid 2 (EP2), and EP4 receptors. *J Biol Chem.* **278**(50), pp.49954-49964.

Bragina, O., Sergejeva, S., Serg, M., Zarkovsky, T., Maloverjan, A., Kogerman, P. and Zarkovsky, A. 2010. Smoothened agonist augments proliferation and survival of neural cells. *Neurosci Lett.* **482**(2), pp.81-85.

Braithwaite, S.S. and Jarabak, J. 1975. Studies on a 15-hydroxyprostaglandin dehydrogenase from human placenta. Purification and partial characterization. *J Biol Chem.* **250**(6), pp.2315-2318.

Breuiller-Fouche, M., Leroy, M.J., Dubois, O., Reinaud, P., Chissey, A., Qi, H., Germain, G., Fortier, M.A. and Charpigny, G. 2010. Differential expression of

the enzymatic system controlling synthesis, metabolism, and transport of PGF2 alpha in human fetal membranes. *Biol Reprod.* **83**(1), pp.155-162.

Brumbaugh, K., Liao, W.C., Houchins, J.P., Cooper, J. and Stoesz, S. 2017. Phosphosite-Specific Antibodies: A Brief Update on Generation and Applications. *Methods Mol Biol.* **1554**, pp.1-40.

Bygdeman, M. 2003. Pharmacokinetics of prostaglandins. *Best Practice & Research Clinical Obstetrics & Gynaecology.* **17**(5), pp.707-716.

Carninci, P., Sandelin, A., Lenhard, B., Katayama, S., Shimokawa, K., Ponjavic, J., Semple, C.A., Taylor, M.S., Engstrom, P.G., Frith, M.C., Forrest, A.R., Alkema, W.B., Tan, S.L., Plessy, C., Kodzius, R., Ravasi, T., Kasukawa, T., Fukuda, S., Kanamori-Katayama, M., Kitazume, Y., Kawaji, H., Kai, C., Nakamura, M., Konno, H., Nakano, K., Mottagui-Tabar, S., Arner, P., Chesi, A., Gustincich, S., Persichetti, F., Suzuki, H., Grimmond, S.M., Wells, C.A., Orlando, V., Wahlestedt, C., Liu, E.T., Harbers, M., Kawai, J., Bajic, V.B., Hume, D.A. and Hayashizaki, Y. 2006. Genome-wide analysis of mammalian promoter architecture and evolution. *Nat Genet.* **38**(6), pp.626-635.

Carpenter, E.P., Beis, K., Cameron, A.D. and Iwata, S. 2008. Overcoming the challenges of membrane protein crystallography. *Current Opinion in Structural Biology.* **18**(5), pp.581-586.

Castellone, M.D., Teramoto, H., Williams, B.O., Druey, K.M. and Gutkind, J.S. 2005. Prostaglandin E2 promotes colon cancer cell growth through a Gs-axin-beta-catenin signaling axis. *Science.* **310**(5753), pp.1504-1510.

Chan, B.S., Bao, Y. and Schuster, V.L. 2002a. Role of Conserved Transmembrane Cationic Amino Acids in the Prostaglandin Transporter PGT. *Biochemistry.* **41**(29), pp.9215-9221.

Chan, B.S., Endo, S., Kanai, N. and Schuster, V.L. 2002b. Identification of lactate as a driving force for prostanoid transport by prostaglandin transporter PGT. *Am J Physiol Renal Physiol.* **282**(6), pp.F1097-1102.

Chan, B.S., Satriano, J.A., Pucci, M. and Schuster, V.L. 1998. Mechanism of prostaglandin E2 transport across the plasma membrane of HeLa cells and Xenopus oocytes expressing the prostaglandin transporter "PGT". *J Biol Chem.* **273**(12), pp.6689-6697.

Chan, B.S., Satriano, J.A. and Schuster, V.L. 1999. Mapping the substrate binding site of the prostaglandin transporter PGT by cysteine scanning mutagenesis. *J Biol Chem.* **274**(36), pp.25564-25570.

Chang, H.Y., Locker, J., Lu, R. and Schuster, V.L. 2010. Failure of postnatal ductus arteriosus closure in prostaglandin transporter-deficient mice. *Circulation.* **121**(4), pp.529-536.

Chen, J.K., Taipale, J., Cooper, M.K. and Beachy, P.A. 2002. Inhibition of Hedgehog signaling by direct binding of cyclopamine to Smoothened. *Genes & Development.* **16**(21), pp.2743-2748.

Chen, Z.-S. and Tiwari, A.K. 2011. Multidrug Resistance Proteins (MRPs/ABCCs) in Cancer Chemotherapy and Genetic Diseases. *The FEBS journal.* **278**(18), pp.3226-3245.

Chi, X., Freeman, B.M., Tong, M., Zhao, Y. and Tai, H.H. 2009. 15-Hydroxyprostaglandin dehydrogenase (15-PGDH) is up-regulated by flurbiprofen and other non-steroidal anti-inflammatory drugs in human colon cancer HT29 cells. *Arch Biochem Biophys.* **487**(2), pp.139-145.

Chi, Y., Jasmin, J.F., Seki, Y., Lisanti, M.P., Charron, M.J., Lefer, D.J. and Schuster, V.L. 2015. Inhibition of the Prostaglandin Transporter PGT Lowers Blood Pressure in Hypertensive Rats and Mice. *PLoS One.* **10**(6), pe0131735.

Chi, Y., Khersonsky, S.M., Chang, Y.T. and Schuster, V.L. 2006. Identification of a new class of prostaglandin transporter inhibitors and characterization of their biological effects on prostaglandin E2 transport. *J Pharmacol Exp Ther.* **316**(3), pp.1346-1350.

Chi, Y., Min, J., Jasmin, J.F., Lisanti, M.P., Chang, Y.T. and Schuster, V.L. 2011. Development of a high-affinity inhibitor of the prostaglandin transporter. *J Pharmacol Exp Ther.* **339**(2), pp.633-641.

Chi, Y., Pucci, M.L. and Schuster, V.L. 2008. Dietary salt induces transcription of the prostaglandin transporter gene in renal collecting ducts. *Am J Physiol Renal Physiol.* **295**(3), pp.F765-771.

Chi, Y. and Schuster, V.L. 2010. The prostaglandin transporter PGT transports PGH(2). *Biochem Biophys Res Commun.* **395**(2), pp.168-172.

Chi, Y., Suadicani, S.O. and Schuster, V.L. 2014. Regulation of prostaglandin EP1 and EP4 receptor signaling by carrier-mediated ligand reuptake. *Pharmacol Res Perspect.* **2**(5), pe00051.

Chiurillo, M.A. 2015. Role of the Wnt/beta-catenin pathway in gastric cancer: An in-depth literature review. *World J Exp Med.* **5**(2), pp.84-102.

Choi, P.M. and Zelig, M.P. 1994. Similarity of colorectal cancer in Crohn's disease and ulcerative colitis: implications for carcinogenesis and prevention. *Gut.* **35**(7), pp.950-954.

Chomczynski, P. 1992. Solubilization in formamide protects RNA from degradation. *Nucleic Acids Res.* **20**(14), pp.3791-3792.

Chulada, P.C., Thompson, M.B., Mahler, J.F., Doyle, C.M., Gaul, B.W., Lee, C., Tiano, H.F., Morham, S.G., Smithies, O. and Langenbach, R. 2000. Genetic disruption of Ptgs-1, as well as Ptgs-2, reduces intestinal tumorigenesis in Min mice. *Cancer Res.* **60**(17), pp.4705-4708.

Cingolani, G., Panella, A., Perrone, M.G., Vitale, P., Di Mauro, G., Fortuna, C.G., Armen, R.S., Ferorelli, S., Smith, W.L. and Scilimati, A. 2017. Structural basis for selective inhibition of Cyclooxygenase-1 (COX-1) by diarylisoxazoles mofezolac and 3-(5-chlorofuran-2-yl)-5-methyl-4-phenylisoxazole (P6). *European Journal of Medicinal Chemistry.* **138**, pp.661-668.

Cobain, E.F., Milliron, K.J. and Merajver, S.D. 2016. Updates on breast cancer genetics: Clinical implications of detecting syndromes of inherited increased susceptibility to breast cancer. *Seminars in Oncology.* **43**(5), pp.528-535.

Coceani, F., Bodach, E., White, E., Bishai, I. and Olley, P.M. 1978. Prostaglandin I2 is less relaxant than prostaglandin E2 on the lamb ductus arteriosus. *Prostaglandins.* **15**(4), pp.551-556.

Coggins, K.G., Latour, A., Nguyen, M.S., Audoly, L., Coffman, T.M. and Koller, B.H. 2002. Metabolism of PGE2 by prostaglandin dehydrogenase is essential for remodeling the ductus arteriosus. *Nature Medicine.* **8**, p91.

Coskun, M., Olsen, A.K., Bzorek, M., Holck, S., Engel, U.H., Nielsen, O.H. and Troelsen, J.T. 2014. Involvement of CDX2 in the cross talk between TNF-alpha and Wnt signaling pathway in the colon cancer cell line Caco-2. *Carcinogenesis.* **35**(5), pp.1185-1192.

Dakin, S.G., Ly, L., Colas, R.A., Oppermann, U., Wheway, K., Watkins, B., Dalli, J. and Carr, A.J. 2017. Increased 15-PGDH expression leads to dysregulated resolution responses in stromal cells from patients with chronic tendinopathy. *Sci Rep.* **7**(1), p11009.

Dalerba, P., Sahoo, D., Paik, S., Guo, X., Yothers, G., Song, N., Wilcox-Fogel, N., Forgo, E., Rajendran, P.S., Miranda, S.P., Hisamori, S., Hutchison, J., Kalisky, T., Qian, D., Wolmark, N., Fisher, G.A., van de Rijn, M. and Clarke, M.F. 2016. CDX2 as a Prognostic Biomarker in Stage II and Stage III Colon Cancer. *N Engl J Med.* **374**(3), pp.211-222.

Davis, B.J., Lennard, D.E., Lee, C.A., Tiano, H.F., Morham, S.G., Wetsel, W.C. and Langenbach, R. 1999. Anovulation in cyclooxygenase-2-deficient mice is restored by prostaglandin E2 and interleukin-1beta. *Endocrinology.* **140**(6), pp.2685-2695.

Dawson, H., Koelzer, V.H., Lukesch, A.C., Mallaev, M., Inderbitzin, D., Lugli, A. and Zlobec, I. 2013. Loss of Cdx2 Expression in Primary Tumors and Lymph Node Metastases is Specific for Mismatch Repair-Deficiency in Colorectal Cancer. *Front Oncol.* **3**, p265.

de Miranda, N.F.C.C., van Dinther, M., van den Akker, B.E.W.M., van Wezel, T., ten Dijke, P. and Morreau, H. 2015. Transforming Growth Factor β Signaling in Colorectal Cancer Cells With Microsatellite Instability Despite Biallelic Mutations in TGFBR2. *Gastroenterology.* **148**(7), pp.1427-1437.e1428.

Desai, A., Zhang, Y., Park, Y., Dawson, D.M., Larusch, G.A., Kasturi, L., Wald, D., Ready, J.M., Gerson, S.L. and Markowitz, S.D. 2018. A second-generation 15-PGDH inhibitor promotes bone marrow transplant recovery independent of age, transplant dose, and G-CSF support. *Haematologica.*

Dienstmann, R., Vermeulen, L., Guinney, J., Kopetz, S., Tejpar, S. and Tabernero, J. 2017. Consensus molecular subtypes and the evolution of precision medicine in colorectal cancer. *Nature Reviews Cancer.* **17**, p79.

Diggle, C.P., Carr, I.M., Zitt, E., Wusik, K., Hopkin, R.J., Prada, C.E., Calabrese, O., Rittinger, O., Punaro, M.G., Markham, A.F. and Bonthron, D.T. 2010. Common and recurrent HPGD mutations in Caucasian individuals with primary hypertrophic osteoarthropathy. *Rheumatology (Oxford).* **49**(6), pp.1056-1062.

Diggle, C.P., Parry, D.A., Logan, C.V., Laissue, P., Rivera, C., Restrepo, C.M., Fonseca, D.J., Morgan, J.E., Allanore, Y., Fontenay, M., Wipff, J., Varret, M., Gibault, L., Dalantaeva, N., Korbonits, M., Zhou, B., Yuan, G., Harifi, G., Cefle, K., Palanduz, S., Akoglu, H., Zwijnenburg, P.J., Lichtenbelt, K.D., Aubry-Rozier, B., Superti-Furga, A., Dallapiccola, B., Accadia, M., Brancati, F., Sheridan, E.G., Taylor, G.R., Carr, I.M., Johnson, C.A., Markham, A.F. and Bonthron, D.T. 2012. Prostaglandin transporter mutations cause pachydermoperiostosis with myelofibrosis. *Hum Mutat.* **33**(8), pp.1175-1181.

Dong, X., Stothard, P., Forsythe, I.J. and Wishart, D.S. 2004. PlasMapper: a web server for drawing and auto-annotating plasmid maps. *Nucleic Acids Res.* **32**(Web Server issue), pp.W660-664.

Dupont, S., Zacchigna, L., Adorno, M., Soligo, S., Volpin, D., Piccolo, S. and Cordenonsi, M. 2004. Convergence of p53 and TGF-beta signaling networks. *Cancer Lett.* **213**(2), pp.129-138.

Dykxhoorn, D.M., St Pierre, R., Van Ham, O. and Linn, T. 1997. An efficient protocol for linker scanning mutagenesis: analysis of the translational regulation of an Escherichia coli RNA polymerase subunit gene. *Nucleic Acids Res.* **25**(21), pp.4209-4218.

Eberhart, C.E., Coffey, R.J., Radhika, A., Giardiello, F.M., Ferrenbach, S. and Dubois, R.N. 1994. Up-regulation of cyclooxygenase 2 gene expression in human colorectal adenomas and adenocarcinomas. *Gastroenterology.* **107**(4), pp.1183-1188.

Edwards, T.L., Shrubsole, M.J., Cai, Q., Li, G., Dai, Q., Rex, D.K., Ulbright, T.M., Fu, Z., Murff, H.J., Smalley, W., Ness, R. and Zheng, W. 2012. A study of prostaglandin pathway genes and interactions with current nonsteroidal anti-inflammatory drug use in colorectal adenoma. *Cancer Prev Res (Phila).* **5**(6), pp.855-863.

Ee, H.C., Erler, T., Bhathal, P.S., Young, G.P. and James, R.J. 1995. Cdx-2 homeodomain protein expression in human and rat colorectal adenoma and carcinoma. *Am J Pathol.* **147**(3), pp.586-592.

Eklund, B. and Carlson, L.A. 1980. Central and peripheral circulatory effects and metabolic effects of different prostaglandins given I.V. to man. *Prostaglandins.* **20**(2), pp.333-347.

Engle, S.J., Hoying, J.B., Boivin, G.P., Ormsby, I., Gartside, P.S. and Doetschman, T. 1999. Transforming growth factor beta1 suppresses nonmetastatic colon cancer at an early stage of tumorigenesis. *Cancer Res.* **59**(14), pp.3379-3386.

Ensor, C.M., Yang, J.Y., Okita, R.T. and Tai, H.H. 1990. Cloning and sequence analysis of the cDNA for human placental NAD(+)-dependent 15-hydroxyprostaglandin dehydrogenase. *J Biol Chem.* **265**(25), pp.14888-14891.

Fabian, I.D., Onadim, Z., Karaa, E., Duncan, C., Chowdhury, T., Scheimberg, I., Ohnuma, S.-I., Reddy, M.A. and Sagoo, M.S. 2018. The management of retinoblastoma. *Oncogene.* **37**(12), pp.1551-1560.

Fanaroff, A.C. and Roe, M.T. 2016. Contemporary Reflections on the Safety of Long-Term Aspirin Treatment for the Secondary Prevention of Cardiovascular Disease. *Drug safety.* **39**(8), pp.715-727.

Fearon, E.R. 2011. Molecular genetics of colorectal cancer. *Annu Rev Pathol.* **6**, pp.479-507.

Fearon, E.R. and Vogelstein, B. 1990. A genetic model for colorectal tumorigenesis. *Cell.* **61**(5), pp.759-767.

Ferlay, J., Colombet, M., Soerjomataram, I., Dyba, T., Randi, G., Bettio, M., Gavin, A., Visser, O. and Bray, F. 2018. Cancer incidence and mortality patterns in Europe: Estimates for 40 countries and 25 major cancers in 2018. *Eur J Cancer.*

Fink, S.P., Yamauchi, M., Nishihara, R., Jung, S., Kuchiba, A., Wu, K., Cho, E., Giovannucci, E., Fuchs, C.S., Ogino, S., Markowitz, S.D. and Chan, A.T. 2014. Aspirin and the risk of colorectal cancer in relation to the expression of 15-hydroxyprostaglandin dehydrogenase (HPGD). *Sci Transl Med.* **6**(233), p233re232.

Fitzgibbons, P.L., Bradley, L.A., Fatheree, L.A., Alsabeh, R., Fulton, R.S., Goldsmith, J.D., Haas, T.S., Karabakhtsian, R.G., Loykasek, P.A., Marolt, M.J., Shen, S.S., Smith, A.T. and Swanson, P.E. 2014. Principles of analytic validation of immunohistochemical assays: Guideline from the College of American Pathologists Pathology and Laboratory Quality Center. *Arch Pathol Lab Med.* **138**(11), pp.1432-1443.

Fitzmaurice, C., Allen, C., Barber, R.M., Barregard, L., Bhutta, Z.A., Brenner, H., Dicker, D.J., Chimed-Orchir, O., Dandona, R., Dandona, L., Fleming, T., Forouzanfar, M.H., Hancock, J., Hay, R.J., Hunter-Merrill, R., Huynh, C., Hosgood, H.D., Johnson, C.O., Jonas, J.B., Khubchandani, J., Kumar, G.A., Kutz, M., Lan, Q., Larson, H.J., Liang, X., Lim, S.S., Lopez, A.D., MacIntyre, M.F., Marczak, L., Marquez, N., Mokdad, A.H., Pinho, C., Pourmalek, F.,

Salomon, J.A., Sanabria, J.R., Sandar, L., Sartorius, B., Schwartz, S.M., Shackelford, K.A., Shibuya, K., Stanaway, J., Steiner, C., Sun, J., Takahashi, K., Vollset, S.E., Vos, T., Wagner, J.A., Wang, H., Westerman, R., Zeeb, H., Zoeckler, L., Abd-Allah, F., Ahmed, M.B., Alabed, S., Alam, N.K., Aldhahri, S.F., Alem, G., Alemayohu, M.A., Ali, R., Al-Raddadi, R., Amare, A., Amoako, Y., Artaman, A., Asayesh, H., Atnafu, N., Awasthi, A., Saleem, H.B., Barac, A., Bedi, N., Bensenor, I., Berhane, A., Bernabe, E., Betsu, B., Binagwaho, A., Boneya, D., Campos-Nonato, I., Castaneda-Orjuela, C., Catala-Lopez, F., Chiang, P., Chibueze, C., Chitheer, A., Choi, J.Y., Cowie, B., Damtew, S., das Neves, J., Dey, S., Dharmaratne, S., Dhillon, P., Ding, E., Driscoll, T., Ekwueme, D., Endries, A.Y., Farvid, M., Farzadfar, F., Fernandes, J., Fischer, F., TT, G.H., Gebru, A., Gopalani, S., Hailu, A., Horino, M., Horita, N., Husseini, A., Huybrechts, I., Inoue, M., Islami, F., Jakovljevic, M., James, S., Javanbakht, M., Jee, S.H., Kasaeian, A., Kedir, M.S., Khader, Y.S., Khang, Y.H., Kim, D., Leigh, J., Linn, S., Lunevicius, R., El Razek, H.M.A., Malekzadeh, R., Malta, D.C., Marcenes, W., Markos, D., Melaku, Y.A., Meles, K.G., Mendoza, W., Mengiste, D.T., Meretoja, T.J., Miller, T.R., Mohammad, K.A., Mohammadi, A., Mohammed, S., Moradi-Lakeh, M., Nagel, G., Nand, D., Le Nguyen, Q., Nolte, S., Ogbo, F.A., Oladimeji, K.E., Oren, E., Pa, M., Park, E.K., Pereira, D.M., Plass, D., Qorbani, M., Radfar, A., Rafay, A., Rahman, M., Rana, S.M., Soreide, K., Satpathy, M., Sawhney, M., Sepanlou, S.G., Shaikh, M.A., She, J., Shiue, I., Shore, H.R., Shrime, M.G., So, S., Soneji, S., Stathopoulou, V., Stroumpoulis, K., Sufiyan, M.B., Sykes, B.L., Tabares-Seisdedos, R., Tadese, F., Tedla, B.A., Tessema, G.A., Thakur, J.S., Tran, B.X., Ukwaja, K.N., Uzochukwu, B.S.C., Vlassov, V.V., Weiderpass, E., Wubshet Terefe, M., Yebyo, H.G., Yimam, H.H., Yonemoto, N., Younis, M.Z., Yu, C., Zaidi, Z., Zaki, M.E.S., Zenebe, Z.M., Murray, C.J.L. and Naghavi, M. 2017. Global, Regional, and National Cancer Incidence, Mortality, Years of Life Lost, Years Lived With Disability, and Disability-Adjusted Life-years for 32 Cancer Groups, 1990 to 2015: A Systematic Analysis for the Global Burden of Disease Study. *JAMA Oncol.* **3**(4), pp.524-548.

Forbes, S.A., Beare, D., Boutselakis, H., Bamford, S., Bindal, N., Tate, J., Cole, C.G., Ward, S., Dawson, E., Ponting, L., Stefancsik, R., Harsha, B., Kok, C.Y., Jia, M., Jubb, H., Sondka, Z., Thompson, S., De, T. and Campbell, P.J. 2017. COSMIC: somatic cancer genetics at high-resolution. *Nucleic Acids Res.* **45**(D1), pp.D777-D783.

Forman, B.M., Tontonoz, P., Chen, J., Brun, R.P., Spiegelman, B.M. and Evans, R.M. 1995. 15-Deoxy-delta 12, 14-prostaglandin J2 is a ligand for the adipocyte determination factor PPAR gamma. *Cell.* **83**(5), pp.803-812.

Freund, J.N., Duluc, I., Reimund, J.M., Gross, I. and Domon-Dell, C. 2015. Extending the functions of the homeotic transcription factor Cdx2 in the digestive system through nontranscriptional activities. *World J Gastroenterol.* **21**(5), pp.1436-1443.

Friedman, E., Gold, L.I., Klimstra, D., Zeng, Z.S., Winawer, S. and Cohen, A. 1995. High levels of transforming growth factor beta 1 correlate with disease progression in human colon cancer. *Cancer Epidemiol Biomarkers Prev.* **4**(5), pp.549-554.

Frolov, A., Yang, L., Dong, H., Hammock, B.D. and Crofford, L.J. 2013. Anti-inflammatory properties of prostaglandin E2: deletion of microsomal prostaglandin E synthase-1 exacerbates non-immune inflammatory arthritis in mice. *Prostaglandins Leukot Essent Fatty Acids.* **89**(5), pp.351-358.

Fujimura, N., Vacik, T., Machon, O., Vlcek, C., Scalabrin, S., Speth, M., Diep, D., Krauss, S. and Kozmik, Z. 2007. Wnt-mediated Down-regulation of Sp1 Target Genes by a Transcriptional Repressor Sp5. *Journal of Biological Chemistry.* **282**(2), pp.1225-1237.

Fujino, H. 2016. The Roles of EP4 Prostanoid Receptors in Cancer Malignancy Signaling. *Biol Pharm Bull.* **39**(2), pp.149-155.

Fujino, H., Xu, W. and Regan, J.W. 2003. Prostaglandin E2 induced functional expression of early growth response factor-1 by EP4, but not EP2, prostanoid receptors via the phosphatidylinositol 3-kinase and extracellular signal-regulated kinases. *J Biol Chem.* **278**(14), pp.12151-12156.

Fung, W.-P., Karim, S.M.M. and Tye, C.Y. 1974. EFFECT OF 15(R)15 METHYLPROSTAGLANDIN E2 METHYL ESTER ON HEALING OF GASTRIC ULCERS: Controlled Endoscopic Study. *The Lancet.* **304**(7871), pp.10-12.

Galiatsatos, P. and Foulkes, W.D. 2006. Familial Adenomatous Polyposis. *The American Journal Of Gastroenterology.* **101**, p385.

Gao, F., Lei, W., Diao, H.L., Hu, S.J., Luan, L.M. and Yang, Z.M. 2007. Differential expression and regulation of prostaglandin transporter and metabolic enzymes in mouse uterus during blastocyst implantation. *Fertil Steril.* **88**(4 Suppl), pp.1256-1265.

Gerling, M., Buller, N.V., Kirn, L.M., Joost, S., Frings, O., Englert, B., Bergstrom, A., Kuiper, R.V., Blaas, L., Wielenga, M.C., Almer, S., Kuhl, A.A., Fredlund, E., van den Brink, G.R. and Toftgard, R. 2016. Stromal Hedgehog signalling is downregulated in colon cancer and its restoration restrains tumour growth. *Nat Commun.* **7**, p12321.

Glaenzer, J., Peter, M.F. and Hagelueken, G. 2018. Studying structure and function of membrane proteins with PELDOR/DEER spectroscopy – A crystallographers' perspective. *Methods.*

Goujon, M., McWilliam, H., Li, W., Valentin, F., Squizzato, S., Paern, J. and Lopez, R. 2010. A new bioinformatics analysis tools framework at EMBL-EBI. *Nucleic Acids Res.* **38**(Web Server issue), pp.W695-699.

Greenland, K.J., Jantke, I., Jenatschke, S., Bracken, K.E., Vinson, C. and Gellersen, B. 2000. The human NAD+-dependent 15-hydroxyprostaglandin dehydrogenase gene promoter is controlled by Ets and activating protein-1 transcription factors and progesterone. *Endocrinology.* **141**(2), pp.581-597.

Gronert, K., Maheshwari, N., Khan, N., Hassan, I.R., Dunn, M. and Laniado Schwartzman, M. 2005. A role for the mouse 12/15-lipoxygenase pathway in promoting epithelial wound healing and host defense. *J Biol Chem.* **280**(15), pp.15267-15278.

Grösch, S., Niederberger, E. and Geisslinger, G. 2017. Investigational drugs targeting the prostaglandin E2 signaling pathway for the treatment of inflammatory pain. *Expert Opinion on Investigational Drugs.* **26**(1), pp.51-61.

Guillem-Llobat, P., Dovizio, M., Bruno, A., Ricciotti, E., Cufino, V., Sacco, A., Grande, R., Alberti, S., Arena, V., Cirillo, M., Patrono, C., FitzGerald, G.A., Steinhilber, D., Sgambato, A. and Patrignani, P. 2016. Aspirin prevents colorectal cancer metastasis in mice by splitting the crosstalk between platelets and tumor cells. *Oncotarget.*

Guinney, J., Dienstmann, R., Wang, X., de Reyniès, A., Schlicker, A., Soneson, C., Marisa, L., Roepman, P., Nyamundanda, G., Angelino, P., Bot, B.M., Morris, J.S., Simon, I.M., Gerster, S., Fessler, E., De Sousa E Melo, F., Missiaglia, E., Ramay, H., Barras, D., Homicsko, K., Maru, D., Manyam, G.C., Broom, B., Boige, V., Perez-Villamil, B., Laderas, T., Salazar, R., Gray, J.W., Hanahan, D., Tabernero, J., Bernards, R., Friend, S.H., Laurent-Puig, P., Medema, J.P., Sadanandam, A., Wessels, L., Delorenzi, M., Kopetz, S., Vermeulen, L. and Tejpar, S. 2015. The consensus molecular subtypes of colorectal cancer. *Nature Medicine.* **21**, p1350.

Gumbiner, B.M. and McCrea, P.D. 1993. Catenins as mediators of the cytoplasmic functions of cadherins. *J Cell Sci Suppl.* **17**, pp.155-158.

Gustafson-Svard, C., Lilja, I., Hallbook, O. and Sjodahl, R. 1996. Cyclooxygenase-1 and cyclooxygenase-2 gene expression in human colorectal adenocarcinomas and in azoxymethane induced colonic tumours in rats. *Gut.* **38**(1), pp.79-84.

Gustafsson, A., Andersson, M., Lagerstedt, K., Lonnroth, C., Nordgren, S. and Lundholm, K. 2010. Receptor and enzyme expression for prostanoid metabolism in colorectal cancer related to tumor tissue PGE2. *Int J Oncol.* **36**(2), pp.469-478.

Hagenbuch, B. and Stieger, B. 2013. THE SLCO (FORMER SLC21) SUPERFAMILY OF TRANSPORTERS. *Molecular aspects of medicine.* **34**(2-3), pp.396-412.

Hamberg, M. and Samuelsson, B. 1971. On the Metabolism of Prostaglandins E1 and E2 in Man. *Journal of Biological Chemistry.* **246**(22), pp.6713-6721.

Hamberg, M., Svensson, J. and Samuelsson, B. 1975. Thromboxanes: a new group of biologically active compounds derived from prostaglandin endoperoxides. *Proc Natl Acad Sci U S A.* **72**(8), pp.2994-2998.

Hanahan, D. 2014. Rethinking the war on cancer. *The Lancet.* **383**(9916), pp.558-563.

Hanahan, D. and Weinberg, Robert A. 2011. Hallmarks of Cancer: The Next Generation. *Cell.* **144**(5), pp.646-674.

Hara, S., Kamei, D., Sasaki, Y., Tanemoto, A., Nakatani, Y. and Murakami, M. 2010. Prostaglandin E synthases: Understanding their pathophysiological roles through mouse genetic models. *Biochimie.* **92**(6), pp.651-659.

Harding, P., Balasubramanian, L., Swegan, J., Stevens, A. and Glass, W.F. 2006. Transforming growth factor beta regulates cyclooxygenase-2 in glomerular mesangial cells. *Kidney International.* **69**(9), pp.1578-1585.

Hashimoto, S., Suzuki, Y., Kasai, Y., Morohoshi, K., Yamada, T., Sese, J., Morishita, S., Sugano, S. and Matsushima, K. 2004. 5'-end SAGE for the analysis of transcriptional start sites. *Nat Biotechnol.* **22**(9), pp.1146-1149.

Hauptmann, S., Zwadlo-Klarwasser, G., Jansen, M., Klosterhalfen, B. and Kirkpatrick, C.J. 1993. Macrophages and multicellular tumor spheroids in co-culture: a three-dimensional model to study tumor-host interactions. Evidence for macrophage-mediated tumor cell proliferation and migration. *Am J Pathol.* **143**(5), pp.1406-1415.

He, N., Zheng, H., Li, P., Zhao, Y.R., Zhang, W., Song, F.J. and Chen, K.X. 2014. miR-485-5p Binding Site SNP rs8752 in HPGD Gene Is Associated with Breast Cancer Risk. *PLoS One.* **9**(7).

Hedrick, E., Cheng, Y., Jin, U.H., Kim, K. and Safe, S. 2016. Specificity protein (Sp) transcription factors Sp1, Sp3 and Sp4 are non-oncogene addiction genes in cancer cells. *Oncotarget.* **7**(16), pp.22245-22256.

Hermansen, S.K., Christensen, K.G., Jensen, S.S. and Kristensen, B.W. 2011. Inconsistent immunohistochemical expression patterns of four different CD133 antibody clones in glioblastoma. *J Histochem Cytochem.* **59**(4), pp.391-407.

Hial, V., Horakova, Z., Shaff, F.E. and Beaven, M.A. 1976. Alteration of tumor growth by aspirin and indomethacin: studies with two transplantable tumors in mouse. *Eur J Pharmacol.* **37**(2), pp.367-376.

Hinck, A.P. and O'Connor-McCourt, M.D. 2011. Structures of TGF-beta receptor complexes: implications for function and therapeutic intervention using ligand traps. *Curr Pharm Biotechnol.* **12**(12), pp.2081-2098.

Hofman, F.M. and Taylor, C.R. 2013. Immunohistochemistry. *Curr Protoc Immunol.* **103**, pUnit 21.24.

Holla, V.R., Backlund, M.G., Yang, P., Newman, R.A. and DuBois, R.N. 2008. Regulation of prostaglandin transporters in colorectal neoplasia. *Cancer Prev Res (Phila).* **1**(2), pp.93-99.

Holstege, H., van Beers, E., Velds, A., Liu, X., Joosse, S.A., Klarenbeek, S., Schut, E., Kerkhoven, R., Klijn, C.N., Wessels, L.F., Nederlof, P.M. and

Jonkers, J. 2010. Cross-species comparison of aCGH data from mouse and human BRCA1- and BRCA2-mutated breast cancers. *BMC Cancer.* **10**, p455.

Hoosein, N.M., Brattain, D.E., McKnight, M.K., Levine, A.E. and Brattain, M.G. 1987. Characterization of the inhibitory effects of transforming growth factor-beta on a human colon carcinoma cell line. *Cancer Res.* **47**(11), pp.2950-2954.

Hou, Y., Lin, Y., Qi, X., Yuan, L., Liao, R., Pang, Q., Cui, L., Jiang, Y., Wang, O., Li, M., Dong, J. and Xia, W. 2017. Identification of mutations in the prostaglandin transporter gene SLCO2A1 and phenotypic comparison between two subtypes of primary hypertrophic osteoarthropathy (PHO): A single-center study. *Bone.*

Houseley, J. and Tollervey, D. 2009. The many pathways of RNA degradation. *Cell.* **136**(4), pp.763-776.

Hryniuk, A., Grainger, S., Savory, J.G. and Lohnes, D. 2014. Cdx1 and Cdx2 function as tumor suppressors. *J Biol Chem.* **289**(48), pp.33343-33354.

Hu, M., Li, K., Maskey, N., Xu, Z., Peng, C., Tian, S., Li, Y. and Yang, G. 2015. 15-PGDH expression as a predictive factor response to neoadjuvant chemotherapy in advanced gastric cancer. *Int J Clin Exp Pathol.* **8**(6), pp.6910-6918.

Hua, H., Zhang, H., Kong, Q., Wang, J. and Jiang, Y. 2018. Complex roles of the old drug aspirin in cancer chemoprevention and therapy. *Med Res Rev.*

Huang, F., Hsu, S., Yan, Z., Winawer, S. and Friedman, E. 1994. The capacity for growth stimulation by TGF beta 1 seen only in advanced colon cancers cannot be ascribed to mutations in APC, DCC, p53 or ras. *Oncogene.* **9**(12), pp.3701-3706.

Huang, X., Taeb, S., Jahangiri, S., Korpela, E., Cadonic, I., Yu, N., Krylov, S.N., Fokas, E., Boutros, P.C. and Liu, S.K. 2015. miR-620 promotes tumor radioresistance by targeting 15-hydroxyprostaglandin dehydrogenase (HPGD). *Oncotarget.*

Hugen, N., van de Velde, C.J.H., de Wilt, J.H.W. and Nagtegaal, I.D. 2014. Metastatic pattern in colorectal cancer is strongly influenced by histological subtype. *Annals of Oncology.* **25**(3), pp.651-657.

Huggins, I.J., Bos, T., Gaylord, O., Jessen, C., Lonquich, B., Puranen, A., Richter, J., Rossdam, C., Brafman, D., Gaasterland, T. and Willert, K. 2017. The WNT target SP5 negatively regulates WNT transcriptional programs in human pluripotent stem cells. *Nature Communications.* **8**, p1034.

Iizuka, Y., Kuwahara, A. and Karaki, S.-I. 2014. Role of PGE2 in the colonic motility: PGE2 generates and enhances spontaneous contractions of longitudinal smooth muscle in the rat colon. *The Journal of Physiological Sciences.* **64**(2), pp.85-96.

Ilyas, M., Efstathiou, J.A., Straub, J., Kim, H.C. and Bodmer, W.F. 1999. Transforming growth factor beta stimulation of colorectal cancer cell lines: type II receptor bypass and changes in adhesion molecule expression. *Proc Natl Acad Sci U S A.* **96**(6), pp.3087-3091.

Ilyas, M., Tomlinson, I.P.M., Rowan, A., Pignatelli, M. and Bodmer, W.F. 1997. β-Catenin mutations in cell lines established from human colorectal cancers. *Proceedings of the National Academy of Sciences of the United States of America.* **94**(19), pp.10330-10334.

Iskit, S., Schlicker, A., Wessels, L. and Peeper, D.S. 2015. Fra-1 is a key driver of colon cancer metastasis and a Fra-1 classifier predicts disease-free survival. *Oncotarget.* **6**(41), pp.43146-43161.

Ito, Y., Takeda, T., Okada, M. and Matsuura, N. 2002. Expression of ets-1 and ets-2 in colonic neoplasms. *Anticancer Res.* **22**(3), pp.1581-1584.

Jabbour, H.N., Milne, S.A., Williams, A.R., Anderson, R.A. and Boddy, S.C. 2001. Expression of COX-2 and PGE synthase and synthesis of PGE(2)in endometrial adenocarcinoma: a possible autocrine/paracrine regulation of neoplastic cell function via EP2/EP4 receptors. *Br J Cancer.* **85**(7), pp.1023-1031.

Jacoby, R.F., Seibert, K., Cole, C.E., Kelloff, G. and Lubet, R.A. 2000. The cyclooxygenase-2 inhibitor celecoxib is a potent preventive and therapeutic agent in the min mouse model of adenomatous polyposis. *Cancer Res.* **60**(18), pp.5040-5044.

Jegerschöld, C., Pawelzik, S.-C., Purhonen, P., Bhakat, P., Gheorghe, K.R., Gyobu, N., Mitsuoka, K., Morgenstern, R., Jakobsson, P.-J. and Hebert, H. 2008. Structural basis for induced formation of the inflammatory mediator prostaglandin E₂. *Proceedings of the National Academy of Sciences.* **105**(32), pp.11110-11115.

Johnson, R.A., Lincoln, F.H., Thompson, J.L., Nidy, E.G., Mizsak, S.A. and Axen, U. 1977. Synthesis and stereochemistry of prostacyclin and synthesis of 6-ketoprostaglandin F1.alpha. *Journal of the American Chemical Society.* **99**(12), pp.4182-4184.

Kahn, M. 2014. Can we safely target the WNT pathway? *Nature reviews. Drug discovery.* **13**(7), pp.513-532.

Kaley, G. and Weiner, R. 1971. Effect of prostaglandin E 1 on leukocyte migration. *Nat New Biol.* **234**(47), pp.114-115.

Kaliberova, L.N., Kusmartsev, S.A., Krendelchtchikova, V., Stockard, C.R., Grizzle, W.E., Buchsbaum, D.J. and Kaliberov, S.A. 2009. Experimental cancer therapy using restoration of NAD+ -linked 15-hydroxyprostaglandin dehydrogenase expression. *Mol Cancer Ther.* **8**(11), pp.3130-3139.

Kamo, S., Nakanishi, T., Aotani, R., Nakamura, Y., Gose, T. and Tamai, I. 2017. Impact of FDA-Approved Drugs on the Prostaglandin Transporter OATP2A1/SLCO2A1. *J Pharm Sci.* **106**(9), pp.2483-2490.

Kanai, N., Lu, R., Satriano, J.A., Bao, Y., Wolkoff, A.W. and Schuster, V.L. 1995. Identification and characterization of a prostaglandin transporter. *Science.* **268**(5212), pp.866-869.

Kang, J., Chapdelaine, P., Parent, J., Madore, E., Laberge, P.Y. and Fortier, M.A. 2005. Expression of human prostaglandin transporter in the human endometrium across the menstrual cycle. *J Clin Endocrinol Metab.* **90**(4), pp.2308-2313.

Kang, J.H., Kang, S.H., Seo, S.H., Shin, J.H., An, M.S., Ha, T.K., Bae, K.B., Kim, T.H., Choi, C.S., Oh, S.H., Kang, M.S. and Kim, K.H. 2014. Relationship between 15-hydroxyprostaglandin dehydrogenase and gastric adenocarcinoma. *Ann Surg Treat Res.* **86**(6), pp.302-308.

Kang, S., Min, A., Im, S.A., Song, S.H., Kim, S.G., Kim, H.A., Kim, H.J., Oh, D.Y., Jong, H.S., Kim, T.Y. and Bang, Y.J. 2015. TGF-beta Suppresses COX-2 Expression by Tristetraprolin-Mediated RNA Destabilization in A549 Human Lung Cancer Cells. *Cancer Res Treat.* **47**(1), pp.101-109.

Kapral, M., Wawszczyk, J., Hollek, A. and Weglarz, L. 2013. Induction of the expression of genes encoding TGF-beta isoforms and their receptors by inositol hexaphosphate in human colon cancer cells. *Acta Pol Pharm.* **70**(2), pp.357-363.

Kasai, H., Allen, J.T., Mason, R.M., Kamimura, T. and Zhang, Z. 2005. TGF-beta1 induces human alveolar epithelial to mesenchymal cell transition (EMT). *Respir Res.* **6**, p56.

Kasai, T., Nakanishi, T., Ohno, Y., Shimada, H., Nakamura, Y., Arakawa, H. and Tamai, I. 2016. Role of OATP2A1 in PGE secretion from human colorectal cancer cells via exocytosis in response to oxidative stress. *Exp Cell Res.*

Kennedy, C.R., Zhang, Y., Brandon, S., Guan, Y., Coffee, K., Funk, C.D., Magnuson, M.A., Oates, J.A., Breyer, M.D. and Breyer, R.M. 1999. Salt-sensitive hypertension and reduced fertility in mice lacking the prostaglandin EP2 receptor. *Nat Med.* **5**(2), pp.217-220.

Kent, W.J., Sugnet, C.W., Furey, T.S., Roskin, K.M., Pringle, T.H., Zahler, A.M. and Haussler, D. 2002. The human genome browser at UCSC. *Genome Res.* **12**(6), pp.996-1006.

Kikuchi, A., Yamamoto, H., Sato, A. and Matsumoto, S. 2012. Wnt5a: its signalling, functions and implication in diseases. *Acta Physiol (Oxf).* **204**(1), pp.17-33.

Kim, H.J., Koo, K.Y., Shin, D.Y., Kim do, Y., Lee, J.S. and Lee, M.G. 2015. Complete form of pachydermoperiostosis with SLCO2A1 gene mutation in a Korean family. *J Dermatol.* **42**(6), pp.655-657.

Kim, H.R., Lee, H.N., Lim, K., Surh, Y.J. and Na, H.K. 2014. 15-Deoxy-Delta(12,14)-prostaglandin J(2) induces expression of 15-hydroxyprostaglandin dehydrogenase through Elk-1 activation in human breast cancer MDA-MB-231 cells. *Mutation Research-Fundamental and Molecular Mechanisms of Mutagenesis.* **768**, pp.6-15.

Kliewer, S.A., Lenhard, J.M., Willson, T.M., Patel, I., Morris, D.C. and Lehmann, J.M. 1995. A prostaglandin J2 metabolite binds peroxisome proliferator-activated receptor gamma and promotes adipocyte differentiation. *Cell.* **83**(5), pp.813-819.

Knudson, A.G. 1971. Mutation and Cancer: Statistical Study of Retinoblastoma. *Proceedings of the National Academy of Sciences of the United States of America.* **68**(4), pp.820-823.

Knudson, A.G. 1985. Hereditary Cancer, Oncogenes, and Antioncogenes. *Cancer Research.* **45**(4), pp.1437-1443.

Knutsen, T., Padilla-Nash, H.M., Wangsa, D., Barenboim-Stapleton, L., Camps, J., McNeil, N., Difilippantonio, M.J. and Ried, T. 2010. Definitive molecular cytogenetic characterization of 15 colorectal cancer cell lines. *Genes Chromosomes Cancer.* **49**(3), pp.204-223.

Kochel, T.J. and Fulton, A.M. 2015. Multiple drug resistance-associated protein 4 (MRP4), prostaglandin transporter (PGT), and 15-hydroxyprostaglandin dehydrogenase (15-PGDH) as determinants of PGE2 levels in cancer. *Prostaglandins Other Lipid Mediat.* **116-117**, pp.99-103.

Koeberle, A. and Werz, O. 2015. Perspective of microsomal prostaglandin E2 synthase-1 as drug target in inflammation-related disorders. *Biochem Pharmacol.* **98**(1), pp.1-15.

Kolesnikov, N., Hastings, E., Keays, M., Melnichuk, O., Tang, Y.A., Williams, E., Dylag, M., Kurbatova, N., Brandizi, M., Burdett, T., Megy, K., Pilicheva, E., Rustici, G., Tikhonov, A., Parkinson, H., Petryszak, R., Sarkans, U. and Brazma, A. 2015. ArrayExpress update--simplifying data submissions. *Nucleic Acids Res.* **43**(Database issue), pp.D1113-1116.

Korinek, V., Barker, N., Morin, P.J., van Wichen, D., de Weger, R., Kinzler, K.W., Vogelstein, B. and Clevers, H. 1997. Constitutive transcriptional activation by a beta-catenin-Tcf complex in APC-/- colon carcinoma. *Science.* **275**(5307), pp.1784-1787.

Ku, E.C., Wasvary, J.M. and Cash, W.D. 1975. Diclofenac sodium (GP 45840, Voltaren), a potent inhibitor of prostaglandin synthetase. *Biochem Pharmacol.* **24**(5), pp.641-643.

Kune, G.A., Kune, S. and Watson, L.F. 1988. Colorectal Cancer Risk, Chronic Illnesses, Operations, and Medications: Case Control Results from the Melbourne Colorectal Cancer Study. *Cancer Research.* **48**(15), pp.4399-4404.

Lampropoulos, P., Zizi-Sermpetzoglou, A., Rizos, S., Kostakis, A., Nikiteas, N. and Papavassiliou, A.G. 2012. Prognostic significance of transforming growth factor beta (TGF-beta) signaling axis molecules and E-cadherin in colorectal cancer. *Tumour Biol.* **33**(4), pp.1005-1014.

Laneuville, O., Breuer, D.K., Xu, N., Huang, Z.H., Gage, D.A., Watson, J.T., Lagarde, M., DeWitt, D.L. and Smith, W.L. 1995. Fatty acid substrate specificities of human prostaglandin-endoperoxide H synthase-1 and -2. Formation of 12-hydroxy-(9Z, 13E/Z, 15Z)- octadecatrienoic acids from alpha-linolenic acid. *J Biol Chem.* **270**(33), pp.19330-19336.

Langenbach, R., Loftin, C., Lee, C. and Tiano, H. 1999. Cyclooxygenase knockout mice: models for elucidating isoform-specific functions. *Biochem Pharmacol.* **58**(8), pp.1237-1246.

Langenbach, R., Morham, S.G., Tiano, H.F., Loftin, C.D., Ghanayem, B.I., Chulada, P.C., Mahler, J.F., Lee, C.A., Goulding, E.H., Kluckman, K.D., Kim, H.S. and Smithies, O. 1995. Prostaglandin synthase 1 gene disruption in mice reduces arachidonic acid-induced inflammation and indomethacin-induced gastric ulceration. *Cell.* **83**(3), pp.483-492.

Lehtinen, L., Vainio, P., Wikman, H., Reemts, J., Hilvo, M., Issa, R., Pollari, S., Brandt, B., Oresic, M., Pantel, K., Kallioniemi, O. and Iljin, K. 2012. 15-Hydroxyprostaglandin dehydrogenase associates with poor prognosis in breast cancer, induces epithelial-mesenchymal transition, and promotes cell migration in cultured breast cancer cells. *J Pathol.* **226**(4), pp.674-686.

Lejeune, M., Leung, P., Beck, P.L. and Chadee, K. 2010. Role of EP4 receptor and prostaglandin transporter in prostaglandin E2-induced alteration in colonic epithelial barrier integrity. *Am J Physiol Gastrointest Liver Physiol.* **299**(5), pp.G1097-1105.

Leprince, D., Gegonne, A., Coll, J., de Taisne, C., Schneeberger, A., Lagrou, C. and Stehelin, D. 1983. A putative second cell-derived oncogene of the avian leukaemia retrovirus E26. *Nature.* **306**(5941), pp.395-397.

Li, L., Wang, X., Li, W., Yang, L., Liu, R., Zeng, R., Wu, Y. and Shou, T. 2017a. miR-21 modulates prostaglandin signaling and promotes gastric tumorigenesis by targeting 15-PGDH. *Biochem Biophys Res Commun.*

Li, S.S., He, J.W., Fu, W.Z., Liu, Y.J., Hu, Y.Q. and Zhang, Z.L. 2017b. Clinical, Biochemical, and Genetic Features of 41 Han Chinese Families With Primary Hypertrophic Osteoarthropathy, and Their Therapeutic Response to Etoricoxib: Results From a Six-Month Prospective Clinical Intervention. *J Bone Miner Res.* **32**(8), pp.1659-1666.

Lieber, M., Todaro, G., Smith, B., Szakal, A. and Nelson-Rees, W. 1976. A continuous tumor-cell line from a human lung carcinoma with properties of type II alveolar epithelial cells. *International Journal of Cancer.* **17**(1), pp.62-70.

Lim, H., Paria, B.C., Das, S.K., Dinchuk, J.E., Langenbach, R., Trzaskos, J.M. and Dey, S.K. 1997. Multiple female reproductive failures in cyclooxygenase 2-deficient mice. *Cell.* **91**(2), pp.197-208.

Liu, W., Cao, D., Oh, S.F., Serhan, C.N. and Kulmacz, R.J. 2006. Divergent cyclooxygenase responses to fatty acid structure and peroxide level in fish and mammalian prostaglandin H synthases. *Faseb j.* **20**(8), pp.1097-1108.

Liu, X. 2008. Inflammatory cytokines augments TGF-beta1-induced epithelial-mesenchymal transition in A549 cells by up-regulating TbetaR-I. *Cell Motil Cytoskeleton.* **65**(12), pp.935-944.

Liu, Y., Jia, Z., Sun, Y., Zhou, L., Downton, M., Chen, R., Zhang, A. and Yang, T. 2014. Postnatal regulation of 15-hydroxyprostaglandin dehydrogenase in the rat kidney. *Am J Physiol Renal Physiol.* **307**(4), pp.F388-395.

Liu, Z., Benard, O., Syeda, M.M., Schuster, V.L. and Chi, Y. 2015. Inhibition of Prostaglandin Transporter (PGT) Promotes Perfusion and Vascularization and Accelerates Wound Healing in Non-Diabetic and Diabetic Rats. *PLoS One.* **10**(7), pe0133615.

Lodygin, D., Epanchintsev, A., Menssen, A., Diebold, J. and Hermeking, H. 2005. Functional epigenomics identifies genes frequently silenced in prostate cancer. *Cancer Res.* **65**(10), pp.4218-4227.

Lu, L., Byrnes, K., Han, C., Wang, Y. and Wu, T. 2014. miR-21 Targets 15-PGDH and Promotes Cholangiocarcinoma Growth. *Molecular Cancer Research.* **12**(6), pp.890-900.

Lu, R., Kanai, N., Bao, Y. and Schuster, V.L. 1996. Cloning, in vitro expression, and tissue distribution of a human prostaglandin transporter cDNA(hPGT). *J Clin Invest.* **98**(5), pp.1142-1149.

Lu, R. and Schuster, V.L. 1998. Molecular cloning of the gene for the human prostaglandin transporter hPGT: Gene organization, promoter activity, and chromosomal localization. *Biochemical and Biophysical Research Communications.* **246**(3), pp.805-812.

MacDonald, B.T., Tamai, K. and He, X. 2009. Wnt/β-Catenin Signaling: Components, Mechanisms, and Diseases. *Developmental Cell.* **17**(1), pp.9-26.

MacKay, S.L., Yaswen, L.R., Tarnuzzer, R.W., Moldawer, L.L., Bland, K.I., Copeland, E.M., 3rd and Schultz, G.S. 1995. Colon cancer cells that are not growth inhibited by TGF-beta lack functional type I and type II TGF-beta receptors. *Ann Surg.* **221**(6), pp.767-776; discussion 776-767.

Maeng, H.-J., Lee, W.-J., Jin, Q.-R., Chang, J.-E. and Shim, W.-S. 2014. Upregulation of COX-2 in the lung cancer promotes overexpression of multidrug resistance protein 4 (MRP4) via PGE2-dependent pathway. *European Journal of Pharmaceutical Sciences.* **62**, pp.189-196.

Magrum, L.J. and Johnston, P.V. 1983. Modulation of prostaglandin synthesis in rat peritoneal macrophages with omega-3 fatty acids. *Lipids.* **18**(8), pp.514-521.

Mahé, M.M., Aihara, E., Schumacher, M.A., Zavros, Y., Montrose, M.H., Helmrath, M.A., Sato, T. and Shroyer, N.F. 2013. Establishment of gastrointestinal epithelial organoids. *Current protocols in mouse biology.* **3**, pp.217-240.

Mallo, G.V., Rechreche, H., Frigerio, J.M., Rocha, D., Zweibaum, A., Lacasa, M., Jordan, B.R., Dusetti, N.J., Dagorn, J.C. and Iovanna, J.L. 1997. Molecular cloning, sequencing and expression of the mRNA encoding human Cdx1 and Cdx2 homeobox. Down-regulation of Cdx1 and Cdx2 mRNA expression during colorectal carcinogenesis. *Int J Cancer.* **74**(1), pp.35-44.

Markowitz, S., Wang, J., Myeroff, L., Parsons, R., Sun, L., Lutterbaugh, J., Fan, R., Zborowska, E., Kinzler, K., Vogelstein, B. and et, a. 1995. Inactivation of the type II TGF-beta receptor in colon cancer cells with microsatellite instability. *Science.* **268**(5215), pp.1336-1338.

Martínez-Colón, G.J. and Moore, B.B. 2018. Prostaglandin E2 as a Regulator of Immunity to Pathogens. *Pharmacology & Therapeutics.* **185**, pp.135-146.

Mathelier, A., Fornes, O., Arenillas, D.J., Chen, C.Y., Denay, G., Lee, J., Shi, W., Shyr, C., Tan, G., Worsley-Hunt, R., Zhang, A.W., Parcy, F., Lenhard, B., Sandelin, A. and Wasserman, W.W. 2016. JASPAR 2016: a major expansion and update of the open-access database of transcription factor binding profiles. *Nucleic Acids Res.* **44**(D1), pp.D110-115.

Matys, V., Fricke, E., Geffers, R., Gossling, E., Haubrock, M., Hehl, R., Hornischer, K., Karas, D., Kel, A.E., Kel-Margoulis, O.V., Kloos, D.U., Land, S., Lewicki-Potapov, B., Michael, H., Munch, R., Reuter, I., Rotert, S., Saxel, H., Scheer, M., Thiele, S. and Wingender, E. 2003. TRANSFAC: transcriptional regulation, from patterns to profiles. *Nucleic Acids Res.* **31**(1), pp.374-378.

McKnight, S. and Kingsbury, R. 1982. Transcriptional control signals of a eukaryotic protein-coding gene. *Science.* **217**(4557), pp.316-324.

Mehdawi, L.M., Prasad, C.P., Ehrnstrom, R., Andersson, T. and Sjolander, A. 2016. Non-canonical WNT5A signaling up-regulates the expression of the tumor suppressor 15-PGDH and induces differentiation of colon cancer cells. *Mol Oncol.* **10**(9), pp.1415-1429.

Mehdawi, L.M., Satapathy, S.R., Gustafsson, A., Lundholm, K., Alvarado-Kristensson, M. and Sjolander, A. 2017. A potential anti-tumor effect of leukotriene C4 through the induction of 15-hydroxyprostaglandin

dehydrogenase expression in colon cancer cells. *Oncotarget.* **8**(21), pp.35033-35047.

Messeguer, X., Escudero, R., Farre, D., Nunez, O., Martinez, J. and Alba, M.M. 2002. PROMO: detection of known transcription regulatory elements using species-tailored searches. *Bioinformatics.* **18**(2), pp.333-334.

Miettinen, P.J., Ebner, R., Lopez, A.R. and Derynck, R. 1994. TGF-beta induced transdifferentiation of mammary epithelial cells to mesenchymal cells: involvement of type I receptors. *J Cell Biol.* **127**(6 Pt 2), pp.2021-2036.

Mohammed, M.K., Shao, C., Wang, J., Wei, Q., Wang, X., Collier, Z., Tang, S., Liu, H., Zhang, F., Huang, J., Guo, D., Lu, M., Liu, F., Liu, J., Ma, C., Shi, L.L., Athiviraham, A., He, T.C. and Lee, M.J. 2016. Wnt/beta-catenin signaling plays an ever-expanding role in stem cell self-renewal, tumorigenesis and cancer chemoresistance. *Genes Dis.* **3**(1), pp.11-40.

Montero-Conde, C., Leandro-Garcia, L.J., Chen, X., Oler, G., Ruiz-Llorente, S., Ryder, M., Landa, I., Sanchez-Vega, F., La, K., Ghossein, R.A., Bajorin, D.F., Knauf, J.A., Riordan, J.D., Dupuy, A.J. and Fagin, J.A. 2017. Transposon mutagenesis identifies chromatin modifiers cooperating with Ras in thyroid tumorigenesis and detects ATXN7 as a cancer gene. *Proc Natl Acad Sci U S A.* **114**(25), pp.E4951-E4960.

Morham, S.G., Langenbach, R., Loftin, C.D., Tiano, H.F., Vouloumanos, N., Jennette, J.C., Mahler, J.F., Kluckman, K.D., Ledford, A., Lee, C.A. and Smithies, O. 1995. Prostaglandin synthase 2 gene disruption causes severe renal pathology in the mouse. *Cell.* **83**(3), pp.473-482.

Morin, P.J., Sparks, A.B., Korinek, V., Barker, N., Clevers, H., Vogelstein, B. and Kinzler, K.W. 1997. Activation of beta-catenin-Tcf signaling in colon cancer by mutations in beta-catenin or APC. *Science.* **275**(5307), pp.1787-1790.

Moser, A.R., Pitot, H.C. and Dove, W.F. 1990. A Dominant Mutation That Predisposes to Multiple Intestinal Neoplasia in the Mouse. *Science.* **247**(4940), pp.322-324.

Munemitsu, S., Albert, I., Souza, B., Rubinfeld, B. and Polakis, P. 1995. Regulation of intracellular beta-catenin levels by the adenomatous polyposis coli (APC) tumor-suppressor protein. *Proceedings of the National Academy of Sciences of the United States of America.* **92**(7), pp.3046-3050.

Myung, D.S., Park, Y.L., Kim, N., Chung, C.Y., Park, H.C., Kim, J.S., Cho, S.B., Lee, W.S., Lee, J.H. and Joo, Y.E. 2014. Expression of early growth response-1 in colorectal cancer and its relation to tumor cell proliferation and apoptosis. *Oncol Rep.* **31**(2), pp.788-794.

Myung, S.J., Rerko, R.M., Yan, M., Platzer, P., Guda, K., Dotson, A., Lawrence, E., Dannenberg, A.J., Lovgren, A.K., Luo, G., Pretlow, T.P., Newman, R.A., Willis, J., Dawson, D. and Markowitz, S.D. 2006. 15-Hydroxyprostaglandin

dehydrogenase is an in vivo suppressor of colon tumorigenesis. *Proc Natl Acad Sci U S A.* **103**(32), pp.12098-12102.

Na, H.K., Park, J.M., Lee, H.G., Lee, H.N., Myung, S.J. and Surh, Y.J. 2011. 15-Hydroxyprostaglandin dehydrogenase as a novel molecular target for cancer chemoprevention and therapy. *Biochem Pharmacol.* **82**(10), pp.1352-1360.

Nagaraj, S.H., Gasser, R.B. and Ranganathan, S. 2007. A hitchhiker's guide to expressed sequence tag (EST) analysis. *Brief Bioinform.* **8**(1), pp.6-21.

Nakamura, Y., Nakanishi, T., Shimada, H., Shimizu, J., Aotani, R., Maruyama, S., Higuchi, K., Okura, T., Deguchi, Y. and Tamai, I. 2018. Prostaglandin Transporter OATP2A1/SLCO2A1 Is Essential for Body Temperature Regulation during Fever. *The Journal of Neuroscience.* **38**(24), pp.5584-5595.

Nakanishi, T., Hasegawa, Y., Mimura, R., Wakayama, T., Uetoko, Y., Komori, H., Akanuma, S., Hosoya, K. and Tamai, I. 2015. Prostaglandin Transporter (PGT/SLCO2A1) Protects the Lung from Bleomycin-Induced Fibrosis. *PLoS One.* **10**(4), pe0123895.

Nakanishi, T., Ohno, Y., Aotani, R., Maruyama, S., Shimada, H., Kamo, S., Oshima, H., Oshima, M., Schuetz, J.D. and Tamai, I. 2017. A novel role for OATP2A1/SLCO2A1 in a murine model of colon cancer. *Scientific Reports.* **7**(1), p16567.

Nakanishi, T. and Tamai, I. 2017. Roles of Organic Anion Transporting Polypeptide 2A1 (OATP2A1/SLCO2A1) in Regulating the Pathophysiological Actions of Prostaglandins. *The AAPS Journal.* **20**(1), p13.

Nakano, J., Anggard, E. and Samuelsson, B. 1969. 15-Hydroxy-prostanoate dehydrogenase. Prostaglandins as substrates and inhibitors. *Eur J Biochem.* **11**(2), pp.386-389.

Nakayama, T., Ito, M., Ohtsuru, A., Naito, S. and Sekine, I. 2001. Expression of the ets-1 proto-oncogene in human colorectal carcinoma. *Mod Pathol.* **14**(5), pp.415-422.

Nandy, A., Jenatschke, S., Hartung, B., Milde-Langosch, K., Bamberger, A.M. and Gellersen, B. 2003. Genomic structure and transcriptional regulation of the human NAD+-dependent 15-hydroxyprostaglandin dehydrogenase gene. *J Mol Endocrinol.* **31**(1), pp.105-121.

Niesen, F.H., Schultz, L., Jadhav, A., Bhatia, C., Guo, K., Maloney, D.J., Pilka, E.S., Wang, M., Oppermann, U., Heightman, T.D. and Simeonov, A. 2010. High-Affinity Inhibitors of Human NAD+-Dependent 15-Hydroxyprostaglandin Dehydrogenase: Mechanisms of Inhibition and Structure-Activity Relationships. *PLOS ONE.* **5**(11), pe13719.

Nishihara, H., Hwang, M., Kizaka-Kondoh, S., Eckmann, L. and Insel, P.A. 2004. Cyclic AMP promotes cAMP-responsive element-binding protein-

dependent induction of cellular inhibitor of apoptosis protein-2 and suppresses apoptosis of colon cancer cells through ERK1/2 and p38 MAPK. *J Biol Chem.* **279**(25), pp.26176-26183.

Nishimura, T., Zhao, X., Gan, H., Koyasu, S. and Remold, H.G. 2013. The prostaglandin E2 receptor EP4 is integral to a positive feedback loop for prostaglandin E2 production in human macrophages infected with Mycobacterium tuberculosis. *Faseb j.* **27**(9), pp.3827-3836.

Nishisho, I., Nakamura, Y., Miyoshi, Y., Miki, Y., Ando, H., Horii, A., Koyama, K., Utsunomiya, J., Baba, S. and Hedge, P. 1991. Mutations of chromosome 5q21 genes in FAP and colorectal cancer patients. *Science.* **253**(5020), pp.665-669.

Nomura, T., Chang, H.Y., Lu, R., Hankin, J., Murphy, R.C. and Schuster, V.L. 2005. Prostaglandin signaling in the renal collecting duct: release, reuptake, and oxidation in the same cell. *J Biol Chem.* **280**(31), pp.28424-28429.

Nomura, T., Lu, R., Pucci, M.L. and Schuster, V.L. 2004. The Two-Step Model of Prostaglandin Signal Termination: In Vitro Reconstitution with the Prostaglandin Transporter and Prostaglandin 15 Dehydrogenase. *Molecular Pharmacology.* **65**(4), pp.973-978.

Nusse, R., Brown, A., Papkoff, J., Scambler, P., Shackleford, G., McMahon, A., Moon, R. and Varmus, H. 1991. A new nomenclature for int-1 and related genes: The Wnt gene family. *Cell.* **64**(2), p231.

Nusse, R., van Ooyen, A., Cox, D., Fung, Y.K. and Varmus, H. 1984. Mode of proviral activation of a putative mammary oncogene (int-1) on mouse chromosome 15. *Nature.* **307**(5947), pp.131-136.

O'Grady, P., Liu, Q., Huang, S.S. and Huang, J.S. 1992. Transforming growth factor beta (TGF-beta) type V receptor has a TGF-beta-stimulated serine/threonine-specific autophosphorylation activity. *J Biol Chem.* **267**(29), pp.21033-21037.

Oida, T. and Weiner, H.L. 2010. Depletion of TGF-beta from fetal bovine serum. *J Immunol Methods.* **362**(1-2), pp.195-198.

Olivarius, S., Plessy, C. and Carninci, P. 2009. High-throughput verification of transcriptional starting sites by Deep-RACE. *Biotechniques.* **46**(2), pp.130-132.

Olsen, A.K., Coskun, M., Bzorek, M., Kristensen, M.H., Danielsen, E.T., Jørgensen, S., Olsen, J., Engel, U., Holck, S. and Troelsen, J.T. 2013. Regulation of APC and AXIN2 expression by intestinal tumor suppressor CDX2 in colon cancer cells. *Carcinogenesis.* **34**(6), pp.1361-1369.

Olsen, J., Eiholm, S., Kirkeby, L.T., Espersen, M.L., Jess, P., Gogenur, I., Olsen, J. and Troelsen, J.T. 2016. CDX2 downregulation is associated with poor differentiation and MMR deficiency in colon cancer. *Exp Mol Pathol.* **100**(1), pp.59-66.

Ongen, H., Andersen, C.L., Bramsen, J.B., Oster, B., Rasmussen, M.H., Ferreira, P.G., Sandoval, J., Vidal, E., Whiffin, N., Planchon, A., Padioleau, I., Bielser, D., Romano, L., Tomlinson, I., Houlston, R.S., Esteller, M., Orntoft, T.F. and Dermitzakis, E.T. 2014. Putative cis-regulatory drivers in colorectal cancer. *Nature.* **512**(7512), pp.87-90.

Oshima, M., Dinchuk, J.E., Kargman, S.L., Oshima, H., Hancock, B., Kwong, E., Trzaskos, J.M., Evans, J.F. and Taketo, M.M. 1996. Suppression of intestinal polyposis in Apc delta716 knockout mice by inhibition of cyclooxygenase 2 (COX-2). *Cell.* **87**(5), pp.803-809.

Oshima, M., Oshima, H., Kitagawa, K., Kobayashi, M., Itakura, C. and Taketo, M. 1995. Loss of Apc heterozygosity and abnormal tissue building in nascent intestinal polyps in mice carrying a truncated Apc gene. *Proceedings of the National Academy of Sciences of the United States of America.* **92**(10), pp.4482-4486.

Patrignani, P., Capone, M.L. and Tacconelli, S. 2003. Clinical pharmacology of etoricoxib: a novel selective COX2 inhibitor. *Expert Opin Pharmacother.* **4**(2), pp.265-284.

Pelus, L.M. and Hoggatt, J. 2011. Pleiotropic effects of prostaglandin E2 in hematopoiesis; prostaglandin E2 and other eicosanoids regulate hematopoietic stem and progenitor cell function. *Prostaglandins & Other Lipid Mediators.* **96**(1), pp.3-9.

Peng, C., Gao, H., Niu, Z., Wang, B., Tan, Z., Niu, W., Liu, E., Wang, J., Sun, J., Shahbaz, M., Agrez, M. and Niu, J. 2014. Integrin alphavbeta6 and transcriptional factor Ets-1 act as prognostic indicators in colorectal cancer. *Cell Biosci.* **4**(1), p53.

Pereira, C., Queiros, S., Galaghar, A., Sousa, H., Pimentel-Nunes, P., Brandao, C., Moreira-Dias, L., Medeiros, R. and Dinis-Ribeiro, M. 2014. Genetic variability in key genes in prostaglandin E2 pathway (COX-2, HPGD, ABCC4 and SLCO2A1) and their involvement in colorectal cancer development. *PLoS One.* **9**(4), pe92000.

Petryszak, R., Keays, M., Tang, Y.A., Fonseca, N.A., Barrera, E., Burdett, T., Füllgrabe, A., Fuentes, A.M.-P., Jupp, S., Koskinen, S., Mannion, O., Huerta, L., Megy, K., Snow, C., Williams, E., Barzine, M., Hastings, E., Weisser, H., Wright, J., Jaiswal, P., Huber, W., Choudhary, J., Parkinson, H.E. and Brazma, A. 2016. Expression Atlas update—an integrated database of gene and protein expression in humans, animals and plants. *Nucleic Acids Research.* **44**(D1), pp.D746-D752.

Piper, P.J., Vane, J.R. and Wyllie, J.H. 1970. Inactivation of Prostaglandins by the Lungs. *Nature.* **225**, p600.

Pollard, M. and Luckert, P.H. 1981. Effect of indomethacin on intestinal tumors induced in rats by the acetate derivative of dimethylnitrosamine. *Science.* **214**(4520), pp.558-559.

Poniatowski, L.A., Wojdasiewicz, P., Gasik, R. and Szukiewicz, D. 2015. Transforming growth factor Beta family: insight into the role of growth factors in regulation of fracture healing biology and potential clinical applications. *Mediators Inflamm.* **2015**, p137823.

Poon, D.C., Ho, Y.S., Chiu, K., Wong, H.L. and Chang, R.C. 2015. Sickness: From the focus on cytokines, prostaglandins, and complement factors to the perspectives of neurons. *Neurosci Biobehav Rev.* **57**, pp.30-45.

Portella, G., Cumming, S.A., Liddell, J., Cui, W., Ireland, H., Akhurst, R.J. and Balmain, A. 1998. Transforming growth factor beta is essential for spindle cell conversion of mouse skin carcinoma in vivo: implications for tumor invasion. *Cell Growth Differ.* **9**(5), pp.393-404.

Potten, C.S., Kellett, M., Roberts, S.A., Rew, D.A. and Wilson, G.D. 1992. Measurement of in vivo proliferation in human colorectal mucosa using bromodeoxyuridine. *Gut.* **33**(1), pp.71-78.

Powell, S.M., Zilz, N., Beazer-Barclay, Y., Bryan, T.M., Hamilton, S.R., Thibodeau, S.N., Vogelstein, B. and Kinzler, K.W. 1992. APC mutations occur early during colorectal tumorigenesis. *Nature.* **359**, p235.

Ptashne, M. 1988. How eukaryotic transcriptional activators work. *Nature.* **335**(6192), pp.683-689.

Qi, Z., Hao, C.M., Langenbach, R.I., Breyer, R.M., Redha, R., Morrow, J.D. and Breyer, M.D. 2002. Opposite effects of cyclooxygenase-1 and -2 activity on the pressor response to angiotensin II. *J Clin Invest.* **110**(1), pp.61-69.

Qualtrough, D., Hinoi, T., Fearon, E. and Paraskeva, C. 2002. Expression of CDX2 in normal and neoplastic human colon tissue and during differentiation of an in vitro model system. *Gut.* **51**(2), pp.184-190.

Quyn, A.J., Appleton, P.L., Carey, F.A., Steele, R.J., Barker, N., Clevers, H., Ridgway, R.A., Sansom, O.J. and Nathke, I.S. 2010. Spindle orientation bias in gut epithelial stem cell compartments is lost in precancerous tissue. *Cell Stem Cell.* **6**(2), pp.175-181.

Rampton, D.S. and Sladen, G.E. 1984. Relationship between Rectal Mucosal Prostaglandin Production and Water and Electrolyte Transport in Ulcerative Colitis. *Digestion.* **30**(1), pp.13-22.

Reid, G., Wielinga, P., Zelcer, N., van der Heijden, I., Kuil, A., de Haas, M., Wijnholds, J. and Borst, P. 2003. The human multidrug resistance protein MRP4 functions as a prostaglandin efflux transporter and is inhibited by nonsteroidal antiinflammatory drugs. *Proceedings of the National Academy of Sciences of the United States of America.* **100**(16), pp.9244-9249.

Reiser, J.-B., Legoux, F., Gras, S., Trudel, E., Chouquet, A., Léger, A., Le Gorrec, M., Machillot, P., Bonneville, M., Saulquin, X. and Housset, D. 2014. Analysis of Relationships between Peptide/MHC Structural Features and Naive T Cell Frequency in Humans. *The Journal of Immunology.* **193**(12), pp.5816-5826.

Reyes, A. and Huber, W. 2018. Alternative start and termination sites of transcription drive most transcript isoform differences across human tissues. *Nucleic Acids Research.* **46**(2), pp.582-592.

Rivière, P.J., Farmer, S.C., Burks, T.F. and Porreca, F. 1991. Prostaglandin E2-induced diarrhea in mice: importance of colonic secretion. *Journal of Pharmacology and Experimental Therapeutics.* **256**(2), pp.547-552.

Rivron, N.C., Raiss, C.C., Liu, J., Nandakumar, A., Sticht, C., Gretz, N., Truckenmuller, R., Rouwkema, J. and van Blitterswijk, C.A. 2012. Sonic Hedgehog-activated engineered blood vessels enhance bone tissue formation. *Proc Natl Acad Sci U S A.* **109**(12), pp.4413-4418.

Robert, A., Schultz, J.R., Nezamis, J.E. and Lancaster, C. 1976. Gastric Antisecretory and Antiulcer Properties of PGE₂, 15-Methyl PGE₂, and 16,16-Dimethyl PGE₂. *Gastroenterology.* **70**(3), pp.359-370.

Roche, J.K. 2001. Isolation of a purified epithelial cell population from human colon. *Methods Mol Med.* **50**, pp.15-20.

Rome, L.H., Lands, W.E., Roth, G.J. and Majerus, P.W. 1976. Aspirin as a quantitative acetylating reagent for the fatty acid oxygenase that forms prostaglandins. *Prostaglandins.* **11**(1), pp.23-30.

Romeo, D., Allison, R.S.H., Kondaiah, P. and Wakefield, L.M. 1997. Recharacterization of the start sites for the major human transforming growth factor-β1 mRNA. *Gene.* **189**(2), pp.289-295.

Ruan, C.H., So, S.P. and Ruan, K.H. 2011. Inducible COX-2 dominates over COX-1 in prostacyclin biosynthesis: mechanisms of COX-2 inhibitor risk to heart disease. *Life Sci.* **88**(1-2), pp.24-30.

Rubinfeld, B., Souza, B., Albert, I., Muller, O., Chamberlain, S.H., Masiarz, F.R., Munemitsu, S. and Polakis, P. 1993. Association of the APC gene product with beta-catenin. *Science.* **262**(5140), pp.1731-1734.

Sabirov, R.Z., Merzlyak, P.G., Okada, T., Islam, M.R., Uramoto, H., Mori, T., Makino, Y., Matsuura, H., Xie, Y. and Okada, Y. 2017. The organic anion transporter SLCO2A1 constitutes the core component of the Maxi-Cl channel. *EMBO J.*

Sabo, P.J., Hawrylycz, M., Wallace, J.C., Humbert, R., Yu, M., Shafer, A., Kawamoto, J., Hall, R., Mack, J., Dorschner, M.O., McArthur, M. and

Stamatoyannopoulos, J.A. 2004. Discovery of functional noncoding elements by digital analysis of chromatin structure. *Proc Natl Acad Sci U S A.* **101**(48), pp.16837-16842.

Sabui, S., Ghosal, A. and Said, H.M. 2014. Identification and characterization of 5'-flanking region of the human riboflavin transporter 1 gene (SLC52A1). *Gene.* **553**(1), pp.49-56.

Sakamoto, K.M. and Frank, D.A. 2009. CREB in the pathophysiology of cancer: implications for targeting transcription factors for cancer therapy. *Clin Cancer Res.* **15**(8), pp.2583-2587.

Salomon, D., Sacco, P.A., Roy, S.G., Simcha, I., Johnson, K.R., Wheelock, M.J. and Ben-Ze'ev, A. 1997. Regulation of beta-catenin levels and localization by overexpression of plakoglobin and inhibition of the ubiquitin-proteasome system. *J Cell Biol.* **139**(5), pp.1325-1335.

Samowitz, W.S. and Slattery, M.L. 1997. Transforming growth factor-beta receptor type 2 mutations and microsatellite instability in sporadic colorectal adenomas and carcinomas. *Am J Pathol.* **151**(1), pp.33-35.

Sano, H., Kawahito, Y., Wilder, R.L., Hashiramoto, A., Mukai, S., Asai, K., Kimura, S., Kato, H., Kondo, M. and Hla, T. 1995. Expression of cyclooxygenase-1 and -2 in human colorectal cancer. *Cancer Res.* **55**(17), pp.3785-3789.

Saunders, J., Wisidagama, D.R., Morford, T. and Malone, C.S. 2016. Maximal Expression of the Evolutionarily Conserved Slit2 Gene Promoter Requires Sp1. *Cell Mol Neurobiol.* **36**(6), pp.955-964.

Schaefer, B.C. 1995. Revolutions in rapid amplification of cDNA ends: new strategies for polymerase chain reaction cloning of full-length cDNA ends. *Anal Biochem.* **227**(2), pp.255-273.

Schuster, V.L., Chi, Y. and Lu, R. 2015. The Prostaglandin Transporter: Eicosanoid Reuptake, Control of Signaling, and Development of High-Affinity Inhibitors as Drug Candidates. *Trans Am Clin Climatol Assoc.* **126**, pp.248-257.

Schuster, V.L., Lu, R. and Coca-Prados, M. 1997. The prostaglandin transporter is widely expressed in ocular tissues. *Surv Ophthalmol.* **41 Suppl 2**, pp.S41-45.

Sebastian, A. and Contreras-Moreira, B. 2014. footprintDB: a database of transcription factors with annotated cis elements and binding interfaces. *Bioinformatics.* **30**(2), pp.258-265.

Seifert, W., Kuhnisch, J., Tuysuz, B., Specker, C., Brouwers, A. and Horn, D. 2012. Mutations in the prostaglandin transporter encoding gene SLCO2A1 cause primary hypertrophic osteoarthropathy and isolated digital clubbing. *Hum Mutat.* **33**(4), pp.660-664.

Seira, N., Yanagisawa, N., Suganami, A., Honda, T., Wasai, M., Regan, J.W., Fukushima, K., Yamaguchi, N., Tamura, Y., Arai, T., Murayama, T. and Fujino, H. 2017. Anti-cancer Effects of MW-03, a Novel Indole Compound, by Inducing 15-Hydroxyprostaglandin Dehydrogenase and Cellular Growth Inhibition in the LS174T Human Colon Cancer Cell Line. *Biol Pharm Bull.* **40**(10), pp.1806-1812.

Seo, T., Tatsuguchi, A., Shinji, S., Yonezawa, M., Mitsui, K., Tanaka, S., Fujimori, S., Gudis, K., Fukuda, Y. and Sakamoto, C. 2009. Microsomal prostaglandin E synthase protein levels correlate with prognosis in colorectal cancer patients. *Virchows Archiv.* **454**(6), pp.667-676.

Serhan, C.N. 2002. Lipoxins and aspirin-triggered 15-epi-lipoxin biosynthesis: an update and role in anti-inflammation and pro-resolution. *Prostaglandins & Other Lipid Mediators.* **68-69**, pp.433-455.

Serhan, C.N. 2007. Resolution Phase of Inflammation: Novel Endogenous Anti-Inflammatory and Proresolving Lipid Mediators and Pathways. *Annual Review of Immunology.* **25**(1), pp.101-137.

Serhan, C.N., Chiang, N., Dalli, J. and Levy, B.D. 2015. Lipid Mediators in the Resolution of Inflammation. *Cold Spring Harbor Perspectives in Biology.* **7**(2), pa016311.

Serhan, C.N., Clish, C.B., Brannon, J., Colgan, S.P., Chiang, N. and Gronert, K. 2000. Novel Functional Sets of Lipid-Derived Mediators with Antiinflammatory Actions Generated from Omega-3 Fatty Acids via Cyclooxygenase 2–Nonsteroidal Antiinflammatory Drugs and Transcellular Processing. *The Journal of Experimental Medicine.* **192**(8), pp.1197-1204.

Serhan, C.N., Hamberg, M. and Samuelsson, B. 1984a. Lipoxins: novel series of biologically active compounds formed from arachidonic acid in human leukocytes. *Proc Natl Acad Sci U S A.* **81**(17), pp.5335-5339.

Serhan, C.N., Hamberg, M. and Samuelsson, B. 1984b. Trihydroxytetraenes: A novel series of compounds formed from arachidonic acid in human leukocytes. *Biochemical and Biophysical Research Communications.* **118**(3), pp.943-949.

Shao, C., Shen, C., Lu, E., Haydon, R.C., Luu, H.H., Athiviraham, A., He, T.C. and Lee, M.J. 2015. Damage control: Harnessing prostaglandin E2 as a potential healing factor of tissue injuries. *Genes Dis.* **2**(4), pp.295-298.

Shi, S.R., Shi, Y. and Taylor, C.R. 2011. Antigen retrieval immunohistochemistry: review and future prospects in research and diagnosis over two decades. *J Histochem Cytochem.* **59**(1), pp.13-32.

Shifera, A.S. and Hardin, J.A. 2010. Factors modulating expression of Renilla luciferase from control plasmids used in luciferase reporter gene assays. *Anal Biochem.* **396**(2), pp.167-172.

Shimada, H., Nakamura, Y., Nakanishi, T. and Tamai, I. 2015. OATP2A1/SLCO2A1-mediated prostaglandin E2 loading into intracellular acidic

compartments of macrophages contributes to exocytotic secretion. *Biochemical Pharmacology.* **98**(4), pp.629-638.

Shimizu, T., Rådmark, O. and Samuelsson, B. 1984. Enzyme with dual lipoxygenase activities catalyzes leukotriene A4 synthesis from arachidonic acid. *Proceedings of the National Academy of Sciences of the United States of America.* **81**(3), pp.689-693.

Shiraki, T., Kondo, S., Katayama, S., Waki, K., Kasukawa, T., Kawaji, H., Kodzius, R., Watahiki, A., Nakamura, M., Arakawa, T., Fukuda, S., Sasaki, D., Podhajska, A., Harbers, M., Kawai, J., Carninci, P. and Hayashizaki, Y. 2003. Cap analysis gene expression for high-throughput analysis of transcriptional starting point and identification of promoter usage. *Proc Natl Acad Sci U S A.* **100**(26), pp.15776-15781.

Shirasaka, Y., Shichiri, M., Kasai, T., Ohno, Y., Nakanishi, T., Hayashi, K., Nishiura, A. and Tamai, I. 2013. A role of prostaglandin transporter in regulating PGE2 release from human bronchial epithelial BEAS-2B cells in response to LPS. *Journal of Endocrinology.* **217**(3), pp.265-274.

Shiraya, K., Hirata, T., Hatano, R., Nagamori, S., Wiriyasermkul, P., Jutabha, P., Matsubara, M., Muto, S., Tanaka, H., Asano, S., Anzai, N., Endou, H., Yamada, A., Sakurai, H. and Kanai, Y. 2010. A novel transporter of SLC22 family specifically transports prostaglandins and co-localizes with 15-hydroxyprostaglandin dehydrogenase in renal proximal tubules. *J Biol Chem.* **285**(29), pp.22141-22151.

Sidhu, R.S., Lee, J.Y., Yuan, C. and Smith, W.L. 2010. Comparison of Cyclooxygenase-1 Crystal Structures: Cross-Talk between Monomers Comprising Cyclooxygenase-1 Homodimers. *Biochemistry.* **49**(33), pp.7069-7079.

Sievers, F., Wilm, A., Dineen, D., Gibson, T.J., Karplus, K., Li, W., Lopez, R., McWilliam, H., Remmert, M., Soding, J., Thompson, J.D. and Higgins, D.G. 2011. Fast, scalable generation of high-quality protein multiple sequence alignments using Clustal Omega. *Mol Syst Biol.* **7**, p539.

Sirois, J., Levy, L.O., Simmons, D.L. and Richards, J.S. 1993. Characterization and hormonal regulation of the promoter of the rat prostaglandin endoperoxide synthase 2 gene in granulosa cells. Identification of functional and protein-binding regions. *J Biol Chem.* **268**(16), pp.12199-12206.

Sizemore, G.M., Pitarresi, J.R., Balakrishnan, S. and Ostrowski, M.C. 2017. The ETS family of oncogenic transcription factors in solid tumours. *Nat Rev Cancer.* **17**(6), pp.337-351.

Sjögren, T., Nord, J., Ek, M., Johansson, P., Liu, G. and Geschwindner, S. 2013. Crystal structure of microsomal prostaglandin E₂ synthase provides insight into diversity in the MAPEG superfamily. *Proceedings of the National Academy of Sciences.* **110**(10), pp.3806-3811.

Smartt, H.J., Greenhough, A., Ordonez-Moran, P., Al-Kharusi, M., Collard, T.J., Mariadason, J.M., Huelsken, J., Williams, A.C. and Paraskeva, C. 2012a. beta-catenin negatively regulates expression of the prostaglandin transporter PGT in the normal intestinal epithelium and colorectal tumour cells: a role in the chemopreventive efficacy of aspirin? *Br J Cancer.* **107**(9), pp.1514-1517.

Smartt, H.J., Greenhough, A., Ordonez-Moran, P., Talero, E., Cherry, C.A., Wallam, C.A., Parry, L., Al Kharusi, M., Roberts, H.R., Mariadason, J.M., Clarke, A.R., Huelsken, J., Williams, A.C. and Paraskeva, C. 2012b. beta-catenin represses expression of the tumour suppressor 15-prostaglandin dehydrogenase in the normal intestinal epithelium and colorectal tumour cells. *Gut.* **61**(9), pp.1306-1314.

Soboleva, T.A., Nekrasov, M., Ryan, D.P. and Tremethick, D.J. 2014. Histone variants at the transcription start-site. *Trends Genet.* **30**(5), pp.199-209.

Soumaoro, L.T., Uetake, H., Higuchi, T., Takagi, Y., Enomoto, M. and Sugihara, K. 2004. Cyclooxygenase-2 expression: a significant prognostic indicator for patients with colorectal cancer. *Clin Cancer Res.* **10**(24), pp.8465-8471.

St John, M.A., Wang, G., Luo, J., Dohadwala, M., Hu, D., Lin, Y., Dennis, M., Lee, J.M., Elashoff, D., Lawhon, T., Zaknoen, S.L., Burrows, F.J. and Dubinett, S.M. 2012. Apricoxib upregulates 15-PGDH and PGT in tobacco-related epithelial malignancies. *Br J Cancer.* **107**(4), pp.707-712.

Stamatakis, K., Jimenez-Martinez, M., Jimenez-Segovia, A., Chico-Calero, I., Conde, E., Galan-Martinez, J., Ruiz, J., Pascual, A., Barrocal, B., Lopez-Perez, R., Garcia-Bermejo, M.L. and Fresno, M. 2015. Prostaglandins induce early growth response 1 transcription factor mediated microsomal prostaglandin E2 synthase up-regulation for colorectal cancer progression. *Oncotarget.* **6**(37), pp.39941-39959.

Steinert, D., Kuper, C., Bartels, H., Beck, F.X. and Neuhofer, W. 2009. PGE2 potentiates tonicity-induced COX-2 expression in renal medullary cells in a positive feedback loop involving EP2-cAMP-PKA signaling. *Am J Physiol Cell Physiol.* **296**(1), pp.C75-87.

Stewart, A.J., Hannenhalli, S. and Plotkin, J.B. 2012. Why Transcription Factor Binding Sites Are Ten Nucleotides Long. *Genetics.* **192**(3), pp.973-985.

Stormo, G.D. 1990. Consensus patterns in DNA. *Methods Enzymol.* **183**, pp.211-221.

Straus, D.S. and Glass, C.K. 2001. Cyclopentenone prostaglandins: new insights on biological activities and cellular targets. *Med Res Rev.* **21**(3), pp.185-210.

Sun, K.H., Karna, S., Moon, Y.-S., Cho, H. and Choi, C.-H. 2017. The wound-healing effect of 7,3′,4′-trimethoxyflavone through increased levels of prostaglandin E2 by 15-hydroxyprostaglandin dehydrogenase inhibition. *Biotechnology Letters.* **39**(10), pp.1575-1582.

Swan, C.E. and Breyer, R.M. 2011. Prostaglandin E2 modulation of blood pressure homeostasis: Studies in rodent models. *Prostaglandins & Other Lipid Mediators.* **96**(1), pp.10-13.

Tai, H.H. 2011. Prostaglandin catabolic enzymes as tumor suppressors. *Cancer Metastasis Rev.* **30**(3-4), pp.409-417.

Tai, H.H., Chi, X. and Tong, M. 2011. Regulation of 15-hydroxyprostaglandin dehydrogenase (15-PGDH) by non-steroidal anti-inflammatory drugs (NSAIDs). *Prostaglandins Other Lipid Mediat.* **96**(1-4), pp.37-40.

Takahashi, E., Nagano, O., Ishimoto, T., Yae, T., Suzuki, Y., Shinoda, T., Nakamura, S., Niwa, S., Ikeda, S., Koga, H., Tanihara, H. and Saya, H. 2010. Tumor Necrosis Factor-alpha Regulates Transforming Growth Factor-beta-dependent Epithelial-Mesenchymal Transition by Promoting Hyaluronan-CD44-Moesin Interaction. *Journal of Biological Chemistry.* **285**(6), pp.4060-4073.

Takahashi, M., Nakamura, Y., Obama, K. and Furukawa, Y. 2005. Identification of SP5 as a downstream gene of the beta-catenin/Tcf pathway and its enhanced expression in human colon cancer. *Int J Oncol.* **27**(6), pp.1483-1487.

Takai, E., Tsukimoto, M. and Kojima, S. 2013. TGF-beta 1 Downregulates COX-2 Expression Leading to Decrease of PGE2 Production in Human Lung Cancer A549 Cells, Which Is Involved in Fibrotic Response to TGF-beta 1. *Plos One.* **8**(10).

Takano, T., Fiore, S., Maddox, J.F., Brady, H.R., Petasis, N.A. and Serhan, C.N. 1997. Aspirin-triggered 15-epi-lipoxin A4 (LXA4) and LXA4 stable analogues are potent inhibitors of acute inflammation: evidence for anti-inflammatory receptors. *J Exp Med.* **185**(9), pp.1693-1704.

Takayama, T., Shiozaki, H., Shibamoto, S., Oka, H., Kimura, Y., Tamura, S., Inoue, M., Monden, T., Ito, F. and Monden, M. 1996. Beta-catenin expression in human cancers. *Am J Pathol.* **148**(1), pp.39-46.

Takeda, S., Tanigawa, T., Watanabe, T., Tatsuwaki, H., Nadatani, Y., Otani, K., Nagami, Y., Tanaka, F., Kamata, N., Yamagami, H., Shiba, M., Tominaga, K., Fujiwara, Y., Muguruma, K., Ohira, M., Hirakawa, K. and Arakawa, T. 2015. Reduction of prostaglandin transporter predicts poor prognosis associated with angiogenesis in gastric adenocarcinoma. *J Gastroenterol Hepatol.*

Tamai, I., Nezu, J., Uchino, H., Sai, Y., Oku, A., Shimane, M. and Tsuji, A. 2000. Molecular identification and characterization of novel members of the human organic anion transporter (OATP) family. *Biochem Biophys Res Commun.* **273**(1), pp.251-260.

Tauriello, D.V.F., Palomo-Ponce, S., Stork, D., Berenguer-Llergo, A., Badia-Ramentol, J., Iglesias, M., Sevillano, M., Ibiza, S., Canellas, A., Hernando-Momblona, X., Byrom, D., Matarin, J.A., Calon, A., Rivas, E.I., Nebreda, A.R., Riera, A., Attolini, C.S. and Batlle, E. 2018. TGFbeta drives immune evasion in

genetically reconstituted colon cancer metastasis. *Nature.* **554**(7693), pp.538-543.

Tetteh, P.W., Kretzschmar, K., Begthel, H., van den Born, M., Korving, J., Morsink, F., Farin, H., van Es, J.H., Offerhaus, G.J.A. and Clevers, H. 2016. Generation of an inducible colon-specific Cre enzyme mouse line for colon cancer research. *Proceedings of the National Academy of Sciences of the United States of America.* **113**(42), pp.11859-11864.

Thaler-Dao, H., Saintot, M., Baudin, G., Descomps, B. and Crastes de Paulet, A. 1974. Purification of the human placental 15 hydroxy prostaglandin dehydrogenase: properties of the purified enzyme. *FEBS Lett.* **48**(2), pp.204-208.

Thermo Fisher Scientific. 2017. *Mutation Generation System Kit - Thermo Fisher Scientific.* [Online]. [Accessed 22/05/2017]. Available from: https://www.thermofisher.com/

Thompson, C.L., Fink, S.P., Lutterbaugh, J.D., Elston, R.C., Veigl, M.L., Markowitz, S.D. and Li, L. 2013. Genetic Variation in 15-Hydroxyprostaglandin Dehydrogenase and Colon Cancer Susceptibility. *Plos One.* **8**(5).

Thun, M.J., Namboodiri, M.M. and Heath, C.W., Jr. 1991. Aspirin use and reduced risk of fatal colon cancer. *N Engl J Med.* **325**(23), pp.1593-1596.

Thuresson, E.D., Lakkides, K.M. and Smith, W.L. 2002. PGG2, 11R-HPETE and 15R/S-HPETE are formed from different conformers of arachidonic acid in the prostaglandin endoperoxide H synthase-1 cyclooxygenase site. *Adv Exp Med Biol.* **507**, pp.67-72.

Thurman, R.E., Rynes, E., Humbert, R., Vierstra, J., Maurano, M.T., Haugen, E., Sheffield, N.C., Stergachis, A.B., Wang, H., Vernot, B., Garg, K., John, S., Sandstrom, R., Bates, D., Boatman, L., Canfield, T.K., Diegel, M., Dunn, D., Ebersol, A.K., Frum, T., Giste, E., Johnson, A.K., Johnson, E.M., Kutyavin, T., Lajoie, B., Lee, B.K., Lee, K., London, D., Lotakis, D., Neph, S., Neri, F., Nguyen, E.D., Qu, H., Reynolds, A.P., Roach, V., Safi, A., Sanchez, M.E., Sanyal, A., Shafer, A., Simon, J.M., Song, L., Vong, S., Weaver, M., Yan, Y., Zhang, Z., Zhang, Z., Lenhard, B., Tewari, M., Dorschner, M.O., Hansen, R.S., Navas, P.A., Stamatoyannopoulos, G., Iyer, V.R., Lieb, J.D., Sunyaev, S.R., Akey, J.M., Sabo, P.J., Kaul, R., Furey, T.S., Dekker, J., Crawford, G.E. and Stamatoyannopoulos, J.A. 2012. The accessible chromatin landscape of the human genome. *Nature.* **489**(7414), pp.75-82.

Tirino, V., Camerlingo, R., Bifulco, K., Irollo, E., Montella, R., Paino, F., Sessa, G., Carriero, M.V., Normanno, N., Rocco, G. and Pirozzi, G. 2013. TGF-beta 1 exposure induces epithelial to mesenchymal transition both in CSCs and non-CSCs of the A549 cell line, leading to an increase of migration ability in the CD133(+) A549 cell fraction. *Cell Death & Disease.* **4**.

Tong, M., Ding, Y. and Tai, H.H. 2006a. Reciprocal regulation of cyclooxygenase-2 and 15-hydroxyprostaglandin dehydrogenase expression in

A549 human lung adenocarcinoma cells. *Carcinogenesis.* **27**(11), pp.2170-2179.

Tong, M., Ding, Y.F. and Tai, H.H. 2006b. Histone deacetylase inhibitors and transforming growth factor-beta induce 15-hydroxyprostaglandin dehydrogenase expression in human lung adenocarcinoma cells. *Biochemical Pharmacology.* **72**(6), pp.701-709.

Tootle, T.L. 2013. Genetic insights into the in vivo functions of prostaglandin signaling. *Int J Biochem Cell Biol.* **45**(8), pp.1629-1632.

Topper, J.N., Cai, J., Stavrakis, G., Anderson, K.R., Woolf, E.A., Sampson, B.A., Schoen, F.J., Falb, D. and Gimbrone, M.A., Jr. 1998. Human prostaglandin transporter gene (hPGT) is regulated by fluid mechanical stimuli in cultured endothelial cells and expressed in vascular endothelium in vivo. *Circulation.* **98**(22), pp.2396-2403.

Torre, L.A., Bray, F., Siegel, R.L., Ferlay, J., Lortet-Tieulent, J. and Jemal, A. 2015. Global cancer statistics, 2012. *CA Cancer J Clin.* **65**(2), pp.87-108.

Tosetto, E., Casarin, A., Salviati, L., Familiari, A., Lieske, J.C. and Anglani, F. 2014. Complexity of the 5'UTR region of the CLCN5 gene: eleven 5'UTR ends are differentially expressed in the human kidney. *BMC Med Genomics.* **7**, p41.

Trop-Steinberg, S. and Azar, Y. 2017. AP-1 Expression and its Clinical Relevance in Immune Disorders and Cancer. *Am J Med Sci.* **353**(5), pp.474-483.

Uchida, K., Nakajima, A., Ushijima, K., Ida, S., Seki, Y., Kakuta, F., Abukawa, D., Tsukahara, H., Maisawa, S.I., Inoue, M., Araki, T., Umeno, J., Matsumoto, T. and Taguchi, T. 2016. Pediatric Onset Chronic Nonspecific Multiple Ulcers of Small Intestine: A Nationwide Survey and Genetic Study in Japan. *J Pediatr Gastroenterol Nutr.*

Uhlen, M., Bjorling, E., Agaton, C., Szigyarto, C.A., Amini, B., Andersen, E., Andersson, A.C., Angelidou, P., Asplund, A., Asplund, C., Berglund, L., Bergstrom, K., Brumer, H., Cerjan, D., Ekstrom, M., Elobeid, A., Eriksson, C., Fagerberg, L., Falk, R., Fall, J., Forsberg, M., Bjorklund, M.G., Gumbel, K., Halimi, A., Hallin, I., Hamsten, C., Hansson, M., Hedhammar, M., Hercules, G., Kampf, C., Larsson, K., Lindskog, M., Lodewyckx, W., Lund, J., Lundeberg, J., Magnusson, K., Malm, E., Nilsson, P., Odling, J., Oksvold, P., Olsson, I., Oster, E., Ottosson, J., Paavilainen, L., Persson, A., Rimini, R., Rockberg, J., Runeson, M., Sivertsson, A., Skollermo, A., Steen, J., Stenvall, M., Sterky, F., Stromberg, S., Sundberg, M., Tegel, H., Tourle, S., Wahlund, E., Walden, A., Wan, J., Wernerus, H., Westberg, J., Wester, K., Wrethagen, U., Xu, L.L., Hober, S. and Ponten, F. 2005. A human protein atlas for normal and cancer tissues based on antibody proteomics. *Mol Cell Proteomics.* **4**(12), pp.1920-1932.

Uhlen, M., Fagerberg, L., Hallstrom, B.M., Lindskog, C., Oksvold, P., Mardinoglu, A., Sivertsson, A., Kampf, C., Sjostedt, E., Asplund, A., Olsson, I.,

Edlund, K., Lundberg, E., Navani, S., Szigyarto, C.A., Odeberg, J., Djureinovic, D., Takanen, J.O., Hober, S., Alm, T., Edqvist, P.H., Berling, H., Tegel, H., Mulder, J., Rockberg, J., Nilsson, P., Schwenk, J.M., Hamsten, M., von Feilitzen, K., Forsberg, M., Persson, L., Johansson, F., Zwahlen, M., von Heijne, G., Nielsen, J. and Ponten, F. 2015. Proteomics. Tissue-based map of the human proteome. *Science.* **347**(6220), p1260419.

Umar, A., Steele, V.E., Menter, D.G. and Hawk, E.T. 2016. Mechanisms of nonsteroidal anti-inflammatory drugs in cancer prevention. *Seminars in Oncology.* **43**(1), pp.65-77.

Umeno, J., Esaki, M., Hirano, A., Fuyuno, Y., Ohmiya, N., Yasukawa, S., Hirai, F., Kochi, S., Kurahara, K., Yanai, S., Uchida, K., Hosomi, S., Watanabe, K., Hosoe, N., Ogata, H., Hisamatsu, T., Nagayama, M., Yamamoto, H., Abukawa, D., Kakuta, F., Onodera, K., Matsui, T., Hibi, T., Yao, T., Kitazono, T. and Matsumoto, T. 2018. Clinical features of chronic enteropathy associated with SLCO2A1 gene: a new entity clinically distinct from Crohn's disease. *Journal of Gastroenterology.*

Umeno, J., Hisamatsu, T., Esaki, M., Hirano, A., Kubokura, N., Asano, K., Kochi, S., Yanai, S., Fuyuno, Y., Shimamura, K., Hosoe, N., Ogata, H., Watanabe, T., Aoyagi, K., Ooi, H., Watanabe, K., Yasukawa, S., Hirai, F., Matsui, T., Iida, M., Yao, T., Hibi, T., Kosaki, K., Kanai, T., Kitazono, T. and Matsumoto, T. 2015. A Hereditary Enteropathy Caused by Mutations in the SLCO2A1 Gene, Encoding a Prostaglandin Transporter. *PLoS Genet.* **11**(11), pe1005581.

Uppal, S., Diggle, C.P., Carr, I.M., Fishwick, C.W., Ahmed, M., Ibrahim, G.H., Helliwell, P.S., Latos-Bielenska, A., Phillips, S.E., Markham, A.F., Bennett, C.P. and Bonthron, D.T. 2008. Mutations in 15-hydroxyprostaglandin dehydrogenase cause primary hypertrophic osteoarthropathy. *Nat Genet.* **40**(6), pp.789-793.

Vainio, P., Gupta, S., Ketola, K., Mirtti, T., Mpindi, J.P., Kohonen, P., Fey, V., Perala, M., Smit, F., Verhaegh, G., Schalken, J., Alanen, K.A., Kallioniemi, O. and Iljin, K. 2011. Arachidonic acid pathway members PLA2G7, HPGD, EPHX2, and CYP4F8 identified as putative novel therapeutic targets in prostate cancer. *Am J Pathol.* **178**(2), pp.525-536.

Van Den Brenk, H.A., Stone, M., Kelly, H., Orton, C. and Sharpington, C. 1974. Promotion of growth of tumour cells in acutely inflamed tissues. *Br J Cancer.* **30**(3), pp.246-260.

van Ooyen, A., Kwee, V. and Nusse, R. 1985. The nucleotide sequence of the human int-1 mammary oncogene; evolutionary conservation of coding and non-coding sequences. *Embo j.* **4**(11), pp.2905-2909.

Van Poucke, M., Melkebeek, V., Erkens, T., Van Zeveren, A., Cox, E. and Peelman, L.J. 2009. Molecular cloning and characterization of the porcine prostaglandin transporter (SLCO2A1): evaluation of its role in F4 mediated neonatal diarrhoea. *BMC Genetics.* **10**, pp.64-64.

Volloch, V., Schweitzer, B. and Rits, S. 1994. Ligation-mediated amplification of RNA from murine erythroid cells reveals a novel class of beta globin mRNA with an extended 5'-untranslated region. *Nucleic Acids Research.* **22**(13), pp.2507-2511.

Wada, M., DeLong, C.J., Hong, Y.H., Rieke, C.J., Song, I., Sidhu, R.S., Yuan, C., Warnock, M., Schmaier, A.H., Yokoyama, C., Smyth, E.M., Wilson, S.J., FitzGerald, G.A., Garavito, R.M., Sui de, X., Regan, J.W. and Smith, W.L. 2007. Enzymes and receptors of prostaglandin pathways with arachidonic acid-derived versus eicosapentaenoic acid-derived substrates and products. *J Biol Chem.* **282**(31), pp.22254-22266.

Wang, D., Fu, L., Sun, H., Guo, L. and DuBois, R.N. 2015. Prostaglandin E Promotes Colorectal Cancer Stem Cell Expansion and Metastasis in Mice. *Gastroenterology.*

Wang, J., Cho, N.L., Zauber, A.G., Hsu, M., Dawson, D., Srivastava, A., Mitchell-Richards, K.A., Markowitz, S.D. and Bertagnolli, M.M. 2018. Chemopreventive efficacy of the cyclooxygenase-2 (Cox-2) inhibitor, celecoxib, is predicted by adenoma expression of Cox-2 and 15-PGDH. *Cancer Epidemiology Biomarkers & Prevention.*

Weirauch, M.T., Yang, A., Albu, M., Cote, A.G., Montenegro-Montero, A., Drewe, P., Najafabadi, H.S., Lambert, S.A., Mann, I., Cook, K., Zheng, H., Goity, A., van Bakel, H., Lozano, J.C., Galli, M., Lewsey, M.G., Huang, E., Mukherjee, T., Chen, X., Reece-Hoyes, J.S., Govindarajan, S., Shaulsky, G., Walhout, A.J., Bouget, F.Y., Ratsch, G., Larrondo, L.F., Ecker, J.R. and Hughes, T.R. 2014. Determination and inference of eukaryotic transcription factor sequence specificity. *Cell.* **158**(6), pp.1431-1443.

Weiss, H.J., Aledort, L.M. and Kochwa, S. 1968. The effect of salicylates on the hemostatic properties of platelets in man. *J Clin Invest.* **47**(9), pp.2169-2180.

Wilkins, M.H.F., Stokes, A.R. and Wilson, H.R. 1953. Molecular Structure of Nucleic Acids: Molecular Structure of Deoxypentose Nucleic Acids. *Nature.* **171**, p738.

Wilson, A.J., Chueh, A.C., Tögel, L., Corner, G.A., Ahmed, N., Goel, S., Byun, D.-S., Nasser, S., Houston, M.A., Jhawer, M., Smartt, H.J.M., Murray, L.B., Nicholas, C., Heerdt, B.G., Arango, D., Augenlicht, L.H. and Mariadason, J.M. 2010. A coordinated Sp1/Sp3-mediated transcriptional response involving immediate-early gene induction is linked to HDAC inhibitor-induced apoptosis in colon cancer cells. *Cancer research.* **70**(2), pp.609-620.

Wolf, I., O'Kelly, J., Rubinek, T., Tong, M., Nguyen, A., Lin, B.T., Tai, H.H., Karlan, B.Y. and Koeffler, H.P. 2006. 15-hydroxyprostaglandin dehydrogenase is a tumor suppressor of human breast cancer. *Cancer Res.* **66**(15), pp.7818-7823.

Woodford-Richens, K.L., Rowan, A.J., Gorman, P., Halford, S., Bicknell, D.C., Wasan, H.S., Roylance, R.R., Bodmer, W.F. and Tomlinson, I.P.M. 2001.

SMAD4 mutations in colorectal cancer probably occur before chromosomal instability, but after divergence of the microsatellite instability pathway. *Proceedings of the National Academy of Sciences of the United States of America.* **98**(17), pp.9719-9723.

Wray, J., Kalkan, T., Gomez-Lopez, S., Eckardt, D., Cook, A., Kemler, R. and Smith, A. 2011. Inhibition of glycogen synthase kinase-3 alleviates Tcf3 repression of the pluripotency network and increases embryonic stem cell resistance to differentiation. *Nat Cell Biol.* **13**(7), pp.838-845.

Wu, C., Zhu, X., Liu, W., Ruan, T. and Tao, K. 2017. Hedgehog signaling pathway in colorectal cancer: function, mechanism, and therapy. *Onco Targets Ther.* **10**, pp.3249-3259.

Wu, Y.Y., Chen, W.Z., Guo, M.S., He, Q. and Hu, Y. 2014. Effects of transforming growth factor-beta 2 on myocilin expression and secretion in human primary cultured trabecular meshwork cells. *International Journal of Clinical and Experimental Pathology.* **7**(8), pp.4827-4836.

Xu, H.G., Liu, L., Gao, S., Jin, R., Ren, W. and Zhou, G.P. 2016. Cloning and characterizing of the murine IRF-3 gene promoter region. *Immunol Res.* **64**(4), pp.969-977.

Xu, H.G., Ren, W., Zou, L., Wang, Y., Jin, R. and Zhou, G.P. 2012. Transcriptional control of human CD2AP expression: the role of Sp1 and Sp3. *Mol Biol Rep.* **39**(2), pp.1479-1486.

Xu, X., Sun, Y.L. and Hoey, T. 1996. Cooperative DNA binding and sequence-selective recognition conferred by the STAT amino-terminal domain. *Science.* **273**(5276), pp.794-797.

Xun, C.Q., Tian, Z.G. and Tai, H.H. 1991. Stimulation of synthesis de novo of NAD(+)-dependent 15-hydroxyprostaglandin dehydrogenase in human promyelocytic leukaemia (HL-60) cells by phorbol ester. *Biochem J.* **279 (Pt 2)**, pp.553-558.

Yamashita, S. and Okada, Y. 2005. Mechanisms of heat-induced antigen retrieval: analyses in vitro employing SDS-PAGE and immunohistochemistry. *J Histochem Cytochem.* **53**(1), pp.13-21.

Yan, M., Rerko, R.M., Platzer, P., Dawson, D., Willis, J., Tong, M., Lawrence, E., Lutterbaugh, J., Lu, S., Willson, J.K., Luo, G., Hensold, J., Tai, H.H., Wilson, K. and Markowitz, S.D. 2004. 15-Hydroxyprostaglandin dehydrogenase, a COX-2 oncogene antagonist, is a TGF-beta-induced suppressor of human gastrointestinal cancers. *Proc Natl Acad Sci U S A.* **101**(50), pp.17468-17473.

Yang, J.E., Park, E., Lee, H.J., Kang, H.J., Kim, K.M., Yu, E., Lee, D., Shim, J.H., Lim, Y.S., Lee, H.C., Chung, Y.H. and Lee, Y.S. 2014. Role of 15-hydroxyprostaglandin dehydrogenase down-regulation on the prognosis of hepatocellular carcinoma. *Clin Mol Hepatol.* **20**(1), pp.28-37.

Yang, X., Lin, L., Zhang, X., Ji, Y., Lv, J., Zhu, Y., Yin, Y., Sun, Y. and Han, X. 2008. IDENTIFICATION OF A NOVEL REPRESSOR ELEMENT IN THE CYCLO-OXYGENASE-2 PROMOTER AND ITS NUCLEAR BINDING PROTEIN. *Clinical and Experimental Pharmacology and Physiology.* **35**(10), pp.1204-1208.

Yao, B., Xu, J., Harris, R.C. and Zhang, M.Z. 2008. Renal localization and regulation of 15-hydroxyprostaglandin dehydrogenase. *Am J Physiol Renal Physiol.* **294**(2), pp.F433-439.

Yeomans, N.D., Tulassay, Z., Juhasz, L., Racz, I., Howard, J.M., van Rensburg, C.J., Swannell, A.J. and Hawkey, C.J. 1998. A comparison of omeprazole with ranitidine for ulcers associated with nonsteroidal antiinflammatory drugs. Acid Suppression Trial: Ranitidine versus Omeprazole for NSAID-associated Ulcer Treatment (ASTRONAUT) Study Group. *N Engl J Med.* **338**(11), pp.719-726.

Yeung, T.L., Leung, C.S., Wong, K.K., Samimi, G., Thompson, M.S., Liu, J., Zaid, T.M., Ghosh, S., Birrer, M.J. and Mok, S.C. 2013. TGF-beta modulates ovarian cancer invasion by upregulating CAF-derived versican in the tumor microenvironment. *Cancer Res.* **73**(16), pp.5016-5028.

Zelenay, S., van der Veen, A.G., Bottcher, J.P., Snelgrove, K.J., Rogers, N., Acton, S.E., Chakravarty, P., Girotti, M.R., Marais, R., Quezada, S.A., Sahai, E. and Reis e Sousa, C. 2015. Cyclooxygenase-Dependent Tumor Growth through Evasion of Immunity. *Cell.* **162**(6), pp.1257-1270.

Zhang, W., Hart, J., McLeod, H.L. and Wang, H.L. 2005. Differential expression of the AP-1 transcription factor family members in human colorectal epithelial and neuroendocrine neoplasms. *Am J Clin Pathol.* **124**(1), pp.11-19.

Zhang, Y., Desai, A., Yang, S.Y., Bae, K.B., Antczak, M.I., Fink, S.P., Tiwari, S., Willis, J.E., Williams, N.S., Dawson, D.M., Wald, D., Chen, W.D., Wang, Z., Kasturi, L., Larusch, G.A., He, L., Cominelli, F., Di Martino, L., Djuric, Z., Milne, G.L., Chance, M., Sanabria, J., Dealwis, C., Mikkola, D., Naidoo, J., Wei, S., Tai, H.H., Gerson, S.L., Ready, J.M., Posner, B., Willson, J.K. and Markowitz, S.D. 2015. TISSUE REGENERATION. Inhibition of the prostaglandin-degrading enzyme 15-PGDH potentiates tissue regeneration. *Science.* **348**(6240), paaa2340.

Zhang, Z., He, J.W., Fu, W.Z., Zhang, C.Q. and Zhang, Z.L. 2013. A novel mutation in the SLCO2A1 gene in a Chinese family with primary hypertrophic osteoarthropathy. *Gene.* **521**(1), pp.191-194.

Zhang, Z., He, J.W., Fu, W.Z., Zhang, C.Q. and Zhang, Z.L. 2014. Two novel mutations in the SLCO2A1 gene in a Chinese patient with primary hypertrophic osteoarthropathy. *Gene.* **534**(2), pp.421-423.

Zhang, Z., Xia, W., He, J., Ke, Y., Yue, H., Wang, C., Zhang, H., Gu, J., Hu, W., Fu, W., Hu, Y., Li, M. and Liu, Y. 2012. Exome sequencing identifies SLCO2A1 mutations as a cause of primary hypertrophic osteoarthropathy. *Am J Hum Genet.* **90**(1), pp.125-132.

Zhao, J., Wen, S., Wang, X. and Zhang, Z. 2017. Helicobacter pylori modulates cyclooxygenase-2 and 15-hydroxy prostaglandin dehydrogenase in gastric cancer. *Oncol Lett.* **14**(5), pp.5519-5525.

Zhao, M., Mishra, L. and Deng, C.X. 2018. The role of TGF-beta/SMAD4 signaling in cancer. *Int J Biol Sci.* **14**(2), pp.111-123.

Zhao, Y. and Stormo, G.D. 2011. Quantitative analysis demonstrates most transcription factors require only simple models of specificity. *Nat Biotechnol.* **29**(6), pp.480-483.

Zhou, R., Xiong, B., Song, H., Liu, S. and Wang, X. 2008. Soluble transforming growth factor beta type II receptor attenuates TGF-beta1 activity in human colorectal cancer LoVo cells. *Oncol Rep.* **20**(6), pp.1449-1456.

Zhu, Q., Liang, X., Dai, J. and Guan, X. 2015. Prostaglandin transporter, SLCO2A1, mediates the invasion and apoptosis of lung cancer cells via PI3K/AKT/mTOR pathway. *Int J Clin Exp Pathol.* **8**(8), pp.9175-9181.

Zolk, O., Schnepf, R., Muschler, M., Fromm, M.F., Wendler, O., Traxdorf, M., Iro, H. and Zenk, J. 2013. Transporter gene expression in human head and neck squamous cell carcinoma and associated epigenetic regulatory mechanisms. *Am J Pathol.* **182**(1), pp.234-243.

Zucker, M.B. and Peterson, J. 1968. Inhibition of adenosine diphosphate-induced secondary aggregation and other platelet functions by acetylsalicylic acid ingestion. *Proc Soc Exp Biol Med.* **127**(2), pp.547-551.

Appendix

Index	PCR Name	Forward Primer Reverse Primer	Primer Sequences
1	HPGD cDNA	HPGDsplice1 HPGDsplice2	CACGTGAACGGCAAAGTG ACATCGCACTGGATGAACAG
2	SLCO2A1	PGTsplice11 PGTsplice10	CCTCTCCACCTTCCTCAACA GGAGCATCCCATGAAGAACA
3	ACTB GeneRacer Nested PCR	Control Primer_A Control Primer_B.1	GCTCACCATGGATGATGATATCGC GACCTGGCCGTCAGGCAGCTCG
4	SLCO2A1 GeneRacer Nested PCR	GeneRacer-5_NESTED SLCO2A1_GSP	GGACACTGACATGGACTGAAGGAGTA TCAAGCTGGAAATGAGACCCGATG
5	Screening cloned RLM-RACE nested PCR products	M13F M13R	GTAAAACGACGGCCAG CAGGAAACAGCTATGAC
6	colony PCR for HPGD GeneRacer clones (forward)	M13F HPGD_exon01_F	GTAAAACGACGGCCAG GTGAACGGCAAAGTGG
7	colony PCR for HPGD GeneRacer clones (reverse)	HPGD_exon01_F M13R	GTGAACGGCAAAGTGG CAGGAAACAGCTATGAC
8	BAC confirming HPGD presence	HPGD_intron1-5 HPGD_exon-2_GSP_new1	GCGTGCCCACTTTGCCACTTCCAAA TGCTCATCCAGGGCAGCTTTACACTGT
9	BAC confirming SLCO2A1 presence	SLCO2A1_intron1-5_1 SLCO2A1_GSP_new1	CTCACGGGCCCATCACTCTTCCCCGCCCAAAGCGCTTCTCAATGGTGGT
10	HPGD -206 to -1 fragment for second cloning step for H-3082	HPGD_NruI_-40bp_F HPGD_NcoI_at-ATG_R	AGGCTTTGAGCCGGTCTG GTTCACGTCCATG**G**TGCA
11	BAC checking HPGD promoter (distal)	HPGD_-3167_F HPGD_-3093_R	GATGTGATGCCCAGGAGTTT AGTTGACATGGAATAACTGTGC
12	BAC checking HPGD promoter (middle)	HPGD_-2015_F HPGD_-1549_R	GCTTCCTGTTCTTCCAGTTGT CTTCAGCTCCTCTAATGGCA
13	BAC checking HPGD promoter (proximal)	HPGD_-943_F HPGD_-491_R	CGCTGACAACCTGAGAAAAAG TCTCGTAATCAGTGGGGTTG
14	BAC checking SLCO2A1 promoter (distal	SLCO2A1_-3324_F SLCO2A1_-2986_R	TCACCCTTGGTTAGAAGCCT CTCTATGGTCTCAGGGTGGG
15	BAC checking SLCO2A1 promoter (middle)	SLCO2A1_-2196_F SLCO2A1_-1444_R	GAACTCCACCCAGTAAAGGTC GAATTCCAGGTCCCATCTGT
16	BAC checking SLCO2A1 promoter (proximal)	SLCO2A1_-709_F SLCO2A1_-207_R	AGTCCTCAACACAAACAGAGC CGGGTGTCAAAGGCGCTAC
17	screening Acc65I-AvrII-10bp-NruI-XhoI adaptor in pGL4.10[luc2]	pGL4_MCR_F pGL4_luc2+329_R	GAGCTCGCTAGCCTCG TTGTAGATGTCGTTAGCTGG
18	screening for Acc65I-AvrII-10bp-NruI-XhoI adaptor in pGL4.10[luc2]	pGL4_adaptor_F pGL4_luc2+329_R	CCCTAGGAGTTAGGCGAT TTGTAGATGTCGTTAGCTGG

19	SLCO2A1 insert 3' check	SLCO2A1_-188_F	GAGAGCGCGTTTCATCATCG
		pGL4_luc2+132_R	TGTCCACCTCGATATGTGCG
20	SLCO2A1 insert 5' check	PGL4_AmpR+831_F	GAGCTCGCTAGCCTCG
		SLCO2A1_-2986_R	TTGTAGATGTCGTTAGCTGG
21	HPGD insert 3' check	HPGD_-943_F	CGCTGACAACCTGAGAAAAAG
		pGL4_luc2+132_R	TGTCCACCTCGATATGTGCG
22	HPGD insert 5' check	PGL4_AmpR+767_F	TACTTTCACCAGCGTTTCGG
		HPGD_-3093_R	AGTTGACATGGAATAACTGTGC
23	HPGD -206 to -1 fragment by PCR	HPGD_NruI_-40bp_F	AGGCTTTGAGCCGGTCTG
		HPGD_NcoI_at-ATG_R	GTTCACGTCCATG**G**TGCA
24	SLCO2A1 deletion series colony PCR	PGL4_AmpR+767_F	TACTTTCACCAGCGTTTCGG
		SLCO2A1_-2074_R	TGGAGAGCCAACCAAAATGAC
25	SLCO2A1 deletion series colony PCR	PGL4_AmpR+767_F	TACTTTCACCAGCGTTTCGG
		SLCO2A1_-2074_R	TGGAGAGCCAACCAAAATGAC
26	Introducing NcoI site for S-805	SLCO2A1_-813_F	CAGTTTACC**A**TGGCTCAGGTC
		pGL4_luc2+132_R	TGTCCACCTCGATATGTGCG
27	Introducing NcoI site for S-1310	SLCO2A1_-1318_F	GCCGTGTCC**A**TGGAACTTG
		pGL4_luc2+132_R	TGTCCACCTCGATATGTGCG
28	Introducing Acc65I site for H-2445	HPGD_-2459_F	TGCTGTTTGCTATC**C**TAGGAG
		HPGD_-1549_R	CTTCAGCTCCTCTAATGGCA
29	Colony PCR S-1310, S-805	SLCO2A1_-709_F	AGTCCTCAACACAAACAGAGC
		pGL4_luc2+132_R	TGTCCACCTCGATATGTGCG
30	Colony PCR S-1579	PGL4_AmpR+767_F	TACTTTCACCAGCGTTTCGG
		SLCO2A1_-1444_R	GAATTCCAGGTCCCATCTGT
31	Colony PCR S-364, S-226	PGL4_AmpR+767_F	TACTTTCACCAGCGTTTCGG
		SLCO2A1_-207_R	CGGGTGTCAAAGGCGCTAC
32	Colony PCR for H-2149, H-2050, H-1570	PGL4_AmpR+767_F	TACTTTCACCAGCGTTTCGG
		HPGD_-1549_R	CTTCAGCTCCTCTAATGGCA
33	Colony PCR for H-1023, H-872	PGL4_AmpR+767_F	TACTTTCACCAGCGTTTCGG
		HPGD_-491_R	TCTCGTAATCAGTGGGGTTG
34	Colony PCR for H-319, H-206, H-34, H-7	PGL4_AmpR+767_F	TACTTTCACCAGCGTTTCGG
		pGL4_luc2+132_R	TGTCCACCTCGATATGTGCG
35	Colony PCR for H-2984	PGL4_AmpR+767_F	TACTTTCACCAGCGTTTCGG
		HPGD_-3093_R	AGTTGACATGGAATAACTGTGC
36	Colony PCR for H-2445, new primer	PGL4_AmpR+767_F	TACTTTCACCAGCGTTTCGG
		HPGD_-2891_R	CGTATCCGTAAACCAGCCTC
37	screening SLCO2A1 internal deletions colonies	>SLCO2A1_-2517_F	TGGGTTACTCCATGTGTAGGTG
		>SLCO2A1_-1823_R	GGTCACAGACACCTTAGGGC
38	SP1 expression from cell line cDNA	SP1_F	CAGGACCCCCTTGAGCTTGTC
		SP1_R	CCTGTTCCCCCTGACTGACT
39	SP2 expression from cell line cDNA	SP2_F	CCAAGCGCTTATTGGTGAAGG
		SP2_R	ATAGGAGGCGCTCAGTTGTG
40		SP3_F	GGCAGCTCAGTGGTGATTCT

	SP3 expression from cell line cDNA	SP3_R	TGGCAAGGTGGTCACTTCTC
41	SP4 expression from cell line cDNA	SP4_F	TGCTCAGATTGCTCCTGTGG
		SP4_R	CTCTTCGAAGCCTCTTGCCA
42	SP5 expression from cell line cDNA	SP5_F	CTTTCTCCAGGACCGCACC
		SP5_R	GATCTGGCTCTGGTACTGCG
43	SP6 expression from cell line cDNA	SP6_F	TCCTAAAAGCTTCTGAGGCCG
		SP6_R	TGCAGGAGCTTGGAAAAGGG
44	SP7 expression from cell line cDNA	SP7_F	CCTGAGTGGAACAGGAGTGG
		SP7_R	AGTTGTTGAGTCCCGCAGAG
45	SP8 expression from cell line cDNA	SP8_F	CAGCCAAACTTGTCCCCTCC
		SP8_R	CGAGGGCTTAAACCACGACT
46	SP9 expression from cell line cDNA	SP9_F	TCTATACTCGGGGAAGAGCCG
		SP9_R	AGCTGAAGTCGGGGTTGTAG
47	EGR1 expression from cell line cDNA	EGR1_F	GGATCCTTTCCTCACTCGCC
		EGR1_R	GAGTGGTTTGGCTGGGGTAA
48	EGR2 expression from cell line cDNA	EGR2_F	AGCGTAGCTCTTAGGGGGAG
		EGR2_R	TTCTAGGTGCAGAGACGGGA
49	EGR3 expression from cell line cDNA	EGR3_F	CTTGCCTGGAAGCTGCGTTA
		EGR3_R	TCGAAGGCGAACTTTCCCAA
50	EGR4 expression from cell line cDNA	EGR4_F	TAGCGAGTTTTCCGAACCCG
		EGR4_R	GATGCCCGACATGAGGTTGA
51	CDX1 expression from cell line cDNA	CDX1_F	CCTCTGGAAACAGCACGAGA
		CDX1_R	GGGAATGTGAGACTCCAGTGA
52	CDX2 expression from cell line cDNA	CDX2_F	AAGGACGTGAGCATGTACCC
		CDX2_R	GTCCTGGTTTTCACTTGGCT
53	CDX4 expression from cell line cDNA	CDX4_F	CACCGGCTTTCTCGCACTAT
		CDX4_R	TTTGTCCTGGTTTTCCCCGTC
54	Introducing NcoI site for S-209	SLCO2A1_NcoI_-209_F	TGACACCC**AT**GGAAAAGAGGG
		pGL4_luc2+132_R	TGTCCACCTCGATATGTGCG
55	Introducing NcoI site for S-87	SLCO2A1_NcoI_-87_F	CCACTGCCGCC**AT**GGTC
		pGL4_luc2+132_R	TGTCCACCTCGATATGTGCG
56	S-364 smaller constructs colony PCR	PGL4_AmpR+767_F	TACTTTCACCAGCGTTTCGG
		pGL4_luc2+132_R	TGTCCACCTCGATATGTGCG
57	S-364 smaller constructs colony PCR	PGL4_AmpR+767_F	TACTTTCACCAGCGTTTCGG
		SLCO2A1_NcoI_-87_F	CCACTGCCGCC**AT**GGTC
58	S-364 smaller constructs colony PCR	SLCO2A1_NcoI_-87_F	CCACTGCCGCC**AT**GGTC
		pGL4_luc2+132_R	TGTCCACCTCGATATGTGCG
59	New GAPDH primers	GAPDH_new_F	GGATTTGGTCGTATTGGGCG
		GAPDH_new_R	GCAAATGAGCCCCAGCCTTC
60	site-directed mutagenesis - first EGR site in S-364	S266_TFmut_EGR_F	CACCTGTCTGAGG**TT**GCGGCGGC GGCGG
		S266_TFmut_EGR_R	CCGCCGCCGCCGC**AA**CCTCAGAC AGGTG
61		S266_TFmut_EGR_second_F	CGGCGGCGGC**TT**CGGGGCGGGG

	site-directed mutagenesis - second EGR site in S-364	S266_TFmut_EGR_second_R	CCCCGCCCCG**AA**GCCGCCGCCG
62	site-directed mutagenesis - SP site in S-364	S266_TFmut_SP_first_F S266_TFmut_SP_first_R	CGGCGGCGGGGC**TT**GGGCTCGTAGCG CGCTACGAGCCC**AA**GCCCCGCCGCCG
63	site-directed mutagenesis - CDX site in S-364	S140_TFmut_CDX _F S140_TFmut_CDX _R	TCGGCGGCGGCCACTT**GG**AAAAACTTCTAGGCGC GCGCCTAGAAGTTTTT**CC**AAGTGGCCGCCGCCGA
64	site-directed mutagenesis - positive control pWhitestript (*lacZ)*	primer 1 primer 2	proprietary primer proprietary primer
65	screening linker scanning mutagenesis insert clones (forward)	PGL4_AmpR+767_F NotI Miniprimer	TACTTTCACCAGCGTTTCGG TGCGGCCGCA
66	screening linker scanning mutagenesis insert clones (reverse)	NotI Miniprimer pGL4_luc2+132_R	TGCGGCCGCA TGTCCACCTCGATATGTGCG
67	PCR for SLCO2A1 on Smoothened Agonist-treated A549 cells cDNA	SLCO2A1_cDNA_3/4_F SLCO2A1_cDNA_5_R	CCAGCACTGGGAACAAGAGC CCCGAAAGCCGGTCCAAATA

Table 1:PCR Reactions and Primers
The PCR reactions, primers and primer sequences are listed. Rows shaded in blue indicate reactions using the Pfx DNA polymerase instead of the conventional *Taq* polymerase. The Index field links the primers to the reaction conditions shown in Table 2.

Index	Initial Denaturation		Denaturation		Annealing		Extension		Final Extension		Total Cycles	Product size
1	95°C	5 min	95°C	30s	64°C	30s	72°C	30s	72°C	5 min	35	191 bp
2	95°C	5 min	95°C	30s	60°C	20s	72°C	30s	72°C	2 min	39	232 bp
3	94°C	5 min	94°C	30s	64°C	20s	72°C	30s	72°C	2 min	38	748 bp, (1323 gDNA)
4	95°C	5 min	95°C	30s	64°C	20s	72°C	30s	72°C	2 min	35	276
5	95°C	3 min	95°C	30s	55°C	20s	72°C	30s	72°C	1 or 2 min	35	variable
6	95°C	3 min	95°C	30s	52°C	20s	72°C	1 min	72°C	2 min	35	variable
7	95°C	3 min	95°C	30s	58°C	20s	72°C	1 min	72°C	2 min	35	variable
8	95°C	3 min	95°C	15s	60°C	15s	72°C	15s	72°C	1 min	35	253 bp
9	95°C	3 min	95°C	15s	60°C	15s	72°C	15s	72°C	1 min	35	124 bp
10	94°C	5 min	94°C	15s	58°C	15s	68°C	15s	68°C	1 min	35	258 bp
11	95°C	3 min	95°C	30s	58°C	20s	72°C	40s	72°C	2 min	35	583 bp
12	95°C	3 min	95°C	30s	58°C	20s	72°C	40s	72°C	2 min	35	467 bp
13	95°C	3 min	95°C	30s	58°C	20s	72°C	40s	72°C	2 min	35	453 bp
14	95°C	3 min	95°C	30s	58°C	20s	72°C	40s	72°C	2 min	35	339 bp
15	95°C	3 min	95°C	30s	58°C	20s	72°C	40s	72°C	2 min	35	618 bp
16	95°C	3 min	95°C	30s	58°C	20s	72°C	40s	72°C	2 min	35	503 bp

17	95°C	3 min	95°C	30s	55°C	20s	72°C	40s	72°C	2 min	35	408 bp
18	95°C	3 min	95°C	30s	55°C	20s	72°C	40s	72°C	2 min	35	420 bp
19	95°C	3 min	95°C	30s	60°C	20s	72°C	30s	72°C	1 min	35	333 bp
20	95°C	3 min	95°C	30s	56-66°C	20s	72°C	40s	72°C	1 min	35	600 bp
21	95°C	3 min	95°C	30s	58°C	20s	72°C	1 min	72°C	2 min	35	958bp (-3082 to -1) 1094bp (-3082 to -1) 261bp (-3082 to -1) 397bp (-3082 to -1)
22	95°C	3 min	95°C	30s	58°C	20s	72°C	30s	72°C	2 min	35	869 bp
23	94°C	5 min	94°C	15s	58°C	20s	68°C	20s	68°C	2 min	35	258 bp
24	94°C	3 min	94°C	30s	55-65°C	20s	68°C	1 min 30s	68°C	2 min	35	1574 bp (-3198), 1234 (-2887), 698 (-2351), 511 (-2164)
25	94°C	3 min	94°C	30s	55-65°C	20s	68°C	1 min 30s	68°C	2 min	35	854 (-1877)
26	94°C	5 min	94°C	30s	58°C	30s	68°C	1 min 30s	68°C	2 min	35	964 bp
27	94°C	5 min	94°C	30s	58°C	30s	68°C	1 min 30s	68°C	2 min	35	1469 bp
28	94°C	5 min	94°C	30s	57°C	30s	68°C	1 min	68°C	2 min	35	911 bp
29	95°C	3 min	95°C	30s	59°C	20s	72°C	1 min	72°C	2 min	35	841 bp
30	95°C	3 min	95°C	30s	59°C	20s	72°C	1 min 30s	72°C	2 min	35	556
31	95°C	3 min	95°C	30s	59°C	20s	72°C	1 min 30s	72°C	2 min	35	1411 bp (-1310), 936 (-805), 578 bp (-364), 480 bp (-226)
32	95°C	3 min	95°C	30s	59°C	20s	72°C		72°C	2 min	35	

								1 min 30s				972 bp (-2419), 1268 bp (-2445), 772 bp (-2050), 319 bp (-1570)
33	95°C	3 min	95°C	30s	59°C	20s	72°C	1 min	72°C	2 min	35	902 bp (-1023), 751 bp (-872),
34	95°C	3 min	95°C	30s	59°C	20s	72°C	1 min	72°C	2 min	35	839 bp (-319), 726 bp (-206), 554 bp (-34), 527 bp (-7)
35	95°C	3 min	95°C	30s	57°C	20s	72°C	1 min	72°C	2 min	35	771 bp
36	95°C	3 min	95°C	30s	59°C	20s	72°C	40s	72°C	2 min	35	484 bp
37	95°C	3 min	95°C	30s	61°C	20s	72°C	40s	72°C	2 min	35	695 bp
38	95°C	3 min	95°C	30s	60°C	20s	72°C	1 min	72°C	2 min	35	307 bp
39	95°C	3 min	95°C	30s	60°C	20s	72°C	1 min	72°C	2 min	35	446 bp
40	95°C	3 min	95°C	30s	60°C	20s	72°C	1 min	72°C	2 min	35	414 bp
41	95°C	3 min	95°C	30s	60°C	20s	72°C	1 min	72°C	2 min	35	347 bp
42	95°C	3 min	95°C	30s	60°C	20s	72°C	1 min	72°C	2 min	35	721 bp
43	95°C	3 min	95°C	30s	60°C	20s	72°C	1 min	72°C	2 min	35	506 bp
44	95°C	3 min	95°C	30s	60°C	20s	72°C	1 min	72°C	2 min	35	300 bp
45	95°C	3 min	95°C	30s	60°C	20s	72°C	1 min	72°C	2 min	35	675 bp
46	95°C	3 min	95°C	30s	60°C	20s	72°C	1 min	72°C	2 min	35	667 bp
47	95°C	3 min	95°C	30s	60°C	20s	72°C	30s	72°C	2 min	35	319 bp
48	95°C	3 min	95°C	30s	60°C	20s	72°C	30s	72°C	2 min	35	463 bp
49	95°C	3 min	95°C	30s	60°C	20s	72°C	30s	72°C	2 min	35	351 bp
50	95°C	3 min	95°C	30s	60°C	20s	72°C	30s	72°C	2 min	35	313 bp

51	95°C	3 min	95°C	30s	60°C	40s	72°C	30s	72°C	2 min	35	607 bp
52	95°C	3 min	95°C	30s	60°C	40s	72°C	30s	72°C	2 min	35	530 bp
53	95°C	3 min	95°C	30s	60°C	40s	72°C	30s	72°C	2 min	35	379 bp
54	94°C	5 min	94°C	30s	60°C	20s	68°C	30s	68°C	2 min	35	366 bp
55	94°C	5 min	94°C	30s	60°C	20s	68°C	30s	68°C	2 min	35	247 bp
56	95°C	3 min	95°C	30s	59°C	20s	72°C	40s	72°C	2 min	35	810bp (-209), 688bp (-87)
57	95°C	3 min	95°C	30s	59°C	20s	72°C	30s	72°C	2 min	35	~600bp
58	95°C	3 min	95°C	30s	59°C	20s	72°C	30s	72°C	2 min	35	~600bp
59	95°C	3 min	95°C	30s	60°C	20s	72°C	30s	72°C	2 min	25	310bp
60	95°C	30s	95°C	30s	55°C	1 min	68°C	5 min	x	x	17	N/A amplify whole S-364 plasmid
61	95°C	30s	95°C	30s	55°C	1 min	68°C	5 min	x	x	17	N/A amplify whole S-364 plasmid
62	95°C	30s	95°C	30s	55°C	1 min	68°C	5 min	x	x	17	N/A amplify whole S-364 plasmid
63	95°C	30s	95°C	30s	55°C	1 min	68°C	5 min	x	x	17	N/A amplify whole S-364 plasmid
64	95°C	30s	95°C	30s	55°C	1 min	68°C	5 min	x	x	17	N/A amplify whole +ve control
65	95°C	3 min	95°C	30s	55°C	20s	72°C	1 min 30s	72°C	2 min	35	430bp - 794bp
66	95°C	3 min	95°C	30s	55°C	20s	72°C	1 min 30s	72°C	2 min	35	163bp - 527bp
67	95°C	3 min	95°C	30s	60°C	20s	72°C	20s	x	x	35.0	278 bp

Table 2: PCR reaction conditions and products
The thermocycler temperatures, times and cycle numbers are shown in the table above. The size of the reaction product or products is also given. The index field corresponds to the primers listed in Table 1. Rows shaded in blue use the Pfx proofreading DNA polymerase in place of *Taq* polymerase.

Step	Temperature settings	Temperature / (°C)	Time
1 initial denaturation	Ramp to target temperature, 1°C/second	96.0	1 minute
2 denaturation	Ramp to target temperature, 1°C/second	96.0	10 seconds
3 annealing	Ramp to target temperature, 1°C/second	50.0	5 seconds
4 extension	Ramp to target temperature, 1°C/second	60.0	4 minutes
5 loop	24 times		
6 final extension	Ramp to target temperature, 1°C/second	60.0	4 minutes
7 incubate	Ramp to target temperature, 1°C/second	4	∞

Table 3: Dye Termination (Sanger) Thermocycler program
The sequencing reactions were run using the above program on an MH Research DNA Engine Dyad Peltier Thermocycler, (Bio-Rad, CA, USA)

Reagent	**1 × /µl**	**Final concentration**
Autoclaved deionized water	35.00	
10X Pfx Amplification Buffer	5.00	1 × buffer solution
50mM $MgCl_2$	1.00	1 mM
10mM dNTP	1.50	300 µM
10µM GeneRacer™ 5′ Primer,	4.50	0.9 µM
10µM Gene-Specific Primer	1.50	0.3 µM
Platinum®Pfx DNA Polymera	0.50	
Master mix total volume	**49.00**	
DNA template	1.00	

Table 4: Setup of the first PCR reaction for the 5'-amplifications of cDNA ends
Reagents were added in the order shown. 3 times the amount of GeneRacer primer is used given that the GeneRacer oligomer is ligated to the 5'-end of mRNAs, and only a subset of them will be from HPGD or SLCO2A1 in the PCRs following there reverse transcription reaction

Temperature	Time	Cycles
94°C	2 minutes	1
94°C	30 seconds	5
72°C	2 minutes	
94°C	30 seconds	5
70°C	2 minutes	
94°C	30 seconds	25
65°C	30 seconds	
68°C	2 minutes	
68°C	10 minutes	1

Table 5:Thermocycler Program for the 5'-amplification of cDNA ends in the first PCR reaction used for SLCO2A1

Temperature	Time	Cycles
94°C	2 minutes	1
94°C	30 seconds	10
67°C - 62°C [-0.5°C/cycle]	30 seconds	
94°C	30 seconds	25
62°C	30 seconds	
68°C	2 minutes	
68°C	10 minutes	1

Table 6:Thermocycler Program for the 5'-amplification of cDNA ends in the first touchdown PCR reaction used for HPGD on the second run of the protocol

Construct	Restriction Endonucleases
H-3082	AvrII, Bsp68I
H-2983	AvrII, NdeI
H-2149	AvrII, BsaI
H2050	AvrII, ZraI
H-1570	AvrII, SphI
H-1023	AvrII, BglII
H-872	AvrII, NheI
H-319	AvrII, XmnI
S-3198	NcoI
S-2887	HindIII-HF, PflF1
S-2351	HindIII-HF, AflII
S-2164	HindIII-HF, AvrII
S-1877	HindIII-HF, StuI
S-1579	HindIII-HF, AclI
S-364	HindIII-HF, XmaI
S-266	HindIII-HF, EcoNI
S-140	SfiI, BssHII
S-3198 (del:-2351 to -2164)	AflII, AvrII
S-3198 (del:-2164 to -1877)	AvrII, StuI

Table 7:Restriction enzymes used for generating the HPGD and SLCO2A1 promoter deletion series

The above table list the constructs generated by double restriction endonuclease digestion

reagent	For each well (100µl) of medium and adherent cells
Opti-MEM	25.00 µl
pRL-CMV (0.35ng/µl)	1.00 µl
Opti-MEM	25.00 µl
Lipofectamine 2000	1.00 µl
Equimolar deletion series plasmids (50ng/µl)	1.00 µl

Table 8:Cell line transfection set up using Lipofectamine 2000, on a 96-well plate format
Cell line transfection set up using Lipofectamine 2000, on a 96-well plate format. A “master mix” of Opti-MEM and the transfection control Renilla plasmid was prepared. This was aliquoted in 0.5ml tubes, to which the equimolar dilutions of the promoter deletion series plasmids were added (50 ng/µl).

Antibody	Manufacturer	Product code	Stock concentration	Dilutions used
Rabbit-anti-Human HPGD polyclonal antibody	Novus Biologicals (Cambridge, UK (EU office))	NBP1-87061	0.1 mg/ml	1:400 (0.25µg/ml) 1:200 (0.5µg/ml) 1:100 (1.0µg/ml)
Rabbit-anti-Human HPGD polyclonal antibody	Novus Biologicals, (Cambridge, UK (EU office))	NBP1-87062	0.1 mg/ml	1:200 (0.5µg/ml) 1:100 (1.0µg/ml) 1:50 (2.0µg/ml)
Rabbit-anti-Human HPGD polyclonal antibody	Cayman Chemicals, (Ann Arbor, Michigan, USA)	160615	0.5 mg/ml	1:800 (0.625µg/ml) 1:400 (1.25µg/ml) 1:200 (2.5µg/ml) 1:100 (5.0µg/ml)
Rabbit-anti-Human SLCO2A1 polyclonal antibody	Abcam, (Cambridge, UK)	ab150788	0.100 mg/ml	1:1600 (0.0625µg/ml) 1:800 (0.125µg/ml) 1:400 (0.25µg/ml) 1:200 (0.5µg/ml) 1:100 (1.0µg/ml) 1:50 (2.0µg/ml) 1:25 (4.0µg/ml)
Rabbit-anti-Human/Mouse/Rat SLCO2A1 polyclonal antibody	Bioss Antibodies Inc. (Massachusetts, USA)	bs-4710R	1.0 mg/ml	1:400 (2.5µg/ml) 1:200 (5.0µg/ml) 1:100 (10.0µg/ml) 1:25 (40.0µg/ml)
Rabbit-anti-Human SLCO2A1 polyclonal antibody	Cayman Chemicals, (Ann Arbor, Michigan, USA)	11860	0.5 mg/ml	1:800 (0.625µg/ml) 1:400 (1.25µg/ml) 1:200 (2.5µg/ml) 1:100 (5.0µg/ml)
Rabbit IgG			2.0 mg/ml	1:1000 (2.0µg/ml)

Table 9: Antibodies used for Immunohistochemistry